UNIVERSITA' DEGLI STUDI
DI MILANO – BICOCCA

SCUOLA DI DOTTORATO DI SCIENZE
Facoltà di Scienze Matematiche, Fisiche e Naturali
Dipartimento di Biotecnologie e Bioscienze

Corso di Dottorato di Ricerca in Biotecnologie industriali, XXVII ciclo

Exploration of new techniques for purification and chemo-selective conjugation of bioreagents for immunodiagnostic applications

Dott.ssa Elisa Mazzoleni

Anno accademico 2013/2014

Dottorato in Biotecnologie Industriali, XXVII ciclo

Dott.ssa Elisa Mazzoleni
Matricola: 064424

Tutor: Prof. Marco Ercole Vanoni

Il lavoro presentato in questa tesi è stato realizzato presso i laboratori di Biochimica e Biologia Molecolare del DiaSorin Research Center, sotto la supervisione del dott. Pier Natale Brusasca

Università degli Studi di Milano-Bicocca
Piazza dell'Ateneo Nuovo 1, 20126, Milano

Dipartimento di Biotecnologie e Bioscienze
Piazza della Scienza 2, 20126, Milano

INDEX

RIASSUNTO

Antigene e anticorpo rappresentano i due reagenti chiave di un saggio immunodiagnostico. L'indagine di nuove tecniche e il miglioramento di processi quali la purificazione e la marcatura sito-specifica di antigeni e anticorpi può promuovere lo sviluppo di nuovi reagenti più efficienti capaci di migliorare la performance dei saggi immunodiagnostici.
La prima parte di questa tesi ha avuto lo scopo di esplorare tecniche biotecnologiche innovative nella produzione di antigeni per il miglioramento dei saggi che permettono la rilevazione di anticorpi diretti contro il virus Epstein-Barr (EBV), nei campioni di siero o plasma umano. EBV è l'agente eziologico della mononucleosi infettiva ed è uno dei virus maggiormente diffusi a livello mondiale. Si stima che circa il 95% della popolazione adulta mondiale sia sieropositiva per EBV. Inoltre, questo virus è associato ad uno spettro ancora crescente di patologie cliniche, che vanno da malattie infiammatorie acute e croniche a tumori linfoidi ed epiteliali; per questo motivo è necessario sviluppare saggi diagnostici per il rilevamento di EBV con elevata specificità e sensibilità. La proteina del capside virale VCA p18 rappresenta uno degli antigeni più importanti per la diagnosi di EBV. Gli attuali saggi Diasorin LIAISON® EBV VCA IgM and IgG si basano principalmente su un singolo antigene corrispondente alla regione C-terminale immuno-dominante della proteina p18, immobilizzata su fase solida. I vari metodi esplorati in questa tesi hanno permesso di ottenere diverse varianti dell'antigene p18 con lo scopo di migliorare le prestazioni dei saggi EBV VCA IgM e IgG a diversi livelli: 1_produzione dell'antigene p18; 2_immobilizzazione dell'antigene p18 su fase solida; 3_formato di saggio.
1_La lunghezza della regione C-terminale immunodominante della proteina p18 (57aa), risulta essere considerevole per il processo sintetico ma, allo stesso tempo, troppo piccola per essere prodotta in modo efficiente per via ricombinante. Per superare questo problema, abbiamo esplorato il sistema Elastin Like Polypeptides (ELP)-Inteina, un metodo basato sull'uso di una proteina in grado di effettuare auto-cleavage (inteina) e un tag responsivo alla temperatura (ELP). Questa tecnica si è rivelata un eccellente sistema per la produzione del peptide p18.
2_L'immobilizzazione su fase solida è stato un altro aspetto investigato al fine di ottimizzare la performance dei saggi immunodiagnostici per la

detection di EBV. Abbiamo esplorato tre differenti tecniche per l'immobilizzazione dell'antigene p18 su fase solida: coating covalente diretto (2.1), attraverso il sistema streptavidina-biotina (2.2) e attraverso l'utilizzo dei "leucine-zipper" o "velcro peptidi" (2.3). (2.1) Il primo metodo ha previsto il coating covalente diretto su fase solida della variante ricombinante dell'antigene p18 ottenuto attraverso il sistema ELP-Inteina. (2.2) Il secondo metodo ha previsto invece l'uso del complesso streptavidina-biotina; in questo caso la biotinilazione dell'antigene è stata effettuata a sua volta attraverso l'investigazione di due diversi metodi. (i) Nel primo caso, abbiamo sfruttato la variante dell'antigene p18 generata con il metodo ELP-Inteina al fine di ottenere una biotinilazione C-terminale sito-specifica dello stesso antigene attraverso l'uso della tecnica chiamata "expressed protein ligation" o "intein-mediated protein ligation". Questa tecnica comporta la reazione tra una proteina ricombinante caratterizzata da un gruppo tioestere al C-terminale (ottenuta attraverso il processo di auto-cleavage dell'inteina) e un peptide sintetico contenente un gruppo tiolo all'N-terminale e, nel nostro caso, un residuo di lisina-biotina al C-terminale al fine di ottenere una biotinilazione sito specifica al C-terminale della proteina target. L'immobilizzazione su fase solida sia della variante ricombinante dell'antigene p18 attraverso coating covalente diretto, che della variante biotinilata in modo sito specifico al C-terminale attraverso il sistema streptavidina-biotina, è avvenuta con successo e l'attività immunochimica di queste varianti è risultata migliore rispetto a quella del peptide sintetico attualmente in uso.
(ii) Nel secondo caso, abbiamo cercato di ottenere la biotinilazione sito-specifica dell'antigene p18 all'N-terminale utilizzando una tecnica innovativa che prevede l'incorporazione genetica di amminoacidi non naturali nella proteina target direttamente in cellule di *E. coli*. In particolare l'incorporazione di una para-azido-fenilalanina (pAzF) a livello della regione N-terminale dell'antigene p18 è stata sfruttata per realizzare una reazione SPAAC (Strain-Promoted Azide-Alkyne Cycloaddition (SPAAC**)** con una molecola di cicloottino-biotina al fine di ottenere un antigene p18 biotinilato all'N-terminale. Sfortunatamente, nonostante numerosi esperimenti abbiano confermato l'incorporazione della pAzF sulla proteina p18, la reazione SPAAC non è avvenuta.

Saranno quindi necessarie future analisi finalizzate alla comprensione della mancanza di reattività del gruppo funzionale azidico incorporato sulla proteina p18 stessa.
(2.3) Infine, la terza tecnica di immobilizzazione su fase solida ha previsto una procedura innovativa basata sull'utilizzo dei leucine zipper (o "velcro") peptidi. Il principio di questo sistema è basato sulla formazione di strutture coiled coil stabili tra i 2 peptidi velcro (il primo -partner acido- legato ad un dominio di ancoraggio alla fase solida, e il secondo -partner basico- legato alla proteina target) al fine di permettere l'immobilizzazione indiretta della proteina target su fase solida. I risultati ottenuti hanno mostrato una buona responsività del sistema, ma allo stesso tempo, hanno rilevato un problema di alto background introdotto dal sistema stesso. Numerose strategie (buffers con specifici detergenti, design dei costrutti, etc.) potranno essere applicate per ottimizzare la tecnica e i problemi ad essa correlati.
3_Nonostante il saggio Diasorin LIAISON® EBV VCA IgM abbia una buona performance analitica, al fine di ottenere un aumento di specificità, è stato esplorato un nuovo tipo di formato di saggio. Partendo da un formato di saggio indiretto (che implica l'immobilizzazione dell'antigene p18 su fase solida), abbiamo cercato di sviluppare un formato "reverse", in cui anticorpi anti-human IgM, capaci di catturare le IgM umane presenti nei campioni, sono usati come elemento di cattura su fase solida, mentre l'antigene p18, legato a una o più molecole chemilumescenti, è usato come tracciante. Sfortunatamente, i risultati indicano che il formato di tipo reverse non è responsivo e quindi non adatto per questo specifico saggio immunodiagnostico. Nonostante i risultati negativi, questa esplorazione ci ha permesso di settare le migliori condizioni per l'utilizzo di un nuovo tipo di chimica, la click chemistry, utilizzata per la sintesi del tracciante p18. Allo stesso tempo abbiamo sviluppato un protocollo per la sintesi di nuovi traccianti caratterizzati dal possedere una molecola scaffold di natura non proteica in grado di legare più molecole chemiluminescenti insieme all'antigene di interesse, con lo scopo di amplificare il segnale e di migliorare quindi la sensibilità del sistema.

La seconda parte di questa tesi è stata focalizzata sull'esplorazione di un metodo innovativo per la produzione di coniugati con molecole anticorpali. Uno degli approcci più promettenti per la marcatura sito specifica degli anticorpi è basato sulla generazione di gruppi tiolo liberi attraverso la riduzione parziale e selettiva dei ponti disolfuro inter-catena presenti a livello della "hinge region" e la loro reazione con molecole marcanti caratterizzate dal possedere gruppi chimici funzionali reattivi verso i gruppi sulfidrilici. Questa tecnologia è stata utilizzata per la biotinilazione di due diversi anticorpi usati attualmente per il rilevamento della proteina virale p24 di HIV e per quella dell'antigene FGF23. I risultati suggeriscono che la biotinilazione sito-specifica rispetto a quella classica random promuove un miglioramento dell'attività immunochimica degli anticorpi con una conseguente ottimizzazione della performance dei saggi immunodiagnostici.

ABSTRACT

Antigen and antibody are the two key reagents for an immunodiagnostic assay. Investigation of new techniques and improvement of processes such as purification and site-specific labeling of antigen and antibody molecules can promote the development of new more powerful bioreagents able of improving the performance of immunodiagnostic assays.

The first part of this thesis aimed to explore innovative biotechnology techniques in antigen production for the improvement of immunoassays that allow the detection of antibodies directed against the Epstein-Barr virus (EBV), in human serum or plasma samples. EBV is the causative agent of infectious mononucleosis and is one of the most successful viruses. It is estimated that nearly 95% of the adult population worldwide is seropositive for EBV. Moreover, it is associated with a still growing spectrum of clinical disorders, ranging from acute and chronic inflammatory diseases to lymphoid and epithelial malignancies; for this reason it is necessary to develop diagnostic assays for EBV detection with high specificity and sensitivity. The minor viral capsid protein VCA p18 appears to be one of the most important antigens for the diagnosis of EBV. The current Diasorin LIAISON® EBV VCA IgM and IgG assays mainly rely on a single antigen, consisting in a synthetic peptide corresponding to the immunodominant C-terminal portion of the p18 protein, which is immobilized on solid phase (indirect format). The several methods explored in this thesis have allowed to obtain different variants of the p18 antigen with the aim to improve the performance of DiaSorin LIAISON® EBV VCA IgM and IgG assays at different levels: 1_production of p18 antigen; 2_immobilization of p18 antigen on solid phase; 3_immunoassay format.

1_The length of the immunodominant C-terminal portion of the p18 protein (57aa) appears to be considerable for the synthetic route but, at the same time, too small to be effectively produced in a recombinant fashion. To overcome this problem, we explored the Elastin Like Polypeptides (ELP)-Intein system, a method based on the use of a self-cleavable protein (the intein) and a temperature responsive tag (ELP). This technique has proved to be an excellent system for the preparation of the p18 peptide.

2_ The immobilization on solid phase was another aspect investigated in order to improve the performance of immunoassays for EBV detection. We explored three different techniques for the immobilization of the p18 antigen on solid phase: direct covalent coating (2.1), through streptavidin/biotin system (2.2) and through the use of leucine zipper (or "velcro") peptides (2.3). (2.1) The first method provided direct covalent coating of the p18 recombinant variant obtained through ELP-Intein system. (2.2) The second involved the use of streptavidin-biotin complex; in this case, the biotinylation of the antigen was carried out in turn through the investigation of two different methods. (i) In the first case, we exploited the p18 antigen variant generated by ELP-intein method in order to obtain the C-terminal site-specific biotinylation of the same antigen by using the technique called "expressed protein ligation" or "intein-mediated protein ligation". This technique involves the reaction between a recombinant protein with a C-terminal thioester group (obtained through the process of intein self-cleavage) and a synthetic peptide containing a thiol group at the N-terminus and, in our case, a lysine-biotin at the C-terminus in order to obtain a C-terminal site-specific biotinylation of target protein.
The immobilization on solid phase of both the p18 recombinant variant through direct covalent coating and the C-terminal site specific biotinylated p18 antigen through streptavidin-biotin system, occurred successfully and the immunochemical activity of these variants resulted much better than that of the synthetic peptide currently in use.
(ii) In the second case, we tried to obtain the N-terminal site-specific biotinylation of the p18 antigen by using an innovative technique that provides the genetic incorporation of unnatural amino acids into target protein directly in *E. coli* cells. In particular the incorporation of a para-azido-phenylalanine (pAzF) at the N-terminus region of the p18 antigen has been exploited to subsequently realize a Strain-Promoted Azide-Alkyne Cycloaddition (SPAAC**)** reaction with a molecule of cyclooctyne-biotin with the aim to obtain a N-terminal biotinylated p18 antigen. Unfortunately, despite numerous experiments have confirmed the incorporation of pAzF into p18 antigen, the SPAAC reaction did not occur. Therefore, future analyses aimed to understand the lack of

reactivity of azido functional group incorporated into p18 antigen will be necessary.
(2.3) Finally, the third immobilization technique provided an innovative procedure based on the use of leucine zipper (or “velcro”) peptides. The principle of this system is based on the formation of stable coiled coil structures between the two velcro peptides (the first -acidic partner- linked to a solid phase anchor domain and the second -basic partner- linked to the target protein) to permit the indirect immobilization of the target protein on solid phase. The results obtained showed a good responsiveness of the system, but at same time revealed a problem of high background introduced by the system itself. Numerous strategies (buffers with specific detergents, constructs design. etc.) will be applied to optimize this technique and to solve correlated problems.
3_ Despite the DiaSorin LIAISON® EBV VCA IgM immunoassay has a good analytical performance, in order to obtain an increase of specificity, a new assay format was explored. Starting from an indirect format (which includes the p18 antigen immobilization on solid phase), we tried to develop a "reverse" format, in which anti-human IgM antibodies, capable of catching the human IgM present in the samples, are used as a capture element on solid phase, while the p18 antigen, linked to one or more chemiluminescent molecules, is used as a tracer. Unfortunately, the results indicated that the reverse type of format is not responsive and therefore not suitable for this specific immunoassay. Despite the negative results, this exploration permitted us to set the best conditions for the use of new type of chemistry, the click chemistry, used for the synthesis of p18-tracer. At the same time, we developed a protocol for the synthesis of new tracer molecules characterized by the presence of a non-proteic scaffold carrying different chemiluminescent molecules together with the antigen of interest, with the aim to amplify the signal and thus to improve the sensitivity of the system.

The second part of this thesis aimed to explore an innovative method for the production of antibody conjugates. One the most promising approach for the site-specific labeling of antibody is based on the generation of free thiol groups by selective partial reduction of the interchain disulfide bridges present at the level of the “hinge region” and their reaction to labels carrying sulfhydryl-reactive chemical groups. This technology was used for the biotinylation of two different antibodies currently used in immunoassays for the HIV p24 viral protein and for FGF23 antigen detection. The results suggest that the site-specific biotinylation compared to the random traditional biotinylation promotes a great improvement of antibodies immunochemical activity with a consequent optimization of immunodiagnostic assays performance.

Chapter 1:

Exploration of various techniques for the production of different p18 antigen variants aimed to improve the immunoassays for EBV detection

INTRODUCTION

As the world population grows, the need for health care increases. Health care today not only means advances in therapy but also requires accurate, sensitive, specific, quick and cost-effective diagnostic systems. With the advances in biotechnology, it has now become possible to develop diagnostic assays for several diseases and pathological conditions. In this context, immunodiagnostics has replaced and is replacing conventional techniques of serum biochemistry and analysis.

Immunodiagnostics is a diagnostic methodology that uses an antigen-antibody reaction as their primary means of detection. The concept of using immunology as a diagnostic tool was introduced in 1960 as a test for serum insulin (1). A second test was developed in 1970 as a test for thyroxine (2). One of the main advantages in the use of immunodiagnostic assays is the high sensitivity, which means the ability to detect even small amounts of biochemical substances in the samples; this characteristic is related to the use of highly selective antigen-antibody recognition reaction. Antibodies specific for a desired antigen can be conjugated with a radiolabel (radioactive immunoassay), fluorescent label (fluorescent immunoassay), color-forming enzyme (e.g. ELISA) or with molecules emitting photons of light (chemilumiscent immunoassay) and are used as a "probe" to detect antigen. The speed, accuracy and simplicity of such tests has led to the development of rapid techniques for the diagnosis of several diseases.

Antigen and antibody are the two key reagents for an immunodiagnostic assay. The investigation of new techniques and the improvement of processes such as the expression, purification and site-specific labeling of antigen and antibody molecules can promote the development of new more powerful reagents with a consequent optimization of immunodiagnostic assay. The aim of this thesis is the exploration of new methods of purification, immobilization on solid phase and chemo-selective conjugation for the development of new reagents and new solutions for immunodiagnostic applications. As model systems, we took into consideration the Diasorin LIAISON® EBV VCA IgM and Diasorin LIAISON® EBV VCA IgG assays, these assays allow the determination of IgM or IgG antibodies directed specifically against the Epstein-Barr virus, in human serum or plasma samples.

EPSTEIN BARR VIRUS (EBV)

The Epstein–Barr virus (EBV) was discovered 36 years ago by electron microscopy of cells cultured from Burkitt's lymphoma tissue by Epstein, Achong, and Barr (3). Four years later, in 1968, EBV was shown to be the etiologic agent of heterophile-positive infectious mononucleosis (4). EBV DNA was detected in tissues from patients with nasopharyngeal carcinoma in 1970 (5). In the 1980s, EBV was found to be associated with non-Hodgkin's lymphoma and oral hairy leukoplakia in patients with the acquired immunodeficiency syndrome (AIDS) (6,7). Since then, EBV DNA has been found in tissues from other cancers, including T-cell lymphomas and Hodgkin's disease (8,9). EBV is one of the most successful viruses, most individuals become infected during childhood, and it is estimated that nearly 95% of the adult population worldwide is seropositive for the virus (10).

VIROLOGIC FEATURES

EBV, or human herpesvirus 4 (HHV4) belongs to the genus Lymphocryptovirus within the subfamily of gammaherpesviruses. Common feature of these viruses are their lymphotropism, their ability to establish latent infection of their host cells and to induce proliferation of the latently infected cells (11). Like other herpesviruses, EBV is a DNA virus with a toroid-shaped protein core that is wrapped with DNA, a nucleocapsid which comprises major and minor capsid proteins and characterized by a common icosahedral structure with 162 capsomers, a protein tegument between the nucleocapsid and the envelope, and an outer envelope with external virus-encoded glycoprotein spikes (Figure 1A). The viral genome is encased within a nucleocapsid, which is, in turn, surrounded by the viral envelope. Before the virus enters the B cell, the major envelope glycoprotein, gp350, binds to the viral receptor, the CD21 molecule (the C3d complement receptor) (12), on the surface of the B cell. Other factors in addition to CD21 are important for infection. The major-histocompatibility-complex (MHC) class II molecule serves as a cofactor for the infection of B cells (13).

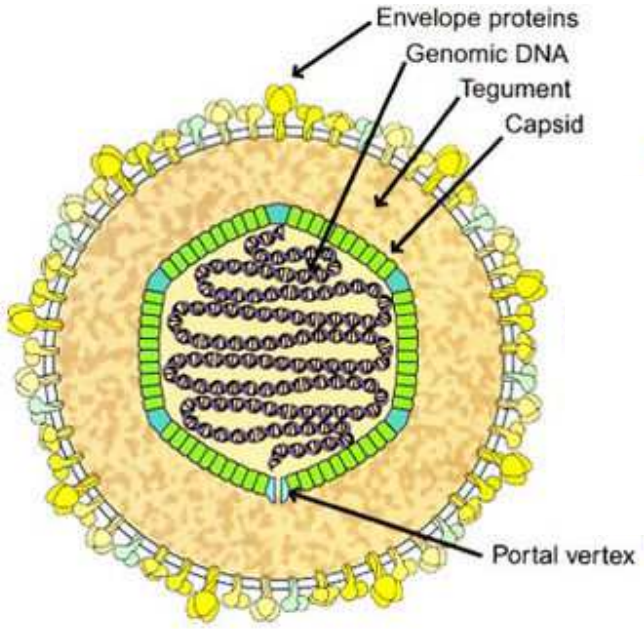

Figure 1A. Structure of Epstein Barr virion.

The EBV genome consists of a linear DNA molecule that encodes nearly 100 viral proteins (14). During viral replication, these proteins are important for regulating the expression of viral genes, replicating viral DNA, forming structural components of the virion, and modulating the host immune response. Infection of epithelial cells by EBV in vitro results in active replication, with production of virus and lysis of the cell (13). In contrast, infection of B cells by EBV in vitro results in a latent infection, with immortalization of the cells (Figure 1B). After infecting B cells, the linear EBV genome becomes circular, forming an episome, and the genome usually remains latent in these B cells. Viral replication is spontaneously activated in only a small percentage of latently infected B cells. Infection of humans with EBV usually occurs by contact with oral secretions. The virus replicates in cells in the oropharynx, and nearly all seropositive persons actively shed virus in the saliva (15). Although earlier studies indicated that the virus replicated in epithelial cells in the oropharynx (16) and investigators postulated that B cells were

subsequently infected after contact with these cells (17), other studies suggest that B cells in the oropharynx may be the primary site of infection (18,19). Resting memory B cells are thought to be the site of persistence of EBV within the body (20). Shedding of EBV from the oropharynx is abolished in patients treated with acyclovir, whereas the number of EBV-infected B cells in the circulation remains the same as before treatment (21). In addition, the observation that EBV can be eradicated in bone marrow–transplant recipients who have received therapy that ablates their hematopoietic cells, but not their oropharyngeal cells (22) provides further evidence that B cells are the site of EBV persistence. In normal adults, from 1 to 50 B cells per million in the circulation are infected with EBV, and the number of latently infected cells within a person remains stable over years (20,23).

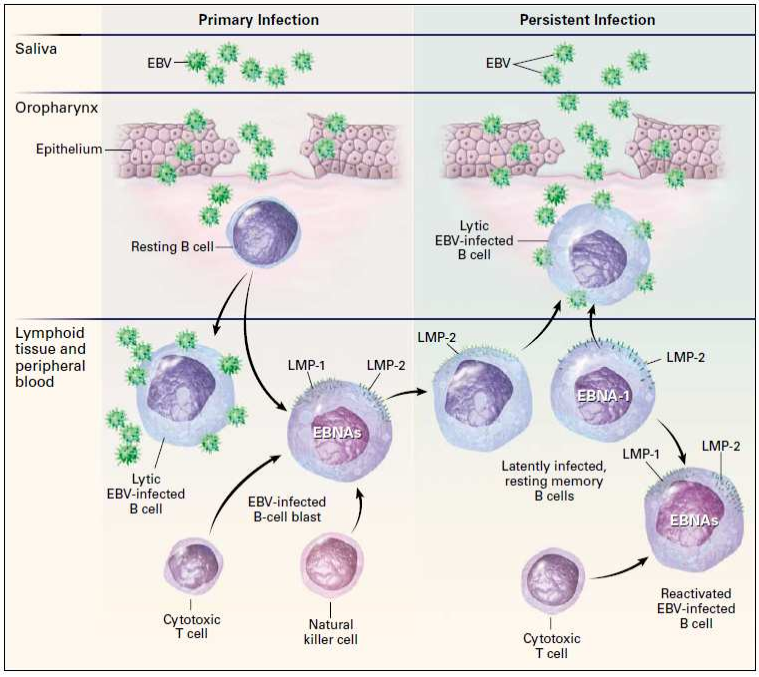

Figure 1B. Model of Epstein-Barr virus (EBV) infection in humans.

Primary infection and lytic replication. Initial infection is thought to occur in the oral (oropharynx) compartment (Figure 1B). The host cells of EBV are mainly lymphocytes and epithelial cells. As mentioned above, EBV attaches to B cells via binding of the viral gp350 protein to CD21 on B cells. EBV gp42 then interacts with B-cell HLA class II molecules and triggers fusion with the host membrane. In epithelial cells, which lack CD21, the EBV BMRF-2 protein interacts with β1 integrins (24,25), and the EBV gH/gL envelope protein triggers fusion via interaction with αvβ6/8 integrins (26). Endocytosis of the virus into vesicles and fusion of the virus with the vesicle membrane release the nucleocapsid into the cytoplasm. Once the viral nucleocapsid is dissolved, the genome is transported to the nucleus, where it is replicated by DNA polymerases. Viral DNA polymerase accomplishes linear viral replication, which occurs during the lytic phase of the viral life cycle. There are three temporal classes of viral lytic gene products (immediate-early [IE], early [E], and late [L]). BZLF1 and BRLF1 are some of the IE products that further act as transactivators of the viral lytic program (27). Activation of lytic replication or reactivation from latency is key to transmission. The early products (e.g., BNLF2a) have a wide array of functions, including replication, metabolism, and blockade of antigen processing, while late products tend to code for structural proteins such as the viral capsid antigens (VCA) and gene products used for immune evasion (e.g., BCRF1). An important consequence of EBV infection in B cells is that they are induced to activate their growth program and trigger differentiation into memory B cells via the germinal center reaction. Infected memory B cells are released into the peripheral circulation, resulting in detectable levels of virus in the blood. The number of infected B cells decreases over time after the onset of symptoms of primary infection (28), but these cells are never eliminated entirely, as discussed below.

Latency. Latency is the state of persistent viral infection without active viral production. EBV persists mostly in the memory B-cell compartment and possibly also in epithelial cells (Figure 1B). It is generally thought that EBV genomes in latently infected B cells exist as episomes, although it is possible that the genomes exist as integrated DNA (29,30). In contrast to lytic replication, episomal replication during the latent phase

occurs via host DNA polymerase. There is limited expression of EBNA and latent membrane protein (LMP) gene products during latency (31). These include EBNA1, EBNA2, EBNA3A, EBNA3B, EBNA3C, EBNA leader protein (EBNA-LP), LMP1, and LMP2. Characterization of gene expression patterns in different cell lines (i.e., Burkitt's tumors and EBV-immortalized lymphoblastoid cell lines [LCLs]) has determined that there are at least three different latency programs (32). By using different transcription programs, latent EBV genomes can multiply in dividing memory cells (type I), induce B-cell differentiation (type II), activate naïve B cells (type III), or completely restrict all gene expression in a context-specific manner (32,33). Only EBNA1 is expressed in the type I latency program, which is seen in Burkitt's lymphoma. CD8+ T cells specific for many EBV antigens arise during the immune response to natural infection, but not for EBNA1, which contributes to evasion during latency (34). EBNA1 and LMP1/2A are expressed in the type II latency program, which is observed in nasopharyngeal carcinoma and Hodgkin's lymphoma. LMP1 and LMP2 are responsible for B-cell activation and induction of a growth (proliferation) program (35). The type III latency program, in which all of the latency gene products are expressed, is often detected during acute infectious mononucleosis or in certain immunocompromised individuals (36).

Reactivation. Latently infected B cells can occasionally be stimulated to reactivate EBV. This produces virus that can reinfect new B cells and epithelial cells, becoming a source of viral transmission. Although much is known about the molecular pathways involved in viral reactivation (37), what triggers reactivation *in vivo* is not known precisely. The presumption is that it occurs when latently infected B cells respond to unrelated infections, because B-cell receptor stimulation triggers reactivation in B-cell lines. It is also not known what fraction of EBV-infected cells are in the lytic or latent phase at any time, although a technique using sera from EBV-infected individuals may prove useful in the future (38). Understanding how each gene product, whether lytic or latent, contributes to the pathogenesis of EBV-related diseases should lead to more rational and effective prevention and treatment strategies.

EBV-ASSOCIATED DISORDERS

Infectious Mononucleosis (IM). IM can be considered the clinically manifest form of a primary EBV-infection. Whereas most EBV infections of infants and children are asymptomatic or have nonspecific symptoms, infections of adolescents and adults frequently result in infectious mononucleosis (39,40). Over 50 percent of patients with infectious mononucleosis manifest fever, lymphadenopathy, and pharyngitis; splenomegaly, palatal petechiae, and hepatomegaly are each present in more than 10 percent of patients. Less common complications include hemolytic anemia, thrombocytopenia, aplastic anemia, myocarditis, hepatitis, genital ulcers, splenic rupture, rash and neurologic complications such as Guillain–Barré syndrome, encephalitis, and meningitis. Its diagnosis relies in the detection of atypical lymphoid cells in the peripheral blood, the occurrence of so-called heterophile antibodies, elevated serum aminotransferase and EBV-seroconversion (41). The atypical lymphocytes are primary T cells, many of which are responding to the EBV-infected B cells.

X-linked lymphoproliferative syndrome (X-LPS). X-LPS, or fatal mononucleosis, is caused by hereditary mutations in the gene encoding the signaling lymphocyte activation molecule (SLAM)-associated protein (SAP) on position q25 of the X-chromosome (42,43). The self-ligand SLAM protein is present on the surface of both B and T-cells. When interactions occur between SLAM molecules on the interface between T- and B-cells, signal transduction pathways are initiated. The T cell protein SAP binds to SLAM and as such acts as a negative regulator (44-45). Individuals that have inherited this trait are usually asymptomatic, but upon primary EBV-infection their immune response becomes over-reactive because of the non functional SAP protein. This usually results in a fulminant IM accompanied by a virus-associated hemophagocytic syndrome by which liver and bone-marrow are destroyed (46). The only curative treatment for this syndrome is allogeneic bone-marrow transplantation (47). However, patients who do survive the infection are prone to developing lymphomas later in life (48).

Nasopharyngeal Carcinoma (NPC). Nasopharyngeal carcinoma is prevalent in southern China, in northern Africa, and among Alaskan Eskimos. In southern China the incidence of nasopharyngeal carcinoma approaches 50 per 100.000 persons per year (49). Nasopharyngeal carcinoma occurs sporadically in the United States and western Europe. Nearly 100 percent of anaplastic or poorly differentiated naso-pharyngeal carcinomas contain EBV genomes and express EBV proteins. The EBV genome is present in the transformed epithelial cells but not in the lymphocytes of the tumor. Clonal EBV genomes are found in the early preinvasive dysplastic lesions or carcinoma in situ, indicating that EBV infection precedes the development of malignant invasive tumors (50). Patients with nasopharyngeal carcinoma often have elevated titers of IgA antibody to EBV structural proteins. Measurement of EBV-specific IgA antibodies is useful in screening patients for early detection of nasopharyngeal carcinoma in southern China (51). An increase in EBV-specific antibody titers after therapy for nasopharyngeal carcinoma is associated with a poor prognosis, whereas a declining or constant level of antibody is associated with a better prognosis (52).

Burkitt's Lymphoma. Burkitt's lymphoma is a high-grade malignant lymphoma of small, noncleaved B cells. In equatorial Africa, Burkitt's lymphoma is associated with *Plasmodium falciparum* malaria; over 90 percent of these cases are associated with EBV. Infection with malaria is thought to diminish the T-cell control of proliferating EBV-infected B cells and enhance their proliferation. In the United States, patients with Burkitt's lymphoma usually present with abdominal tumors, only 20 percent of which are associated with EBV. Burkitt's lymphoma cells contain a chromosomal translocation involving chromosomes 8 and 14, 22, or 2. These translocations result in the positioning of the c*myc* oncogene (chromosome 8) near the immunoglobulin heavy-chain (chromosome 14) or lightchain (chromosome 2 or 22) constant region, leading to abnormal regulation of the c*myc* gene. Expression of c*myc* in EBV immortalized B cells results in increased tumorigenicity of the cells (53).

Epidemiologic studies suggest that EBV may have a causal role in the development of Burkitt's lymphoma in Africa. Children in Uganda who have elevated titers of antibody to EBV structural proteins are at high risk

for Burkitt's lymphoma (54). Tissue from patients with Burkitt's lymphoma in Africa usually contains EBV DNA and expresses only one EBV protein, EBNA-1. As in nasopharyngeal carcinoma, clonal EBV genomes are found in Burkitt's lymphoma tissues, indicating that the tumor arises from a single EBV-infected cell.

Hodgkin's disease (HD). EBV DNA has been detected in tumors from about 40 to 60 percent of patients with Hodgkin's disease in the United States. The EBV genome is present in the Hodgkin's and Reed-Sternberg cells, and the viral genomes are monoclonal (55). Histologically, HD is characterized by mononuclear Hodgkin cells and their multinucleated variant, the Reed-Sternberg cells (H-RS) cells mentioned above. These are embedded in a background of reactive cells, including lymphocytes, plasma cells, histiocytes and eosinophils (56). Most recent studies indicate that the H-RS cells in many (but not all) cases of HD are derived from B-cells (57). The most characteristic epidemiological feature of HD as seen in most western populations is the bimodal age-incidence curve. In these populations, very few cases occur among children; the incidence then increases, peaking at about age 25; the incidence decreases to a plateau level through middle age and increases again with age to a second peak. Males are more often affected than females, which is most clearly observed in the older age group. There is clear evidence that the risk for HD occurring from early childhood through middle age is associated with factors in the childhood environment that influence the age at which infection with EBV takes place, (i.e. social class, population density, geographic region) (58). Moreover, several independent studies have shown that people who have had IM run a threefold higher risk for getting HD. Interestingly, the majority of HDs in patients who have had IM is not associated with EBV (59,60). It has been suggested that EBV is an important cofactor in the pathogenesis of HD, but that in patients with relatively intact immune systems, EBV-positive neoplastic cells are eradicated and only cells capable of virus-independent growth survive (hit-and-run mechanism (61)). Patients with Hodgkin's disease often have higher titers of antibody to EBV structural proteins before the onset of lymphoma or with the development of lymphoma than the general population.

Lymphoproliferative Disease. EBV is associated with lymphoproliferative disease in patients with congenital or acquired immunodeficiency. These include patients with severe combined immunodeficiency, recipients of organ or bone marrow transplants, and patients with AIDS. These patients have impaired T-cell immunity and are unable to control the proliferation of EBV-infected B cells. They present with symptoms of infectious mononucleosis or with fever and localized or disseminated lymphoproliferation involving the lymph nodes, liver, lung, kidney, bone marrow, central nervous system, or small intestine (62,63). Patients who receive T-cell–depleted or HLA-mismatched bone marrow, receive antilymphocyte antibodies, have cytomegalovirus disease, or acquire primary EBV infection after receiving a transplant are at higher risk for lymphoproliferative disease. Increases in EBV viral load in peripheral blood have been detected in patients before the development of disease, and these levels decrease with effective therapy (64,65). Similarly, EBV RNA was detected in liver-biopsy specimens from 71 percent of patients before the development of lymphoproliferative disease, but in only 10 percent of those in whom the disease did not develop (66). Patients with EBV lymphoproliferative disease often have elevated serum levels of interleukin-6, a B-cell growth factor that may increase the proliferation of EBV-infected B cells (67). Tissues from patients with EBV lymphoproliferative disease show plasmacytic hyperplasia, B-cell hyperplasia, B-cell lymphoma, or immunoblastic lymphoma. Lymphoproliferative lesions usually do not have the chromosomal translocations typical of Burkitt's lymphoma. The diagnosis of EBV lymphoproliferative disease requires the demonstration of EBV DNA, RNA, or protein in biopsy tissue.

Other Cancers. EBV DNA or proteins may have a pathogenic role in several other tumors in which they have been detected, including nasal T-cell/natural-killer-cell lymphomas, lymphomatoid granulomatosis, angioimmunoblastic lymphadenopathy, central nervous system lymphomas in non-immunocompromised patients (68), smooth-muscle tumors in transplant recipients (69) and gastric carcinomas (70). Viral DNA or proteins have also been found in peripheral T-cell lymphomas, which can be accompanied by virus-associated hemophagocytic syndrome (71).

EBV AND HIV

Patients with AIDS have 10 to 20 times as many circulating EBV-infected B cells as healthy persons. T cells from patients with AIDS suppress EBV-infected B cells less effectively than do cells from normal controls. Patients with HIV have increased amounts of EBV in their oropharyngeal secretions (72) and have higher EBV antibody titers than HIV-seronegative persons. A decline in EBV specific cytotoxic T cells and an elevated and increasing EBV viral load preceded the development of EBV-associated non-Hodgkin's lymphomas in patients with HIV infection; however, these changes were not seen in patients with HIV before the development of opportunistic infections (73). HIV viral load and the progression of HIV disease were not affected by primary infection with EBV (72-74).

Oral Hairy Leukoplakia. Oral hairy leukoplakia occurs in HIV-infected patients as well as in some immunosuppressed transplant recipients. It presents as raised, white, corrugated lesions of the oral mucosa, especially on the lateral aspect of the tongue. It is a nonmalignant hyperplastic lesion of epithelial cells. EBV DNA and herpesvirus particles are present in the upper, keratinized epithelial cells of the lesions. Multiple EBV strains are often present in the same lesion. Unlike EBV-associated cancers, oral hairy leukoplakia lesions show active viral replication and expression of lytic viral proteins (7,75).

Lymphoid Interstitial Pneumonitis. Lymphoid interstitial pneumonitis occurs primarily in children, but it also occurs in adults infected with HIV. It is characterized by diffuse interstitial pulmonary infiltrates. The pathological changes in the lesions include infiltration of the alveolar septa by lymphocytes, plasma cells, and immunoblasts. EBV DNA and proteins have been detected in pulmonary lesions from children with HIV and lymphoid interstitial pneumonitis (76).

Non-Hodgkin's Lymphoma. EBV was detected more frequently in biopsy specimens from benign-appearing lymph nodes of HIV infected patients who subsequently or concurrently had non-Hodgkin's lymphoma than in specimens from patients without lymphoma (77). About 50 to 60 percent of these tumors contain EBV DNA or proteins (78,79). Most of

the tumors are classified as either immunoblastic lymphomas or Burkitt type lymphomas, and a smaller number are large-cell lymphomas; most are monoclonal. Burkitt-type lymphomas in patients with AIDS often present before the development of severe immunodeficiency and usually have c-*myc* rearrangements. In contrast, immunoblastic lymphomas develop in the later stages of AIDS, lack c-*myc* rearrangements, and are more frequently EBV positive. Unlike other cancers in patients with AIDS, virtually all central nervous system lymphomas contain EBV DNA (64). These tumors are usually immunoblastic lymphomas and occur in patients with very low CD4+ cell counts. A positive polymerase-chain-reaction test for EBV DNA in the cerebrospinal fluid is a useful predictor of lymphoma in patients with AIDS and focal brain lesions (80). Primary effusion lymphomas in patients with AIDS often contain genomes from both EBV and Kaposi's sarcoma–associated herpesvirus (human herpesvirus 8). EBV has also been detected in leiomyosarcomas from patients with AIDS (81).

NOVEL THERAPEUTIC APPROACHES

Given the significant burden of EBV-associated tumours worldwide, an important priority is to design novel therapies that specifically target viral proteins or otherwise exploit the presence of the virus in malignant cells.

Pharmacological approaches. One potential approach is the use of gene-therapy constructs to express either cytotoxic or inhibitory proteins selectively in tumor cells. For example, OriP-based constructs that are responsive to endogenous EBNA1 (Epstein-Barr Nuclear Antigen 1) in infected cells have been used to express cytotoxic proteins (for example, FAS ligand) or wild-type p53 *in vitro* and *in vivo* models of NPC (82,83). Other approaches are based on the induction of the EBV lytic cycle, either by pharmacological agents or by delivery of EBV immediate-early genes, thereby inducing virus encoded kinases (EBV thymidine kinase and BGLF4, a protein kinase) that phosphorylate the nucleoside analogue gancyclovir to produce its active cytotoxic form (84,85). Demethylating agents such as 5-azacytidine are able to de-repress lytic, as well as potentially immunogenic, latent genes (86) and are now in early-stage clinical trials in patients with NPC, Hodgkin's lymphoma and AIDS-

associated lymphoma. Another common chemotherapeutic agent, hydroxyurea (87), is able to induce the loss of EBV episomes *in vitro* models and has shown some limited clinical efficacy in patients with EBV-positive AIDS-related CNS lymphoma (88). More focused pharmacological approaches aim to abrogate the functions of individual EBV proteins. In model systems, LMP1 (latent membrane protein 1) effector function has been targeted directly, using single-chain antibodies or antisense RNA approaches (89,90) and indirectly, by the genetic or pharmacological interception of its downstream effects on NF-kB (91). More recently, LCL (Lymphoblastoid Cell Lines) growth *in vitro* has been impaired by blocking the transactivating function of EBNA2 (Epstein-Barr Nuclear Antigen 2) using a short-peptide mimic of the RBP-Jk-interaction domain of the viral protein (92). EBNA1 - the one viral protein that is expressed in all EBV-positive tumors - is a particularly attractive target, and a dominant-negative form of the protein that blocks its genome-maintenance function might have therapeutic potential (93).

Immunotherapy. A large part of work attempting to target EBV-positive malignancies with T cells that are specific for EBV antigens is important for tumor immunotherapy. The approach was first used to target EBV-positive PTLs (Post-Transplant Lymphomas). Bone-marrow-transplant patients were infused with EBV latent-antigen-specific effector T cells that were prepared from the bone marrow donor by autologous LCL (Lymphoblastoid Cell Lines) stimulation and expansion *in vitro*. This strategy was highly effective, both as a therapy for the treatment of existing disease, and in prophylaxis (94). Similar adoptive-transfer approaches have now been used to treat PTLs in solid-organ transplant settings using T cells that are expanded *in vitro* and are prepared either from the patient (95) or, where necessary, from a partially HLA (Human Leukocyte Antigen)-matched donor (96). However, these LCL-stimulated effector preparations tend to be dominated by CD8+ T cells that are specific for the immunodominant EBNA3A, EBNA3B and EBNA3C proteins - antigens that are not expressed in all EBV-associated tumors. For Hodgkin's lymphoma and NPC, therefore, clinical trials with LCL-stimulated effectors (97) represent just a first step. Strategies are now being developed either to generate T-cell preparations for transfer that are

enriched in CD8+, and possibly CD4+, reactivities to available sub-dominant targets (such as LMP2A and EBNA1) (98,99), or to immunize the patient with appropriate antigenic constructs to boost these particular responses *in vivo* (100). These tumors might also be capable of evading or suppressing T-cell immune attack - in the case of Hodgkin's lymphoma, possibly through immunosuppressive cytokines that are produced by the HRS (Hodgkin's and Reed-Sternberg) cells themselves (101). More work is needed to determine the influence of the tumor microenvironment on T-cell attack and to explore ways of modifying the cytokine milieu, such as the use of EBV-specific T cells to deliver immunostimulatory cytokines (102).

EBV SERODIAGNOSIS

As described before, EBV virus is the etiological agent of infectious mononucleosis and is largely diffused worldwide, moreover, it is considered to be associated with a still increasing number of human malignancies; for this reason it is important to develop diagnostic assays for EBV detection with high specificity and sensitivity. Furthermore, since the clinical symptoms of infections such as CMV, rubella virus, mumps virus, HIV, HAV, HBV, HCV and neurotropic viruses as well as brucellosis, listeriosis, leptospirosis, toxoplasmosis, and neoplastic diseases like lymphomas and leukemias can be similar to those of an EBV infection, specific EBV serology is still often required for the differential diagnosis. It is used to unequivocally differentiate between EBV infections and other infections listed above. In the serologic EBV diagnosis a distinction is made mainly between antibodies against three antigen classes: EA - early antigens (p138; p54), VCA - capsid/structural antigens (p23; p18), EBNA- nuclear antigens (p72) (Table 1).

Name	Classification	Assessment of the EBV status
EBNA-1	Epstein-Barr nuclear antigen	IgG titer regularly lacking in fresh infections, central marker for past infection. Importance in IgM and IgA not yet described.
p138 and p54	EA, early antigens	Reactivity in IgG, IgM and IgA in all stages possible except in overcome infection. Probable in all subclasses in fresh infections.
p23	VCA	Often detectable in IgG and IgM even at the start of an EBV infection; remains detectable in IgG also in past infections.
p18	VCA	IgG titer usually lacking in fresh infections; marker for past infection; Detection of IgM possible even in the early stage.
gp250/350	Membrane antigen	Very often IgM titer in primary infections, not regularly detectable in IgG.

Table 1. Key antigens of the different stages of EBV infection.

The profile of EBV antigen-specific antibodies present in the sample distinguishes acute primary, convalescent, and past infections (103) (Figure 2). Acute primary EBV infection is characterized by IgM antibodies to the early antigens (EA) and viral capsid antigens (VCA) in the absence of IgG antibodies to the latent antigen EBNA1 (104,105). VCA IgG antibodies may be present in acute infection, but in smaller quantities than VCA IgM antibodies. During convalescence (from the third week to the third month after onset of illness), VCA IgM antibodies dwindle, while VCA IgG antibodies rise and persist for life. Between the third and sixth months, VCA IgM antibodies disappear, whereas EBNA1 IgG antibodies become detectable and persist for life (106).
Characteristic for most NPC patient or persons likely to develop NPC is the IgA antibody response to EBV proteins of all classes. This response can be used in the diagnosis of NPC and in monitoring tumor progression before, during and after antitumor treatment (107).

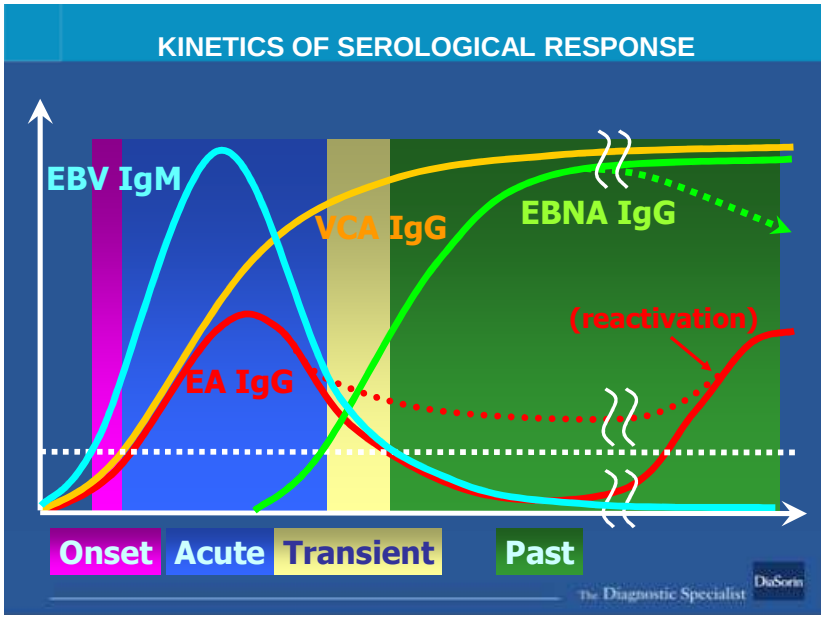

Figure 2. Levels of EBV antigen-specific antibodies in different stages of infection.

THE VIRAL CAPSID ANTIGEN p18

The minor viral capsid or tegument protein of 18kDa (VCA p18) is recognized predominantly by healthy EBV-seropositive persons worldwide indicating that this antigen is an important and fundamental molecule for EBV serologic testing. In particular, the presence of IgG antibodies against p18 (VCA) in the sample, excludes a fresh infection; the titer of anti-p18 (VCA)-IgGs is similar to the EBNA-1 response (Figure 3). However, it has the decisive advantage that persons with a loss of anti- EBNA-1 generally do not lose this late marker. Consequently, they can be serologically evaluated correctly. As regards the IgMs, antibodies against p18 (VCA) are frequently found simultaneously with antibodies against EAs and p23 (VCA) in acute primary infections.
VCA p18 is a highly basic protein of 18 kDa encoded within the open reading frame BFRF3 and appears to have no sequence homologues to other human herpes viruses. Through a specific mapping analysis of

antigenic domains of the p18 protein (108), the C-terminal region has been identified as the immunodominant portion of the antigen: the 95% of VCA IgG-positive sera reacted positively when a peptide corresponding to the C-terminal portion of p18 protein was used as antigen, and the same antigen was reactive with IgM antibodies in 95% of sera from EBV-IgM positive IM patients.

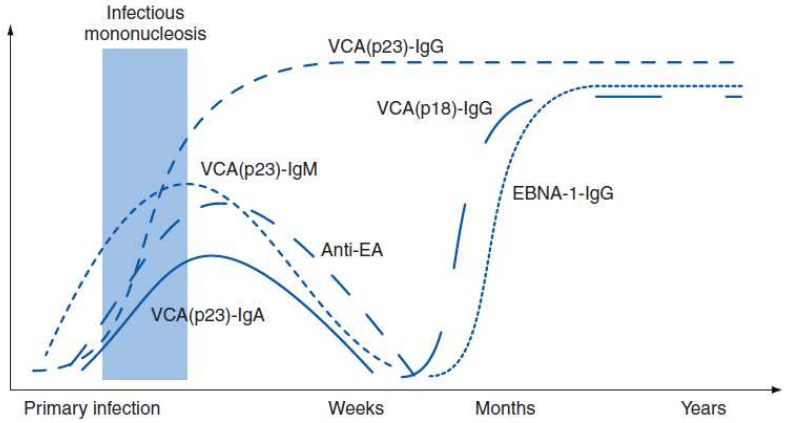

Figure 3. Change in antibodies titers directed against specific EBV antigens with the progress of the stages of infection.

THE LIAISON® SYSTEM

The Liaison® system is an instrument designed to perform immunometric analyses of biological fluid samples (such as serum or plasma) in a completely automated way (Figure 4). Up to 15 different tests can be performed at once on up to 144 samples in a sequential or random access mode. The output of the analysis is generated through the formation of an immune complex, followed by a chemiluminescent reaction that produces an emission of light.

Figure 4. The Liaison® system.

The instrument is composed of two modules, designed to be both allocated on a single workbench; the first module is a personal computer with touch screen, that hosts the user interface software and all the system data (assay protocols, reagent cartridges database, output of analyses, calibration history, network controls etc.). The second module is the actual analyzer, that performs the analysis from sample loading all the way to the final output for the user. Key components of the analyzer include:

- cuvette loader and stacker: two conveyor belts allow continuous loading of the reaction modules, that are stored on a multilevel rack (7 levels).
- Sample rack slots: in the left-hand part of the instrument, a storage area can hold up to 12 sample racks, each carrying up to 12 samples. A barcode reader allows error-free catalogation of samples.
- Reagent slots: in the right-hand part of the instrument, another storage area can hold up to 15 different reagent cartridge simultaneously. This area is kept at a constant temperature of 15°C for optimal conservation of the reagents, while a stirring device keeps the microbeads always in homogenous suspension. Barcode reader for cartridge identification.
- Robot dispense arms: two robotic arms each carrying a dispensing needle. One arm is usually dedicated to dispensing samples, another to dispensing reagents. Each one has a separate washing well to clean the needle after each pipetting.
- Incubator: this area hosts the reaction cuvettes during incubation times, at a constant temperature of 37°C.
- Washing station: through the application of a magnetic field, this part allows retention of the paramagnetic microbeads and removal of the reaction liquids. Any number of washing steps with the desired washing buffer can be set.
- Read area: contains the injection devices of trigger reagents and the photomultiplier tube.

The Liaison® system is based on two key features: the use of paramagnetic microbeads as the solid phase and the generation of signal by means of chemiluminescence. The adoption of microbeads as the solid phase instead of the classic immunoassay supports, as the ELISA microwells gives a clear edge in terms of available reaction surface, which in turn increases the kinetic rates of the antigen-antibody complex formation. Moreover, diffusion of both the analyte and the solid phase in the reaction volume is allowed, while in ELISA system only the analyte can diffuse, decreasing the possibility of the immune complex formation. The microbeads adopted in the Liaison® system (Figure 5) are colloidal

particles composed of a ferric oxide core covered by a polystyrene layer formed by spontaneous coalescence of polystyrene linear chains. This structure is in turn coated with another layer composed of polyurethane activated with tosyl-groups. The tosyl-group (4-toluenesulfonyl chloride) can undergo nucleophilic attack, allowing the beads to covalently bind proteins through their available amino groups (ε-amino groups of lysines, N-terminal end). The paramagnetic properties of these microbeads allow easy manipulation through the application of a magnetic field. The particles respond to a magnet but are not magnetic themselves and retain no residual magnetism after removal of the magnet.

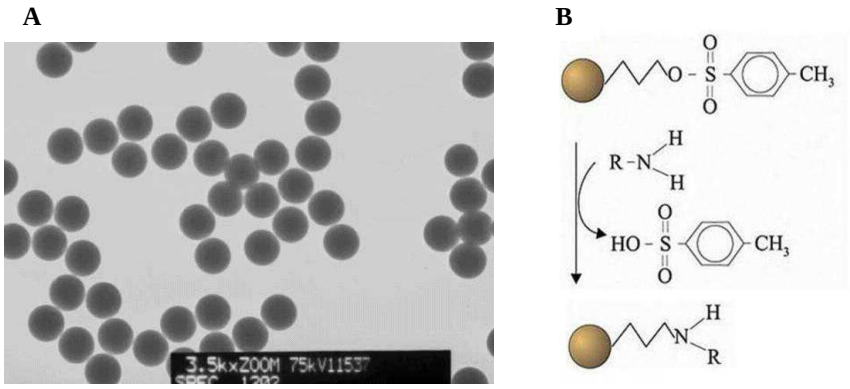

Figure 5. (A) The paramagnetic microbeads used in the Liaison® system.
(B) Chemistry of the covalent binding of amines to the tosyl-activated beads.

The tracer molecule is an antigen or antibody conjugated to a signal generating compound. Chemiluminescent tracers are formed by conjugating the antibody or antigen to a molecule that can generate a photon emission upon addition of certain reagents. The entity of this photon emission is measured with a luminometer, usually equipped with a photomultiplier tube. The chemiluminescent molecule used in the Liaison® system is the luminol derivate ABEI (N-(4-Amino-Butyl)-N Ethyl-Isoluminol), which is converted to its activated ester to allow conjugation with the antibody or antigen (Figure 6).

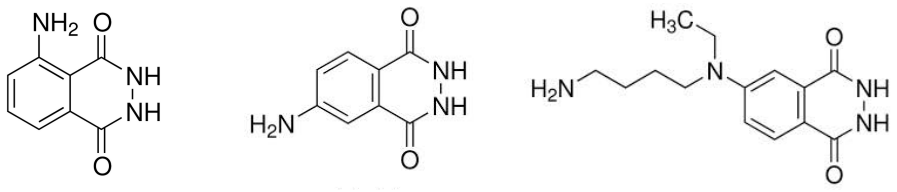

Figure 6. Structure of luminol, isoluminol and ABEI molecules.

In presence of H_2O_2 and a microperoxidase (deuteroferriheme), ABEI achieves an excited state in consequence of a chemical reaction. This excited level decays to the ground level generating energy in form of light (Figure 7). The emission of light is recorded by the photomutiplier tube for an interval of just 3 seconds ("flash" chemiluminescence) and the signal is integrated over this interval. The final result is expressed in RLUs (Relative Light Units).

Using chemiluminescence is a great improvement over enzymatic signal generation of classic ELISA format assays. Sensitivity is highly increased and a greater dynamic range can be achieved. Lower molecular weight and steric hindrance of ABEI compared to horseradish peroxidase allow conjugation of more signal generating molecules per tracer molecule. Moreover, generation and recording of signal is completed in a very short time (3 seconds), with a sensible throughput increase.

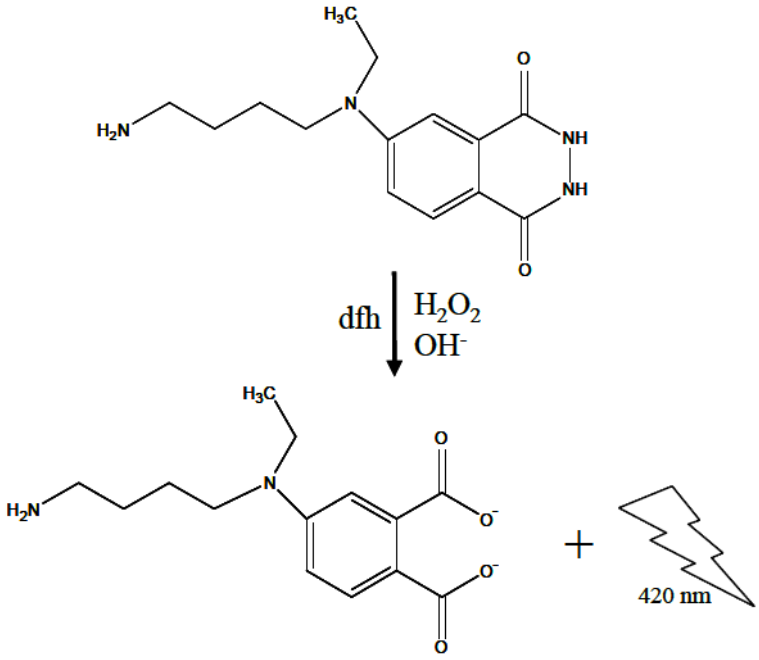

Figure 7. Chemilumiscent reaction of ABEI.

THE LIAISON® EBV VCA IgM AND IgG ASSAYS

The LIAISON® EBV VCA IgM and the LIAISON® EBV VCA IgG assays permit the qualitative determination of specific IgM (acute primary infection) or IgG (past infection) antibodies to Epstein-Barr virus (EBV) viral capsid antigen (VCA) respectively, in human serum or plasma samples. When performed in conjunction with other EBV markers, these assays can be used as aid in the clinical laboratory for the diagnosis of Epstein-Barr Viral Syndrome in patients with signs and symptoms of EBV infection such as infectious mononucleosis. The principal components of these immunoassays are magnetic particles (solid phase) coated with EBV VCA p18 synthetic peptide and mouse monoclonal antibodies to human IgM or IgG linked to the isoluminol-derivative (ABEI) (Figure 8). In the first step (first incubation) EBV IgM or IgG antibodies present in calibrators, samples or controls bind to the solid phase. During the second incubation, the antibody conjugate reacts with EBV IgM or IgG that is already bound to the solid phase. After each incubation, unbound material is removed with a wash cycle. Subsequently, the signal reagents are added and a flash chemiluminescence reaction is thus induced. The light signal, and hence the amount of isoluminol-antibody conjugate, is measured by a photomultiplier as relative light units (RLU) and is indicative of the presence of EBV VCA IgG or IgM antibodies present in calibrators, samples or controls.

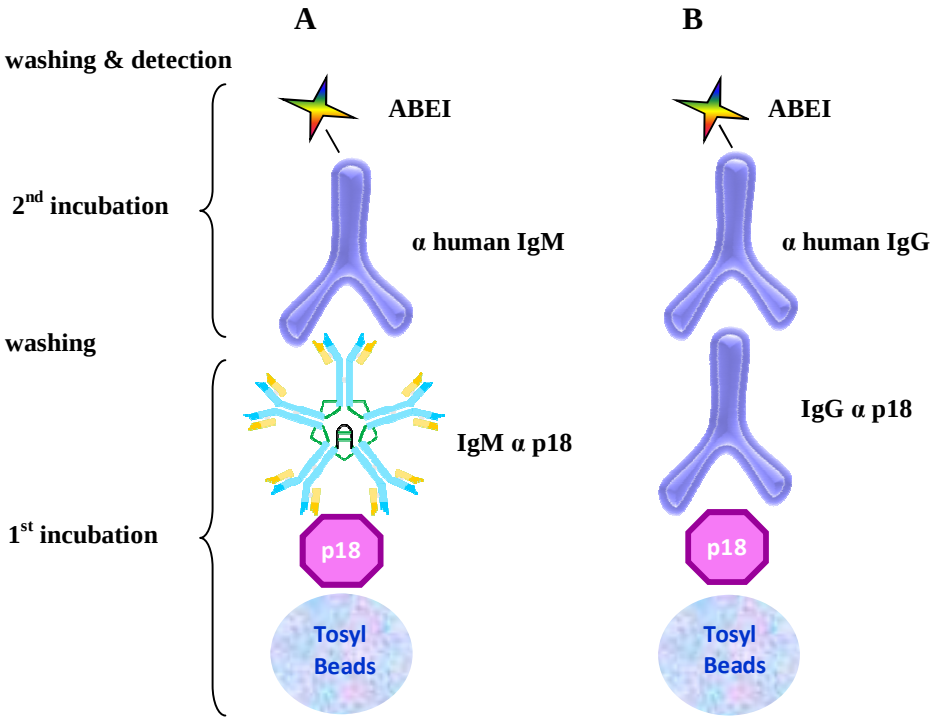

Figure 8. (A) Schematic representation of the Liaison® EBV VCA IgM assay. (B) Schematic representation of the Liaison® EBV VCA IgG assay. On the left side of figure, the various steps of the assay protocol are shown.

INNOVATIVE METHODS FOR PROTEIN PURIFICATION, IMMOBILIZATION ON SOLID PHASE AND CHEMO-SELECTIVE CONJUGATION

ELP-INTEIN SYSTEM: SELF–CLEAVABLE TEMPERATURE RESPONSIVE TAG FOR PROTEIN PURIFICATION

Applications for recombinant proteins in the therapeutic, diagnostic and commodity enzyme fields are rapidly increasing. Fermentation and cell culture methods have been engineered to accommodate this trend by increasing expression efficiency, but bottlenecks in protein purification still remain. Examples of commercially available purification systems include maltose binding protein, glutathione*S*-transferase, biotin carboxyl carrier protein, thioredoxin, and cellulose binding domain. Similarly, vectors for fusion to short peptide tags such as oligohistidine, S-peptide, and the FLAG^{tm} peptide are also available. All these systems typically allow one-step purification of a recombinant protein from cell extract by affinity. However, these traditional affinity-based purification methods are not always easy to scale-up and in any case are cost-prohibitive on an industrial scale. Moreover, one of the major expenses associated with recombinant protein production is the use of chromatography in the isolation and purification stages of a bioprocess. Recently, an economical, non-chromatographic purification method has been developed that relies on the combination of two technological tools, a biochemical (intein auto-cleavage activity) (109) and a physico-chemical one (ELP aggregation ad solvation (110).

INTEINS AND PROTEIN SPLICING

Inteins were identified 20 years ago, when two groups reported an in-frame insertion in the *VMA1* gene, which encodes a vacuolar membrane H^+-ATPase of the yeast *Saccharomyces cerevisiae*, called *Sce*VMA1 (111,112). The N- and C-terminal regions of the deduced sequence were shown to be very similar to the catalytic subunits of vacuolar membrane H^+-ATPases of other organisms, while an internal region of 454 amino acid residues displayed no detectable sequence similarity to any known

ATPase subunits. Instead, this internal sequence exhibits similarity to an *S. cerevisiae* endonuclease encoded by the *HO* gene. It was found to be present in the mRNA, translated with the Vma1 protein, and excised posttranslationally (112). By analogy to pre-mRNA introns and exons, the segments are called *intein* for internal protein sequence, and *extein* for external protein sequence, with upstream exteins termed N-exteins and downstream exteins called C-exteins. The post-translational process that excises the internal region from the precursor protein, with subsequent ligation of the N- and C-exteins, is termed protein splicing (113). The products of the protein splicing process are two stable proteins, the mature protein and the intein (Figure 9). Large-scale genome sequencing approaches have identified inteins in all three domains of life, as well as in phages and viruses. By the end of 2009, the intein registry InBase (114) listed more than 450 inteins in the genomes of Eubacteria, Archaea, and Eukarya.

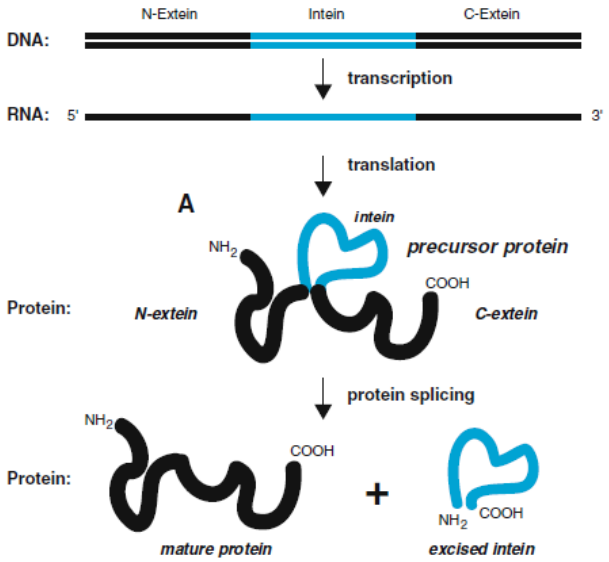

Figure 9. Protein splicing mechanism.

Inteins are classified into two groups, large and minimal (mini) (Figure 10) (115). Large inteins contain a homing endonuclease domain that is absent in mini-inteins. Homing endonucleases are site-specific, double-strand DNA endonucleases that promote the lateral transfer between genomes of their own coding region with flanking sequences, in a recombination-dependent process known as "homing". Usually, homing endonucleases are encoded by an open reading frame within an intron or intein (116). Large inteins are bi-functional proteins, with a protein splicing domain, and a central endonuclease domain. Splicing-efficient mini-inteins have been engineered from large inteins by deleting the central endonuclease domain, demonstrating that the endonuclease domain is not involved in protein splicing (117).

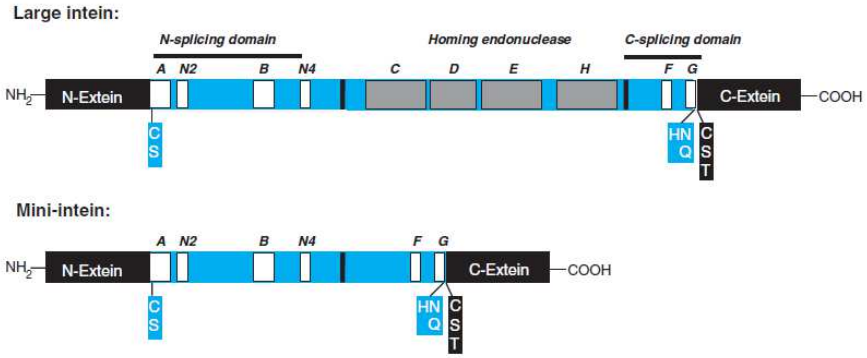

Figure 10. Structure of large and mini-inteins.

All known inteins share a low degree of sequence similarity, with conserved residues only at the N- and C-termini. Most inteins begin with Ser or Cys and end in His-Asn, or in His-Gln. The first amino acid of the C-extein is an invariant Ser, Thr, or Cys, but the residue preceding the intein at the N-extein is not conserved (Figure 11) (114). However, residues proximal to the intein-splicing junction at both the N- and C-terminal exteins were recently found to accelerate or attenuate protein splicing (118).

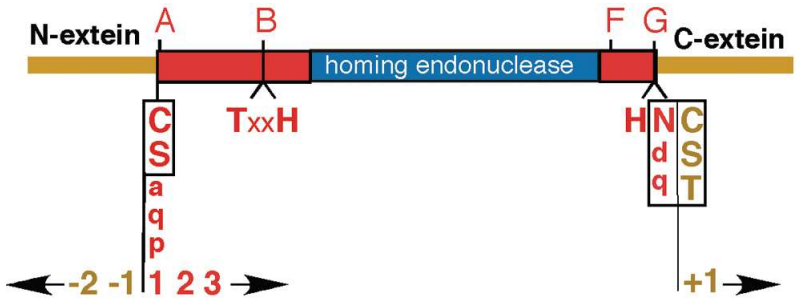

Figure 11. Organization of a splicing precursor with a homing endonuclease domain. Capital letters mean that the corresponding aa occurs frequently in intein or extein sequence, while small letters indicates that the corresponding amino acid is rarely found in that position. Boxes surround nucleophilic residues.

Protein splicing is a rapid process of four nucleophilic attacks, mediated by three of the four conserved splice junction residues (Figure 12) (119).

1. In **step 1**, the splicing process begins with an **N−O shift** if the first intein residue is Ser, **or N−S acyl shift**, if the first intein residue is Cys. This forms a (thio)ester bond at the N-extein/intein junction.
2. In **step 2**, the (thio)ester bond is attacked by the OH- or SH-group of the first residue in the C-extein (Cys, Ser, or Thr). This leads to a **transesterification**, which transfers the N-extein to the side-chain of the first residue of the C-extein.
3. In **step 3**, the **cyclization of the conserved Asn** residue at the C-terminus of the intein releases the intein and links the exteins by a (thio)ester bond.
4. Finally, **step 4** is a rearrangement of the (thio)ester bond to a peptide bond by a spontaneous **S−N or O−N acyl shift**.

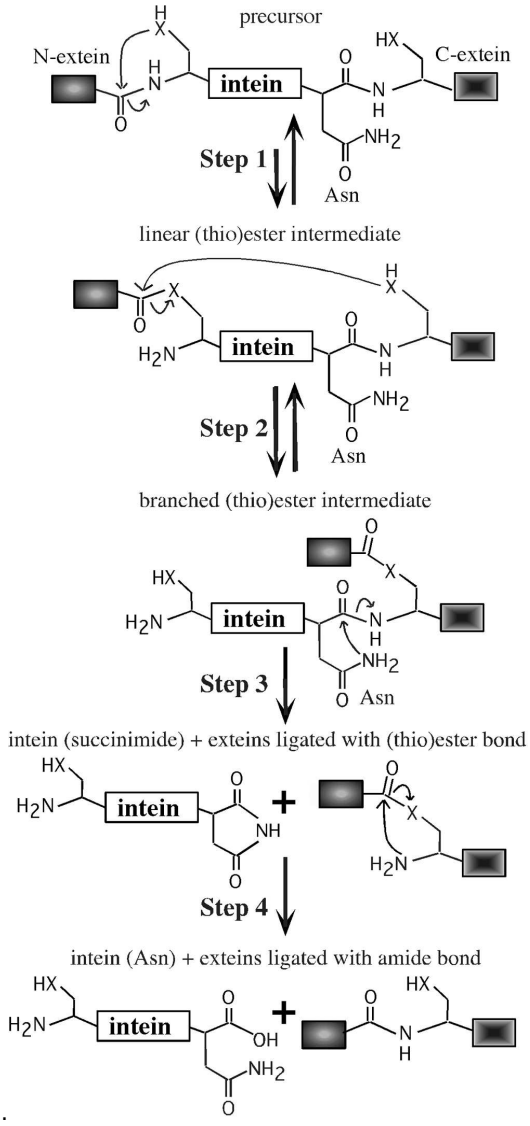

Figure 12. The standard intein-mediated protein splicing mechanism.

The identification of the residues directly participating in the breakage and formation of peptide bonds has paved the way for modulating the protein splicing reaction for various applications. An interesting application in biotechnology field is the site-specific cleavage of inteins. Inteins mutated at one of the two splice-junctions, at the level of the conserved residues, maintains their ability to self cleave at only the non-mutated splice junctions. This property can be exploited during the purification process.

N-terminus cleavage. Mutation of the Asn residue at the intein C-terminus abolishes steps 3 and 4 of the splicing reaction (Asn cyclization and subsequent cleavage of the peptide bond at the C-terminal junction) and results in N-terminal cleavage (Figure 13). Since step 1 still occurs, the (thio)ester bond can spontaneously hydrolyze, separating the N-extein from the intein/C-extein portion; usually, however, N-terminus cleavage requires the addition/presence of a nucleophilic group (typically thiol group or hydroxylamine) able to perform a transesterification reaction on the -1 carbonyl residue.

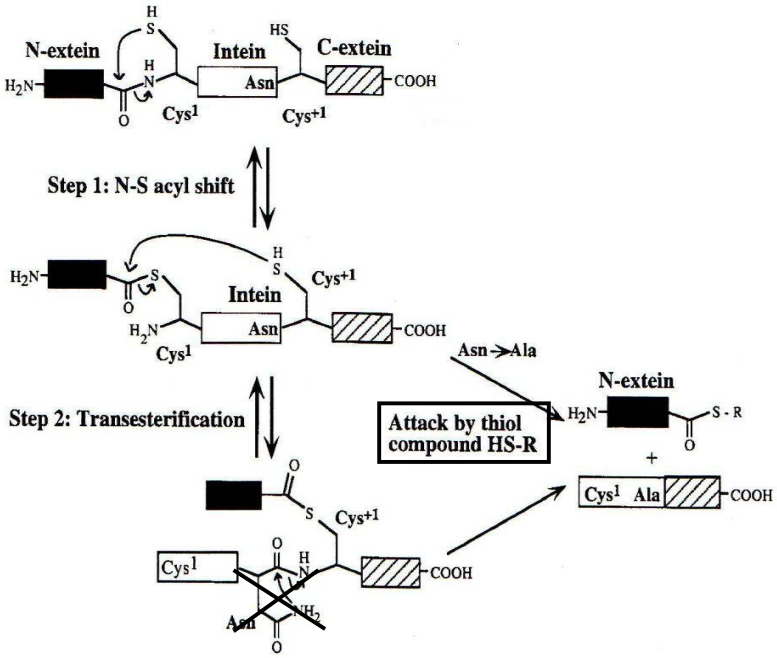

Figure 13. N-terminus cleavage (C-terminus mutation of intein).

C-terminus cleavage. Mutation of the conserved first residue of the intein abolishes steps 1, 2, and 4 of the splicing reaction and leads to C-terminal cleavage (Figure 14). In such a mutated intein, Asn cyclization (step 3) still occurs, to separate the C-extein from the N-extein/intein portion. C–terminal cleavage is usually induced by change in temperature and/or pH conditions.

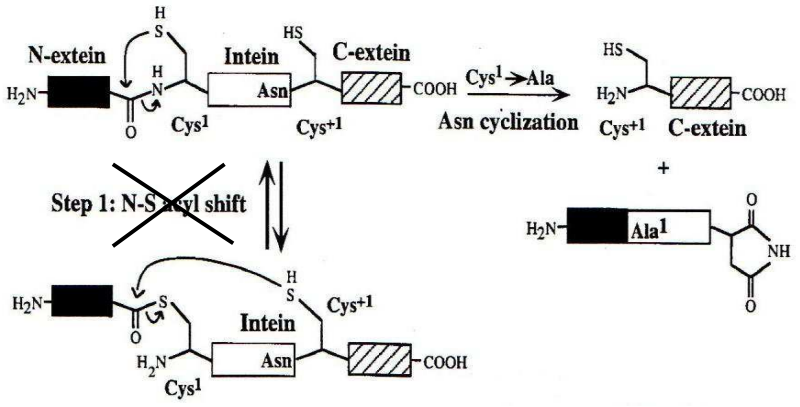

Figure 14. C-terminus cleavage (N-terminus mutation of intein).

Controllable cleavage of modified *cis*-splicing inteins has been adapted for a wide range of useful applications in molecular biology and biotechnology (e.g. IMPACT ™ Kit; a commercial available expression system from New England Biolabs used in proteins purification process).

Most of the inteins used in biotechnology are derived from prokaryotic organisms, or are engineered variants of the *S. cerevisiae* VMA1-intein.
One of the most popular intein employed for the purification of proteins is a 198 aminoacids in-frame insertion in the *gyrA* gene of *Mycobacterium xenopi* (called then *Mxe*GyrA) (120). Compared to other mycobacterial gyrA inteins, *Mxe*GyrA intein has lost more than 200 aminoacids of the central intein domain, which is involved in the homing endonuclease activity, and gained a linker of unrelated residues. This linker is necessary to maintain the splicing activity. The mini-intein *Mxe*GyrA (with the lack of the endonuclease activity, but not of the splicing capability) has then a

primary structure made of 198 amino acids and a molecular weight of 21.3 kDa. The C-terminal mutated version of this intein (*Mxe*GyrA N198A; in which the C-terminal asparagine residue was replaced with an alanine residue) able to perform a thiol-induced cleavage at its N-terminus, is currently exploited in many commercial systems of purification (e.g. IMPACT ™ Kit). As illustrated in Figure 15, in this specific case the target protein is fused at its C-terminus to a self-cleavable intein tag that contains, in addition to the C-terminus mutated intein sequence, a domain necessary for the purification of the target protein (for example in the commercial system IMPACT ™ Kit is used the chitin binding domain for affinity purification of the fusion precursor on a chitin column). Induction of intein self-cleavage activity, using thiol reagents such as dithiothreitol (DTT), releases the target protein from the intein tag (Figure 15).
Therefore, these innovative protein purification systems exploit the site-specific inducible self-cleavage activity of inteins to separate in a simple way the target protein from the affinity tag during the purification process.

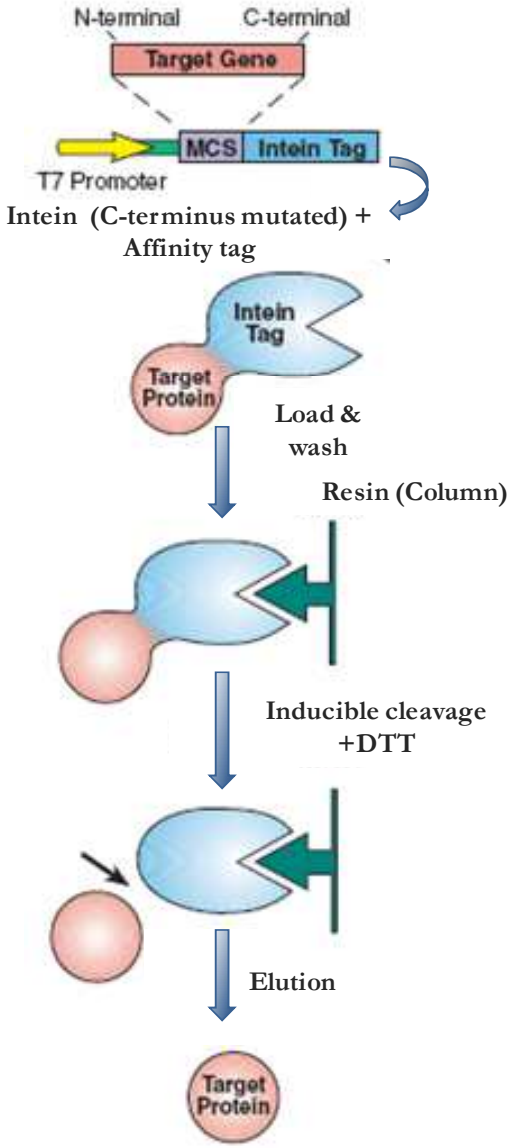

Figure 15. Schematic illustration of an expression/purification system that exploits C-terminus mutation of intein.

Intein-mediated Protein Ligation (IPL) or Expressed Protein Ligation (EPL) technique. As described above, inteins are valuable tools in a wide range of biotechnological applications. Inteins have been used for segmental labeling of proteins for NMR analysis, cyclization of proteins, controlled expression of toxic proteins, conjugation of quantum dots to proteins, and incorporation of unnatural amino acids (from 121 to 125). In basic research studies, they have been used to monitor in vivo protein-protein interactions, or specifically translocate proteins into cellular organelles (126,127).

However, one of the principal and most important applications of intein remains the technique known as intein-mediated protein ligation (IPL) or expressed protein ligation (EPL), that provides the ligation of peptides and proteins using the natural splicing activity of inteins (128,129). The use of this innovative method permits the site-specific modification of protein structure and function by introducing specific chemical functional groups, leading to new biochemical insights in biological systems and creating new tools for biomedical and diagnostic research. Before the use of EPL technique, numerous protein site-specific ligation and modification methods have been explored. Solid-Phase Peptide Synthesis (SPPS) provides the possibility of introducing non-nonical amino acids into peptides but is restricted to peptides of up to 60 amino acids in length. By using expression systems in bacteria or yeast, the recombinant generation of larger peptides and proteins has become possible (130-131). The size of the constructs is not restricted but the insertion of non-canonical amino acids is difficult (132,133).The limitation of peptide size in SPPS was circumvented by several approaches developed for the synthesis of proteins by segment condensation (134). Dawson et al. (135) introduced a simple and elegant method called Native Chemical Ligation (NCL) for the synthesis of peptides by condensation of their unprotected segments. The coupling of synthetic peptide-thioesters with peptides carrying an N-terminal Cys leads to an amide-bond at the ligation site. The reaction proceeds in aqueous conditions at neutral pH. The first step of this process is the chemoselective transthioesterification of an unprotected peptide Cα-thioester with an N-terminal Cys of a second peptide. The so-formed thioester spontaneously undergoes an S-N-acyl transfer to form a native peptide bond and the resulting peptide product is

obtained in the final disposition (Figure 16). Internal Cys residues within both peptide segments are permitted because the initial transthioesterification step is reversible and no side products are obtained, thus, no protecting groups are necessary. To prevent the thiol of the N-terminal Cys from oxidation, and thus forming an unreactive disulfide linked dimer, it is necessary to add thiols or other reducing reagents like tris(2-carboxyethyl)phosphine (TCEP) (136) to the reaction mixture. Furthermore, the addition of an excess of thiols not only keeps the thiol-functions reduced but also increases the reactivity by forming new thioesters through transthioesterification (137).

This approach has proven to be useful for the synthesis of smaller proteins up to 120 amino acids in length; larger proteins cannot be obtained easily in one ligation step. Multistep NCL of different peptide-segments, however, can lead to larger proteins. However, native chemical ligation has proven very useful for the total synthesis of small proteins and protein domains, but has not been extended to the synthesis of proteins beyond ~ 15 kDa.

A useful application of NCL is Solid-Phase Chemical Ligation (SPCL) (138). In this approach, one of the two segments is bound to a polymer, while the other is applied in aqueous solution and can be used in excess. A simple washing step completely removes the solubilized peptides and the assembled full length protein can be cleaved from the resin. In addition to Cys, related amino acids, including selenoCys and selenohomoCys, have been reported to work in a similar manner.

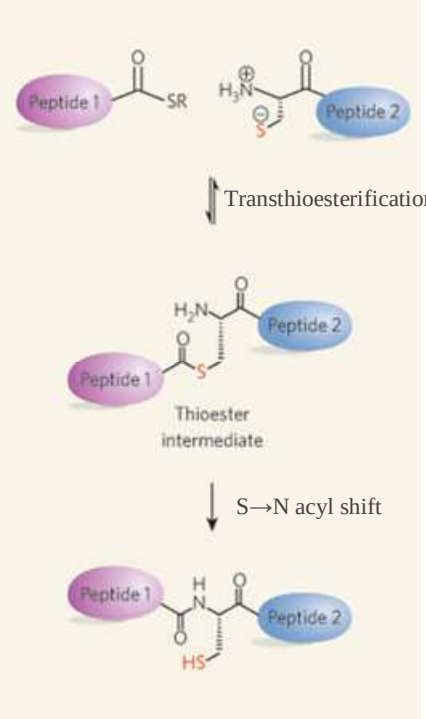

Figure 16. Native Chemical Ligation (NCL) method.

Expressed protein ligation (EPL) (139-141), also named intein-mediated protein ligation, is an extension of the NCL method. A recombinant Cα-thioester protein reacts with a chemically synthesized or expressed peptide/protein possessing an N-terminal Cys under the conditions of NCL to form a native peptide bond (Figure 17). This ligation method combines the advantages of molecular engineering and chemical peptide synthesis in many cases and allows site-specific introduction of unnatural amino acids and chemical or biophysical tags into large proteins.

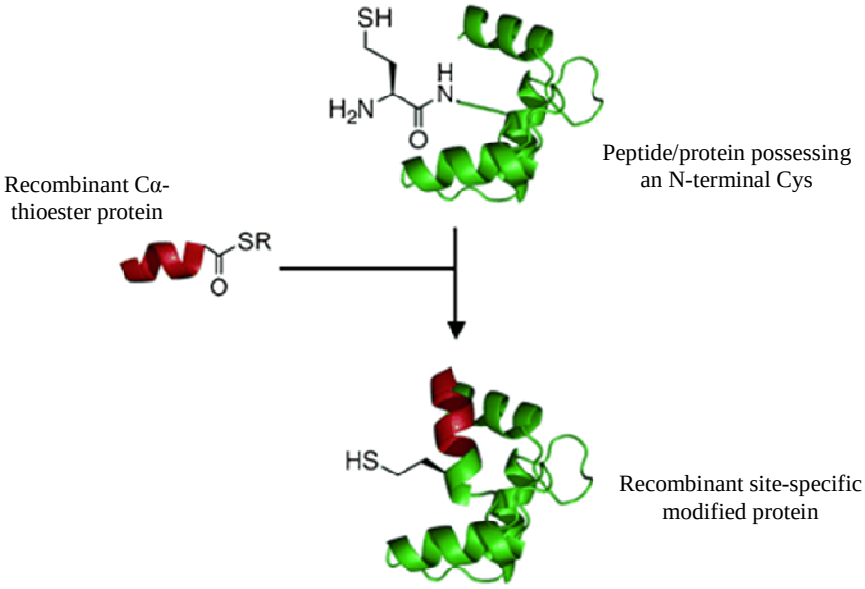

Figure 17. Expressed Protein Ligation (EPL) method.

As mentioned above, peptide ligation via NCL requires the specific generation of C-terminal thioester-tagged peptide allowing ligation with a second peptide containing an N-terminal Cys residue. The efficient and potent synthesis of Cα-thioesters of bacterially expressed proteins was found through studies of the N-terminal cleavage mechanism of inteins. As described above in details, this last is obtained using a C-terminal modified intein (substitution of the C-terminal asparagine with a residue of alanine). Incubation of this modified intein with thiols, like dithiothreitol (DTT), releases the corresponding free C-terminal thioester tagged extein from the N-terminal splicing junction (Figure 18). For the thiolysis of the intein fusion proteins, a broad range of thiols have been investigated. The choice of a certain thiol depends on the accessibility of the catalytic pocket of the intein/extein splicing domain and the properties of the target protein of interest. In general, the thiols should be small, nucleophilic molecules that can enter the catalytic pocket to attack the thioester bond connecting the extein and the intein. For further

application of protein thioesters in EPL two things have to be considered to be dependent on the synthesis strategy. On one hand, the protein thioester should be stable to hydrolysis in order to be isolated. On the other hand, the thioester should also be reactive enough in EPL. Simple alkyl thioesters are quite stable to hydrolysis but not very reactive. Mixtures of alkylthiols and thiophenol or 2-mercaptoethansulfonic acid (MESNA) (141) improved the reactivity.
Expressed protein ligation has proven to be a powerful method to engineer the molecules in a site-specific way; indeed this technique is very simple, involving a single chemical step, and effectively unites the fields of synthetic peptide chemistry and recombinant protein biotechnology.

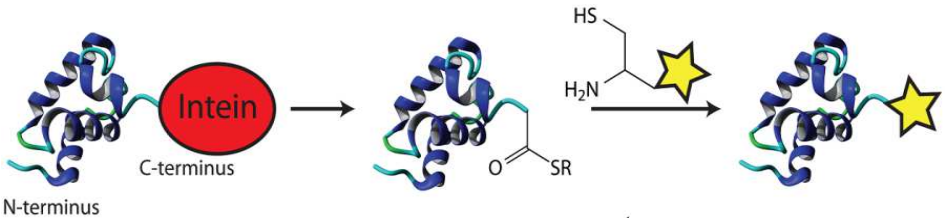

Figure 18. Intein-mediated Protein Ligation (IPL) method. The role of intein in the formation of Cα-thioester protein necessary in the expressed protein ligation mechanism.

ELASTIN-LIKE POLYPEPTIDES (ELPS)

Elastin is a structural extracellular matrix protein that is present in all vertebrate connective tissue. Its functions include the provision of elasticity and resilience to tissues, such as large elastic blood vessels (aorta), elastic ligaments, lung and skin, which are subjected to repetitive and reversible deformation (142,143). The soluble precursor of elastin, tropoelastin, which is deposited into the extracellular space, is highly cross-linked through the action of lysyl oxidase. This is actually the property that confers the prominent physical features of the natural elastin protein (144). The sequence of tropoelastin is characterized by two major domains: the first is hydrophilic and contains many cross-linked Lys and Ala residues, whereas the second is hydrophobic and rich in nonpolar residues, in particular Val, Pro, Ala and Gly, characteristically present as tetra-, penta- and hexa-repeats, such as Val-Pro-Gly-Gly, Val-Pro-Gly-Val-Gly and Ala-Pro-Gly-Val-Gly-Val. These repeats are responsible principally for the elasticity of the protein.

ELPs (Elastin-Like Polypeptides) are artificial biopolymers comprised of the pentapeptide repeat motif Val-Pro-Gly-Xaa-Gly (VPGXG; where the guest residue Xaa can be any amino acid, except Pro), that is derived from the hydrophobic domain of tropoelastin. The principal characteristic of ELPs is that they are thermally responsive polypeptides that undergo an inverse temperature phase transition. The temperature-dependent, reversible self-aggregation (termed inverse phase transition) of ELPs occurs within a 2–3 °C range and can be monitored spectrophotometrically by measuring the turbidity of the protein solution (optical density at 600 nanometer of wavelength). Below the transition temperature (Tt), ELPs are monomeric and soluble, whereas, at temperatures higher than Tt, they aggregate and become insoluble (145-146) (Figure 19). One possible explanation for this process is the development of closer associations between single β-strands of ELP and the subsequent formation of interstrand β-sheet structures that mediate close association or aggregation of different ELP chains (147).

The ELP aggregation is a reversible process, so the polypeptide is completely re-solubilised in buffer when the solution temperature is reduced below its transition temperature, which is in turn determined and controlled by a combination of several factors such as buffer

composition, salt concentration, ELP concentration, chain length, the degree of ionization of any functional side chains, the guest residue Xaa and the polarity arrangement along the molecule (148-151). Thus, for example, Tt is decreased as the ELP chain length or the salt concentration or ELP concentration is raised.

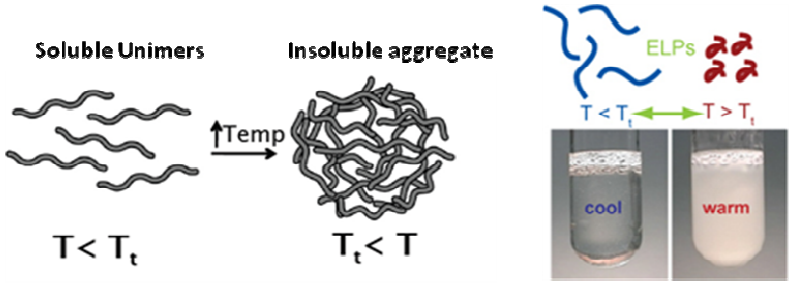

Figure 19. Representation of ELPs inverse phase transition in response to thermal changes.

Inverse Transition cycling. This unique property of ELPs make them attractive for a wide range of applications in biotechnology and biomedicine, for example, non-chromatographic protein purification by a method named inverse transition cycling (ITC). This method is based on the principle that ELP fusion proteins, which are produced by joining the gene encoding a protein of interest with an ELP gene segment, can also undergo a reversible phase transition similar to that of the free ELPs. Thus, the environmental responsiveness of ELPs can be easily imparted by genetic fusion to a protein of interest. Figure 20 shows a schematic ITC purification. Initially, the ELP fusion protein is below its Tt and is soluble. The inverse temperature transition is triggered by increasing the solution temperature to above the Tt or by adding salt to depress isothermally the Tt to below the solution temperature, or by a combination of both. Upon triggering the transition, the fusion protein aggregates and can be separated from other molecules present in solution by centrifugation or filtration. The remaining soluble molecules are removed by decanting or pipetting off the supernatant. The purified fusion protein is then resolubilized at a temperature below its Tt in the buffer and volume of choice. The resolubilized fusion protein is often

centrifuged (or filtered) a final time at a temperature below its Tt to remove any remaining insoluble matter that may have been trapped in the pellet along with the aggregated ELP fusion protein. Additional rounds of ITC can be undertaken until the fusion protein is purified to the desired degree.

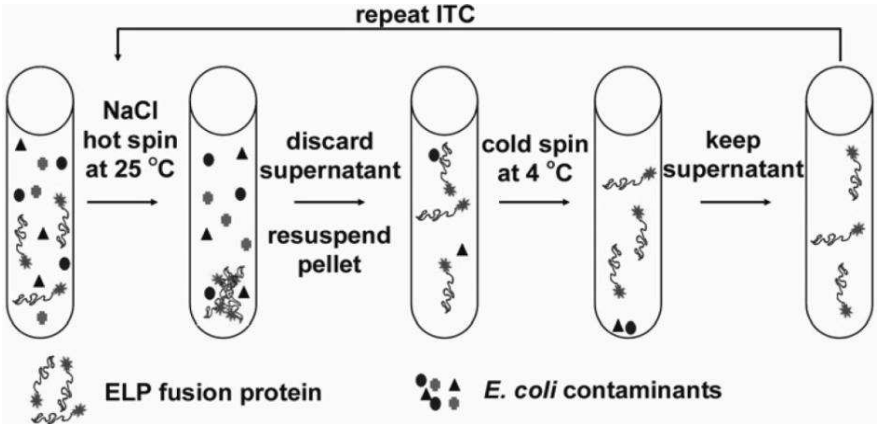

Figure 20. Schematic representation of protein purification by inverse transition cycling (ITC).

ITC protein purification that provides the use of an ELP tag offers several advantages over conventional chromatography. ITC is technically simple, fast, economical, and requires no specialized equipment or reagents. Separations can be completed in minutes using standard laboratory centrifuges and NaCl solution. For these reasons it is a very easy to scale-up process. Because it avoids the expense associated with traditional chromatographic separations, ITC is also likely to be useful for the purification of single proteins at the gram-to-kilogram scale in industrial bioprocessing. Furthermore for microliter-scale expression and purification, ITC can be employed in parallel for high-throughput applications.

At the end of the ITC process, in order to obtain the purified protein of interest, the ELP tag must be cleaved from the fusion protein. Traditionally, the strategy was the insertion between the fusion protein and the ELP genes of a DNA sequence encoding for an amino acid

sequence recognized by a protease. The addition of protease after the ITC process permits the cleavage of the target protein from the ELP tag. It is however necessary to consider that the use of protease in the purification process involves numerous problems, including (I) additional relevant costs, (II) the need to perform a further chromatographic step in order to remove and to separate the proteases from the target protein and finally, (III) the possibility of undesired proteolytic cuts on the protein of interest due to the low specificity of proteases themselves.

ELP-INTEIN SYSTEM

Recently, the study of inteins and in particular the investigation of site-specific cleavage process of these particular enzymes has allowed to exploit this system to separate the target proteins from related tags during the purification process, and then to replace the use of protease overcoming the many drawbacks associated with their use.
Also in the case of ELP-fusion construct, the insertion of an intein at the right position gives the opportunity to isolate the target protein from the ELP tag avoiding the use of proteases. The combination of these two technological tools, the intein auto-cleavage activity (biochemical tool) and ELP aggregation ad solvation properties (physico-chemical tool), has enabled the development of a highly innovative and efficient purification method. Figure 21 schematically illustrates an example of purification process based on the use of the ELP-intein system. Starting from a construct characterized by the fusion to the C-terminus of the target protein with an intein-ELP tag, where the intein is a C-terminal mutated version (e.g. *Mxe*GrA N198A), a ITC process is carried out as first step to purify the ELP-fusion protein of interest from the other contaminating proteins present in the sample. At the end of the ITC process, the addition of a thiol reagent, such as dithiothreitol (DTT), permits the induction of N-terminal intein self-cleavage activity and the consequent release of target protein from the intein-ELP tag.
This new non-chromatographic method, based on the combination of ITC purification process (ELPs tag) with self-cleaving properties of inteins, results in the use of a self–cleavable temperature responsive tag and offers a viable option for protein purification.

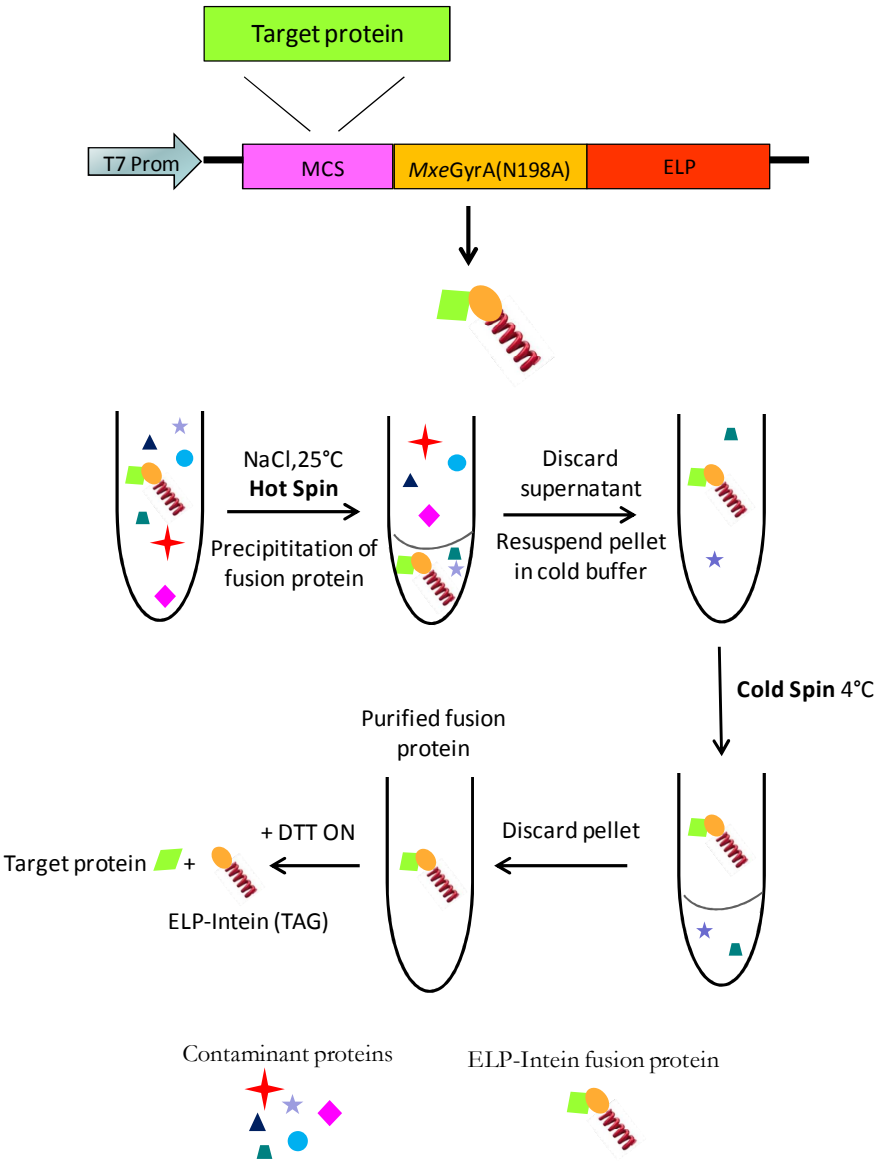

Figure 21. Schematic representation of protein purification by ELP-Intein system.

SITE-SPECIFIC MODIFICATION OF RECOMBINANT PROTEINS BY INCORPORATION OF UNNATURAL AMINO ACIDS IN *E. coli* CELLS

Although proteins are involved in almost every biological process, they are biosynthesized from the same 20 common amino acids and contain a limited set of functional groups (nitrogen bases, carboxylic acids, amides, alcohols, and thiols). The ability to genetically incorporate into proteins amino acids containing "unnatural" functional groups would provide powerful tools for modifying protein and controlling its function. Genetic code expansion (152) is one of the most powerful approaches to generate protein-containing unnatural functional groups because the method is site specific and, in principle, can produce quantities of modified protein sufficient for biochemical and biophysical analyses. Moreover, this method has the advantage to produce modified proteins in a variety of host cells (*E. coli*; *S. Cerevisiae; P. pastoris*; mammalian cells; etc.). The technique is based on the use of an engineered tRNA/aminoacyl-tRNA synthetase (aaRS) pair to insert the Unnatural Amino Acid (UAA) of interest in response to a nonsense or frameshift codon. During the translation process, the ribosome translates mRNA into a polypeptide by complementing triplet-codons with matching aminoacylated tRNAs. Three of the 64 different triplet-codons do not code for any amino acids, but cause recruitment of a release factor resulting in disengagement of the ribosome and termination of the synthesis of the growing polypeptide. These codons are called; ochre (TAA), opal (TGA), and amber (TAG). Of the three stop codons, the amber codon is the least used in *E. coli* (∼7%) and rarely terminates essential genes (153,154). As mentioned above, the mRNA triplet UAG of the amber codon, or any other stop codon normally causes the termination of translation by recruitment of one of two release factors, RF1, and RF2 (Figure 22A). Certain species of methanogenic bacteria do not use the amber codon as a stop codon, but instead use it to introduce an amino acid at a stop codon. For example *Methanococcus jannaschii* introduces a tyrosine at a UAG codon (155). These UAG-tRNAs have been used with great success to introduce

Unnatural Amino Acids (UAAs) into proteins in *E. coli* expression systems. In order to achieve this, a series of essential steps are required. The first of these is the evolution of an orthogonal tRNA and its related aminoacyl-tRNA synthetase (aaRS) so that it does not recognize a natural amino acid, but instead recognizes a UAA of interest (156). The evolved aaRS needs to be orthogonal to the tRNA loading machinery of the expression host, as otherwise cross-loading of natural amino acids onto the $tRNA^{CUA}$ can occur (Figure 22B). The first reported aaRS and iso-tRNA pair that was orthogonal to the *E. coli* expression machinery was derived from the already mentioned archaea *Methanococcus jannaschii*, where it normally encodes for a tyrosine residue (155). The $tRNA^{CUA}$ pair could be readily mutated to accept an unnatural amino acid, because the aaRS has minimal interaction with the anticodon of its $tRNA^{CUA}$. The minimum anticodon recognition of the aaRS to its tRNA makes it possible to mutate the aaRS amino acid binding pocket from tyrosine to an UAA with little loss of affinity and aminoacylation efficiency of the aaRS for the tRNA (157). Furthermore, the lack of an editing mechanism capable of deacylating the UAA and high expression levels are the features that have made this pair so successful for *E. coli* (158). When the crystal structure of an evolved *M. jannaschii* tyrosyl-RS, the *p*-cyanophenylalanine-specific aaRS, was solved, it has been used for a study that uses molecular modeling and docking to design optimal mutations for a given UAA (159). The list of UAAs incorporated into proteins is rapidly growing. The aim is to use the UAAs for chemical couplings, in order to modify the target protein in a chemo-selective and site-specific way, preserving the fold, and function of the proteins (Figure 22C).

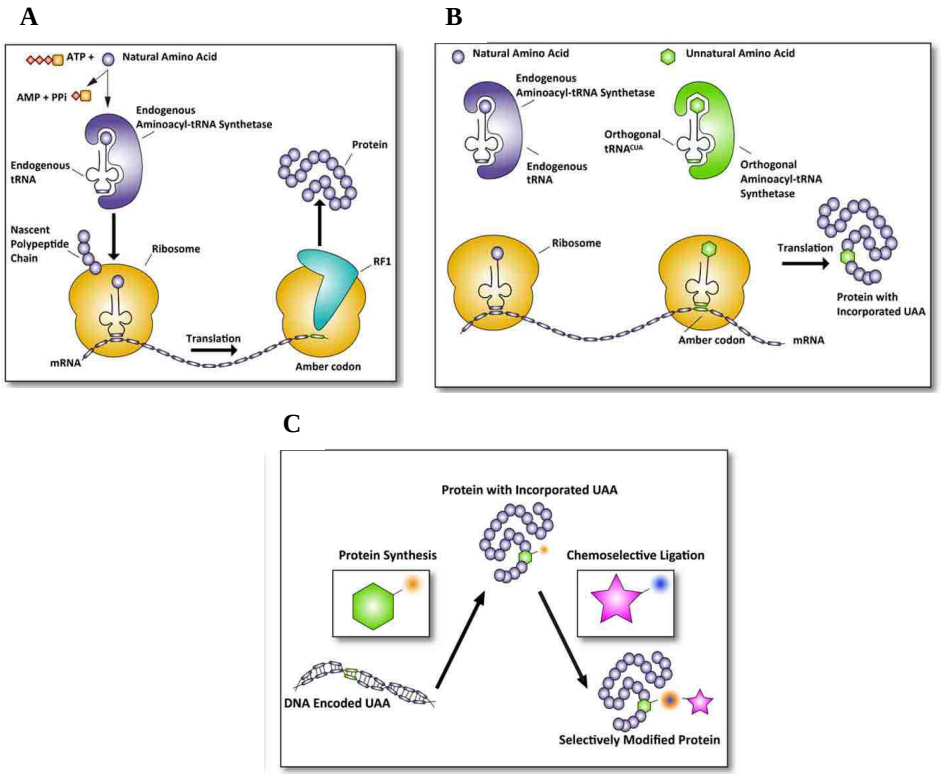

Figure 22. Incorporation of UAAs into proteins in *E. coli* cells.
(A) In normal translation, the recruitment of release factors is required to terminate the process. In the presence of an amber codon (TAG) in mRNA sequence, release factor 1 (RF1) is recruited and this determines the stop of translation and the release the newly synthesized protein.
(B) In amber codon suppression technique to incorporate unnatural amino acids (UAA), the amber codon is used as a coding codon in translation. The complementary amber $tRNA^{CUA}$ is aminoacylated by an orthogonal aminoacyl-tRNA synthetase (aaRS) that is specifically designed to accept only unnatural amino acids. The result is a protein with an UAA incorporated.
(C) The protein containing UAA can be selectively modified via chemoselective chemical modification.

In the classical method to express a protein of interest containing a desired UAA at a specific site in *E. coli* cells, an expression plasmid encoding its corresponding nonsense or frameshift mutant is co-transformed with a suppressor plasmid that harbors the tRNA/aaRS pair, specific for the desired UAA. An early version of this suppressor plasmid employed an *lpp* promoter and a *glnS* promoter to express the tRNA and aaRS, respectively (155). To improve the suppression efficiency of this system, a second generation of suppressor plasmid pSup (160) was developed with an enhanced glnS′ promoter to increase the level of synthetase expression and six copies of the tRNA expression cassette under the proK promoter. A variation of this plasmid, pSUPAR (161) that harbors an additional araBAD-driven aaRS expression cassette and three copies of the tRNA driven by proK was also generated. Further optimization of this system is pEVOL plasmid (162) which harbors one copy of the tRNA expression cassette under the efficient proK promoter and two copies of the aaRS under araBAD and glnS promoters (Figure 23). This latter vector results in a substantial improvement in suppression efficiency, approaching expression levels of the wild-type protein (without nonsense suppression), when used in conjunction with the efficient tRNA/aaRS pairs derived from the *M. jannaschii tyrosyl* (MjTyr) system.

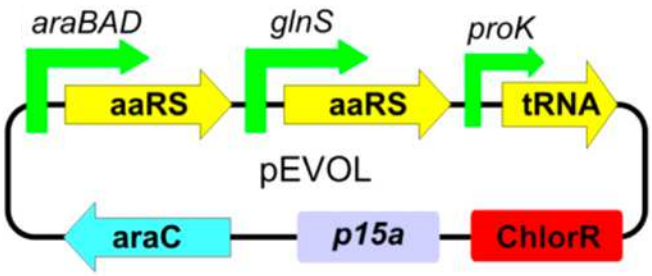

Figure 23. pEVOL vector map.

In addition to the incorporation of a single UAA, the availability of mutually orthogonal tRNA/aaRS pairs, suppressing distinct codons in *E. coli*, has made possible the site specific incorporation of multiple, different UAAs into the same protein (163). To express proteins containing multiple, distinct UAAs, the relevant suppressor tRNA/aaRS pairs must be coexpressed with the target gene containing appropriately positioned nonsense and/or frameshift codons specifying the sites for UAA insertion. The suppressor plasmid designed for this type of process is named pUltra; it is characterized by the presence of two different tRNA/aaRS pairs allowing the generation of a single plasmid capable of dual suppression (Figure 24).

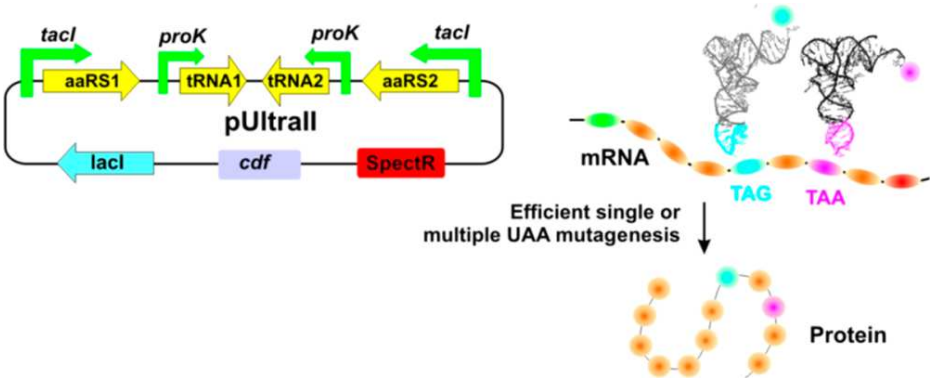

Figure 24. pUltraII vector map of used for multiple-UAA mutagenesis in *E.coli.*

The ability to incorporate unnatural amino acids directly into proteins *in vivo* offers considerable advantages over both chemical and *in vitro* biosynthetic strategies, including the site-specific and homogeneous modification of recombinant proteins under physiological conditions, with the possibility to select a specific position (amino acid) for the incorporation of unnatural specific functional group and then the possibility to chemoselective modify the protein preserving its fold, function and reactivity.

PROTEIN IMMOBILIZATION ON SOLID PHASE THROUGH THE USE OF LEUCINE ZIPPER (OR "VELCRO") PEPTIDES

Protein immobilization is a critical step in the surface-based analysis of protein-protein (or antigen-antibody) interactions, including immunodiagnostic assays, microarray-based proteome analysis, drug screening and others. Covalent attachment methods using functional side groups of protein (amine, carboxyl, thiol, etc) have been widely used for protein immobilization to solve the problem of weak attachment in the traditional physical adsorption methods. Furthermore, various indirect attachment methods using chemical cross-linkers or terminal fusion tags through NHS-biotin, biotin ligase, His-tag, or oligonucleotide-mediated immobilization have been developed (164). Most of these methods, however, still provide limited orientation and applications to antibodies, and they have some problems of a loss of activity and low binding efficiency mainly due to uncontrolled immobilization and random modification. Hence, despite many advances, immobilization of proteins in a controlled and oriented manner still remains a challenge.

Recently, a new and innovative method for the antigen immobilization on solid phase was generated. It is based on the use of Leucine Zipper (LZ) ("velcro") peptides (165). Velcro peptides (VP) are synthetic peptides derived from the sequence of human transcription factor domain B-ZIP; they contain natural leucine zipper domains that allow tight and stable association between them through coiled coil formation. The coiled coil is a common structural motif, formed by approximately 3 ± 5% of all amino acids in proteins (166). Typically, it consists of two to five helices wrapped around each other into a left-handed helix to form a supercoil. Whereas regular helices go through 3.6 residues for each complete turn of the helix, the distortion imposed upon each helix within a left-handed coiled coil lowers this value to around 3.5. Thus a heptad repeat occurs every two turns of the helix (167). The coiled coil was first described by Crick in 1953. The most commonly observed type of coiled coil is left-handed; here each helix has a periodicity of seven (a heptad repeat) (168). This repeat is usually denoted $(a\text{-}b\text{-}c\text{-}d\text{-}e\text{-}f\text{-}g)_n$ in one helix, and $(a'\text{-}b'\text{-}c'\text{-}d'\text{-}e'\text{-}f'\text{-}g')_n$ in the other (Figure 25). In this model, a and d are typically non-polar core residues (e.g. leucine, valine, or isoleucine), thus stabilizing helix dimerization through hydrophobic and van der Waals

interactions. Residues e and g must be charged (e.g. glutamate or lysine) in order to form interhelical electrostatic interactions. Such interaction patterns should be of the opposite charge in heterodimers to stabilize their interaction, and of the same charge in homodimers to destabilize them. The remaining three positions (b, c, and f) must all be hydrophilic, as these will form helical surfaces that are exposed to the solvent.

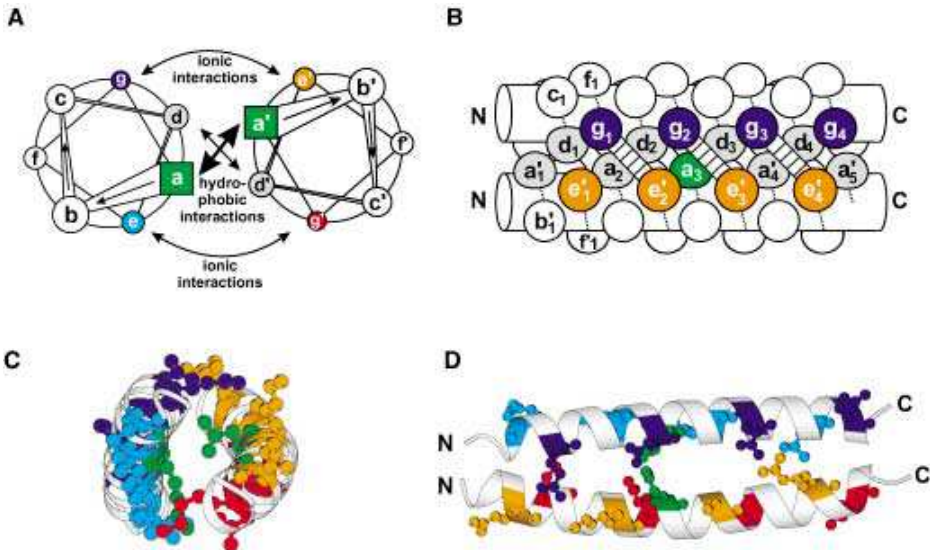

Figure 25. A parallel dimeric coiled coil in a schematic representation (A and B) and as ribbon plot of the X-ray structure of the leucine zipper of GCN4 (C and D) (169). Selected side chains are shown as balls and sticks. The helical wheel diagram in (A) and the plot in (C) look down the axis of the helices from N-terminus to C-terminus. Panel (B) and (C) provide a side view.

This new method of proteins immobilization on solid phase is based on the creation of two different constructs. The first consists of an artificial polypeptide scaffold that can be used to immobilize recombinant proteins on substrates (Figure 26A). The polypeptide contains separate surface anchor and protein capture domains; in particular the surface anchor is represented by an elastin mimetic domain or elastin like polipeptide

(ELP) sequence (described above in details) named ELF, for the presence of a photoreactive unnatural amino acid, *para*-azidophenylalanine, within the sequence. This moiety can be used to generate covalent linkages to substrates (glass slides) upon UV irradiation. ELF consists of five repeats of 25 amino acids with the sequence $(VPGVG)_2VPG\boldsymbol{F}G\text{-}(VPGVG)_2$. Because of its hydrophobic character, ELF provides strong adhesion to hydrophobic surfaces. The protein capture domain of the first construct is a synthetic peptide, called ZE (the acidic partner of velcro peptides), that functions through coiled coil association of a designed parallel heterodimeric leucine zipper pair; the corresponding partner is called ZR (the basic partner of velcro peptides) and it is fused to target proteins as an affinity tag in the second construct. The idea of this system is based on the interaction of the two velcro peptides, through the formation of coiled coil structures, to enable the indirect immobilization of the target protein on solid phase, in a oriented and stable way (Figure 26B). To reduce possible steric hindrance, in both constructs, the ZE velcro peptide and the ELF scaffold for the first construct, and the ZR velcro peptide and the target protein for the second construct, are linked by a flexible spacer. These two structures (velcro peptides) are based on the sequences developed by Vinson et al. (170) with minor modifications (Figure 26). The acidic partner ZE is so named for the presence of several glutamic acid residues (E) in its sequence, while the name of the basic partner ZR derives from the fact that it contains several residues of arginine (R). The presence of opposite charges on the two velcro peptides allows to stabilize their association through the formation of electrostatic interactions in the coiled coil formation. It has been demonstrated that this leucine zipper system has a heterodimerization affinity of 10^{-15} M, while homodimerization affinities are in the micromolar range.

A

B

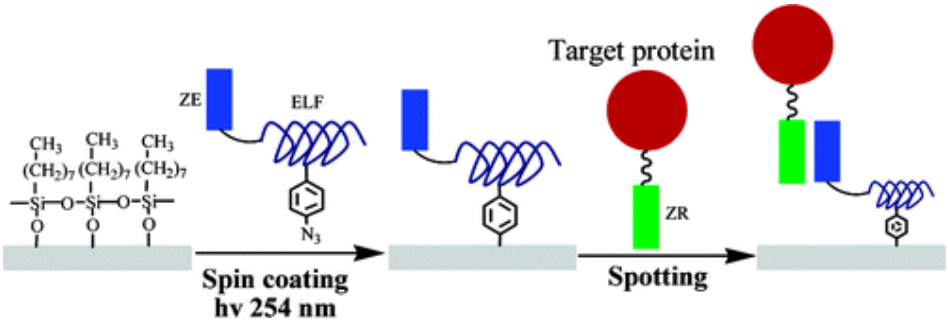

Figure 26. (A) Design of artificial polypeptide scaffold with the surface anchor (ELF) and protein capture domain (ZE) and related amino acid sequence. Sequence of the two "velcro" peptides.
(B) Scheme of surface functionalization and coiled coil mediated immobilization of proteins.

Due to their intrinsic characteristics, the use of the velcro peptides as indirect immobilization method of proteins on solid phase can make many benefits including: (i) specific, oriented immobilization of target protein, (ii) protein structure unaltered and minimized shielding effects (small size of VP), (iii) low background (VP not immunogenic; no known VP circulating in the blood), (iiii) affinities comparable to streptavidin/biotin system (10^{-15} M).

THE USE OF CLICK CHEMISTRY FOR BIOCONJUGATION REACTIONS

The term “click chemistry” defines a powerful set of chemical reactions that are rapid, selective, and high-yielding. A good click reaction satisfies many criteria: it should be high yielding, produce minimal byproducts, and be stereospecific, when applicable. Further, it should involve readily available starting materials, take place in mild conditions, and allow simple isolation of products. In practice, click reactions tend to have large negative free energies and hence involve carbon-heteroatom bond forming processes. Thus, unlike many conventional synthetic reactions, the power of click chemistry lies in its simplicity and ease of use. For these reasons, the click reactions have been applied in different areas, including drug discovery (171), materials science (172), and chemical biology (173). The success of this type of reaction is primarily related to their application in chemical biology field; in fact click chemistry has been used in the selective labeling of biomolecules within living systems, allowing proteins, glycans, and other important biomolecules to be monitored in a physiologically relevant environment rather than in an *in vitro* setting. There has been a recent explosion of interest in the selective covalent labeling of biomolecules in cells and living organisms. Given the functional complexity of biological systems, the major challenge is a chemical one: the labeling reaction must be “bioorthogonal”, meaning that the two components are non-interacting (orthogonal) to the functionality presented in biological systems. Further, the reaction must proceed in water at neutral or near-neutral pH at temperatures ranging from 25 to 37°C without any cytotoxic reagents or byproducts. The concept of click chemistry provides an ideal platform from which to develop bioorthogonal reactions in living systems. Few chemical reactions satisfy both the bioorthogonal and click requirements. Most bioconjugation reactions, such as thiol-maleimide and amine-carboxylic acid couplings, cannot be used for selective biomolecule labeling in complex biological systems because of competing nucleophiles and electrophiles on proteins, nucleic acids, and other biopolymers that would interfere with the reaction. Historically, the first “bioorthogonal click reactions” involved the condensation of ketones or aldehydes with α-

amines such as hydrazides or aminooxy reagents (174). A major breakthrough occurred in 2000, with the introduction of the azide as a functional handle for bioorthogonal chemical reactions (175). Unlike the ketone, the azide is truly bioorthogonal, in fact does not interact with the functional groups presented in biological systems. Despite its kinetic stability, the azide is thermodynamically a high-energy species prone to specific reactivity both as a soft electrophile and as a 1,3-dipole (176). In the subsequent years, most studies in the field have focused on the development of chemical reactions for azide ligation and their application to selective biomolecule labeling *in vitro* and *in vivo*.

Staudinger Ligation. In 2000, it was reported a modification of the classical Staudinger reaction of phosphines and azides, termed the Staudinger ligation, in which an intramolecular electrophile traps the aza-ylide intermediate to form an amide and the corresponding phosphine oxide (Figure 27) (175). Perhaps, the Staudinger ligation was the first truly bioorthogonal reaction, it takes place at room temperature, in water at neutral pH, and involves two fully abiotic functional groups. Its impact on chemical biology was immediate, with many applications of biomolecule labeling relying on this chemistry (177). Nevertheless, the Staudinger ligation suffers from the inconvenience of air oxidation of the phosphine reagents, which can limit their shelf life, and more problematically, from sluggish reaction kinetics.

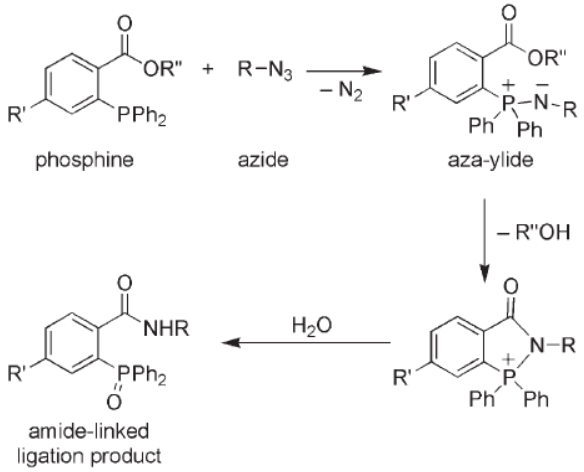

Figure 27. The mechanism of Staudinger ligation.

Cu-Catalyzed [3+2] Azide-Alkyne Cycloaddition (CuAAC).
The most popular click reaction is the Huisgen 1,3-dipolar cycloaddition between a terminal alkyne and an azide (171). This reaction, already discovered and developed many years ago, occurs, as just mentioned, between of unactivated alkynes and azides and requires high temperatures or pressures. For these reasons, it was relatively ignored for years after its discovery by Huisgen in the 1960's. The reaction was again evaluated in 2001 when different authors independently (178,179) reported a Cu(I)-catalyzed variant, that proceeds rapidly at room temperature to regiospecifically form 1,4 disubstituted 1,2,3-triazoles (Figure 28). The CuAAC (Cu-Catalyzed [3+2] Azide-Alkyne Cycloaddition) which is often simply referred to as “click chemistry”, has been employed in several chemoselective bioconjugation applications. These myriad applications have led to the exploration of the interesting physicochemical properties of triazoles, including their polarity, stability, and metal-binding abilities. Its greatly enhanced rate compared to both the aldehyde/ketone ligations and the Staudinger ligation, as well as the commercial availability or synthetic accessibility of both terminal alkynes and azides, are the main characteristics that have led to the ever more frequent use of CuAAC in chemical biology field for different applications, such as labeling of biomolecules in complex mixtures and imaging of fixed cells and tissues. However, the major limitation of this technique is due to the strict requirement for copper, a heavy metal highly toxic to cells and organisms.

Strain-Promoted [3+2] Azide-Alkyne Cycloaddition (SPAAC).
Inspired by the power of Cu catalysis in accelerating the rate of triazole formation, recently it was developed a Cu-free variant of click chemistry that provides a ring strain as an alternative means of alkyne activation (180) (Figure 28). Cu-free variant of click chemistry overcomes the intrinsic toxicity of the canonical Cu-catalyzed reaction. The critical reagent, a substituted cyclooctyne (a cyclic alkyne), possesses ring strain that confers an high steric constraint on alkyne functional group; due to this sever deformation from the ideal 180°, the triple bond in cycloalkynes having less than nine ring atoms displays high reactivity for azides without the need for copper catalysis.

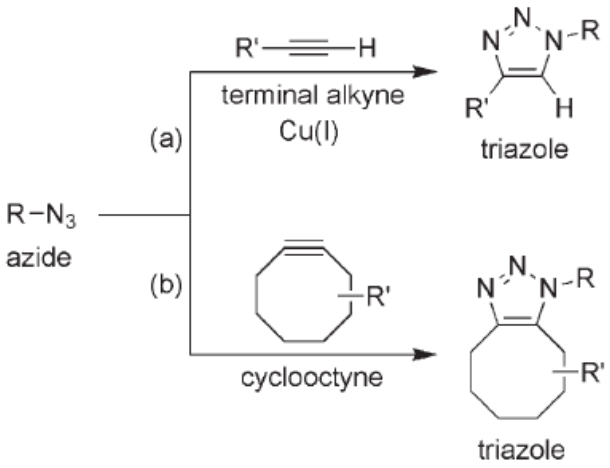

Figure 28. Azide-alkyne [3+2] cycloadditions. (a) Cu-catalyzed Azide-Alkyne Cycloaddition (CuAAC) of azides and terminal alkynes to form 1,4-disubstituted 1,2,3-triazoles. (b) Strain-promoted (Cu-free) cycloaddition of azides and cyclooctynes to form triazole products.

The first generation of cyclooctynes suffered from relatively slow reaction rates; in fact, the reaction rate constants of regular cyclooctynes with azides did not surpass those of the Staudinger ligation (181). However, it has been found that the rate of strain-promoted cycloaddition can be increased by structural modification and in particular by appending electron-withdrawing groups adjacent to the triple bond. For example, by fluorination (Figure 29; molecule n.1) (182), by sp2-hybridization of ring atoms (Figure 29; molecule n.2) (183), or by fusion to cyclopropane (Figure 29; molecule n.3) (184). In this latter case, the developed cycloctyne (BCN: bicyclo nonyne) results extremely powerful and reactive due to its small size and low lipophilicity.

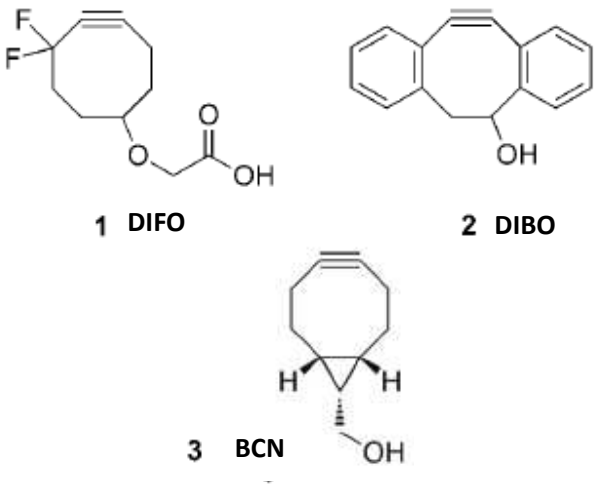

Figure 29. Substituted ring-strained cyclooctynes for bioorthogonal cycloaddition reactions with azides. (**1.** Difluorinated cyclooctyne; **2.** 4-dibenzocyclooctynol; **3.** bicyclo nonyne).

As mentioned above, the power of click chemistry lies in its simplicity. The bioorthogonal click chemistry is rapid, selective, and non-toxic covalent reaction to link biomolecules. The availability of reliable, robust and efficient chemistry for site-specifically label proteins represents a powerful tool in different areas of chemical biology.

AIM OF THE PROJECT

As described in detail in the introduction, the investigation of new methods for the improvement of processes such as the expression, purification and site-specific labeling of antigen and antibody molecules, can promote the development of new more powerful bioreagents and new solutions able of improving the specificity and the sensitivity of immunodiagnostic assays.

The first part of this thesis aimed to explore innovative biotechnology techniques in antigen production for the improvement of Diasorin LIAISON® EBV VCA IgM and IgG immunoassays that allow the detection of antibodies directed specifically against the Epstein-Barr virus (EBV), in human serum or plasma samples. EBV is the causative agent of infectious mononucleosis (IM) and, as extensively mentioned before, the virus infection is largely diffused worldwide. By adulthood, 95% to 99% of most of the world's population has demonstrable EBV antibodies. Moreover, it is considered to be etiologically associated with a still increasing number of disease syndromes including several human malignancies; for this reason it is important to develop diagnostic assays for EBV detection with high specificity and sensitivity.

The minor viral capsid protein VCA p18 appears to be one of the most important antigens for the diagnosis of EBV. The current Diasorin LIAISON® EBV VCA IgM and IgG assays rely on a single antigen, consisting in a synthetic peptide corresponding to the immunodominant C-terminal portion of the p18 protein, which is immobilized on solid phase (indirect format). The several methods explored in this thesis aimed to obtain different variants of the p18 antigen with the purpose to improve the performance of DiaSorin LIAISON® EBV VCA IgM and IgG assays at different levels (1) production process of the p18 antigen; (2) immobilization of the same antigen on solid phase; (3) format of immunoassay (Figure 30).

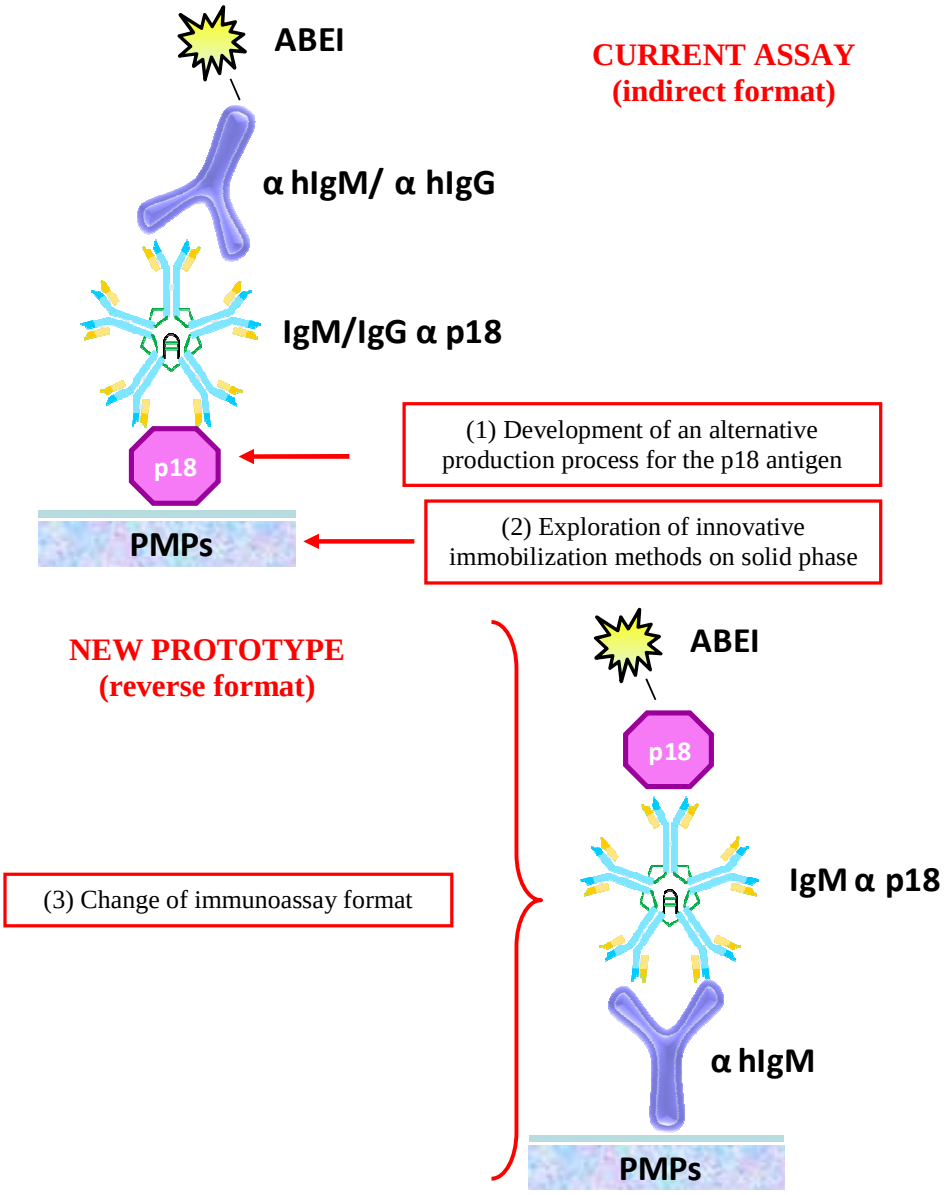

Figure 30. Explored strategies for the improvement of EBV VCA IgM and EBV VCA IgG immunoassays.

(1) Production process of the p18 antigen

The length of the immunodominant C-terminal portion of the p18 protein (57aa), used as capture element coated on solid phase in LIAISON® EBV VCA IgM and IgG assays (Figure 30), appears to be considerable for the synthetic route (necessity to prepare a disulfide-linked heterodimer; Figure 31) but, at the same time, too small to be effectively produced in a recombinant fashion. To overcome this problem, we explored the ELP-Intein system, a method based on the use of a self-cleavable protein (the intein) and a temperature responsive tag (ELP), as described in detail in the introduction.

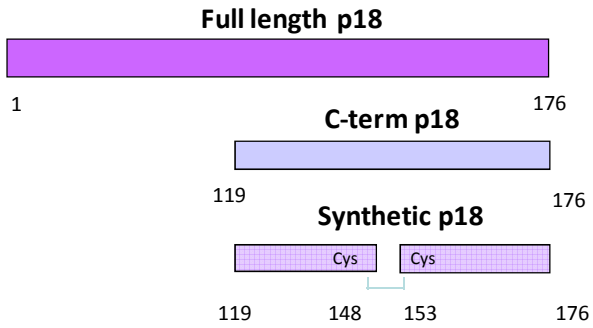

Figure 31. Schematic diagram of p18 components**.** The synthetic peptide used in LIAISON® EBV VCA IgM and IgG assays corresponds to the immunodominant C-terminal portion of the p18 protein. The considerable length of this peptide (57aa) makes the synthetic process quite complex. In fact, its preparation requires the synthesis of 2 separate peptides, which are then joined together through the formation of a disulfide bridge between two cysteine residues, positioned respectively at the C-terminal of the first peptide and at the N-terminal of the second one.

(2) Immobilization of the p18 antigen on solid phase.

The development of different variants of the p18 antigen has enabled to explore different techniques for the immobilization of the same antigen on solid phase:

2.1 _ direct covalent coating;

2.2 _through streptavidin-biotin complex.

In this case, the biotinylation of the antigen was carried out through the investigation of two different methods.

(2.2.1) In the first case, we exploited the p18 antigen variant generated by ELP-intein method in order to obtain the C-terminal site-specific biotinylation of the same antigen by using the technique called “expressed protein ligation” or “intein-mediated protein ligation”. This technique involves the reaction between a recombinant protein with a C-terminal thioester group (obtained through the process of intein self-cleavage) and a synthetic peptide containing a thiol group at the N-terminus and, in our case, a lysine-biotin at the C-terminus in order to obtain a C-terminal site-specific modification (biotinylation) of target protein.

(2.2.2) In the second case, we tried to obtain the N-terminal site-specific biotinylation of the p18 antigen by using an innovative technique that provides the genetic incorporation of unnatural amino acids into target protein directly in *E. coli* cells. In particular the incorporation of a para-azido-phenylalanine at the N-terminal region of the protein has been exploited to subsequently realize a Strain-Promoted Azide-Alkyne Cycloaddition (SPAAC**)** reaction with a molecule of cyclooctyne-biotin with the result of a N-terminal biotinylated p18 antigen.

2.3_ Through an innovative procedure based on the use of leucine zipper (or “velcro”) peptides.

(3) Development of the LIAISON® EBV VCA IgM immunoassay "reverse" format.

Despite the DiaSorin LIAISON® EBV VCA IgM immunoassay has a good analytical performance, in order to obtain an increase of specificity, a new assay format was explored. Starting from an indirect format (which includes the p18 antigen immobilization on solid phase), we tried to develop a "reverse" format, in which anti-human IgM antibodies, capable of catching the human IgM present in the sample, are used as a capture element on solid phase, while the p18 antigen, linked to one or more chemiluminescent molecules, is used as a tracer (Figure 30). For the synthesis of this new tracer characterized by the presence of the p18 antigen, it was decided to use a highly selective and efficient type of chemistry, the click chemistry.

MATERIALS AND METHODS

REAGENTS

Tryptone, peptone were purchased by BD; IPTG was purchased by Inalco; Sodium phosphate, potassium phosphate, sodium acetate, EDTA (Ethylenediaminetetraacetic acid), NaCl and methanol were purchased by Carlo Erba; Ampicillin, Kanamicin, Chloramphenicol, L-Arabinose, DTT (Dithiothreitol), MESNA (2-mercaptoethanesulfonate Na), Urea, Trizma base, SDS (Sodium dodecyl sulphate), APS (Ammonium persulfate), TEMED (N,N,N',N'-Tetramethylethylenediamine), Glycine, 2-mercaptoethanol, BBF (Bromophenol Blue), Pyronin, Glycerol, 4-Chloro-1-naphthol, Hydrogen Peroxide (H_2O_2) DMSO, Hepes, NDSB-195 (Dimethylethylammoniumpropane sulfonate), Phenol, DIPEA (N,N-Diisopropylethylamine), TIPS (triisopropylsilane), piperidine, diethyl ether, tert-butyl-methyl ether, glacial acetic acid were purchased by Sigma-Aldrich. TFA (tri-fluoroacetic acid), CH3CN (acetonitrile) and Tween20 were purchased by Merck; pAzF (para-azido-phenylalanine) was purchased by Bachem; BCN-PEO3-NHS and BCN-PEO3-Biotin were purchased by Synaffix; 40% Acrylamide/Bis solution was purchased by BIORAD; DMF (N,N-Dimethylformamide) was purchased by Sharlau; NMP (N-Methylpyrrolidone) was purchase by Biosolve; Hobt and HBTU were purchased by GL Biochem Ltd; Agarose was purchased by IBI scientific; GelRed™ nucleic acid gel stain was purchased by Biotium.

CLONING

- Plasmid extraction was performed with Wizard Plus SV Minipreps kit (Promega).
- DNA purification (from agarose gel, PCR and digestions) was performed with Kit Wizard SV Gel and PCR Clean-Up System (Promega).
- High Fidelity Expand System Polymerase for PCR and relative buffer were purchased by Roche.
- *NdeI, NheI, XhoI EcoRI, HindIII, BamHI* endonucleases and relative buffers , Quick T4 DNA Ligase and relative buffer were purchased by New England Biolabs (NEB).

CLONING OF EXPRESSION VECTORS

A) pTME-MCS expression vector

pTME vector is a modification of pET32 expression vector (Novagen, Merck Chemicals Ltd) and includes the gene encoding for the Trx-*Mxe*GyrA-ELP90 fusion protein; it was a gentle gift from Prof. Chilkoti (Duke University, Durham, NC, USA).
The expressed protein had the following amino acids sequence, Figure 32:

MSDKIIHLTDDSFDTDVLKADGAILVDFWAEWCGPCKMIAPILDEIADEYQGKLTA
KLNIDQNPGTAPKYGIRGIPTLLLFKNGEVAATKVGALSKGQLKEFLDANLAGSGG
MRMCITGDALVALPEGESVRIADIVPGARPNSDNAIDLKVLDRHGNPVLADRLFHG
EHPVYTVRTVEGLRVTGTANHPLLCLVDVAGVPTLLWKLIDEIKPGDYAVIQRSAS
VDCAGFARGKPEFAPTTYTVGVPGLVRFLEAHHRDPDAQAIADELTDGRFYYAKVS
VTDAGVQPVYSLRVDTADHAFITNGFVSHATGLTGLNSGLHMHHHHHHSSGLVPRS
GKGPGVGVPGVGVPGGGVPGAGVPGVGVPGVGVPGVGVPGGGVPGAGVPGGGVPGG
VPGVGVPGGGVPGAGVPGVGVPGVGVPGVGVPGGGVPGAGVPGGGVPGVGVPGVGP
GGGVPGAGVPGVGVPGVGVPGVGVPGGGVPGAGVPGGGVPGVGVPGVGVPGGGVPA
GVPGVGVPGVGVPGVGVPGGGVPGAGVPGGGVPGVGVPGVGVPGGGVPGAGVPGVV
PGVGVPGVGVPGGGVPGAGVPGGGVPGVGVPGVGVPGGGVPGAGVPGVGVPGVGVG
VGVPGGGVPGAGVPGGGVPGVGVPGVGVPGGGVPGAGVPGVGVPGVGVPGVGVPGG
VPGAGVPGGGVPGVGVPGVGVPGGGVPGAGVPGVGVPGVGVPGVGVPGGGVPGAGP
GGGVPGVGVPGVGVPGGGVPGAGVPGVGVPGVGVPGVGVPGGGVPGAGVPGGGVPG
WP

Thioredoxin (11.805 kDa)-Intein (*Mxe*GyrA N198A)-ELP90 (- linkers)

Figure 32. Trx-*Mxe*GyrA-ELP90 fusion protein sequence (799 amino acids; 72.6 kDa) encoded by the pTME vector.

The main drawback of pTME vector was that the Trx gene could not be replaced by other DNA sequences because no endonuclease restriction sites were anymore available at both the 5’ and 3’ terminus of the Trx sequence.

For this reason it was modified by replacing the Trx gene with a multiple cloning site according to the following protocols, Figure 33A:

1. pTME plasmid was digested with *Nde*I, in order to excise the Trx-Intein DNA sequence.
2. A multiple cloning site-Intein fragment was generated by PCR amplification using as template the Intein sequence of pTME vector. This fragment is characterized by sticky ends to *Nde*I.

The following primers were used:

Fw:

NdeI *EcoRI* **BamHI** *HindIII*
5'_AG**CATATG***GAATTC***GGATCC***AAGCTT*AGATCTGGTTCTGGTTCTGG CATGCGTATG_3'

Rev:

NdeI
5'_GC**CATATG**AGATCTGAGGCCTGAGTTCAGACCGGTGAG_3'

3. Ligation of the open vector from step1 with the PCR product of step 2 digested with *Nde*I gave the new expression vector pTME-MCS.

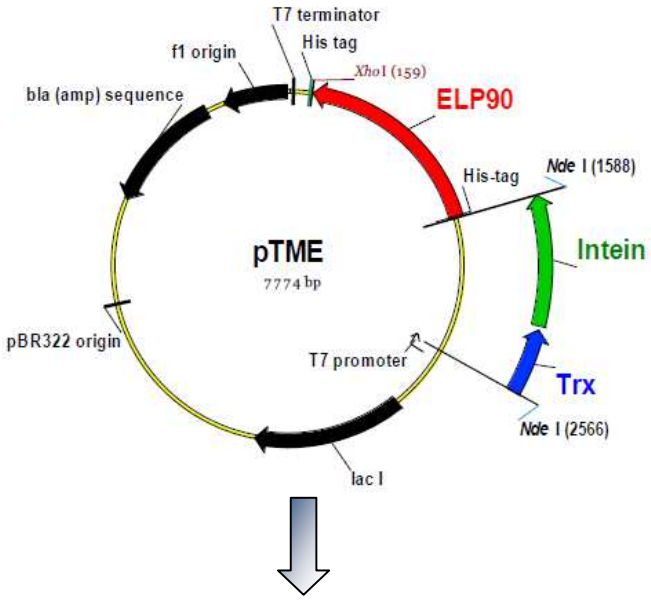

Trx-Intein sequence was excised by *Nde*I and replaced by a MCS-Intein sequence obtained by PCR

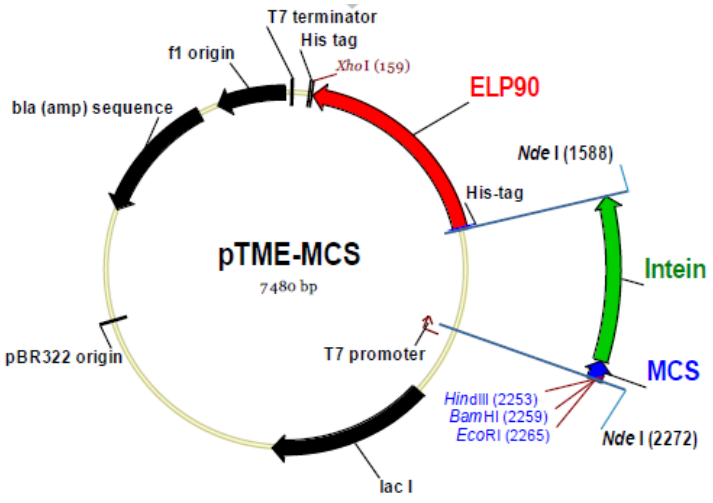

Figure 33A. A schematic representation of the cloning strategy of pTME-MCS vector.

pTME-MCS vector is characterized by the following multiple cloning site, Figure 33B:

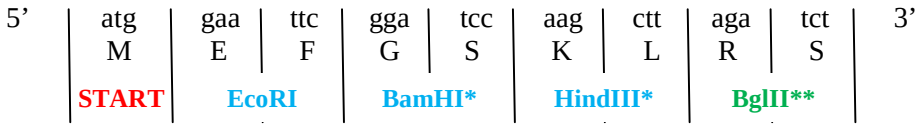

Figure 33B. Nucleotide sequence of the multiple cloning site of pTME-MCS vector. (*) Unique restriction sites usable for cloning. (**) The BglII restriction site is present twice in the pTME-MCS vector, before and after the Intein sequence and cannot be used for cloning but for eventual Intein deletion**.**

The amino acid sequence of the MCS-*Mxe*GyrA-ELP90 protein encoded by pTME-MCS vector resulted then as shown in Figure 34.

MEFGSKLRSGSGSGMRMCITGDALVALPEGESVRIADIVPGARPNSDNAIDLK
VLDRHGNPVLADRLFHSGEHPVYTVRTVEGLRVTGTANHPLLCLVDVAGVPTL
LWKLIDEIKPGDYAVIQRSAFSVDCAGFARGKPEFAPTTYTVGVPGLVRFLEA
HHRDPDAQAIADELTDGRFYYAKVASVTDAGVQPVYSLRVDTADHAFITNGFV
SHATGLTGLNSGLRSHMHHHHHHSSGLVPRGSGKGPGVGVPGVGVPGGGVPGA
GVPGVGVPGVGVPGVGVPGGGVPGAGVPGGGVPGVGVPGVGVPGGGVPGAGVP
GVGVPGVGVPGVGVPGGGVPGAGVPGGGVPGVGVPGVGVPGGGVPGAGVPGVG
VPGVGVPGVGVPGGGVPGAGVPGGGVPGVGVPGVGVPGGGVPGAGVPGVGVPG
VGVPGVGVPGGGVPGAGVPGGGVPGVGVPGVGVPGGGVPGAGVPGVGVPGVGV
PGVGVPGGGVPGAGVPGGGVPGVGVPGVGVPGGGVPGAGVPGVGVPGVGVPGV
GVPGGGVPGAGVPGGGVPGVGVPGVGVPGGGVPGAGVPGVGVPGVGVPGVGVP
GGGVPGAGVPGGGVPGVGVPGVGVPGGGVPGAGVPGVGVPGVGVPGVGVPGGG
VPGAGVPGGGVPGVGVPGVGVPGGGVPGAGVPGVGVPGVGVPGVGVPGGGVPG
AGVPGGGVPGWP

MCS-Intein (*Mxe*GyrA N198A)-ELP90 (- linkers)

Figure 34. Protein sequence encoded by the pTME-MCS vector.

B) pET24-MCS-Intein-ELP(KV7F-36) vector

A synthetic gene encoding for a new ELP (ELP[KV7F]36) linked to the *Mxe*GyrA gene and a multiple cloning site was purchased by GeneArt (Regensburg, Germany) and cloned via *Nde*I-*Xho*I in pET24a vector (Novagen, Merck Chemicals Ltd) (Figure 35A).

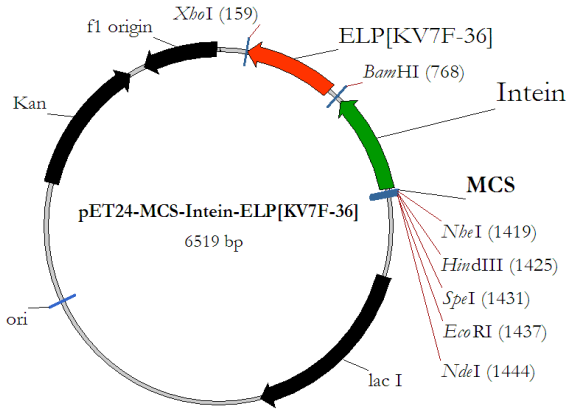

Figure 35A. A schematic representation of pET24-MCS-*Mxe*GyrA-ELP[KV7F]36 vector.

The amino acid sequence of the MCS-*Mxe*GyrA- ELP[KV7F]36 protein encoded by pET24-MCS-*Mxe*GyrA-ELP[KV7F]36 vector resulted as shown in Figure 35B:

MEFTSKLASGSGMRMCITGDALVALPEGESVRIADIVPGARPNSDNAIDLKVLDRH
GNPVLADRLFHSGEHPVYTVRTVEGLRVTGTANHPLLCLVDVAGVPTLLWKLIDEI
KPGDYAVIQRSAFSVDCAGFARGKPEFAPTTYTVGVPGLVRFLEAHHRDPDAQAIA
DELTDGRFYYAKVASVTDAGVQPVYSLRVDTADHAFITNGFVSHATGGGSGGGSGG
GSGGGSGGGSGGGSGGGSGGGVGVPGKGVPGVGVPGVGVPGVGVPGVGVPGVGVPG
VGVPGFGVPGVGVPGKGVPGVGVPGVGVPGVGVPGVGVPGVGVPGVGVPGFGVPGV
GVPGKGVPGVGVPGVGVPGVGVPGVGVPGVGVPGVGVPGFGVPGVGVPGKGVPGVG
VPGVGVPGVGVPGVGVPGVGVPGVGVPGFGVPG

MCS-Intein (*Mxe*GyrA N198A)-ELP36 (- linkers)

Figure 35B. Protein encoded by the pET24-MCS-Intein-ELP]KV7F]36.

C) Cloning of p18 antigen

A synthetic gene encoding for EBV viral capsid antigen p18 was purchased by GeneArt and cloned via *Eco*RI-*Hind*III in:
- pTME-MCS to obtain pTME-p18 vector
-pET24-MCS-*Mxe*GyrA-ELP(KV7F-36) to obtain pET24-p18-*Mxe*GyrA-ELP(KV7F-36) vector

pTME-p18 vector encodes for p18-*Mxe*GyrA-ELP90 fusion protein (757 amino acids; 66.22 kDa; Figure 36).

MEFSTAVAQSATPSVSSSISSLRAATSGATAAASAAAAVDTGSGGGGQPHDTAPRG
ARKKQKLRSGSGSGMRMCITGDALVALPEGESVRIADIVPGARPNSDNAIDLKVLD
RHGNPVLADRLFHSGEHPVYTVRTVEGLRVTGTANHPLLCLVDVAGVPTLLWKLID
EIKPGDYAVIQRSAFSVDCAGFARGKPEFAPTTYTVGVPGLVRFLEAHHRDPDAQA
IADELTDGRFYYAKVASVTDAGVQPVYSLRVDTADHAFITNGFVSHATGLTGLNSG
LRSHMHHHHHHSSGLVPRGSGKGPGVGVPGVGVPGGGVPGAGVPGVGVPGVGVPGV
GVPGGGVPGAGVPGGGVPGVGVPGVGVPGGGVPGAGVPGVGVPGVGVPGVGVPGGG
VPGAGVPGGGVPGVGVPGVGVPGGGVPGAGVPGVGVPGVGVPGVGVPGGGVPGAGV
PGGGVPGVGVPGVGVPGGGVPGAGVPGVGVPGVGVPGVGVPGGGVPGAGVPGGGVP
GVGVPGVGVPGGGVPGAGVPGVGVPGVGVPGVGVPGGGVPGAGVPGGGVPGVGVPG
VGVPGGGVPGAGVPGVGVPGVGVPGVGVPGGGVPGAGVPGGGVPGVGVPGVGVPGG
GVPGAGVPGVGVPGVGVPGVGVPGGGVPGAGVPGGGVPGVGVPGVGVPGGGVPGAG
VPGVGVPGVGVPGVGVPGGGVPGAGVPGGGVPGVGVPGVGVPGGGVPGAGVPGVGV
PGVGVPGVGVPGGGVPGAGVPGGGVPGWP

p18-Intein (*Mxe*GyrA N198A)-ELP90 (- linkers)

Figure 36. p18-*Mxe*GyrA-ELP90 sequence.

pET24-p18-*Mxe*GyrA-ELP(KV7F-36) vector encodes for p18-*Mxe*GyrA-ELP36 fusion protein (481 amino acids; 45.15 kDa; Figure 37).

MEFSTAVAQSATPSVSSSISSLRAATSGATAAASAAAAVDTGSGGGGQPHDTAPRG
ARKKQKLASGSGMRMCITGDALVALPEGESVRIADIVPGARPNSDNAIDLKVLDRH
GNPVLADRLFHSGEHPVYTVRTVEGLRVTGTANHPLLCLVDVAGVPTLLWKLIDEI
KPGDYAVIQRSAFSVDCAGFARGKPEFAPTTYTVGVPGLVRFLEAHHRDPDAQAIA
DELTDGRFYYAKVASVTDAGVQPVYSLRVDTADHAFITNGFVSHATGGGSGGGSGG
GSGGGSGGGSGGGSGGGSGGGVGVPGKGVPGVGVPGVGVPGVGVPGVGVPGVGVPG
VGVPGFGVPGVGVPGKGVPGVGVPGVGVPGVGVPGVGVPGVGVPGVGVPGFGVPGV
GVPGKGVPGVGVPGVGVPGVGVPGVGVPGVGVPGVGVPGFGVPGVGVPGKGVPGVG
VPGVGVPGVGVPGVGVPGVGVPGVGVPGFGVPG

p18-Intein (*Mxe*GyrA N198A)-ELP36 (- linkers)

Figure 37. p18-*Mxe*GyrA-ELP36 sequence.

D) Cloning of MalEp18 antigen

A gene encoding for EBV viral capsid antigen p18 with the first six amino acids of Maltose Binding Protein (MBP) at N-terminus was obtained by digestion with *NdeI* and *NheI* endonucleases of pMA-ZE-p18-ZR template, purchased by GeneArt (Figure 38). This template was designed to realize the constructs necessary for the application of velcro peptides system described in the following paragraphs. This template encodes the first 6 amino acids of MBP followed by the sequence of p18 antigen. MalEp18 gene was characterized by the *NdeI* and *NheI* restriction sites at its 5' and 3' ends, respectively.

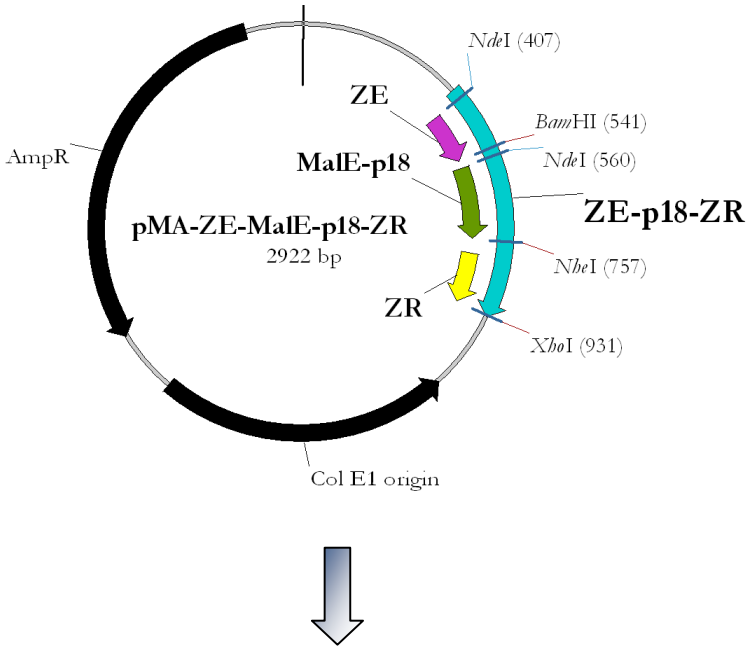

MalEp18 sequence was isolated by the digestion with *NdeI* and *NheI* endonucleases of pMA-ZE-p18-ZR template.

Figure 38. Schematic representation of pMA-ZE-p18-ZR template from which MalEp18 gene was isolated.

MalEp18 was then cloned via *NdeI/NheI* in pET24-MCS-*Mxe*GyrA-ELP(KV7F-36) to obtain pET24-MalEp18-*Mxe*GyrA-ELP(KV7F-36) vector.

pET24-MalEp18-*Mxe*GyrA-ELP(KV7F-36) vector encodes for MalEp18-*Mxe*GyrA-ELP36 fusion protein (483 amino acids; 45.31 kDa; Figure 39).

MKIEEGKSTAVAQSATPSVSSSISSLRAATSGATAAASAAAAVDTGSGGGGQPHDTAPR
GARKKQASGSGMRMCITGDALVALPEGESVRIADIVPGARPNSDNAIDLKVLDRHGNPV
LADRLFHSGEHPVYTVRTVEGLRVTGTANHPLLCLVDVAGVPTLLWKLIDEIKPGDYAV
IQRSAFSVDCAGFARGKPEFAPTTYTVGVPGLVRFLEAHHRDPDAQAIADELTDGRFYY
AKVASVTDAGVQPVYSLRVDTADHAFITNGFVSHATGGGSGGGSGGGSGGGSGGGSGGG
SGGGSGGGVGVPGKGVPGVGVPGVGVPGVGVPGVGVPGVGVPGVGVPGFGVPGVGVPGK
GVPGVGVPGVGVPGVGVPGVGVPGVGVPGVGVPGVGVPGFGVPGVGVPGKGVPGVGVPG
VGVPGVGVPGVGVPGVGVPGFGVPGVGVPGKGVPGVGVPGVGVPGVGVPGVGVPGVGVP
GVGVPGFGVPG

MalEp18-Intein (*Mxe*GyrA N198A)-ELP36 (- linkers)

Figure 39. MalEp18-*Mxe*GyrA-ELP36 sequence.

E) Cloning of MalEp18(pAzF) antigen

A gene encoding for EBV viral capsid antigen p18 with the first six amino acids of Maltose Binding Protein (MBP) at N-terminus and characterized by the presence of an amber stop codon (TAG) at the level of third amino acid position of MBP sequence, was generated by PCR site-directed mutagenesis using as template the MalEp18 sequence of pMA-ZE-p18-ZR vector. Therefore, the new generated gene was characterized by the substitution of the third codon corresponding to isoleucine residue (ATT) with the amber stop codon (TAG). Moreover it was designed to contain the *Nde*I/*NheI* specific restriction site at 5’ and 3’ends, respectively.
The insertion of an amber stop codon within the sequence (third position) was necessary for the genetically incorporation of a para-azido-phenylalanine residue in the corresponding position, directly in *E.coli* cells, as described in detail in the introduction.

The following primers were used:

Fw:

NdeI
5’_TGC**CATATG**AAATAGGAAGAAGGTAAAAGCACCGCAGTTG_3’

Rev:

NheI
5’_ GGA**GCTAGC**CTGTTTTTTACGTGCACCA_3’

MalEp18 (TAG) was then cloned via *NdeI/NheI* in pET24-MCS-*Mxe*GyrA-ELP(KV7F-36) to obtain pET24-MalEp18(TAG)-*Mxe*GyrA-ELP(KV7F-36) vector.

pET24-MalEp18(TAG)-*Mxe*GyrA-ELP(KV7F-36) vector encodes for MalEp18(pAzF)-*Mxe*GyrA-ELP36 fusion protein (483 amino acids; 45.38 kDa; Figure 40).

MK(pAz)FEEGKSTAVAQSATPSVSSSISSLRAATSGATAAASAAAAVDTGSGGGGQPH
DTAPRGARKKQASGSGMRM**CITGDALVALPEGESVRIADIVPGARPNSDNAIDLKVLDR
HGNPVLADRLFHSGEHPVYTVRTVEGLRVTGTANHPLLCLVDVAGVPTLLWKLIDEIKP
GDYAVIQRSAFSVDCAGFARGKPEFAPTTYTVGVPGLVRFLEAHHRDPDAQAIADELTD
GRFYYAKVASVTDAGVQPVYSLRVDTADHAFITNGFVSHAT**GGGSGGGSGGGSGGGSGG
GSGGGSGGGSGGG**VGVPGKGVPGVGVPGVGVPGVGVPGVGVPGVGVPGFGVPGV
GVPGKGVPGVGVPGVGVPGVGVPGVGVPGVGVPGVGVPGFGVPGVGVPGKGVPGVGVPG
VGVPGVGVPGVGVPGVGVPGVGVPGFGVPGVGVPGKGVPGVGVPGVGVPGVGVPGVGVP
GVGVPGVGVPGFGVPG**

MalE(pAzF)p18-Intein (*Mxe*GyrA N198A)-ELP36 (- linkers)

Figure 40. MalEp18(pAzF)-*Mxe*GyrA-ELP36 sequence.

F) pEVOL-pAzF vector

pEVOL-pAZF vector encoding for the tRNA/aaRS pair, specific for the para-azido-phenylalanine unnatural amino acid, is a commercial plasmid purchased by Addgene.

G) Cloning of ZE-ELP(KV7F-36) antigen

The ZE-ELP(KV7F-36) construct characterized by the fusion of genes encoding for the ZE acidic velcro peptide and for the ELP(KV7F-36) thermal responsive polypeptide was obtained with the following procedure (Figure 42):

1. pET24-MCS-*Mxe*GyrA-ELP(KV7F-36) plasmid was digested with *NdeI/BamHI*, in order to excise the Intein DNA sequence.
2. pMA-ZE-p18-ZR plasmid was digested with *NdeI/BamHI*, in order to isolate the ZE DNA sequence of interest.
3. Ligation of the open vector from step1 with the digestion product of step 2 gave the new expression vector pET24-ZE-ELP(KV7F-36).

pET24-ZE-ELP(KV7F-36) vector encodes for ZE-ELP36 fusion protein (245 amino acids; 21.55 kDa; Figure 41).

M**LEIEAAFLEQENTALETEVAELEQEVQRLENIVSQYRTRYGPL**GSGGGSGGGSGG
GSGGGSGGG**VGVPGKGVPGVGVPGVGVPGVGVPGVGVPGVGVPGVGVPGFGVPGVG**
VPGKGVPGVGVPGVGVPGVGVPGVGVPGVGVPGVGVPGFGVPGVGVPGKGVPGVGV
PGVGVPGVGVPGVGVPGVGVPGVGVPGFGVPGVGVPGKGVPGVGVPGVGVPGVGVP
GVGVPGVGVPGVGVPGFGVPG

ZE-ELP36 (- linker)

Figure 41. ZE-ELP36 sequence.

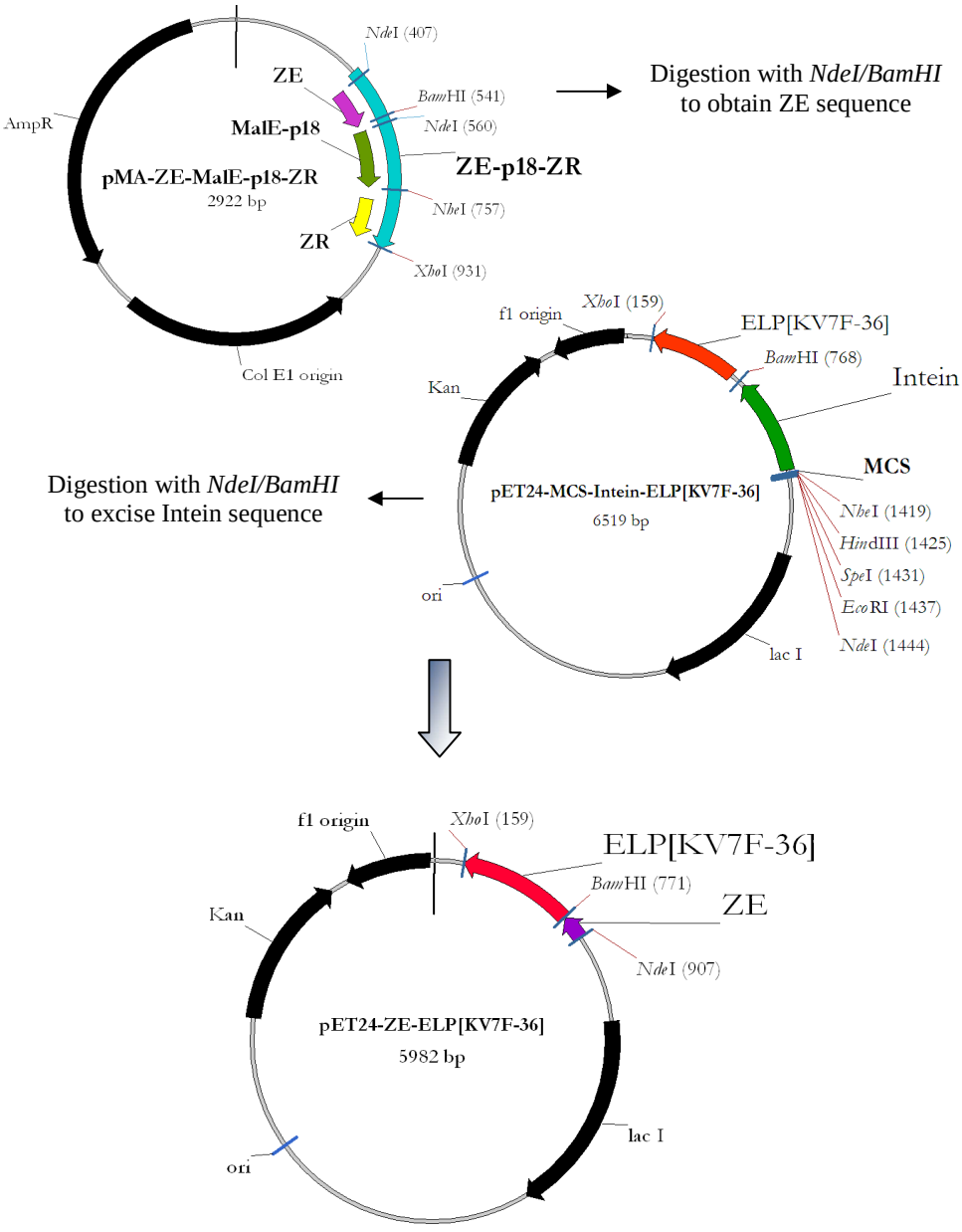

Figure 42. Schematic representation of the pET24-ZE-ELP(KV7F-36) vector cloning strategy.

H) Cloning of MalEp18-ZR antigen

The MalEp18-ZR construct was characterized by the fusion of ZR basic velcro peptide gene to the 3' end of MalEp18 gene.
MalEp18-ZR construct was obtained with the following procedure (Figure 44):

1. pET24-MCS-*Mxe*GyrA-ELP(KV7F-36) plasmid was digested with *NdeI/XhoI*, in order to excise the Intein-ELP(KV7F-36) DNA sequence.
2. pMA-ZE-p18-ZR plasmid was digested with *NdeI/XhoI*, in order to isolate the MalEp18-ZR fragment of interest.
3. Ligation of the open vector from step1 with the digestion product of step 2 gave the new expression vector pET24-MalEp18-ZR.

pET24-MalEp18-ZR vector encodes for MalEp18-ZR fusion protein (121 amino acids; 12.24 kDa; Figure 43).

MKIEEGKSTAVAQSATPSVSSSISSLRAATSGATAAASAAAAVDTGSGGGGQPHDT
APRGARKKQASGGGSGGGSGGGLEIRAAFLRRRNTALRTRVAELRQRVQRLRNEVS
QYETRYGPL

MalEp18-ZR (- linker)

Figure 43. MalEp18-ZR sequence.

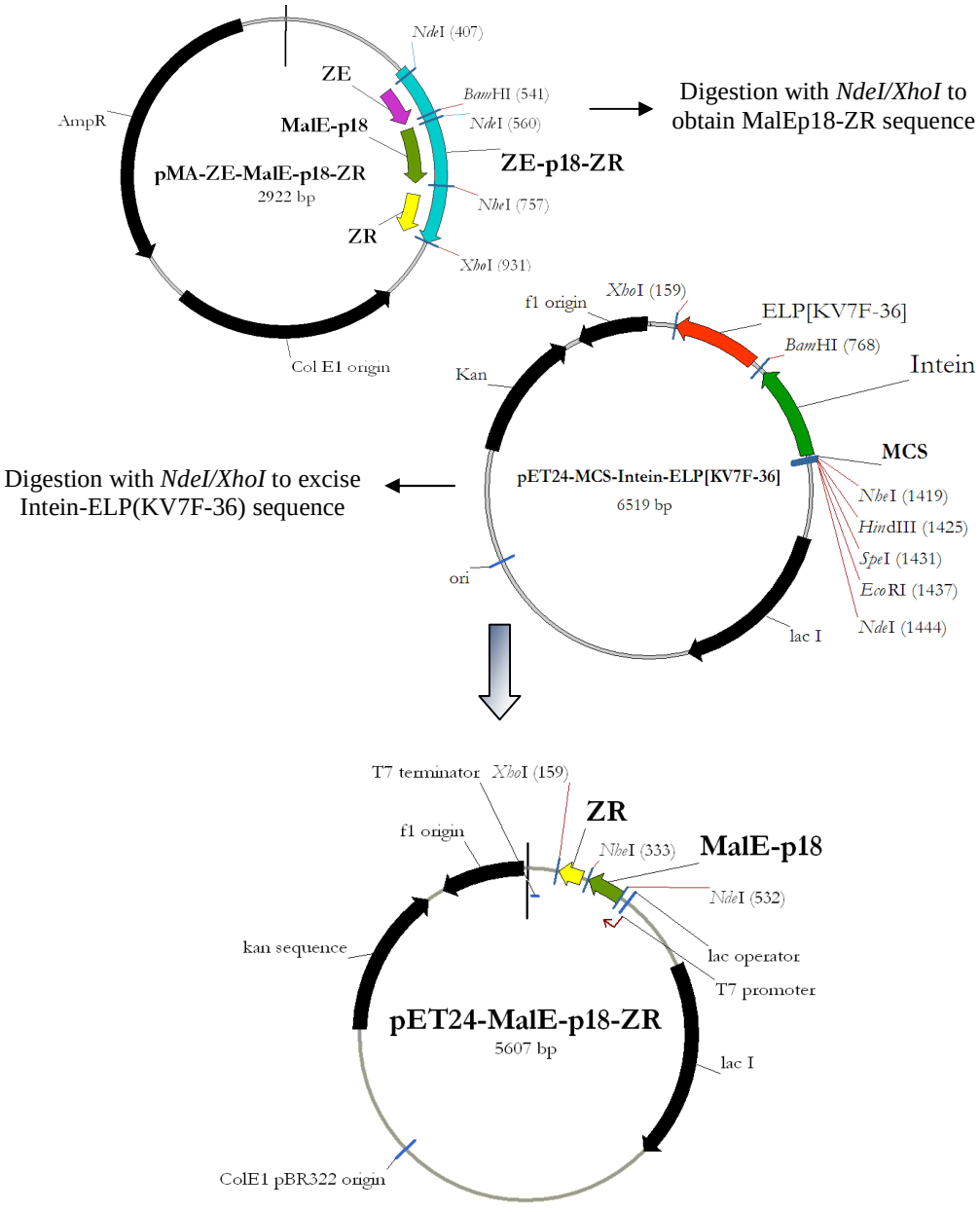

Figure 44. Schematic representation of the pET24-MalEp18-ZR vector cloning strategy.

STRAINS

E. coli XL1-Blue strain (Stratagene, Agilent Technologies, Santa Clara, USA) was used for mutagenesis and cloning operations and plasmid maintenance.
E. coli BL21(DE3) strain (Novagen, Merck Chemicals Ltd) was used for protein expression.
E. coli BL21 Star™ (DE3) pLysS (Innovagen) was used for p18-*Mxe*GyrA-ELP90 and p18-*Mxe*GyrA-ELP36 target proteins expression.
E. coli Rosetta (DE3) pLysS (Novagen, Merck Chemicals Ltd) was used for p18-*Mxe*GyrA-ELP90 and p18-*Mxe*GyrA-ELP36 target proteins expression.

FERMENTATIONS

Pre-inoculum: few µL of glycerinated BL21(DE3), BL21 Star™ (DE3) pLysS or Rosetta (DE3) pLysS cells were poured in 50 mL of culture medium (LB) supplemented with antibiotics (ampicillin 50 µg/ml, kanamycin 30 µg/ml, chloramphenicol 34 µg/mL, depending on the vector), and left on oscillating device (180 rpm) at 37°C, overnight.
Inoculum: the following day the sample was diluted (1:50 for fermentations performed at 30-37°C or 1:30 for fermentations performed at 15-25°C). Bacterial cells, grown in the same medium of pre-inoculum (LB with specific antibiotics), were induced with 0.1 mM (for fermentations performed at 15-25°C) or 1 mM IPTG (for fermentations performed at 30-37°C) when the absorbance at 600 nm reached usually a value of 0.6, but in some cases a value of 1.5 (late induction). Protein expression was continued for 3 hours for fermentations at 30-37 °C or for 16-24 hours for fermentations at 15-25 °C.

Fermentation for the expression of MalEp18(pAzF)*Mxe*GyrA-ELP36 protein (Amber codon suppression system).

1- w/o pre-induction

Pre-inoculum: few µL of glycerinated BL21(DE3) *E. coli* cells carrying the expression plasmid (pET24- MalEp18(TAG)*Mxe*GyrA-ELPKV7F36) and the suppressor plasmid (pEVOL-pAzF) were grown in LB medium supplemented with kanamycin 30 µg /ml and chloramphenicol 34 µg/mL, and left on oscillating device (180 rpm) at 37°C, overnight.

Inoculum: Bacterial cells diluted 1:50 or 1:30 (depending on conditions) in LB medium supplemented with kanamycin 30 µg/ml (w/o chloramphenicol), were grown until the optical density at 600 nm of wavelength reached a value of 1.5 (late induction). At this point the expression of the target gene and the tRNA/aaRS pair were co-induced with 1 mM IPTG and 0.01% L-arabinose, respectively. The pAzF unnatural aminoacid was also added at this point to a final concentration of 1 mM. Protein expression was continued for 20 h at 20°C, 25°C, 30°C or 37°C.

2- with pre-induction

Pre-inoculum: in the same conditions described for fermentation w/o pre-induction.

Inoculum: Bacterial cells diluted 1:50 or 1:30 (depending on conditions) in LB medium supplemented with kanamycin 30 µg/ml (w/o chloramphenicol) and with half dose of L-arabinose and pAzF concentration (0.05% and 0.5 mM, respectively) were grown until the optical density at 600 nm of wavelength reached a value of 1.5 (late induction). At this point cells were induced with IPTG (1 mM; entire dose) and with the other half dose of L-arabinose and pAzF (0.05% and 0.5 mM, respectively). Protein expression was continued for 20 h at 20°C, 25°C, 30°C or 37°C.

PROTEIN INDUCTION TEST PROTOCOL

Aliquots of a fermentation culture corresponding to 0.6 optical density at 600 nm of wavelength per ml of cellular culture were withdrawn at the moment of protein induction (T0), after fixed times from protein

induction (e.g. 1 hour, 2 hours), and at the end of the fermentation. Samples were spinned-down at 10.000xg in a bench top centrifuge and the related bacteria pellets treated with 100 µL of reducing loading buffer at +99ºC for five minutes and then analyzed by SDS-PAGE.

SOLUBILITY TEST PROTOCOL

At the end of fermentation, 15 milliliters of the cell colture were centrifuge (2000xg at 4°C). Then, the following working scheme was performed:

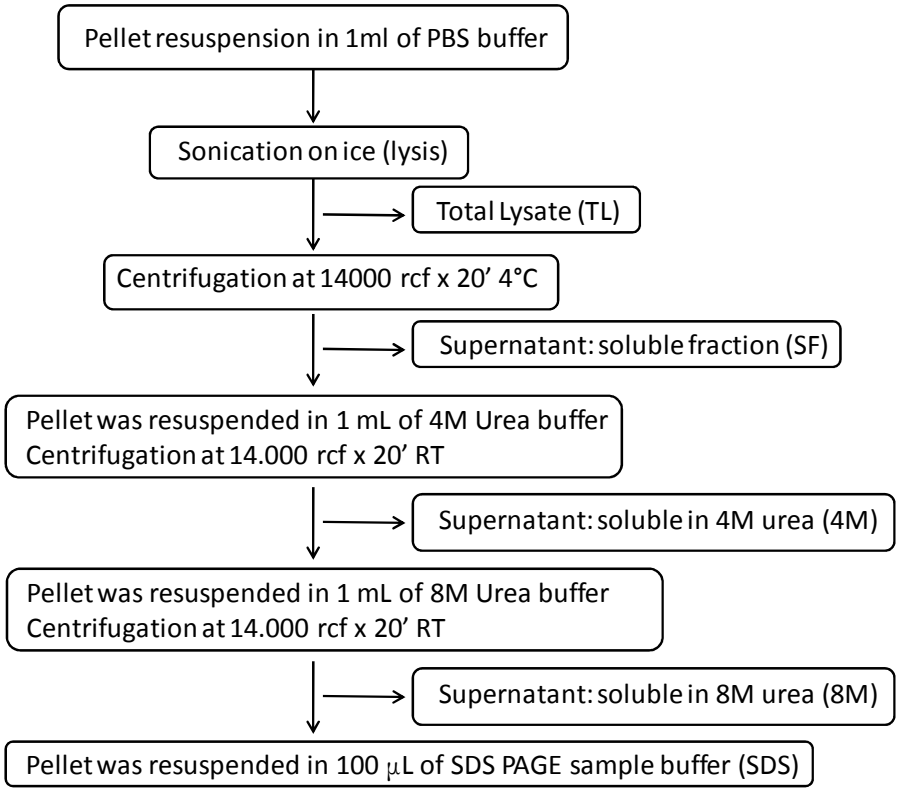

50 µL of each collected fraction (TL; SF; 4M; 8M, sds) were treated with 50 µL of reducing loading buffer (1:1) at +99ºC for five minutes and then analyzed by SDS-PAGE.

SDS-PAGE PROTOCOL

Electrophoresis on polyacrylamide gels was performed using the Mini-PROTEAN® III electrophoresis cell apparatus from BIO-RAD. Separation gels were home casted following the recipe:

Compound	10%	12.5%	Stacking gel
Acrylamide/Bis 19:1	2.0 mL	2.5 mL	0.75 mL
MilliQ water	2.6 mL	2.1mL	3.71 mL
Tris 1M pH 8.7	3 mL	3 mL	-
Tris pH 6.8	-	-	0.625 mL
SDS 20%	40 µL	400 µL	25 µL
APS 10%	70 µL	70 µL	50 µL
TEMED	8 µL	8 µL	6 µL

Running buffer composition:

Compound	Concentration
Tris base	25 mM
Glycine	192 mm
SDS	0.1 (w/v)

Reducing loading buffer:

Compound	Concentration
Tris base	125mM (pH 6.8)
Glycerol	22 % (v/v)
β-OH	2.5 % (v/v)
SDS	2.5 % (w/v)
Bromophenol Blue	0.0025 (w/v)
Pyronin	0.0025 (w/v)

Electrophoresis condition: 100 Volts for 1.5 hours using the power supplier Power-Pac 3000 from BIO-RAD.
Staining solution: Coomassie blue G250 3 g/Liter, Methanol 50 % (v/v), Acetic acid 10 (v/v).
Destaining solution: Methanol 20 % (v/v), Acetic acid 10 (v/v).

WESTERN BLOT PROTOCOL

After electrophoresis separation on a polyacrylamide gel, protein bands were transfer to a PVDF membrane (Immobilon-P, MILLIPORE) using the Mini Trans-Blot Electrophoretic Transfer Cell from BIO-RAD.

Western Blot conditions

Transfer conditions :
Voltage (V): 100 *time*: 1,0 hour
Membrane: Immobilon-P (Millipore)
Buffer composition: H20 / SDS-PAGE running buffer 10% / Glycerol 8.5%

Blocking:
Buffer composition: PBS / BSA 0,5%
Incubation temp: RT *Incubation time*: about 1h

Tracer: Polyclonal rat anti-p18 HRP
Dilution: 1:5000
Dilution Buffer: PBS / BSA 0,5%
Incubation temp : RT *Incubation time :* 1h

Washing:
Buffer composition: PBS/ TWEEN20 0,1%
Incubation temp: RT *Incubation time*: 10 min for three time

Coloration/Development :
5 mL of 4-chloro naphtol
20mL of PBS
20 µL of H_2O_2

PROTEIN PURIFICATION

Chromatographic steps were carried out using an Akta™ Explorer 100 HPLC system and the Unicorn™ software from GE Healthcare.

MalEp18-*Mxe*GyrA-ELP36 and MalEp18(pAzF)-*Mxe*GyrA-ELP36 purification protocol

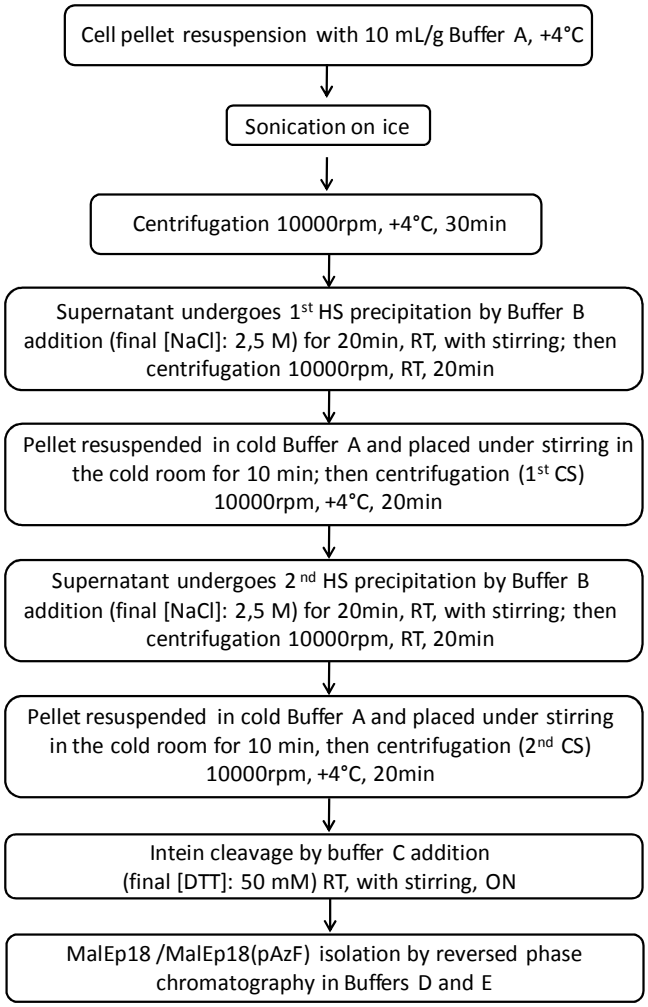

Figure 45A. MalEp18/MalEp18(pAzF) purification scheme from MalEp18-*Mxe*GyrA-ELP36/ MalEp18(pAzF)-*Mxe*GyrA-ELP36.

Buffer	Composition
A	50mM Na2HPO4*2H2O; 5mM EDTA; pH 8
B	NaCl 5M
C	DTT 1M
D	H2O, Trifluoroacetic acid 0.1% (v/v)
E	CH3CN, Trifluoroacetic acid 0.1% (v/v)

Table 2A. List of buffers used in purification protocol of MalEp18-*Mxe*GyrA-ELP36/MalEp18(pAzF)-*Mxe*GyrA-ELP36.

Chromatographic conditions:

- Column: Source15RPC 15µm 8.5x100mm ; CV=6.7 mL (GE)
- Flow rate: 2.5 mL/min
- Wavelengths: 214 nm
- Starting conditions: 90% buffer D, 10% buffer E
- Sample loading and washing: 90% buffer D, 10% buffer E
- Gradient: 10-60% buffer E in 70 mL

MalEp18-*Mxe*GyrA-ELP36 purification protocol for the subsequent EPL reaction (C-terminal site-specific biotinylation)

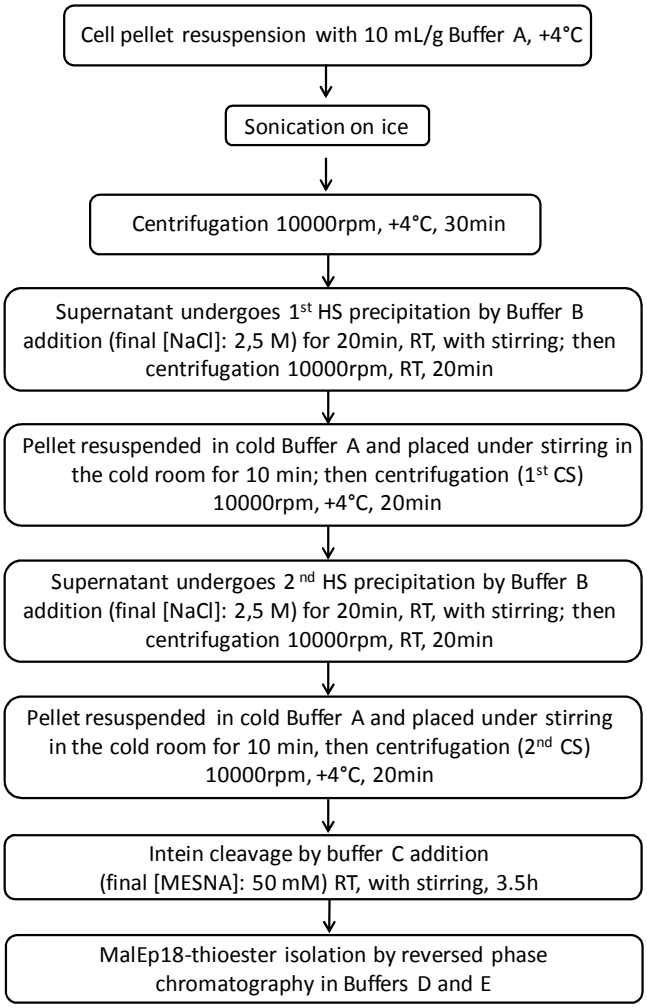

Figure 45B. MalEp18-thioester purification scheme from MalEp18-*Mxe*GyrA-ELP36 for the subsequent EPL reaction (C-terminal site-specific biotinylation of MalEp18 antigen).

Buffer	Composition
A	50mM Na2HPO4*2H2O; 5mM EDTA; pH 8
B	NaCl 5M
C	MESNA 1M
D	H2O, Trifluoroacetic acid 0.1% (v/v)
E	CH3CN, Trifluoroacetic acid 0.1% (v/v)

Table 2B. List of buffers used in purification protocol of MalEp18-*Mxe*GyrA-ELP36 to obtain MalEp18-thioester for the subsequent EPL reaction.

Chromatographic conditions:

- Column: Source15RPC 15μm 8.5x100mm ; CV=6.7 mL (GE)
- Flow rate: 2.5 mL/min
- Wavelengths: 214 nm
- Starting conditions: 90% buffer D, 10% buffer E
- Sample loading and washing: 90% buffer D, 10% buffer E
- Gradient: 10-60% buffer E in 70 mL

MalEp18-biotin purification protocol

Procedure

After biotinylation reaction through EPL (Expressed Protein Ligation) with (Cys)-GGE-(Lys-Biotin) peptide (described in detail in the following paragraphs), sample was loaded onto the column HiLoad 16/ 600 Superdex 30 pg (1 CV = 120.6 mL). This column was equilibrated with PBS buffer. Protein elution is done with a isocratic gradient of the same buffer at a flow rate of 1.3 mL/min.

Chromatographic conditions:

- Column: HiLoad 16/600 Superdex 30 pg; CV=120.6 mL (GE)
- Flow rate: 1.3 mL/min
- Wavelengths: 214 nm
- Gradient: isocratic in PBS buffer

ZE-ELP[KV7F-36] purification protocol

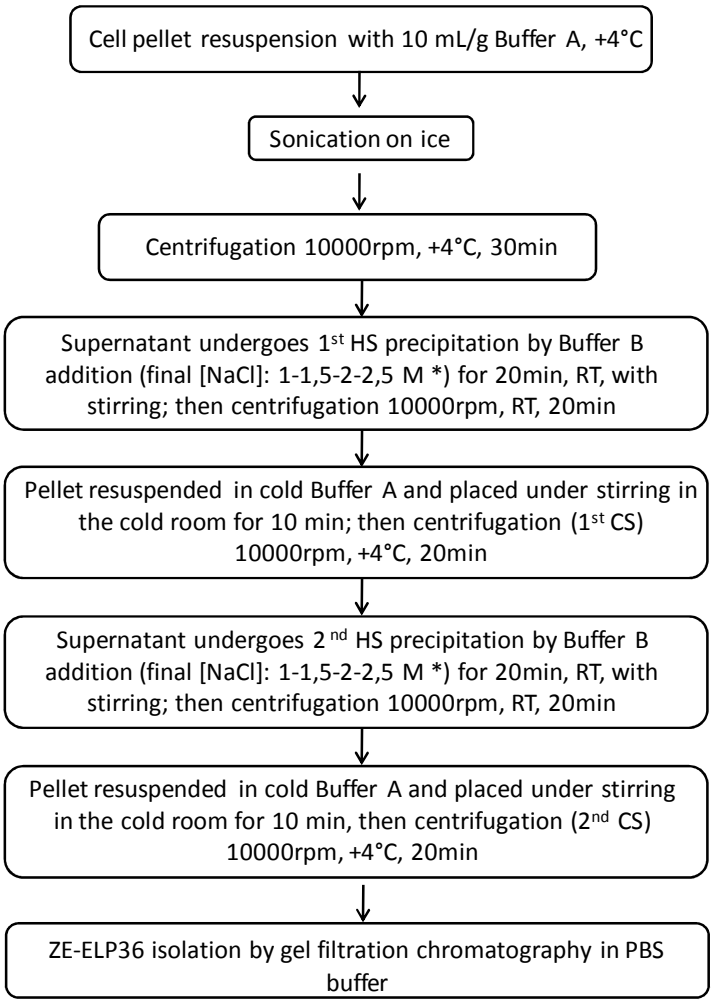

Figure 46. ZE-ELP36 purification scheme. * Various NaCl concentrations used in setting conditions to find the lowest NaCl concentration able to completely precipitate the ZE-ELP36 fusion protein. The best chosen condition was 1.5 M NaCl concentration.

Chromatographic conditions:

- Column: HiLoad 16/600 Superdex 200 pg; CV=120.6 mL (GE)
- Flow rate: 1.3 mL/min
- Wavelengths: 214 nm
- Gradient: isocratic in PBS buffer

MalEp18-ZR purification protocol

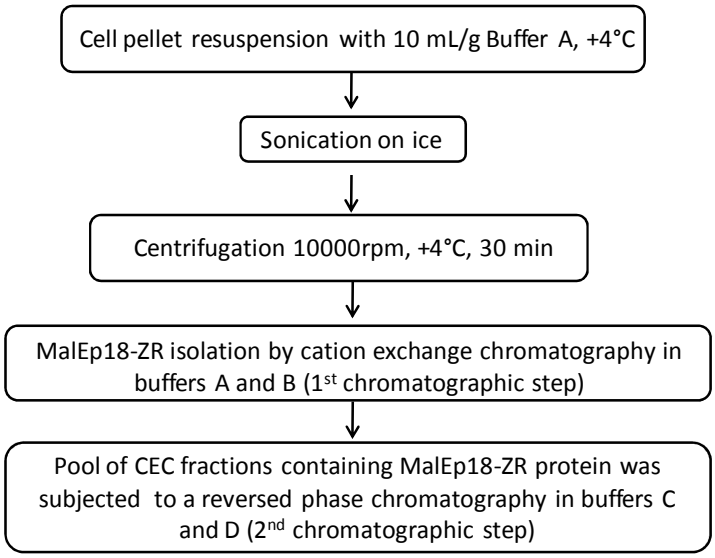

Figure 47. MalEp18-ZR purification scheme.

Buffer	Composition
A	25mM $NaOOCCH_3$; pH 5
B	25mM $NaOOCCH_3$; 1M NaCl; pH 5
C	H2O, Trifluoroacetic acid 0.1% (v/v)
D	CH3CN, Trifluoroacetic acid 0.1% (v/v)

Table 3. List of buffers used in MalEp18-ZR purification protocol.

CEC (Cation Exchange Chromatography) chromatographic conditions:

- Column: Ceramic_HyperD_F_XK_16/5.5; CV=12 mL (PALL)
- Flow rate: 2.0 mL/min
- Wavelengths: 214 nm
- Loading and washing buffer: buffer A
- Gradient: 0-100% buffer B in 60 mL

RPC (Reversed Phase Chromatography) chromatographic conditions:

- Column: Source15RPC 15µm 8.5x100mm ; CV=6.7 mL (GE)
- Flow rate: 2.5 mL/min
- Wavelengths: 214 nm
- Starting conditions: 90% buffer C, 10% buffer D
- Sample loading and washing: 90% buffer C, 10% buffer D
- Gradient: 10-60% buffer D in 35 mL

Purification protocol for HTLVI/II tracers, p18 tracer and scaffold-ABEI 6x-BCN intermediate

Procedure

After synthesis reaction (described in detail in the following paragraphs), samples were loaded onto the column HiLoad 16/600 Superdex 200 pg (1 CV = 120.6 mL). This column was equilibrated with PBS buffer. Protein elution is done with a isocratic gradient of the same buffer at a flow rate of 1.3 mL/min.

Chromatographic conditions:

- Column: HiLoad 16/600 Superdex 200 pg; CV=120.6 mL (GE)
- Flow rate: 1.3 mL/min
- Wavelengths: 260-280-329 nm
- Gradient: isocratic in PBS buffer

SOLID PHASE PEPTIDE SYNTHESIS (SPPS)

The peptides presented in this work were prepared by automated SPPS using Fmoc chemistry on an APEX396 synthesizer (AAPPTEC). The starting resin was a polystyrene Rink amide resin with a functionality of 0.33 mmol/g. Each coupling step was achieved by *in situ* activation of the aminoacidic carboxylic function using HBTU/HOBt as activator agents and DIPEA (N, N-diisopropylethylamine) as base, in DMF. 5-fold molar excess of amino acid/ HBTU/ HOBt and 10-fold excess of DIPEA, over the resin functional groups, were used, with a coupling time of 45 min. After each coupling, Fmoc cleavage was accomplished by treating the peptidyl-resin with 20% piperidine in DMF for 10 min. At the end of the synthesis, the resin was washed with diethylether and dried under vacuum. The final cleavage of the peptides from the resin and simultaneous side-chain deprotection was achieved by treatment for 1h30' with a cleavage mixture consisting in 88% TFA, 5% phenol, 5% water, 2% triisopropylsilane. The peptides were then precipitated from ice-cold tert-butyl-methyl ether, centrifuged and subjected to three ether-washing/centrifugation cycles to remove the scavengers. The crude peptides dried from ether were then lyophilized and characterized by UPLC-MS. Afterwards they were purified by reversed phase HPLC.

The following peptides were synthesized:

- peptide for MalEp18 biotinylation through EPL.
  Sequence: CGGEK-Biotin; MW: 687 Da;
- peptide 1 for the study of click chemistry basic reaction.
  Sequence: K(N3)-TtdsLLPHSNLDHILEPSIPWKSK; MW: 2780 Da;
- peptide 2 for the study of click chemistry basic reaction.
  Sequence: BCN-S-Ttds-AGGTGPEGSRPWARFI; MW: 2467.51 Da;
- HTLVI-N3 peptide.
  Sequence: K(N3)-TtdsLLPHSNLDHILEPSIPWKSK; MW: 2780 Da;
- HTLVII-N3 peptide.
  Sequence:
  K(N3)-TtdsTQPPPTSPPLVHDSDLEHVLTPSTSWTTKILKF;
  MW: 4223.3.

p18 peptide with N-terminal azido-group for the synthesis of p18-tracer was purchased by Polypeptide.
Sequence:K(N3)STAVAQSATPSVSSSISSLRAATSGATAAASAAAA VDTGSGGGGQPHDTAPRGARKKQ;
MW: 5589.8 Da.

UPLC/MS analysis (peptides synthesis)

UPLC-MS analyses were performed using a Waters Acquity® system on a reverse phase Acquity UPLC® BEH C18 1.7um 2.1x100 mm column heated at 45°C. Eluents: H2O, Trifluoroacetic acid 0.02% (v/v) (A), CH3CN, Trifluoroacetic acid 0.02% (v/v) (B). Flow: 0.4 mL/min. Absorbance read at 214 nm.
Gradients used:

- peptide 1 and 2 (click chemistry basic reaction): 1 min isocratic condition at 20% B, then to 50% B in 4 min, afterwards to 80% B in 0.2 min followed by 0.5 min isocratic run and return to the starting conditions.
- HTLVI/II-N3 peptides: 1 min isocratic condition at 20% B, then to 50% B in 4 min, afterwards to 80% B in 0.2 min followed by 0.5 min isocratic run and return to the starting conditions.
- peptide for MalEp18 biotinylation through EPL: 1 min isocratic condition at 5% B, then to 15% B in 4 min, afterwards to 80% B in 0.2 min followed by 0.5 min isocratic run and return to the starting conditions.

HPLC purification

The peptides were purified through reversed phase HPLC using a Waters preparative system on a XBridge™ Prep C18 5µm 30 x150 mm column (Waters). H2O, Trifluoroacetic acid 0.1% (v/v) (A), CH3CN, Trifluoroacetic acid 0.1% (v/v) (B). Absorbance read at 214 nm.

Gradients used:

- peptide 1 and 2 (click chemistry basic reaction): 20% eluent B for 5 min, 20 to 50% eluent B in 20 min, to 80% eluent B in 5 min, flow rate 30 mL/min.
- HTLVI/II-N3 peptides: 20% eluent B for 5 min, 20 to 50% eluent B in 20 min, to 80% eluent B in 5 min, flow rate 30 mL/min.
- peptide for MalEp18 biotinylation through EPL: 5% eluent B for 5 min, 5 to 15% eluent B in 20 min, to 80% eluent B in 5 min, flow rate 30 mL/min.

The collected fractions were analyzed by UPLC and those containing the target species with high purity grade were pooled together and lyophilized. The analytical characterization of the purified pools by UPLC/MS was finally carried out.

UPLC/MS analysis (reactions monitoring)

In order to monitor the following reactions:

- formation of MalEp18-thioester (addition of MESNA);
- biotinylation of MalEp18 with CGGEK-Biotin through EPL;
- SPAAC reaction between MalEp18(pAzF)/pep1 and BCN biotin;
- click chemistry basic reaction between pep1 and pep2;

UPLC-MS analyses were performed using a Waters Acquity® system on a reversed phase Acquity UPLC® BEH300 C4 1.7μm, 2.1x100 mm column heated at 45°C. Eluents: H2O, Trifluoroacetic acid 0.02% (v/v) (A), CH3CN, Trifluoroacetic acid 0.02% (v/v) (B). Flow: 0.4 mL/min. Absorbance read at 214 nm. Gradient used: 1 min isocratic condition at 10% B, then to 60% B in 4 min, afterwards to 80% B in 0.2 min followed by 0.5 min isocratic run and return to the starting conditions.

THIOLYSIS REACTION WITH MESNA: MalEp18-THIOESTER FORMATION

For the cleavage of MalEp18 target protein from *Mxe*GyrA-ELP36 tag and the formation of thioester on the same target protein, MESNA reactive (stock solution 1M in water) was added to the sample, at the end of ITC process, at a final concentration of 50mM. The reaction was

carried out in phosphate buffer at room temperature and reaction time course was followed by UPLC/MS analysis: 3,5 hours of reaction was the time to completely convert MalEp18- *Mxe*GyrA -ELP KV7F36 into the MalEp18-thioester.

Phosphate buffer: 50mM Na2HPO4*2H2O; 5mM EDTA; pH 8.

BIOTINYLATION OF MalEp18 ANTIGEN THROUGH EXPRESSED PROTEIN LIGATION TECHNIQUE

The EPL reaction between MalEp18-thioester (stock solution 4 mg/ml in phosphate buffer) and (Cys)-GGE-(Lys-Biotin) peptide (stock solution 8 mg/ml in phosphate buffer) was carried out in phosphate buffer, over night, at room temperature, in presence of 8 fold molar excesses of peptide. The reaction was monitored by UPLC/MS analysis.

MalEp18-thioester MW: 7055 Da; (Cys)-GGE-(Lys-Biotin) peptide MW: 687 Da; MalEp18-biotin (product) MW: 7760 Da.
Phosphate buffer: 50mM Na2HPO4*2H2O; 5mM EDTA; pH 8.

CLICK CHEMISTRY BASIC REACTION: peptide1-N3 + peptide2-BCN

Peptide1-N3 and peptide2-BCN were resuspended in different buffers (PBS pH 7.4; Hepes pH 6.8; Borate pH 8.3; DMSO) at a final concentration of 10 mg/ml and 2,5 mg/ml, respectively.
The click chemistry reaction was performed in the different buffers mentioned above (PBS pH 7.4; Hepes pH 6.8; Borate pH 8.3; DMSO), at different temperatures (-20°C; 4°C; RT; 15°C and 37°C) and different molar ratios (1:1; 1:2; 1:3 → pep2-BCN:pep1-N3), in combination between them. In particular, the following reaction concentrations were used: 0,15 mg/ml for peptide2-BCN in presence of 1 (0,176 mg/ml), 2 (0,35 mg/ml) or 3 (0,53 mg/ml) fold molar excesses of peptide1-N3.The kinetic of each reaction (t0; t1h; t2,5h; t4h; t24h; t48h) was monitored by UPLC/MS analysis.

Peptide1-N3 MW: 2780 Da; peptide2-BCN MW: 2467.51 Da; product (pep1+pep2) MW: 5247.51 Da.

SPAAC REACTION BETWEEN MalEp18(pAzF) ANTIGEN OR PEPTIDE1-N3 AND BCN-BIOTIN

MalE-p18(pAzF) protein or peptide1-N3 were resuspended at a final concentration of 2 mg/ml in different buffers: (1) phosphate buffer, (2) phosphate buffer with the addition of sulfo-betaine (NDSB-195), (3) phosphate buffer with the addition of UREA 8M and (4) DMSO. BCN-biotin reactive was solubilized in DMSO at a final concentration of 50 mg/ml.
SPAAC reactions (MalEp18(pAzF)+BCN-biotin and peptide1-N3+BCN-biotin) were carried out in the different buffers mentioned above, over night, at 37°C, and in presence of 8 fold molar excesses of BCN-biotin. Reactions were monitored by UPLC/MS analysis.

MalEp18(pAzF) MW: 6981 Da; peptide1-N3 MW: 2780 Da; BCN-biotin MW: 550.71 Da; MalEp18-biotin (product) MW: 7531.71 Da; pep1-biotin (product) MW: 3330.71 Da.
Phosphate buffer: 50mM Na2HPO4*2H2O; 5mM EDTA; pH 8.

SCAFFOLD-ABEI-BCN INTERMEDIATE SINTHESYS (for p18-tracer and HTLVI/II tracers)

10 mg of scaffold (stock solution 10 mg/mL in DMSO) was reacted with 1,12 mg of ABEI cyclic (stock solution 2 mg/mL in DMSO) at a molar ratio of 1:6. This reaction was performed in presence of DIPEA as base at a final concentration of 1% (v/v). Sample was swirled and allowed to react overnight, at RT, in the darkness. 2,68 mg of BCN-NHS reactive (stock solution 50 mg/mL in DMSO) were added to Scaffold-ABEI conjugate (molar ratio = 1:10). The reaction was performed for 2 hour, at RT, in the darkness. Final Scaffold-ABEI-BCN conjugate was purified on a gel filtration column type Superdex 200 16/60 on a AKTA system, as described above.

p18-TRACER AND HTLVI/II-TRACERS SINTHESYS

0,8 mg of scaffold-ABEI-BCN intermediate previously purified (stock solution 0.47 mg/mL in PBS), was reacted with 0,77 mg of HTLVI-N3 peptide or with 1,17 mg of HTLVII-N3 peptide or with 1,55 mg of p18-

N3 peptide, at a molar ratio of 1:8 in each case (stock solution for all three peptides: 10 mg/mL in PBS).
Samples were swirled and allowed to react overnight, at 37°C, in the darkness. Final scaffold-ABEI-HTLVI/II or scaffold-ABEI-p18 conjugates were purified on a gel filtration column type Superdex 200 16/60 on a AKTA system, as described above.

LIAISON® EBV VCA IgM AND IgG ASSAYS

As already described in the introduction, these immunoassays permit to obtain the determination of specific IgM or IgG to EBV viral capsid antigen (VCA) in human serum or plasma samples. In particular, both immunoassays provide an indirect format in which the p18 synthetic peptide acts on solid phase (magnetic particles with tosyl groups) as capture binder for specific anti-p18 IgM or IgG, while a monoclonal antibody anti-human IgM or IgG linked to isoluminol-derivative (ABEI), is used as chemiluminescent tracer.

Coating protocol

The PMPs used for the coating of EBV viral capsid antigen (VCA) p18 were the Dynabeads® M-280 Tosylactivated. The coating were made following the procedure recommended by DYNAL:

1. Resuspension of microparticles in resuspension buffer (0.1 M Borate, pH 9.5) at 1% of concentration
2. Addition of the VCA p18 antigen (100 μg/ml)
3. 18 h at 37°C
4. Washing twice with 0.2 M Tris, 0.1% BSA (w/v), pH 8.5
5. 18 h at 37°C
6. Washing with 10 mM PBS, 0.1% BSA (w/v), pH 7.4
7. Resuspension in 10 mM PBS, 0.1% BSA (w/v), pH 7.4 at a final concentration of 0.25%

Assay protocol

In the first step (first incubation) EBV IgM or IgG antibodies present in calibrators, samples or controls bind to the solid phase (p18 synthetic peptide coated on magnetic particles). During the second incubation, the antibody linked to isoluminol-derivative (ABEI) reacts with EBV IgM or

IgG that is already bound to the solid phase. After each incubation, unbound material is removed with a wash cycle. Subsequently, the starter reagents (hydrogen peroxide and 800 ng/ml deuteroferriheme in 1M NaOH) are added and a flash chemiluminescence reaction is thus induced. The light signal, and hence the amount of isoluminol-antibody conjugate, is measured by a photomultiplier as relative light units (RLU) and is indicative of the presence of EBV VCA IgG or IgM antibodies present in calibrators, samples or controls.
MalEp18 recombinant antigen obtained through the use of ELP-Intein system was tested with the same coating protocol (coating concentration: 100 μg/ml) and with the same assay protocol described above.
For MalEp18-biotin recombinant antigen, obtained through the Expressed Protein Ligation (EPL) technique, both the coating protocol and the assay protocol presented some differences described below.

Coating protocol

In this specific case the M-280 Streptavidin-coupled Dynabeads® microparticles were used as solid phase at a final concentration of 0.25%. The MalEp18-biotin recombinant antigen was diluted at a final concentrations of 25 μg/ml or 1 μg/ml in the assay buffer that was added as an additional component in the first incubation provided by the assay protocol described below.

Assay protocol

In the first step (first incubation), MalEp18-biotin recombinant antigen diluted in the assay buffer, binds to the solid phase (streptavidinated magnetic particles) and then EBV IgM or IgG antibodies present in calibrators, samples or controls react with MalEp18-biotin coated on solid phase. During the second incubation, the antibody linked to isoluminol-derivative (ABEI) reacts with EBV IgM or IgG that is already bound to the solid phase. After each incubation, unbound material is removed with a wash cycle. Subsequently, the starter reagents (hydrogen peroxide and 800 ng/ml deuteroferriheme in 1M NaOH) are added and a flash chemiluminescence reaction is thus induced. The light signal, and hence the amount of isoluminol-antibody conjugate, is measured by a photomultiplier as relative light units (RLU) and is indicative of the presence of

EBV VCA IgG or IgM antibodies present in calibrators, samples or controls.

LIAISON® EBV VCA IgM ASSAY WITH VELCRO PEPTIDES

Velcro peptides system was used as indirect immobilization method for the p18 antigen on solid phase in LIAISON® EBV VCA IgM assay.
Two different coating protocols were explored:

1_ with pre-incubation: ZE-ELP36 was coated on tosyl beads, then a off-line pre-incubation was performed with the MalEp18-ZR construct for 2 hours at RT (the molar ratio used for the two construct was 1:1; see coating protocol below). The paramagnetic beads thus obtained (with the p18 antigen indirectly immobilized through the velcro peptides system), were then used in the current assay following the assay protocol described above.

Coating protocol

1. Resuspension of microparticles (Dynabeads® M-280 Tosyl-activated) in resuspension buffer (0.1 M Borate, pH 9.5) at 1% of concentration
2. Addition of the ZE-ELP36 protein (50 μg/ml)
3. 18 h at 37°C
4. Washing twice with 0.025 M Tris, pH 6.8
5. 18 h at 37°C
6. Washing with 10 mM PBS, pH 7.4
8. Resuspension in 10 mM PBS, pH 7.4 at a final concentration of 0.25%. The ZE-ELP36 protein (MW 21,55 kDa) was thus coated at 12,5 μg/ml
7. Addition of MalEp18-ZR antigen (7.09 μg/ml).
   The MalEp18-ZR antigen (MW 12.24 kDa) was reacted with ZE-ELP36 protein at molar ratio 1:1
8. 2h at 37°C
9. Washing twice with 10 mM PBS, pH 7.4

2_ without pre-incubation: ZE-ELP36 was coated on tosyl beads (see coating protocol below) and MalEp18-ZR construct was diluted to a suitable concentration (in order to have the molar ratio 1:1 between the two constucts) in the assay buffer. This last was added as an additional component in the first incubation provided by the assay protocol described below. In detail, 0.25 μg of ZE-ELP36 protein (MW 21,55 kDa; coated at 12,5 μg/ml) were reacted with 0.14 μg of MalEp18-ZR antigen (MW 12.24 kDa; stock solution 1.4 μg/ml) during the first step of assay protocol. In this way the interaction between the two constructs occured during assembly steps of the assay directly on the LIAISON® instrument.

Coating protocol

1. Resuspension of microparticles (Dynabeads® M-280 Tosyl-activated) in resuspension buffer (0.1 M Borate, pH 9.5) at 1% of concentration
2. Addition of the ZE-ELP36 protein (50 μg/ml)
3. 18 h at 37°C
4. Washing twice with 0.025 M Tris, pH 6.8
5. 18 h at 37°C
6. Washing with 10 mM PBS, pH 7.4
7. Resuspension in 10 mM PBS, pH 7.4 at a final concentration of 0.25%. The ZE-ELP36 protein was thus coated at 12,5 μg/ml.

Assay protocol

In this case, in the first step (first incubation) MalEp18-ZR antigen diluted in the assay buffer , reacts with ZE-ELP36 protein coated on solid phase (tosyl magnetic particles), and then EBV IgM antibodies present in calibrators, samples or controls bind to the solid phase (p18 antigen indirectly coated on magnetic particles through velcro peptides system). During the second incubation, the antibody linked to isoluminol-derivative (ABEI) reacts with EBV IgM that is already bound to the solid phase. After each incubation, unbound material is removed with a wash cycle. Subsequently, the starter reagents (hydrogen peroxide and 800 ng/ml deuteroferriheme in 1M NaOH) are added and a flash chemiluminescence reaction is thus induced. The light signal, and hence the amount of isoluminol-antibody conjugate, is measured by a photomul-

tiplier as relative light units (RLU) and is indicative of the presence of EBV VCA IgM antibodies present in calibrators, samples or controls.

LIAISON® EBV VCA IgM REVERSE FORMAT

In the reverse format of LIAISON® EBV VCA IgM, the anti-human IgM antibodies, able to recognize the human IgM present in the sample, are used as a capture element on solid phase, while the p18 antigen is used as a tracer.

Coating protocol

The M-280 Streptavidin-coupled Dynabeads® microparticles were used as solid phase at a final concentration of 0.25%. The biotinylated mAbs anti-human IgM were diluted at a final concentration of 500 ng/ml in the assay buffer that was added as an additional component in the first incubation provided by the assay protocol described below

Assay protocol

In the first step (first incubation) biotinylated anti-human IgM antibodies, diluted in the assay buffer, binds to the solid phase (streptavidinated magnetic particles) and then EBV IgM antibodies present in calibrators, samples or controls react with biotinylated anti-human IgM antibodies coated on solid phase. During the second incubation, the p18-tracer linked to more ABEI molecules (scaffold-ABEI-p18 conjugate) reacts with EBV IgM that is already bound to the solid phase. After each incubation, unbound material is removed with a wash cycle. Subsequently, the starter reagents (hydrogen peroxide and 800 ng/ml deuteroferriheme in 1M NaOH) are added and a flash chemiluminescence reaction is thus induced. The light signal, and hence the amount of isoluminol-antibody conjugate, is measured by a photomultiplier as relative light units (RLU) and is indicative of the presence of EBV VCA IgM antibodies present in calibrators, samples or controls.

LIAISON ® EBV VCA IgG REVERSE FORMAT (mouse sera screening)

In the reverse format of LIAISON ® EBV VCA IgG, the anti-mouse IgG antibodies, able to recognize the IgG present in the sera derived from mice immunized with p18 antigen, are used as a capture element on solid phase, while the p18 antigen is used as a tracer.

Coating protocol

The M-280 Streptavidin-coupled Dynabeads® microparticles were used as solid phase at a final concentration of 0.25%. The biotinylated mAbs anti-mouse IgG were diluted at a final concentration of 500 ng/ml in the assay buffer that was added as an additional component in the first incubation provided by the assay protocol described below

Assay protocol

In the first step (first incubation) biotinylated anti-mouse IgG antibodies, diluted in the assay buffer, binds to the solid phase (streptavidinated magnetic particles) and then EBV IgG antibodies present in mouse sera react with biotinylated anti-mouse IgG antibodies coated on solid phase. During the second incubation, the p18-tracer linked to more ABEI molecules (scaffold-ABEI-p18 conjugate) reacts with EBV IgG that is already bound to the solid phase. After each incubation, unbound material is removed with a wash cycle. Subsequently, the starter reagents (hydrogen peroxide and 800 ng/ml deuteroferriheme in 1M NaOH) are added and a flash chemiluminescence reaction is thus induced. The light signal, and hence the amount of isoluminol-antibody conjugate, is measured by a photomultiplier as relative light units (RLU) and is indicative of the presence of EBV VCA IgG antibodies present in mouse sera.

RESULTS

p18 ANTIGEN PRODUCTION WITH ELP-INTEIN SYSTEM

The Elastin Like Polypeptides (ELP)-intein system based on the use of a self-cleavable temperature responsive tag, as described in detail in the introduction, was explored as an alternative production method for the p18 peptide, in order to solve the problems related to the complexity of the synthetic process of the same antigen.

The gene corresponding to the p18 antigen was cloned in vectors encoding the fusion tag ELP-Intein; in particular for the expression of the resulting p18-*Mxe*GyrA-ELP fusion protein different constructs were tested in order to select the best one. In literature there are some examples in which the variation of the guest residue ("X" residue) in the ELP sequence can help to lower the total number of repeated motifs with a consequent shortening of the ELP-fusion protein sequence (210,211). Among these variants, one of the most promising and used sequences is the following: [KV_7F]. The main difference of this sequence, compared to traditional motif [$V_5A_2G_3$], lies in the nature of the guest residue; in particular the presence of a polar residue of lysine is able to increase the salt sensitivity of the entire ELP sequence, but, at the same time, the polarity of the same residue obstructs the hydrophobic collapse of the polypeptide. To solve this aspect, a highly hydrophobic residue (Phe) was inserted in the motif in order to promote hydrophobic interactions and thus the ELP precipitation process. The sequence ELP [KV_7F] requires a smaller amount of salt to precipitate than the sequence [$V_5A_2G_3$] with the same length. Consequently, ELP [KV_7F] sequence can be used for the precipitation process of ELP-fusion proteins at the same transition temperature used for ELP[$V_5A_2G_3$] sequence but with a lower number of repetitions: 36 repetitions of the ELP [KV_7F] pentapeptide, instead of 90 of [$V_5A_2G_3$] were enough to have an almost equal transition temperature (211; internal data not shown).

On the basis of this background, we transformed the BL21(DE3) *E.coli* strain with two different plasmids: the first is pTME-p18 which encodes for the p18-*Mxe*GyrA-ELP90 fusion protein characterized by the presence of 90 pentapeptide [$V_5A_2G_3$] ELP repeat; the second is pET24-p18-*Mxe*GyrA-ELP36 which encodes for the p18-*Mxe*GyrA-ELP36 fusion protein with 36 pentapeptide [KV_7F] ELP repeat. Table 4 shows the different expression conditions explored for both constructs.

Fermentation	Vector	Temperature (°C)	Induction Time (h)	[IPTG] (mM)
A	pTME-p18	37°C	3	1
B	pET24-p18-*Mxe*GyrA-ELP36	37°C	3	1
C	pTME-p18	15°C	20	0,1
D	pET24-p18-*Mxe*GyrA-ELP36	15°C	20	0,1

Table 4. Different conditions used for p18-*Mxe*GyrA-ELP fusion proteins expression.

No expression is detected in BL21 (DE3) *E. coli* strain, fermented at 37°C, for any of the two constructs: p18-*Mxe*GyrA-ELP90 (A) and p18-*Mxe*GyrA-ELP36 (B) (Figure 48). Instead, for fermentations performed at 15°C, SDS-PAGE analysis shows the expression at very low levels of both proteins: p18-*Mxe*GyrA-ELP90 (C; black arrow; expected molecular weight of 67,22 kDa) and p18-*Mxe*GyrA-ELP36 (D; gray arrow; expected molecular weight of 45,15 kDa).

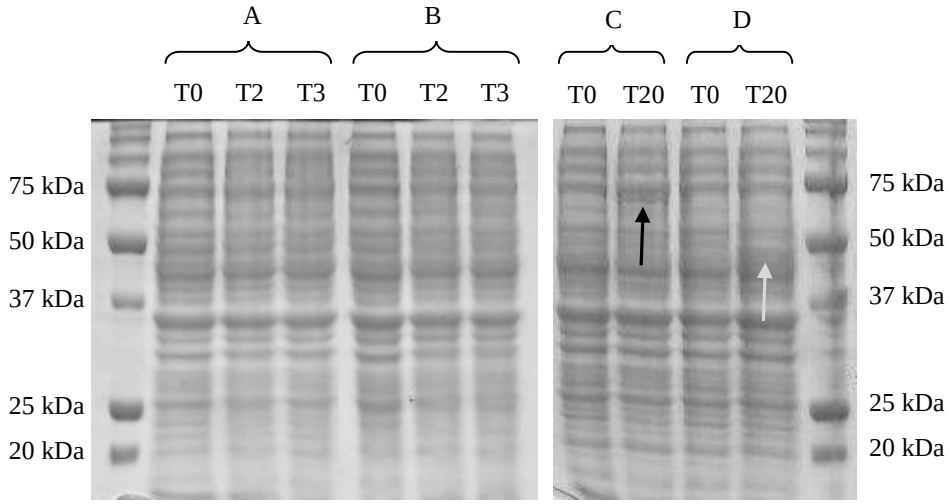

Figure 48. SDS-PAGE analysis showing the induction test of BL21(DE3) pTME-p18 and BL21(DE3) pET24-p18-*Mxe*GyrA-ELP36, fermented at 37°C and 15°C: see table 4 for experimental conditions. Black arrow indicates p18-*Mxe*GyrA-ELP90 target protein and gray arrow indicates p18-*Mxe*GyrA-ELP36 target protein.

In addition, a western blot analysis (Figure 49) was performed in order to confirm the expression of both target proteins in BL21(DE3) *E. coli* cells fermented at 15°C. The presence of bands at lower molecular weight in addition to that relative to the entire target protein (black arrow for p18-*Mxe*GyrA-ELP90 and gray arrow for p18-*Mxe*GyrA-ELP36), indicates that the fusion proteins undergo a partial degradation during the fermentation process.

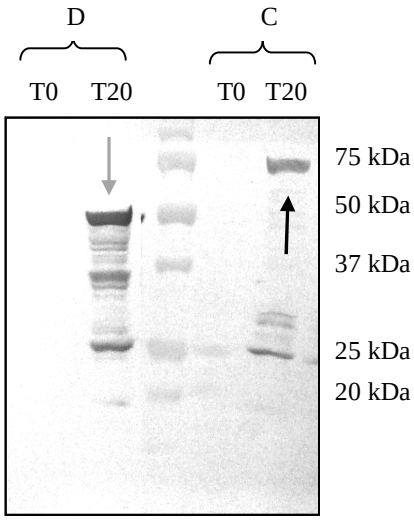

Figure 49. Western Blot analysis of BL21(DE3) pTME-p18 and BL21(DE3) pET24-p18-*Mxe*GyrA-ELP36, fermented at 15°C. Black arrow indicates p18-*Mxe*GyrA-ELP90 target protein and gray arrow indicates p18-*Mxe*GyrA-ELP36 target protein. The staining was performed with rat anti-p18 HRP probe (see Materials and Methods).

To try to improve the low level of expression of the two ELP-fusion proteins, the next step was the use of different *E. coli* strains: BL21 Star™ (DE3) pLysS and Rosetta(DE3) pLysS.
The first strain (BL21 Star™ (DE3) pLysS) is ideal for high-level expression of toxic recombinant proteins. The expression system is based on T7 promoter; all BL21(DE3) strains contain the DE3 lysogen that carries the T7 RNA polymerase gene under control of the *lac*UV5 promoter, and IPTG is required to induce expression of the T7 RNA polymerase and then of genes under the control of the T7 promoter. The pLysS Cam^R (chloramphenicol resistance) plasmid carried by the BL21 Star™ (DE3) pLysS strain expresses T7 lysozyme, a T7 RNA polymerase inhibitor that prevents leaky expression in uninduced cells. The presence of T7 lysozyme lowers the background expression level of target genes under the control of the T7 promoter but does not interfere with the level of expression achieved following induction by IPTG. Moreover, the absence of some proteases (*lon* and *OmpT*) reduces degradation of heterologous proteins. Finally, the system offers enhanced mRNA stability thanks to a mutation in the RNaseE gene (*rne*131), which is involved in mRNA degradation.
The second type of cells, Rosetta(DE3) pLysS, are BL21 derivatives designed to enhance the expression of eukaryotic proteins that contain codons rarely used in *E. coli*. Thus the Rosetta strains provide for "universal" translation which is otherwise limited by the codon usage of *E. coli*. The tRNA genes are driven by their native promoters and these rare tRNA genes are present on the same plasmids that carries the T7 lysozyme gene. As BL21 Star™ (DE3) pLysS, also Rosetta(DE3) pLysS strain expresses T7 lysozyme, which further suppresses basal expression of T7 RNA polymerase prior to induction, thus stabilizing pET recombinants encoding target proteins that affect cell growth and viability.
Also in this case, for each strain, we used the same fermentation conditions previously listed for BL21(DE3) (Table 4).

- **BL21 Star™ (DE3) pLysS strain**

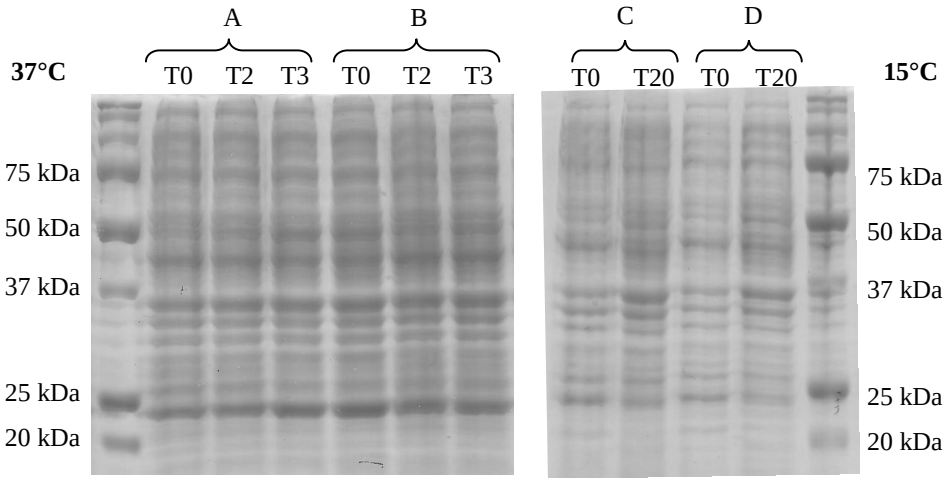

Figure 50. SDS-PAGE analysis showing the induction test of BL21 Star™ (DE3) pLysS pTME-p18, at 37°C (A) and 15°C (C) and BL21 Star™ (DE3) pLysS pET24-p18-*Mxe*GyrA-ELP36, at 37°C (B) and 15°C (D).

- **Rosetta(DE3) pLysS strain**

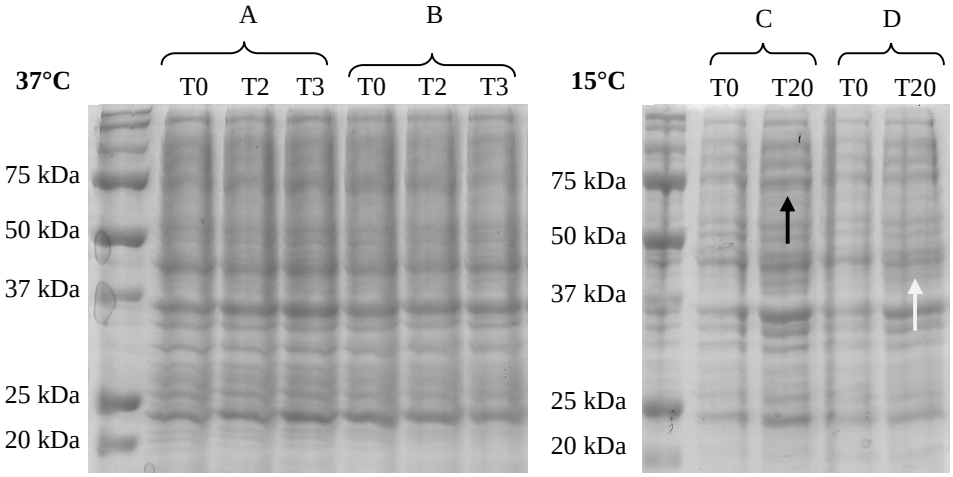

Figure 51. SDS-PAGE analysis showing the induction test of Rosetta (DE3) pLysS pTME-p18, at 37°C (A) and 15°C (C) and Rosetta (DE3) pLysS pET24-p18-*Mxe*GyrA-ELP36, at 37°C (B) and 15°C (D). Black arrow indicates p18-*Mxe*GyrA-ELP90 target protein and gray arrow indicates p18-*Mxe*GyrA-ELP36 target protein.

The induction test performed in BL21 Star™ (DE3) pLysS *E. coli* strain, at 37°C and 15°C (Figure 50), shows the lack of expression for both target proteins (p18-*Mxe*GyrA-ELP90 and p18-*Mxe*GyrA-ELP36). Whereas, the induction test performed in Rosetta (DE3) pLysS *E. coli* strain (Figure 51) shows the expression, but at very low levels, of both proteins p18-*Mxe*GyrA-ELP90 (C; black arrow; expected molecular weight of 67,22 kDa) and p18-*Mxe*GyrA-ELP36 protein (D; gray arrow; expected molecular weight of 45,15 kDa), only for fermentations performed at 15°C. In fermentations carried out at 37°C (A and B; Figure 51), none of the two target proteins is expressed.
The use of different *E. coli* strains (BL21 Star™ (DE3) pLysS and Rosetta (DE3) pLysS) with characteristics aimed to improve the expression of heterologous proteins, however, didn't not allow an increase of expression for our specific ELP fusion proteins.

Therefore, we tried to optimize the expression of our fusion proteins working on the design of the related constructs. Previous constructs encoding for fusion proteins which include the sequence of the p18 peptide, developed in the past in our laboratories, showed a good level of expression in *E. coli* cells if the p18 antigen sequence was positioned at the C-terminus than the fusion partner sequence and a very low level of expression in the opposite case (positioning at the N-terminus), as in our current fusion proteins (p18-*Mxe*GyrA-ELP). Assuming that in our constructs we have available a C-terminal mutated intein (*Mxe*GyrA N198A) and therefore an intein able to perform an N-terminal cleavage (as described previously in detail), it is not possible to change the position of the p18 antigen which must necessarily remain at N-terminus, to be separated by ELP tag after purification through the auto-cleavage activity of the above mentioned intein. Other strategies to try to improve the expression of our fusion proteins rely on the optimization of N-terminal nucleotide sequence. In literature it is widely reported that initiation of protein biosynthesis is a determinant for the efficiency of gene expression at the translational level; in particular some papers (212) have shown that the characteristics (in terms of codon type) of nucleotide sequence at N-terminal region (in particular the codon that follows the AUG initiation triplet) affect gene expression in *E. coli*: a difference up to 20-fold can be detected in gene expression on the basis of the different sequences used.

The authors are not, however, arrived at a final rule concerning the optimization of the N-terminal sequence to ameliorate protein expression at the translational level and even at a conclusive explanation of the process: in fact the effects of this optimization did not correlate with the levels of intracellular cognate tRNA, with putative secondary mRNA structures, or with mRNA stability. Consequently it is difficult, on the basis of this information, to perform an optimization of the N-terminal region of the nucleotide sequence of our target ELP-fusion protein, also considering that a similar type of sequence optimization was already performed on the entire sequence of the p18 target protein during the preparation of the synthetic gene. During this process, in fact, a specific software generates several optimized variants of target sequence in an evolutionary approach that addresses the most important sequence parameters in parallel (identification of the best way to incorporate the requested sequence elements; elimination of cryptic splice sites and RNA destabilizing sequence elements for increased RNA stability; addition of RNA stabilizing sequence elements; codon optimization and G/C content adaptation for the expression system; intron removal; avoidance of stable RNA secondary structures). At the end, the software selects one optimized DNA sequence that best suits specific requirements.

Therefore, to optimize the expression of our ELP-fusion proteins, we decided to adopt the following strategy conceived in order to support the translation process in the initial steps: the strategy relies on the addition at N-terminus of our constructs (before the sequence of the p18 antigen) of a short sequence (the first 6 amino acids) of maltose binding protein, a protein often used as fusion tag for the purification of heterologous proteins in *E. coli* cells. It is always well expressed in *E. coli* cells and for this reason the presence of its first 6 amino acids at N-terminus could promote the initiation of translation of our fusion proteins and consequently of the whole process.

Only the construct containing 36 repetitions of the ELP [KV_7F] pentapeptide has been cloned with this new type of strategy; the cloning of this construct named MalEp18-*Mxe*GyrA-ELP36 is described in detail in materials and methods section.

Even for MalEp18-*Mxe*GyrA-ELP36 fusion protein, the same expression conditions used for the previous constructs were explored (Table 5).

Fermentation	Temperature (°C)	Induction Time (h)	[IPTG] (mM)
A	37°C	3	1
B	15°C	20	0,1

Table 5. Different conditions used for MalEp18-*Mxe*GyrA-ELP36 fusion protein expression.

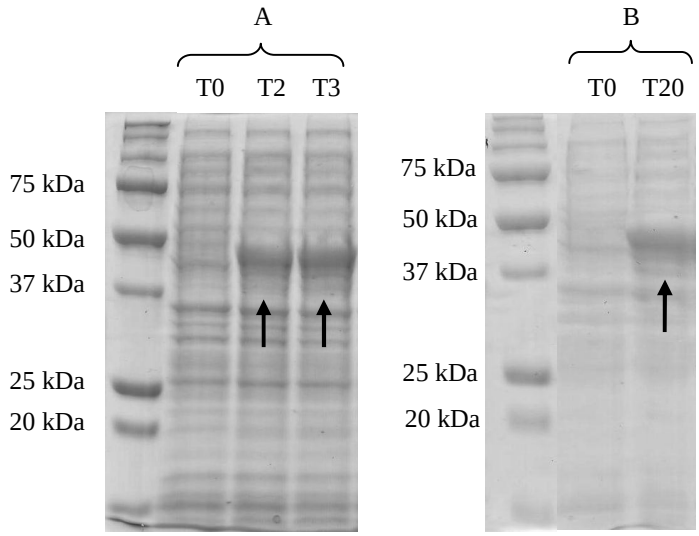

Figure 52. SDS-PAGE analysis showing the induction test of BL21 (DE3) pET24-MalEp18-*Mxe*GyrA-ELP36, fermented at 37°C and 15°C. Black arrows indicate MalEp18-*Mxe*GyrA-ELP36 target protein.

The induction test (Figure 52) shows that the target protein MalEp18-*Mxe*GyrA-ELP36 (expected molecular weight of 45,31 kDa) is well expressed in both conditions (37°C; panel A and 15°C; panel B). The strategy, which involves the placement of the first six amino acids of MBP (Maltose Binding Protein) at the N-terminus, before the sequence of the p18 antigen, had proven to be successful.
Before proceeding to the purification step by using Inverse Transition Cycling (ITC) process, we verified the solubility of the fusion protein in both conditions (37°C and 15°C) as detailed in Materials and Methods section.

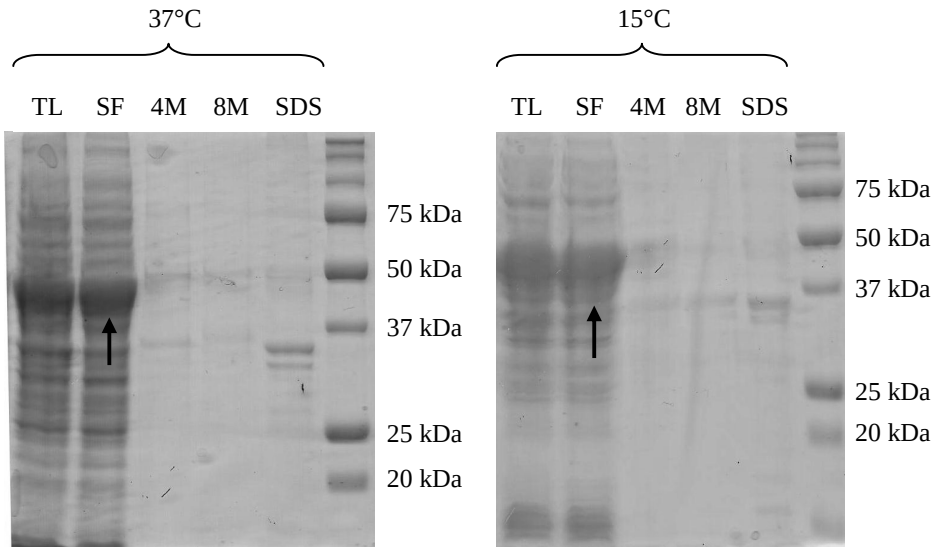

Legend:
TL= Total Lysate
SF= Soluble Fraction
4M= 4M UREA
8M= 8M UREA
SDS= SDS Sample buffer

Figure 53. SDS-PAGE analysis showing the solubility test of BL21 (DE3) pET24-MalEp18-*Mxe*GyrA-ELP36, fermented at 37°C and 15°C. Black arrows indicate the MalEp18-*Mxe*GyrA-ELP36 present in soluble fraction.

As suggested by the SDS PAGE of solubility test (Figure 53), the MalEp18-*Mxe*GyrA-ELP36 target protein is completely soluble in both conditions of fermentation (37°C and 15°C). In fact, the band corresponding to MalEp18-*Mxe*GyrA-ELP36 (expected molecular weight of 45,31 kDa) is visible, in both cases, in the total lysate (TL lane) and in the soluble fraction (SF lane), but it is not present in fractions containing urea or SDS sample buffer (insoluble fractions).
For the purification we chose to use the fermentation carried out at 15°C; normally the amount of cell paste obtained at the end of the fermentation process performed at 15°C is greater than that obtained at the end of

fermentation at 37°C, and therefore potentially greater is also the amount of target protein to be purified.

For purification of the MalEp18-*Mxe*GyrA-ELP36 fusion protein, we exploited the aggregation and solvation properties of ELPs by using the Inverse transition Cycling (ITC) process, as described in the introduction and as shown schematically in Figure 54. The phase transition can occur by varying the temperature of the solution containing the ELP-fusion proteins depending on ELP sequence, or in isothermal conditions by varying the salt concentration in the buffer. We decided to promote the ELP-fusion proteins precipitation (phase transition) through the addition of NaCl, in order to obtain the precipitation of our target protein avoiding to overcome the room temperature and thus avoiding possible problems of protein denaturation.

In order to determine the best NaCl concentration to be used in the purification process, we explored a range of NaCl concentrations between 1.0 and 2.5 M. The optical analysis of solutions containing the target ELP-fusion protein (turbidity of the ELP-fusion protein solution) has shown that, at room temperature (~25°C), only with a salt concentration of 2.5 M, the fusion protein undergoes to the inverse phase transition (precipitation). For this reason, in steps of ITC purification that provide the ELP-fusion protein precipitation, we worked at a NaCl concentration of 2.5 M, as indicated in Figure 54. One round of ITC process (salt-induced precipitation of ELP followed by a hot spin and resuspension in a low ionic buffer followed by a cold spin) was repeated twice, with the aim to obtain a good purity degree of the ELP fusion protein (Figure 54).

At the end of ITC process, the adding of DDT with free thiol groups, promoted the self-cleavage activity of *Mxe*GyrA intein and therefore the release of the MalEp18 antigen from the ELP-Intein tag (Figure 54). The reaction was performed overnight at room temperature, in the low ionic strength buffer used for the resuspension of ELP-fusion protein and in presence of a large excess of DTT (50 mM).

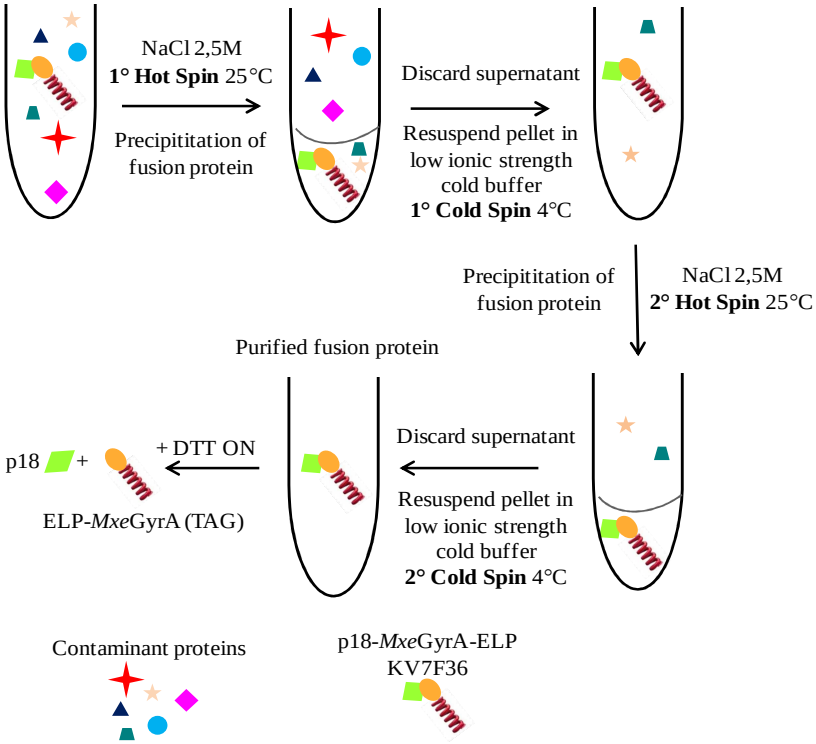

Figure 54. ITC purification scheme and cleavage with DTT.

The SDS-PAGE analyzing the ITC process described above is shown in Figure 55. HS (Hot Spin) lanes represent the supernatant obtained after precipitation process and centrifugation at room temperature; in these lanes the ELP-fusion target protein is therefore not present. CS (Cold Spin) lanes represent the supernatant obtained after resuspension process and centrifugation at +4°C; in these fractions the ELP-fusion protein is present. After the first precipitation-solvation round (1st CS lane), the MalEp18-*Mxe*GyrA-ELP36 target protein reached a good purity grade which was further increased by a second precipitation-resuspension cycle (2nd CS lane). DTT lane indicates the sample after cleavage with DTT. As

clearly shown in the SDS-PAGE analysis, the cleavage reaction occurred successfully (both cleavage products, MalEp18 target protein and *Mxe*GyrA-ELP36 tag, are visible) and only a small amount of the entire precursor protein (MalE-*Mxe*GyrA-ELP36) remains.

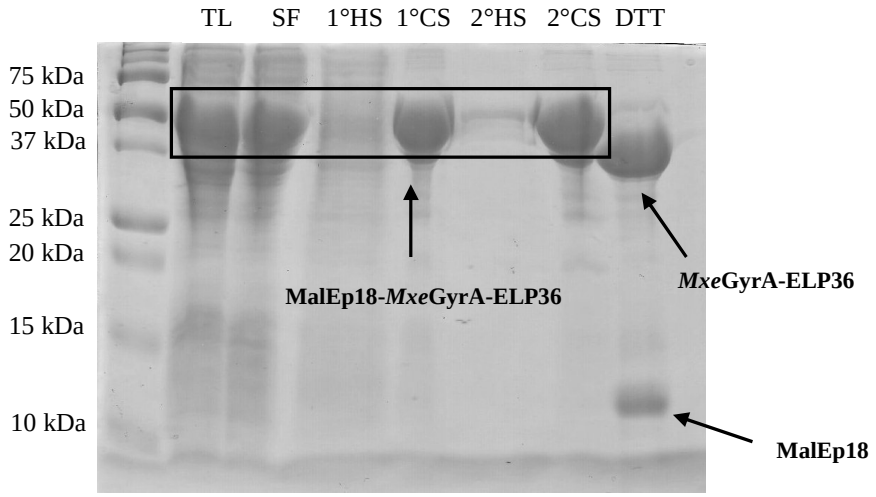

Legend:
TL= Total Lysate
SF= Soluble Fraction
1°HS= 1st Hot Spin supernatant
1°CS= 1st Cold Spin supernatant
2°HS= 2nd Hot Spin supernatant
2°CS= 2nd Cold Spin supernatant
DTT= cleavage with DTT

Figure 55. SDS PAGE analysis monitoring ITC purification process and cleavage with DTT.

To separate the cleaved tag from the target protein, a third round of inverse transition cycling was performed. The addition of salt (NaCl 2.5 M) at this level of the purification process, promotes the intein-ELP tag precipitation, while the MalEp18 target protein remains in solution.
Figure 56 shows the SDS PAGE analysis monitoring the 3th inverse transition cycling round after cleavage with DTT.

In 3°HS lane is present a band corresponding to the soluble MalEp18 protein, while in 3°CS lane is present the *Mxe*GyrA-ELP36 tag after precipitation and resuspension.

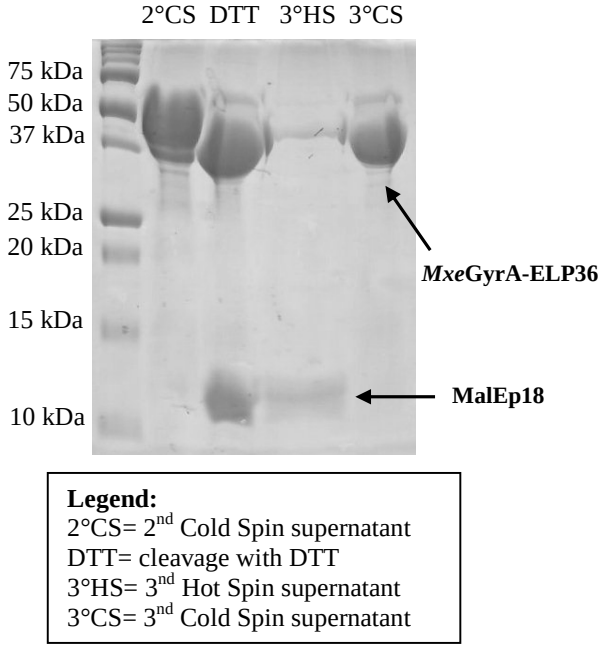

Figure 56. SDS PAGE analysis monitoring the 3th ITC round after cleavage with DTT.

With this third cycle of ITC purification, the two species (MalEp18 target protein and *Mxe*GyrA-ELP36 tag) were separated quite well, as shown by the SDS-PAGE analysis (Figure 56; 3° HS and 3° CS lanes). However, the fraction containing the purified target protein (3° HS lane) showed a slight contamination of *Mxe*GyrA-ELP36 tag; at the same time, this step resulted in a considerable loss of the target protein (3° HS lane). For these reasons, we decided to isolate the MalEp18 target protein from the *Mxe*GyrA-ELP36 tag, after cleavage with DTT, through a chromatographic step. In particular, we performed a Reversed Phase Chromatography (RPC) to try to optimize the purity and the yield of the purified target protein. The choice of this chromatographic technique was determined by peptidic nature of the MalEp18 target protein.

After cleavage with DTT, the sample was loaded on a reversed phase column (Source 15RPC, see materials and methods section) previously equilibrated with water/TFA 0.1% and CH3CN/TFA 0.1%. Elution was performed with a linear gradient of 10-60% CH3CN/TFA 0.1% in 70 mL. A good separation of the MalEp18 target protein from the *Mxe*GyrA-ELP36 tag was achieved (Figure 57).

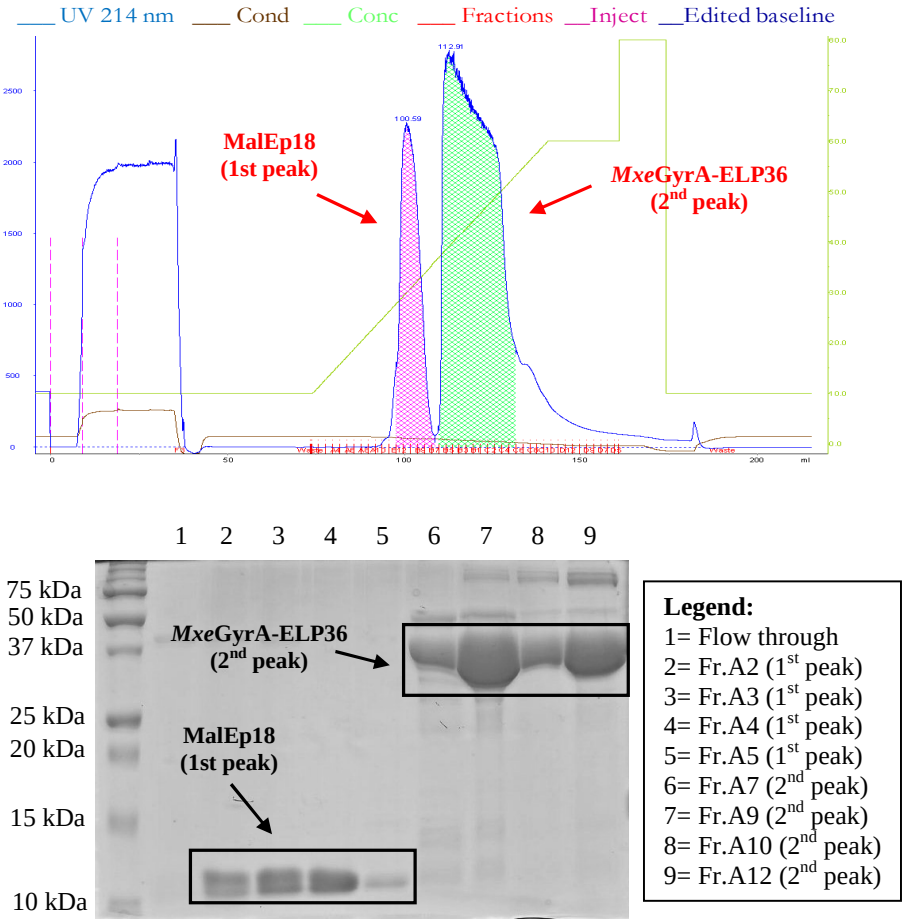

Figure 57. Chromatographic profile of reversed phase purification of the cleaved MalEp18 target protein and *Mxe*GyrA-ELP36 tag (above) and corresponding SDS-PAGE analysis of eluted fractions (below).

The pool of fractions corresponding to the MalEp18 target protein (1st peak of RPC chromatographic profile) was then subjected to lyophilization and quantified. The complete process was repeated three times, and as illustrated in Table 6, showing the data regarding the yield of purification, the ELP-Intein system has proven to be a good and quite reproducible method for the production of the p18 antigen.

Batch	Liter of fermentation	Bacterial pellet weight (g)	Final amount of purified protein (mg)	mg/g cell pellet
A	1	3,95	12,1	3.06
B	1	3,75	10,5	2,8
C	0,5	1,15	2,8	2,43

Table 6. Data regarding the yield of three different batch of purification for the production of the p18 antigen through ELP-Intein system.

SITE-SPECIFIC BIOTYNILATION OF p18 ANTIGEN THROUGH INTEIN-MEDIATED PROTEIN LIGATION TECHNIQUE

As described in the introduction, a C-terminal mutant version of the splicing protein (e.g. *Mxe*GyrA(N198A) intein) has been demonstrated to be defective in completion of the splicing reaction but still capable of thioester intermediate formation (step 1 of intein-mediated protein splicing mechanism). Proteins expressed as in-frame N-terminal fusions to such mutant inteins can be cleaved by thiols to give the corresponding protein-thioester derivatives. In the expressed protein ligation technique, the nucleophilic attack on this thioester by the N-terminal cysteine of a synthetic peptide leads to the ligation of the two reactants through a native peptide bond.
The C-terminal thioester variant of the p18 antigen resulting from the intein-auto-cleavage activity at the end of purification process through ELP-intein system, was used in the expressed protein ligation technique (or intein-mediated protein ligation technique) to obtain the site-specific biotinylation of the same p18 antigen. In particular a synthetic peptide containing a thiol group (Cys residue) at the N-terminus and, a lysine-biotin at the C-terminus was used for the reaction with the recombinant C-terminal thioester p18 in order to obtain a C-terminal site-specific modification (biotinylation) of our target protein.

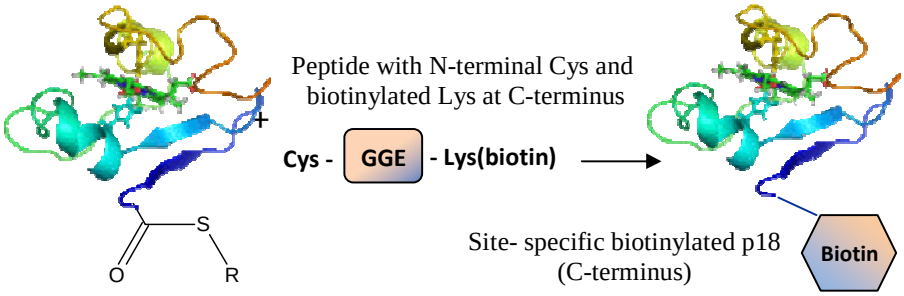

Figure 58. Schematic representation of p18 antigen C-terminal site-specific biotinylation through expressed protein ligation technique.

Therefore, we carried out the MalEp18-*Mxe*GyrA-ELP36 protein purification by using the Inverse transition Cycling (ITC) process, exactly as described above (scheme in Figure 54). The only difference is related to the reagent used to induce transthioesterification and then to promote the C-terminal thioester formation. A variety of molecules can be used to induce thiolysis of intein fusion proteins, the choice is based on two main factors: the formed protein thioester should be stable to hydrolysis in order to be isolated and the thioester should also be reactive enough in the subsequent expressed protein ligation (EPL) reaction. The majority of the molecules used, including DTT, guarantees the stability of the thioester but simple alkyl thioesters are not very reactive in EPL. Other molecules, such as 2-mercaptoethanesulfonic acid (MESNA), instead, permit to generate more reactive α-thioesters in situ through transthioesterification. For these reason, we performed the cleavage reaction at the end of ITC process with MESNA. The transthioesterification reaction was monitored by UPLC/MS analysis until the completeness; in this way we avoided that the reaction proceeded for an excessive time, trying so to limit or exclude any phenomena of hydrolysis of the thioester, the stability of which appears to be necessary for the subsequent EPL reaction. Figure 59 shows the SDS-PAGE analyzing the ITC process and thiolysis with MESNA, whereas in Figure 60 is reported the UPLC analysis monitoring the cleavage reaction of the MalEp18-*Mxe*GyrA-ELP36 fusion protein with MESNA.

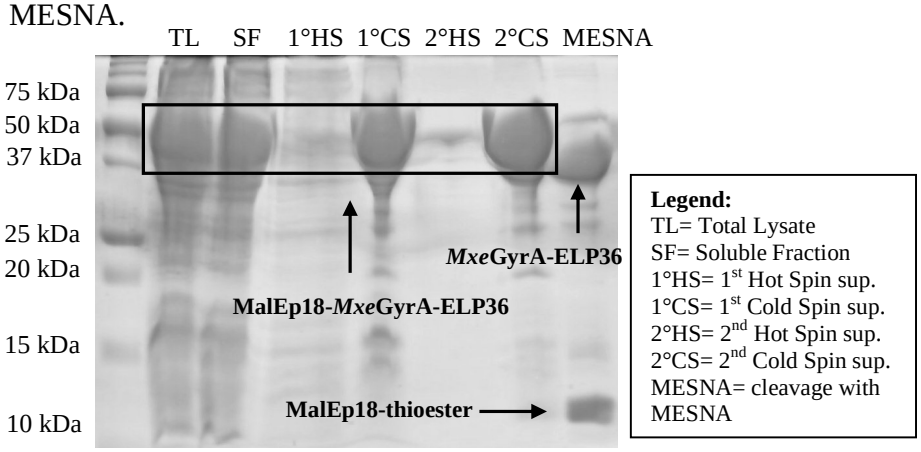

Figure 59. SDS PAGE analysis monitoring ITC purification process and cleavage with MESNA.

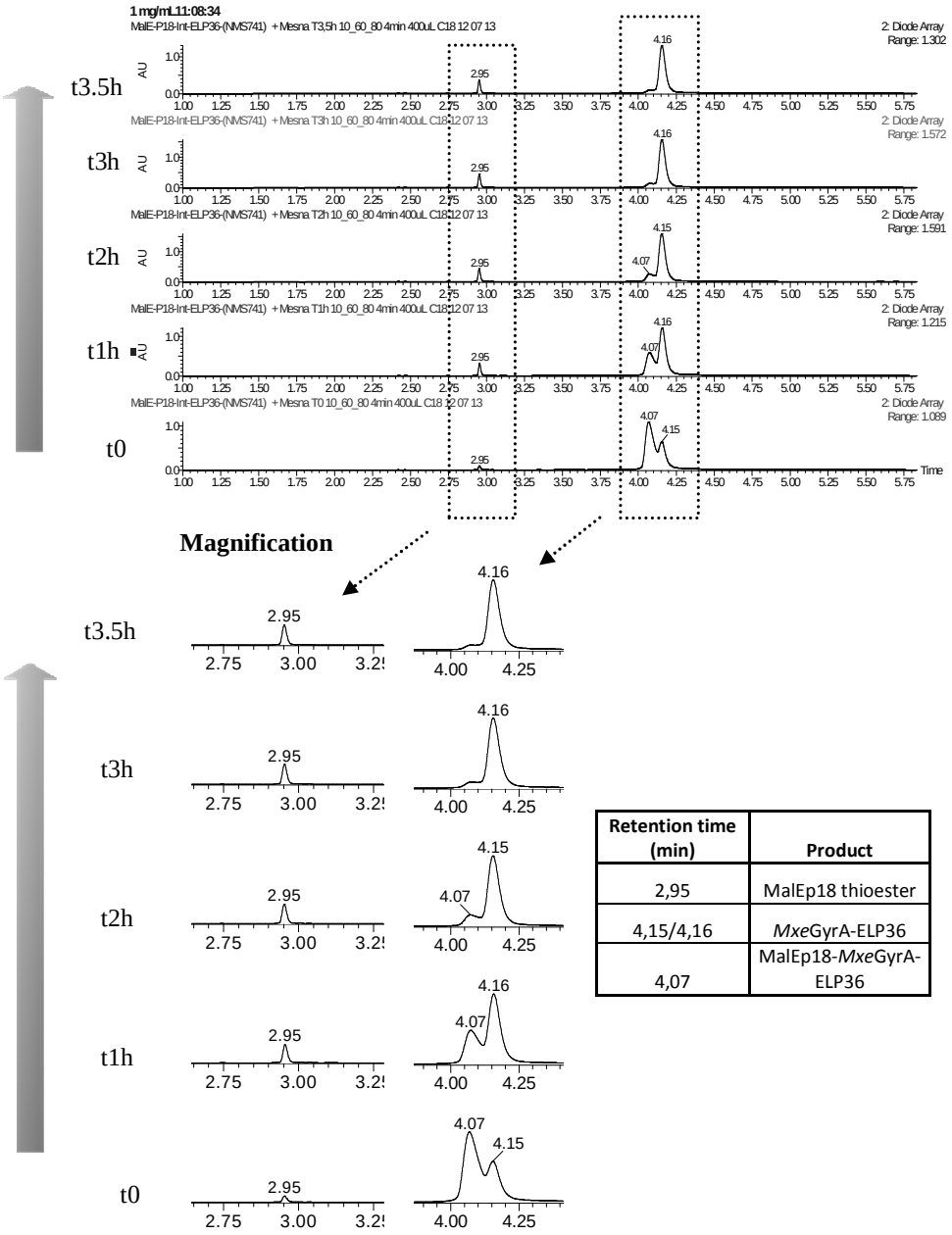

Retention time (min)	Product
2,95	MalEp18 thioester
4,15/4,16	*Mxe*GyrA-ELP36
4,07	MalEp18-*Mxe*GyrA-ELP36

Figure 60. UPLC analysis monitoring thiolysis reaction with MESNA.

UPLC analysis (Figure 60. Column Acquity UPLC BEH300 C4 1.7µm, 2.1x100 mm, Waters; buffer A: H2O/TFA 0.1% v/v, buffer B: CH3CN/TFA 0.1% v/v; gradient 10-60% buffer B in 4 minutes) showed that the cleavage reaction with MESNA occurs already after 1 hour with the appearance of the peak related to the MalEp18 target protein (peak with retention time of 2.95 min) and to that relative to the *Mxe*GyrA-ELP36 tag (peak with retention time of 4.15/4.16 min). The reaction is complete approximately after 3.5 hours (complete disappearance of the peak at 4.07 min, relative to the entire protein MalEp18-*Mxe*GyrA-ELP36). Mass analysis, for the identification of the species involved in the reaction, was performed only for the peak relative to the MalEp18 thioester (MW 7055.98 Da; data not shown). MalEp18-*Mxe*GyrA-ELP36 precursor and *Mxe*GyrA-ELP36 tag have masses too high to be identified through the used mass analysis system.

After cleavage reaction with MESNA, to separate the cleaved tag *Mxe*GyrA-ELP36 from the target protein MalEp18-thioester, we performed a Reversed Phase Chromatography (RPC) in the same conditions described above (see pag. 15). Figure 61 shows the chromatogramic profile of purification and Figure 62 the corresponding SDS-PAGE analysis of eluted fractions.

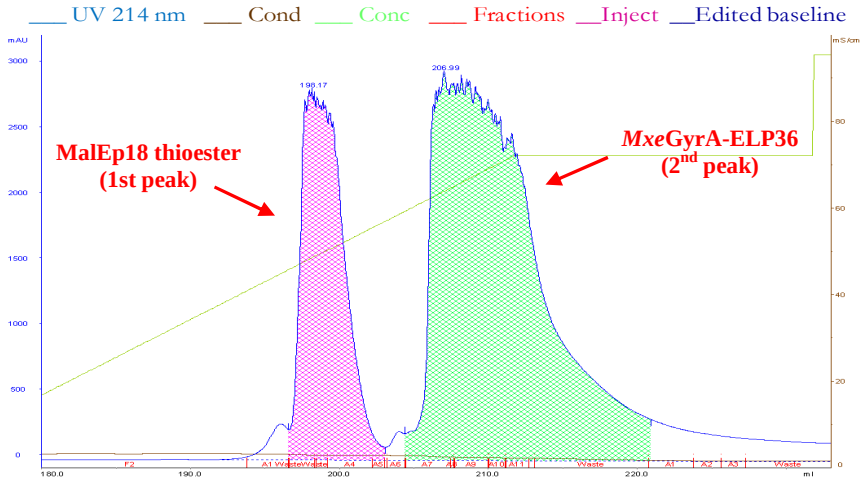

Figure 61. Chromatographic profile of reversed phase purification of the cleaved MalEp18 target protein and *Mxe*GyrA-ELP36 tag (Column: Source 15RPC; Gradient: 10-60% CH3CN/TFA 0.1% in 70 mL).

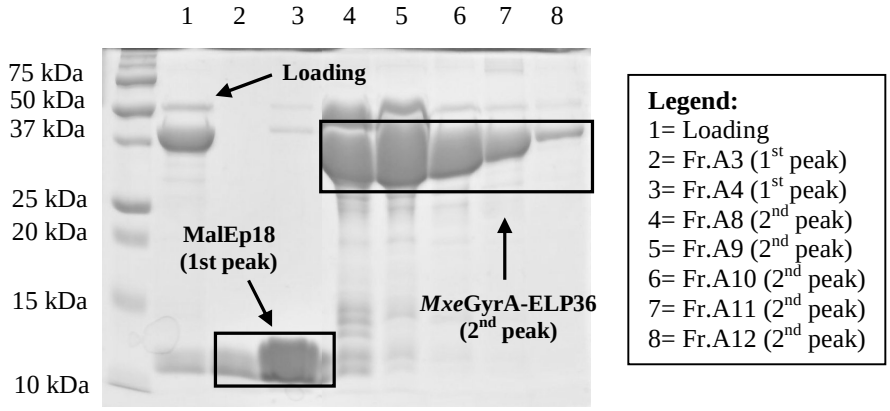

Figure 62. SDS-PAGE analysis of Reversed Phase Chromatography eluted fractions.

Fractions corresponding to the MalEp18 target protein (1st peak of RPC chromatographic profile) were then pooled together, lyophilized and quantified.
Once obtained the MalEp18-thioester purified target protein, we performed the reaction between the purified MalEp18-thioester and the (Cys)-GGE-(Lys-Biotin) peptide, synthesized ad hoc for EPL reaction. The reaction was carried out in a phosphate buffer, over night at room temperature, and in presence of 8 fold molar excess of peptide (more details are provided in the Materials and Methods section).
The EPL reaction aimed to the C-terminal site-specific biotinylation of the p18 antigen, like that of the thiolysis with MESNA previously carried out, was monitored by UPLC/MS analysis under the same conditions used above (Figure 63).

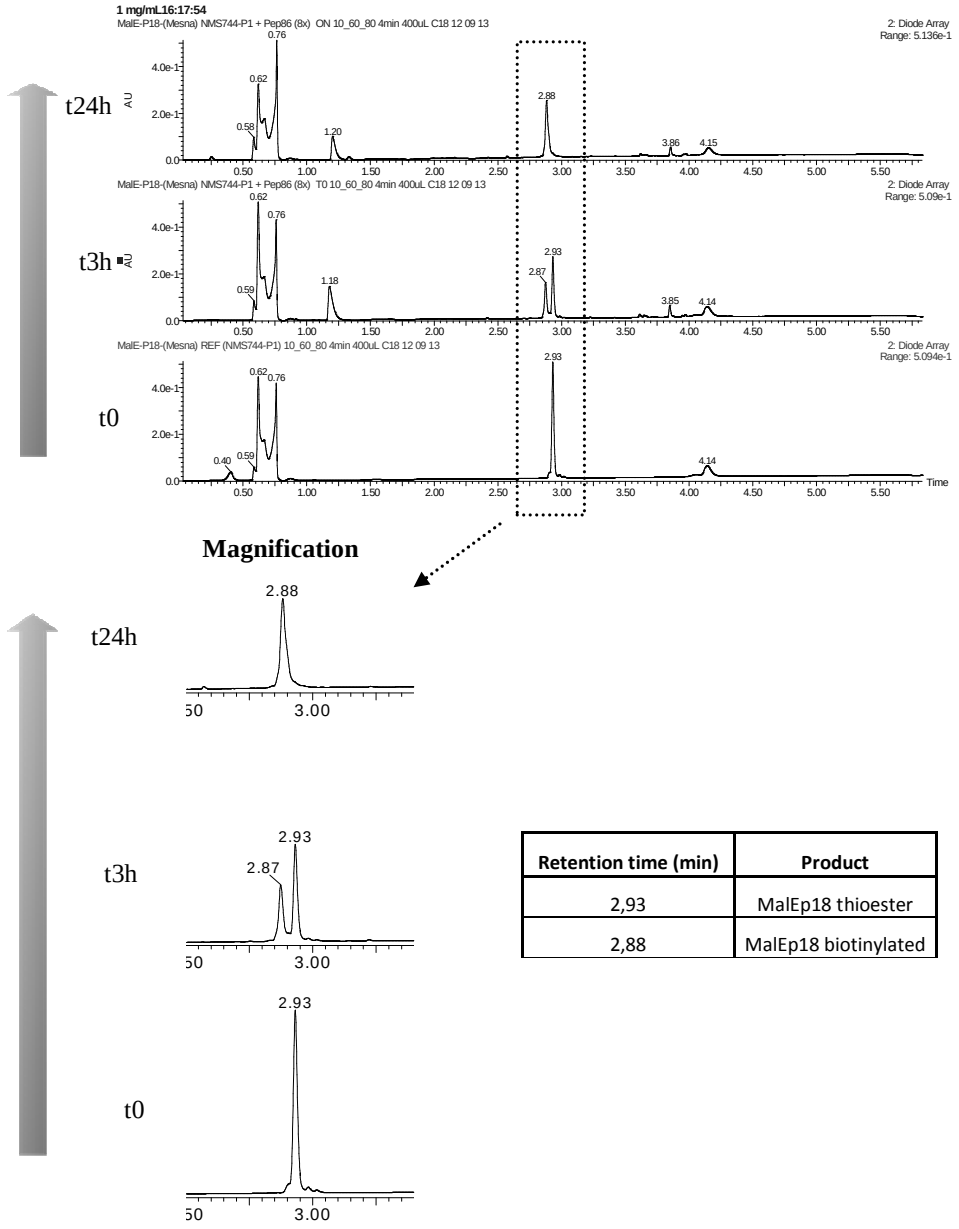

Retention time (min)	Product
2,93	MalEp18 thioester
2,88	MalEp18 biotinylated

Figure 63. UPLC analysis monitoring the C-terminal site-specific biotinylation of p18 antigen through Expressed Protein Ligation technique.

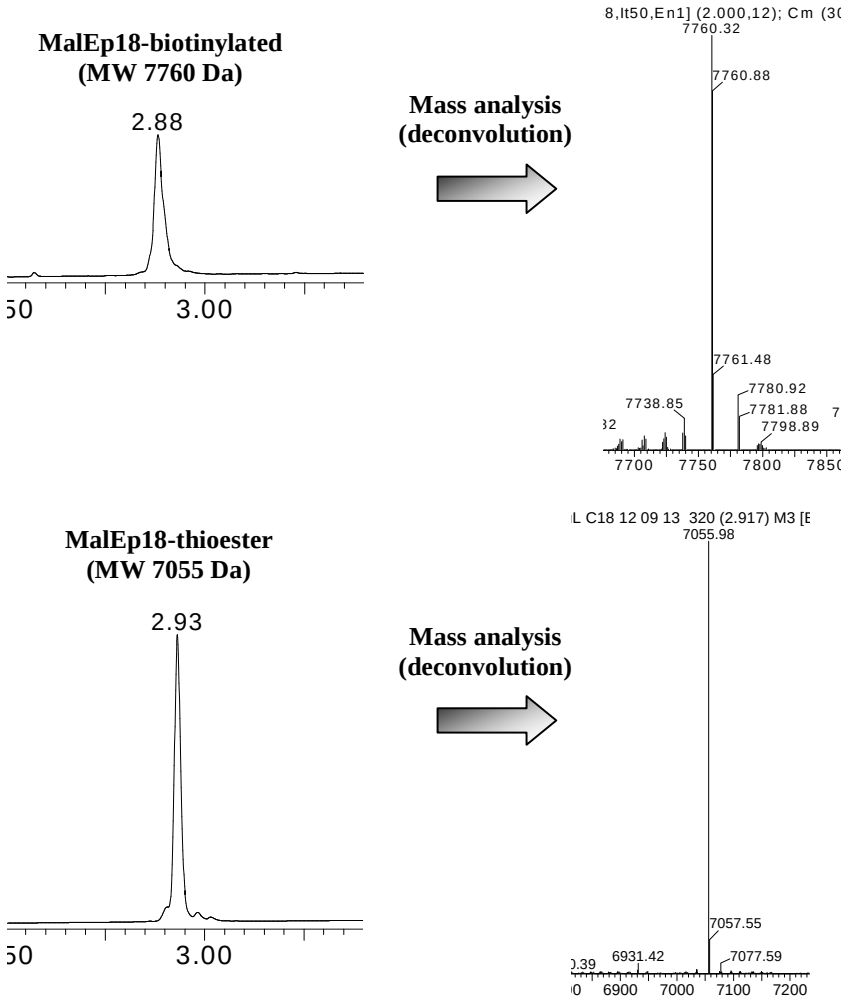

Figure 64. MS analysis monitoring the C-terminal site-specific biotinylation of p18 antigen through Expressed Protein Ligation technique.

The UPLC/MS analysis (Figure 63 and Figure 64. Column Acquity UPLC BEH300 C4 1.7µm, 2.1x100 mm, Waters; buffer A: H2O/TFA 0.1% v/v, buffer B: CH3CN/TFA 0.1% v/v; gradient 10-60% buffer B in 4 minutes) showed that the biotinylation reaction is almost complete after 3 hours and it is complete after 24 hours. The peak with a retention time of 2.92 min, relative to the active product (with the C-terminal thioester), disappears after 24 hours of reaction and, in correspondence, there is the increase of the peak at 2.87 min corresponding to the biotinylated product.
The significant difference between the molecular weights of the biotinylated p18 antigen (7760 Da) and the peptide used for the biotinylation (687 Da) has allowed to performe a Gel Filtration Chromatography (GFC) purification step (Column HiLoad 16/60 Superdex 30 prep grade, GE; see materials and methods section for more details) in order to remove the excess of peptide present in the preparation (Figure 65).

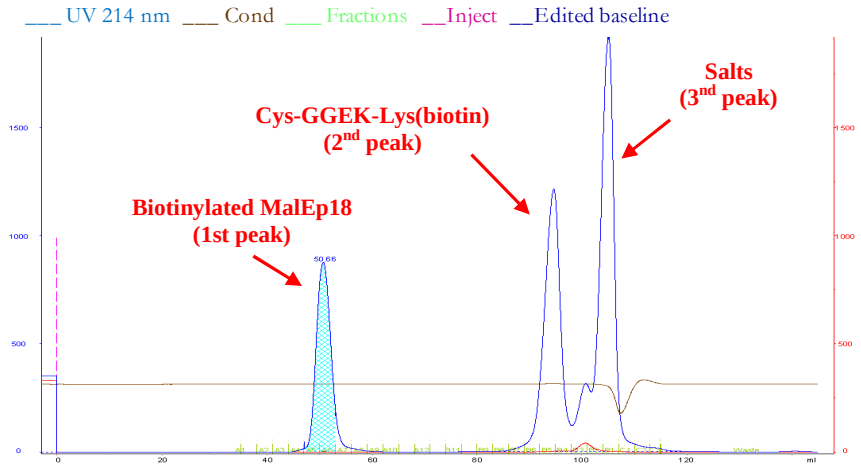

Figure 65. Chromatographic profile of GFC purification performed after EPL reaction in order to remove the excess of synthetic peptide (Cys-GGE-Lys(biotin)) used for the biotinylation of MalEp18-thioester target protein.

The fractions corresponding to the MalEp18 target protein biotinylated in a site-specific way at the C-terminal (1st peak of GFC chromatographic profile) were then pooled together and quantified through densitometric analysis of bands corresponding to the purified target protein on SDS-PAGE (Biorad Image Lab software; data not shown).

p18 RECOMBINANT ANTIGENS ACTIVITY TEST

MalEp18 (non-biotinylated derivative) and MalEp18-biotin (biotinylated derivative) recombinant antigens, obtained in the first case through ELP-Intein method and in the second exploiting the expressed protein ligation (EPL) technique, as previous explained, were subsequently tested in the current LIAISON® EBV VCA IgG and IgM assays (Figure 66). Their performance was then directly compared with that of the synthetic peptide currently in use in the immunoassays. Whereas the immobilization on solid phase of the MalEp18 antigen was performed with direct covalent coating (interaction of the lysines amino groups present on the MalEp18 antigen with the tosyl groups of paramagnetic beads), the immobilization of the MalEp18-biotin antigen was performed with the streptavidin-biotin complex.

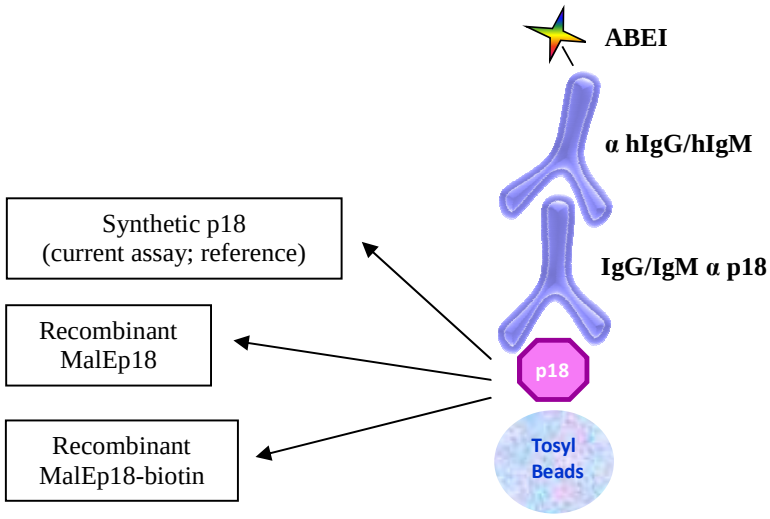

Figure 66. Different p18 antigen variants obtained with innovative techniques (ELP-Intein and EPL methods) were tested in the LIAISON® EBV VCA IgG and IgM assays and compared with p18 synthetic peptide currently in use.

Initially the different variants of p18 antigen were tested on a standard curve composed by a high positive human serum sample in dilution. In this curve, therefore, there are known increasing concentrations of antibodies (IgG or IgM) directed specifically against the p18 antigen. Each test was conducted in triplicate and the response, in RLU, was plotted versus the increasing concentration (U/ml) of α p18 antibodies present in the standard curve.

Figure 67 shows the direct comparison between the immunochemical activity of the synthetic p18 peptide (gray) and the recombinant MalEp18 antigen (blue) used at the same concentration of 100 µg/ml (concentration of current kit) in the EBV VCA IgG immunoassay.

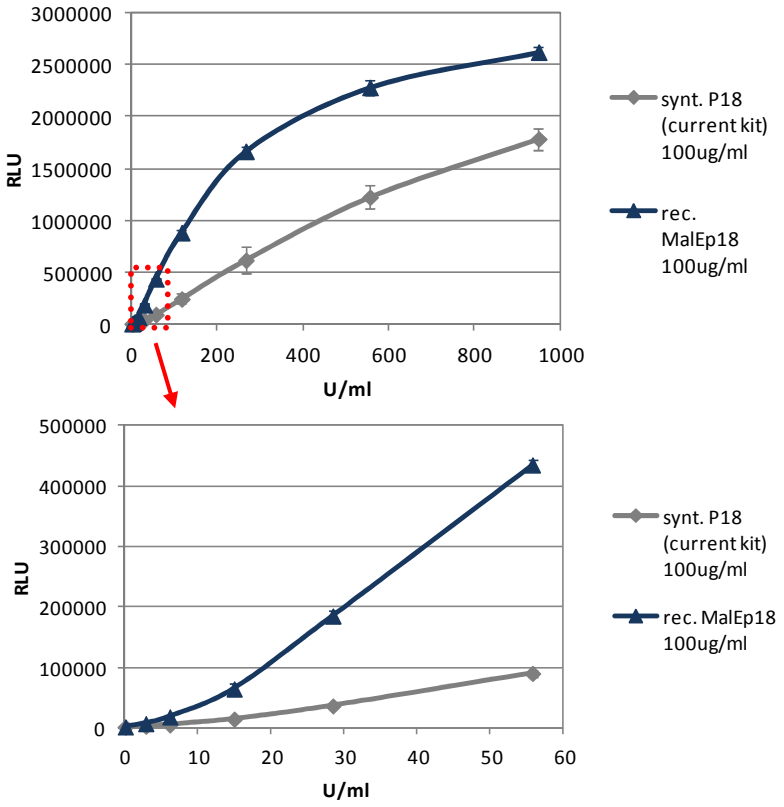

Figure 67. Comparison between synthetic p18 and recombinant MalEp18 antigen immunochemical activity in LIAISON® EBV VCA IgG immunoassay on a standard curve (both antigens were used at the same conc. of 100 µg/ml).

Results showed that MalEp18 recombinant antigen is immunoresponsive: the RLUs in fact followed the concentration increase of IgG α p18 antibodies of standard curve. Furthermore, the response given by the recombinant antigen was considerably higher than that obtained with the use of the synthetic peptide, with a consequent increase in the assay sensitivity (detection of low antibodies concentrations with RLUs higher than those of the current assay). Using a concentration 4 times lower than the previous one (25 µg/ml; Figure 68), the MalEp18 recombinant antigen (blue) showed again a good immunochemical activity comparable, if not slightly better, than that of the synthetic peptide (gray) currently in use.

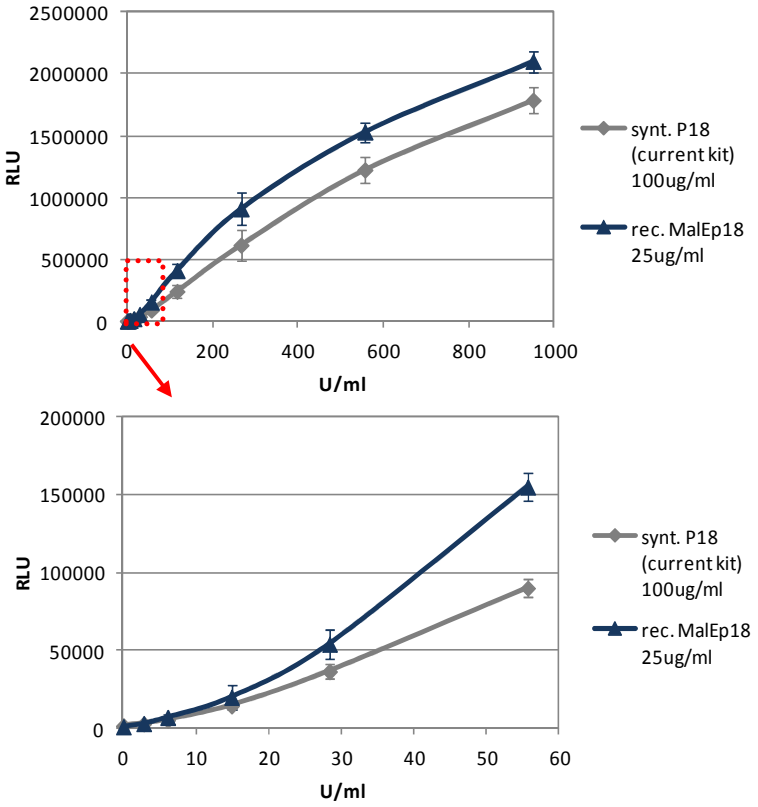

Figure 68. Comparison between synthetic p18 and recombinant MalEp18 antigen immunochemical activity in LIAISON® EBV VCA IgG immunoassay on the standard curve (p18 recombinant antigen was used at a concentration 4 times lower than synthetic p18 antigen).

Similarly to the MalEp18 recombinant antigen obtained through the use of ELP-intein method, also the biotinylated recombinant antigen obtained by EPL technique (MalEp18-biotin), has shown to be immunoreactive and to possess an immunochemical activity much higher than the synthetic p18 peptide (Figure 69). The MalEp18-biotin recombinant antigen worked at a concentration 100 times lower than the synthetic peptide of current kit, 1 µg/ml versus 100 µg/ml. Probably, the C-terminal site-specific biotinylation of the p18 antigen allowed an oriented and specific immobilization of the same p18 on solid phase and then permitted to work at much lower concentrations of antigen.

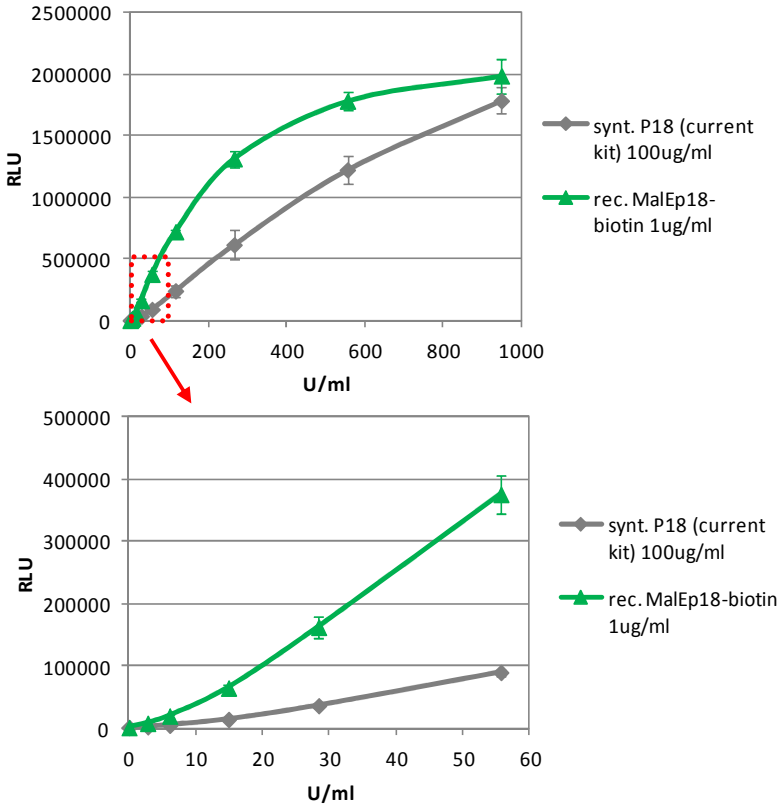

Figure 69. Comparison between synthetic p18 and recombinant MalEp18-biotin antigen immunochemical activity in LIAISON® EBV VCA IgG immunoassay on the standard curve (MalEp18-biotin recombinant antigen was used at a concentration 100 times lower than synthetic p18 peptide).

The different variants of the p18 recombinant antigen were then tested for their ability to bind IgG antibodies α p18 (EBV VCA IgG immunoassay) on a panel of positive and negative sera (Figure 70), in the same conditions previously used for the standard curve. Final evaluation of the immunochemical activity of the p18 antigen variants was done on the average of the signals obtained for the panels of positive and negative samples. The MalEp18 antigen (non-biotinylated version) showed a slight increase of the signal relating to the positive samples (panel B; blue bar) compared to the synthetic peptide (panel B; gray bar); at the same time the signal of negative samples (panel A; blue bar) was much lower than that detected for the synthetic peptide (panel A; gray bar). The result was an increase of the ratio between the signal of the positive and negative samples; this last parameter is an index that proportionally correlates with the good performance of an immunodiagnostic assay. The data obtained from the use of the biotinylated recombinant antigen (MalEp18-biotin) showed a great increase of the signal relative to the positive samples (panel B; green bar) compared to the synthetic peptide (panel B; gray bar); also in this case the background (signal of the negative samples; panel A; green bar), was found to be lower than that of the synthetic peptide (panel A; gray bar) with a resulting better separation positive/negative signal samples.

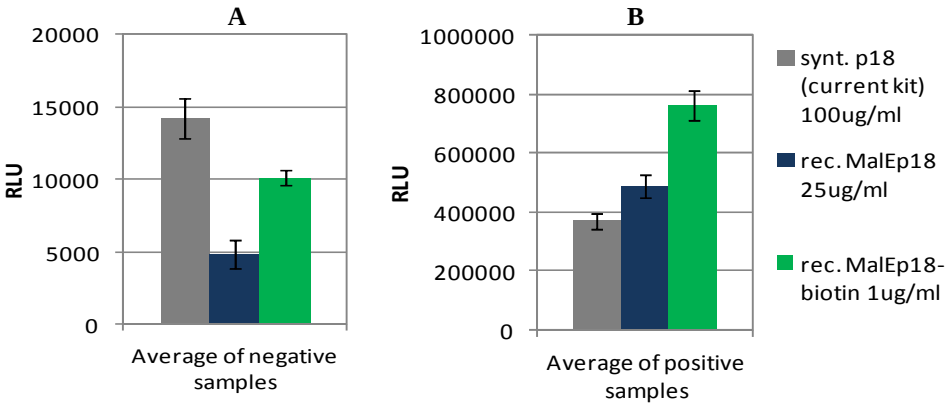

Figure 70. Immunochemical activity of three variants of p18 antigen (synthetic, recombinant non-biotinylated, recombinant biotinylated) was tested in the LIAISON® EBV VCA IgG immunoassay on a panel of negative and positive samples.

The same type of analysis was performed in the LIAISON® EBV VCA IgM immunoassay only for the non-biotinylated p18 recombinant antigen (Figure 71). The results obtained from the analysis of the standard curve showed a performance almost comparable between the recombinant MalEp18 (blue; panel A) and the synthetic p18 peptide (gray; panel A). These data were confirmed by the analysis of a panel of negative and positive samples for IgM antibodies α p18 (panel B); the two antigens showed in fact very similar values regarding the panel of positive samples (panel B, right). The positive aspect was that the signal relative to the negative samples (panel B, left) appeared to be lower for the recombinant antigen, whose use in this immunoassay then allowed a lowering of the background with a consequent optimization of the assay performance.

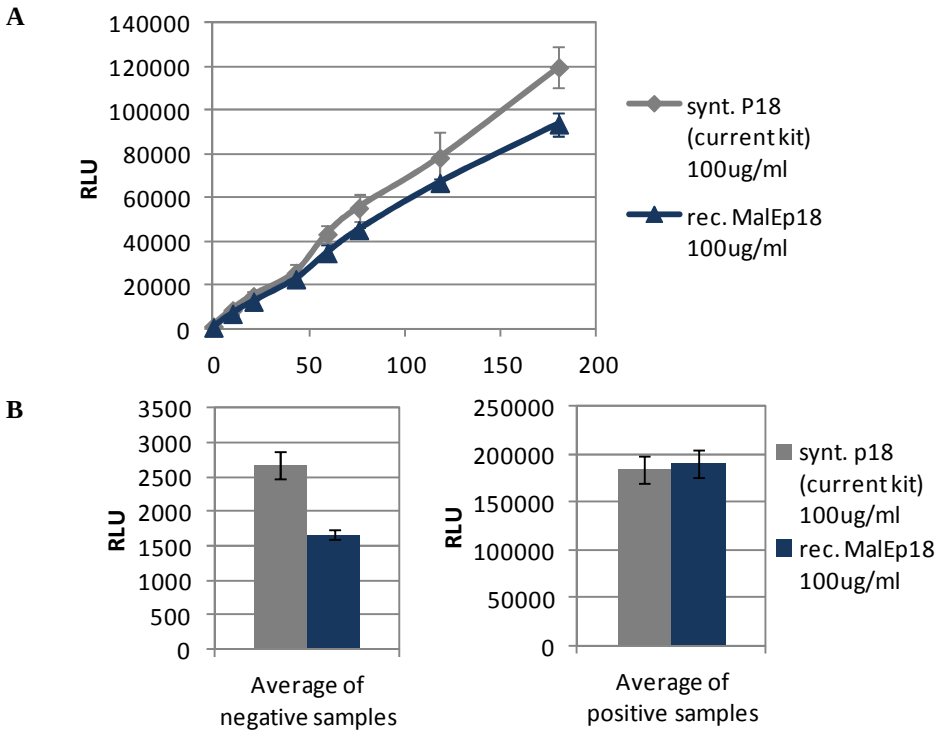

Figure 71. Immunochemical activity of synthetic p18 and recombinant MalEp18 antigen was tested in the LIAISON® EBV VCA IgM immunoassay on a standard curve (A) and on a panel of negative and positive samples (B).

SITE-SPECIFIC BIOTYNILATION OF p18 ANTIGEN THROUGH GENETIC INCORPORATION OF UNNATURAL AMINO ACIDS

Once obtained the C-terminal site-specific biotinylated p18 variant and verified the good reactivity of the same, we tried to get the N-terminal biotinylated version of the same antigen. The aim was to determine if the biotinylation on a different site could have benefits in terms of immunochemical activity of the p18 antigen. For this purpose, the genetic incorporation of Unnatural Amino Acids (UAA) into a target protein directly in *E. coli* cells was used as a strategy; in particular the incorporation of a para-azido-phenylalanine (pAzF) at the N-terminus of the p18 protein has been exploited to subsequently realize a Strain-Promoted Azide-Alkyne Cycloaddition (SPAAC**)** reaction with a molecule of cyclooctyne-biotin with the potential resulting formation of a N-terminal biotinylated p18 antigen.

In order to express the target protein containing the desired UAA at a specific site in *E. coli* cells, as extensively described in the literature and in the introduction, BL21 (DE3) *E. coli* cells were co-transformed with two plasmids. The first expression plasmid contains the MalEp18 gene with a stop codon (TAG; amber codon) in third position and the gene encoding for the ELP-Intein tag (pET24-MalEp18(TAG)-*Mxe*GyrA-ELP36; see materials and methods for cloning details) The second plasmid was a commercial suppressor plasmid (pEVOL-pAzF) that harbors the tRNA/aaRS pair, specific for the pAzF. For the expression of MalEp18(pAzF)-*Mxe*GyrA-ELP36 mutated protein, this system requires a double induction: IPTG for the target protein present in the pET24 expression plasmid and Arabinose for the expression of tRNA/aaRS pair present in the pEVOL suppressor plasmid. It is also necessary add in the culture medium (LB), at the time of induction, the unnatural amino acid (pAzF) to be incorporated in the target protein (see materials and methods section). Initially, we explored some of the classic fermentation conditions (in terms of temperature, induction time and O.D, IPTG concentration) that are generally used for the expression of heterologous proteins in *E. coli* cells (Table 7).

Fermentation	Temperature (°C)	Induction Time (h)	Induction O.D.	[IPTG] (mM)	[Arabinose] (% m/v)	[pAzF] (mM)
A	37°C	3	0,6	1	0,1	1
B	37°C	3	1,5	1	0,1	1
C	30°C	3	0,6	1	0,1	1
D	20°C	20	0,6	0,1	0,1	1

Table 7. Different conditions used for MalEp18(pAzF)-*Mxe*GyrA-ELP36 fusion protein expression.

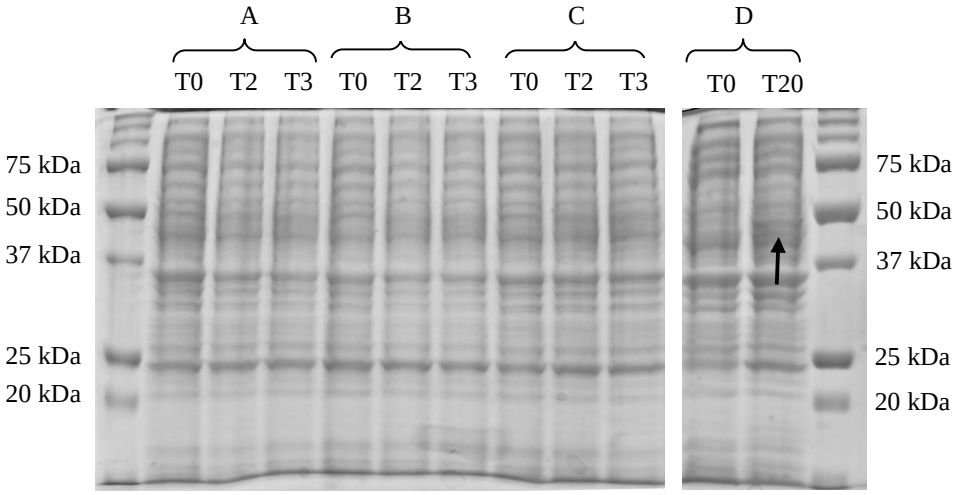

Figure 72. SDS-PAGE analysis showing the induction test of BL21(DE3) pEVOL/pET24-MalEp18(TAG)-*Mxe*GyrA-ELP36, fermented in different conditions reported in Table 7. Black arrow indicates MalEp18(pAzF)-*Mxe*GyrA-ELP36 target protein.

SDS PAGE analysis (Figure 72) shows that MalEp18(pAzF)-*Mxe*GyrA-ELP36 target protein (expected molecular weight of 45.3 kDa; black arrow) is expressed at low levels only in conditions used in fermentation D (20°C, 20 hours of induction time, 0.6 of induction O.D., 0.1 mM IPTG, 0.1% arabinose and 1mM pAzF). In other conditions (fermentations A,B,C) no expression is detected.

In order to improve the levels of expression of the target protein, we decided to follow the fermentation conditions reported in literature for this particular expression system which involves the use of suppression plasmids (160-162). These conditions provide a late induction (in terms of cells O.D.), long induction times both at low and at high temperatures; concentrations of the inductors and of unnatural amino acid remained unchanged (1 mM IPTG, 0.1% arabinose and 1% pAzF; Table 8).

Fermentation	Temperature (°C)	Induction Time (h)	Induction O.D.	[IPTG] (mM)	[Arabinose] (% m/v)	[pAzF] (mM)
A	20°C	20	1,5	1	0,1	1
B	25°C	20	1,5	1	0,1	1
C	37°C	20	1,5	1	0,1	1
D	30°C	20	1,5	1	0,1	1

Table 8. Other conditions used for MalEp18(pAzF)-*Mxe*GyrA-ELP36 fusion protein expression (similar to those reported in literature).

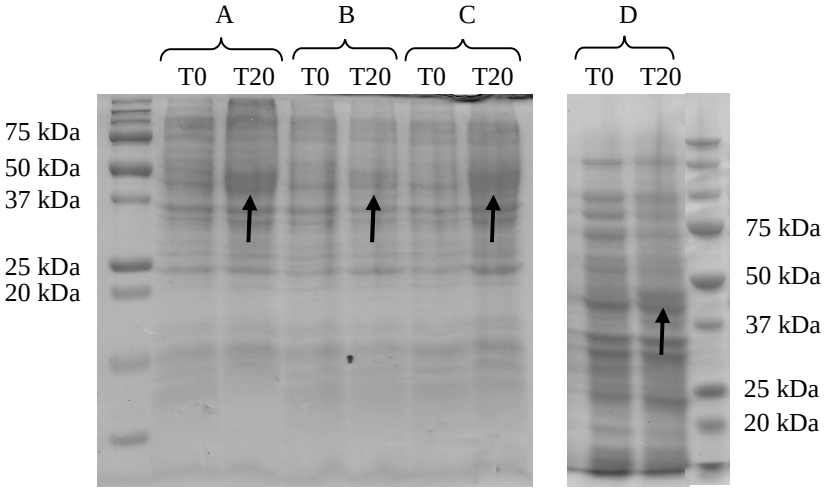

Figure 73. SDS-PAGE analysis showing the induction test of BL21(DE3) pEVOL/pET24-MalEp18(TAG)-*Mxe*GyrA-ELP36, fermented in different conditions reported in Table 8. Black arrows indicate MalEp18(pAzF)-*Mxe*GyrA-ELP36 target protein.

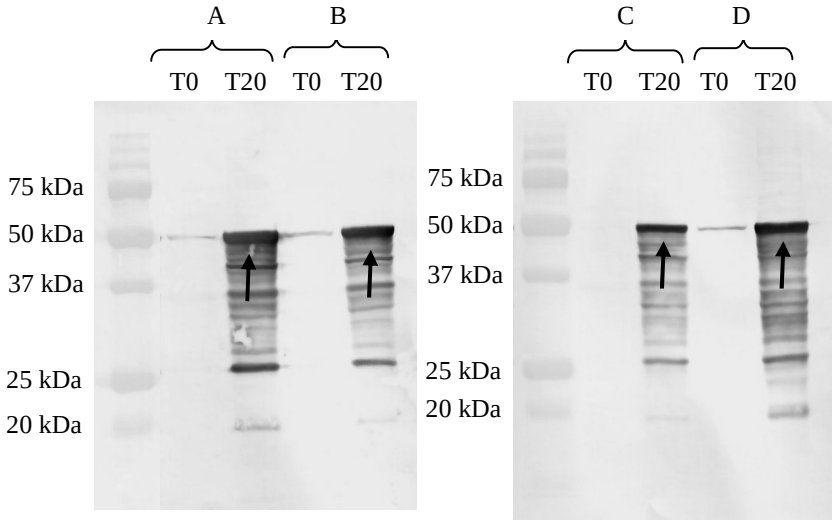

Figure 74. Western Blot analysis of BL21(DE3) pEVOL/pET24-MalEp18(TAG)-*Mxe*GyrA-ELP36 fermented in different conditions reported in Table 8. Black arrows indicate MalEp18(pAzF)-*Mxe*GyrA-ELP36 target protein. The staining was performed with rat anti-p18 HRP probe (see Materials and Methods).

SDS-PAGE analysis (Figure 73) and WB analysis (Figure 74) show that the target protein MalEp18(pAzF)-*Mxe*GyrA-ELP36 (expected molecular weight of 45.3 kDa) is expressed in all conditions at low levels (fermentations A, B, C, D; black arrows in Figures 73 and 74). The presence of bands at lower molecular weight, visible from the WB analysis (Figure 74), in addition to that relative to the entire target protein (black arrows), as seen above for the p18-*Mxe*GyrA-ELP36/90 constructs, indicates that also the MalEp18(pAzF)-*Mxe*GyrA-ELP36 target protein undergoes a partial degradation during the fermentation processes.

Finally, to try to increase the expression degree of the target protein, we decided to carry out a final test of expression at 2 different temperatures: 25°C and 30°C (Table 9; Figures 75 and 76). Compared to the previous, the difference is the following: for each of these two conditions, we

performed a pre-induction of the cells with half doses of arabinose and pAzF. We then induced at time 0 with IPTG (entire dose) and with the other half doses of arabinose and pAzF. The idea is that the pre-induction would give a way for the cells to express the tRNA/aaRS pair specific for pAzF and to have part of para-azido-phenylalanine amount to be loaded onto tRNA molecule before the induction of the target protein. This strategy could lead a potential positive effect on the levels of protein expression.

Fermentation	Temp. (°C)	Induction O.D./Time	[IPTG] (mM)	[Arabinose] (% m/v)	[pAzF] (mM)	pre-induction
A	30°C	1,5/20h	1	0,05 + 0,05	0,5 + 0,5	yes
B	30°C	1,5/20h	1	0,1	1	no
C	25°C	1,5/20h	1	0,05 + 0,05	0,5 + 0,5	yes
D	25°C	1,5/20h	1	0,1	1	no

Table 9. Different conditions (with and without pre-induction) used for MalEp18(pAzF)-*Mxe*GyrA-ELP36 fusion protein expression.

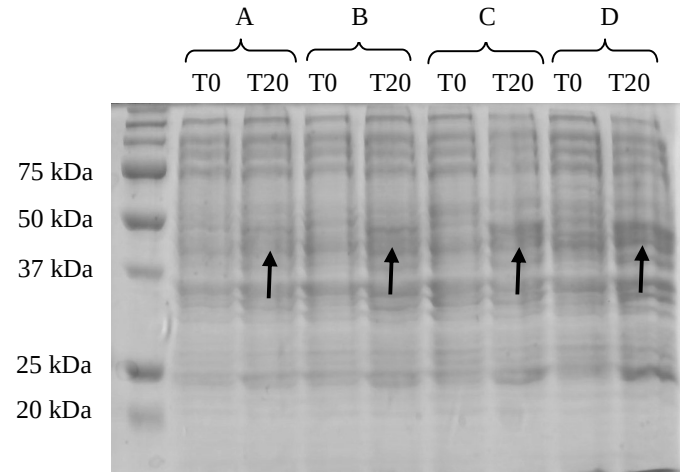

Figure 75. SDS-PAGE analysis showing the induction test of BL21(DE3) pEVOL/pET24-MalEp18(TAG)-*Mxe*GyrA-ELP36, fermented in different conditions reported in Table 9. Black arrows indicate MalEp18(pAzF)-*Mxe*GyrA-ELP36 target protein.

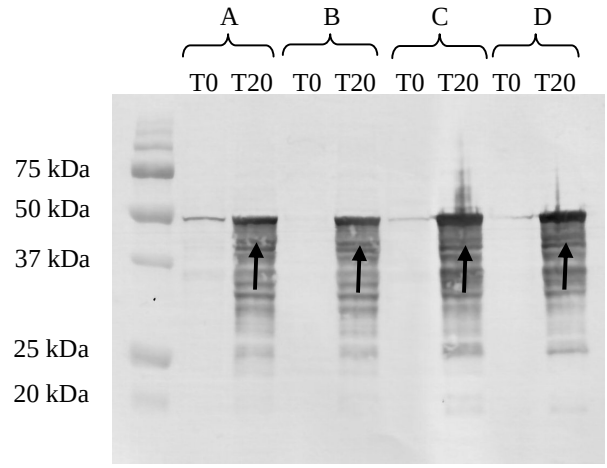

Figure 76. Western Blot analysis of BL21(DE3) pEVOL/pET24-MalEp18(TAG)-*Mxe*GyrA-ELP36, fermented in different conditions reported in Table 9. Black arrows indicate MalEp18(pAzF)-*Mxe*GyrA-ELP36 target protein. The staining was performed with rat anti-p18 HRP probe (see Materials and Methods).

SDS-PAGE analysis (Figure 75) and WB analysis (Figure 76) show that the MalEp18(pAzF)-*Mxe*GyrA-ELP36 target protein (expected molecular weight of 45.3 kDa) is expressed in all conditions at satisfactory levels (fermentations A, B, C, D; black arrows in Figures 75 and 76). At 25°C (fermentations C and D in Figures 75 and 76), the level of expression of the target protein appears to be higher than that of fermentations performed at 30°C (fermentations A and B in Figures 75 and 76). In particular, between the two fermentations carried out at 25°C (with and without pre-induction, fermentations C and D respectively), the condition in which the target protein expression level appears to be little higher (Figure 76; WB analysis) seems to be the fermentation C (25°C with pre-induction). All subsequent fermentations were performed using the parameters of the fermentation C (Table 9).

Before proceeding with the purification of the target protein, we wanted to check two different aspects: 1_ the ability of cells transformed with the pET24 expression vector only (and not with the pEVOL suppression plasmid encoding for tRNA/aaRS pair) to express the target protein with

a stop codon in third position. 2_ The specificity of the tRNA/aaRS pair for the pAzF unnatural amino acid; for this purpose we carried out fermentations in presence and absence of pAzF unnatural amino acid in the culture medium.
The conditions in which we performed the fermentation tests described above are listed in Table 10.

Fermentation	Vector	Temp. (°C)	Induction O.D./Time	[IPTG] (mM)	[Arabinose] (% m/v)	[pAzF] (mM)
A	pET24 only	25°C	1,5/20h	1	/	/
B	pEVOL+pET24	25°C	1,5/20h	1	0,05 + 0,05	/
C	pEVOL+pET24	25°C	1,5/20h	1	0,05 + 0,05	0,5 + 0,5

Table 10. Different fermentation conditions used to test 2 different aspects of MalEp18(pAzF)-*Mxe*GyrA-ELP36 fusion protein expression: the ability of BL21(DE3) cells transformed with the pET24 expression vector only to express the target protein (fermentation A) and the specificity of the tRNA/aaRS pair for the pAzF (fermentations B and C).

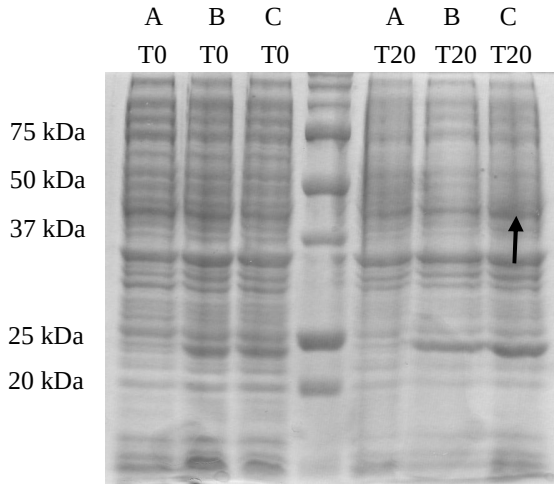

Figure 77. SDS-PAGE analysis showing the induction test of BL21(DE3) pET24-MalEp18(TAG)-*Mxe*GyrA-ELP36 and BL21(DE3) pEVOL / pET24-MalEp18(TAG)-*Mxe*GyrA-ELP36, fermented in different conditions reported in Table 10. Black arrow indicates MalEp18(pAzF)-*Mxe*GyrA-ELP36 target protein.

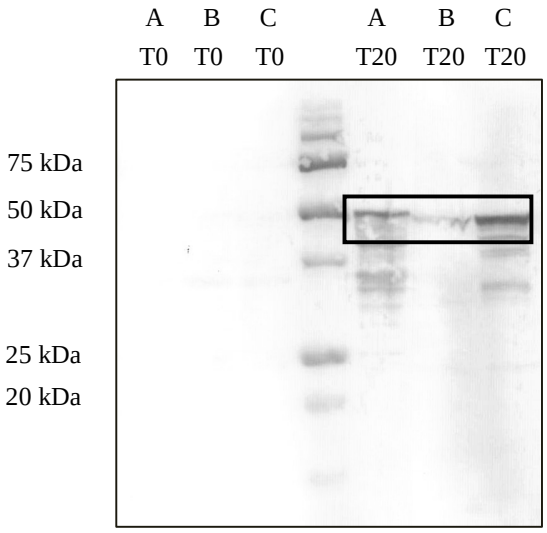

Figure 78. Western Blot analysis of BL21(DE3) pET24-MalEp18(TAG)-*Mxe*GyrA-ELP36 and BL21(DE3) pEVOL / pET24- MalEp18(TAG)-*Mxe*GyrA-ELP36, fermented in different conditions reported in Table 10. Black square indicates MalEp18(pAzF)-*Mxe*GyrA-ELP36 target protein. The staining was performed with rat anti-p18 HRP probe (see Materials and Methods).

SDS PAGE analysis (Figure 77) shows that the BL21(DE3) cells transformed with the pET24 expression vector only are not able to express the target protein (A; T20h); in addition, BL21(DE3) cells co-transformed with both vectors (pET24 and pEVOL) seem to be not able to express the target protein in absence of pAzF in the culture medium (B; T20h) but only in its presence (C; T20h; black arrow). Given the low expression levels of the target protein, before advancing concluding remarks, it was needed to perform a WB analysis (Figure 78). This analysis revealed that the target protein MalEp18(pAzF)-*Mxe*GyrA-ELP36 is expressed, even if at low levels, in BL21(DE3) cells transformed with pET24 plasmid only (A; T20h). This indicates that the cells are able to express the target protein even in the absence of specific aminoacyl tRNA synthetase and tRNA pair necessary to incorporate unnatural aa (pAzF) and in the absence of pAzF in the culture medium. Probably *E. coli* cells are able to circumvent the problem by incorporating another amino acid at the position of the pAzF or by shifting the

translation reading frame. In BL21(DE3) cells co-transformed with both plasmids (pEVOL and pET24), the target protein MalEp18(pAzF)-*Mxe*GyrA-ELP36 is expressed only in the presence of pAzF in the growth medium (C; T20h). In the absence of this latter, the cells are not able to express the protein except at very low levels (B; T20h). This result indicates that the tRNA and the aminoacyl tRNA synthetase pair is specific for the pAzF unnatural aminoacid. In the absence of pAzF in the medium, the cells are not able to bypass the problem by incorporating another amino acid or by shifting the translation reading frame as happens instead for the BL21(DE3) cells transformed with pET24 plasmid only.
The next step was the purification of the MalEp18(pAzF)-*Mxe*GyrA-ELP36 target protein. Being expressed as a fusion protein with the *Mxe*GyrA-ELP36 tag, we exploited the ELP-Intein system for the purification process, exactly under the same conditions used for the MalEp18-*Mxe*GyrA-ELP36 protein. Therefore, we made the inverse transition cycling (ITC) process followed by cleavage with DTT (Figure 54); then to separate the cleaved tag (*Mxe*GyrA-ELP36) from the target protein (MalEp18(pAzF)), a reversed phase chromatography (RPC) was performed. The ITC process and the cleavage reaction with DTT were monitored by SDS-PAGE analysis (Figure 79); Figure 80 shows instead the chromatographic profile of RPC purification (above) and the corresponding SDS-PAGE analysis of eluted fractions (below).

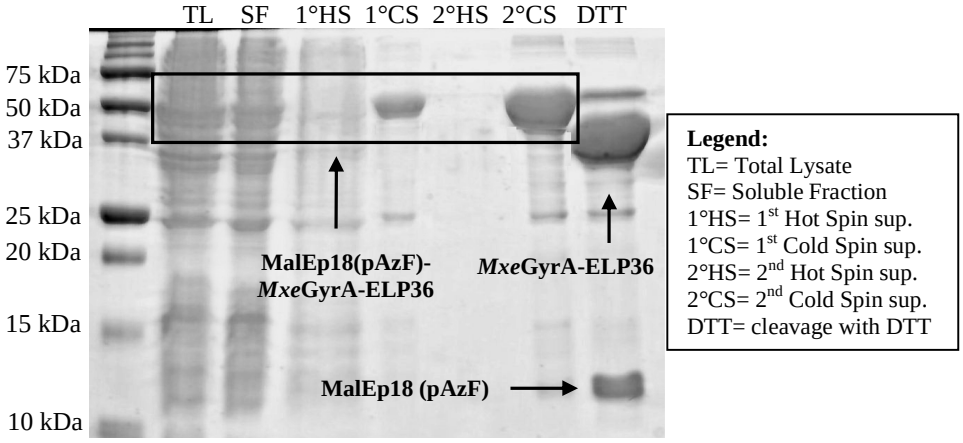

Figure 79. SDS PAGE analysis monitoring ITC purification process and cleavage with DTT.

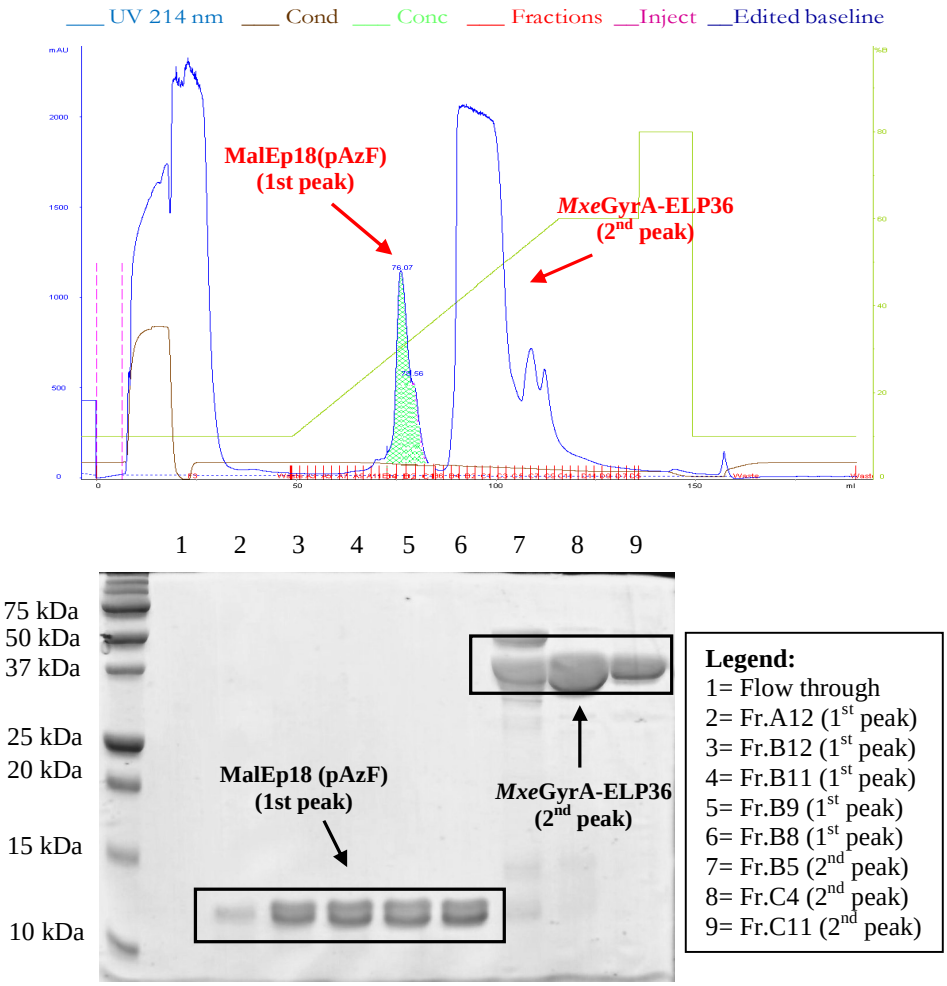

Figure 80. Chromatographic profile of reversed phase purification of the cleaved MalEp18(pAzF) target protein and *Mxe*GyrA-ELP36 tag (Column: Source 15RPC; Gradient: 10-60% CH3CN/TFA 0.1% in 70 mL) (above) and corresponding SDS-PAGE analysis of eluted fractions (below).

The pool of fractions corresponding to the MalEp18(pAzF) target protein (1st peak of RPC chromatographic profile) was then subjected to lyophilization and quantified for subsequent analysis.

In order to verify the incorporation of pAzF at N-terminus of our target protein (third position), we commissioned in outsourcing (CNR ISPA Colleretto Giacosa (T0)) a N-terminal sequencing of the first six amino acids of the MalEp18(pAzF) and of the wild type MalEp18 proteins. The following sequences were identified:

- MalEp18(wt): MKIEEG
- MalEp18(pAzF): MKXEEG

In particular, the results obtained have revealed that MalEp18(wt) protein presents correctly an isoleucine residue at the level of third position, while MalEp18(pAzF) protein shows at the level of third amino acidic residue a signal not attributable to anyone of known amino acid (indicated in sequence with "X"). This finding potentially confirms the insertion of para-azido-phenylalanine unnatural amino acid in the third position of the MalEp18 (pAzF) sequence.

Once the incorporation of pAzF at the N-terminus of the protein was confirmed, this unnatural aminoacid was exploited to realize a Strain-Promoted Azide-Alkyne Cycloaddition (SPAAC**)** reaction with a molecule of cyclooctyne-biotin; the scope was to obtain a N-terminal biotinylated p18 antigen. The SPAAC reaction consists in the use a new type of highly selective and efficient chemistry called click chemistry. As described in the introduction, this type of chemistry provides a 1,3-dipolar cycle-addition between an azido group and an alkyne to give a stable triazole ring. Having our laboratory any previous experience with this particular type of chemistry, as a first step, we preliminary studied the basic reaction conditions through the evaluation of different parameters (pH, temperature, buffers, reagent concentration, etc.) and through the evaluation of the reaction efficiency (yield, reproducibility, etc.). For this purpose, two peptides were synthesized as model systems (see appendix section for experimental details of these analyses).
The data obtained revealed that the SPAAC reaction is simple to handle; another positive feature is its robustness, in fact SPAAC reaction takes place efficiently in a wide range of conditions (pH, temperature, buffers, molar concentration of the reagents). However, it is not an extremely fast reaction: the time necessary to reach the completeness is approximately 24 hours. In summary, the best conditions in which the reaction kinetic

appears to be favored are aqueous buffers instead of organic media, temperatures around at 37°C than room temperature; moreover the presence of a slight molar excess (2-3x) of one of the 2 components (azide or alkyne) seems to improve the reaction kinetic.

Once identified the best reaction conditions, we applied those conditions to carry out the reaction of click chemistry (SPAAC) between the MalEp18(pAzF) protein and the molecule of cyclooctyne-biotin (BCN-biotin), as shown schematically in Figure 81.

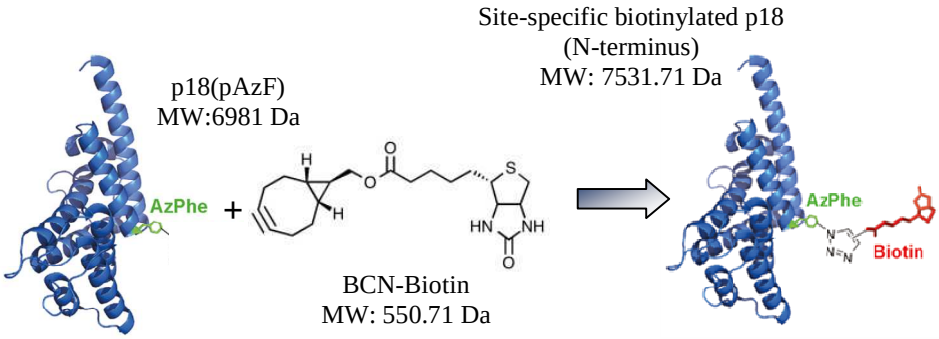

Figure 81. Schematic representation of SPAAC reaction between the para-azido-phenylalanine residue of MalEp18(pAzF) protein and a cyclooctyne-biotin molecule.

The reaction was carried out in a phosphate buffer, over night at 37°C, and in presence of 8 fold molar excess of BCN-biotin (more details are provided in the Materials and Methods section). The SPAAC reaction, aimed to the N-terminal site-specific biotinylation of the p18 antigen, was monitored by UPLC/MS analysis (Figure 82).
As a positive control, we performed in parallel a click chemistry reaction between the peptide1 (the same one used for the analysis of the click chemistry basic reaction; see appendix) containing an azido-group at N-terminal and the BCN-biotin reactive (Figure 83).

The UPLC/MS analysis (Figure 82 and Figure 83. Column Acquity UPLC BEH300 C4 1.7μm, 2.1x100 mm, Waters; buffer A: H2O/TFA 0.1% v/v, buffer B: CH3CN/TFA 0.1% v/v; gradient 10-60% buffer B in 4 minutes) showed that both reactions have the same chromatographic profile at time 0 and after 24 hours; however, the mass analysis revealed that the reaction between the peptide 1 and the BCN-biotin (Figure 83; positive control) occured: in fact a change was detected for the molecular mass of peak relative to peptide 1 (MW 2780 Da). This after 24 hours of reaction resulted to have a mass exactly coincident with that of the product (MW 3331 Da), indicating a co-elution between the peak of the peptide itself and that of the product. In the case of reaction involving our target protein MalEp18 (pAzF) and the cyclooctyne-biotin (Figure 82) not only the chromatographic profile did not change, but also the masses relative to the peaks remained unvaried, indicating that the reaction did not take place.

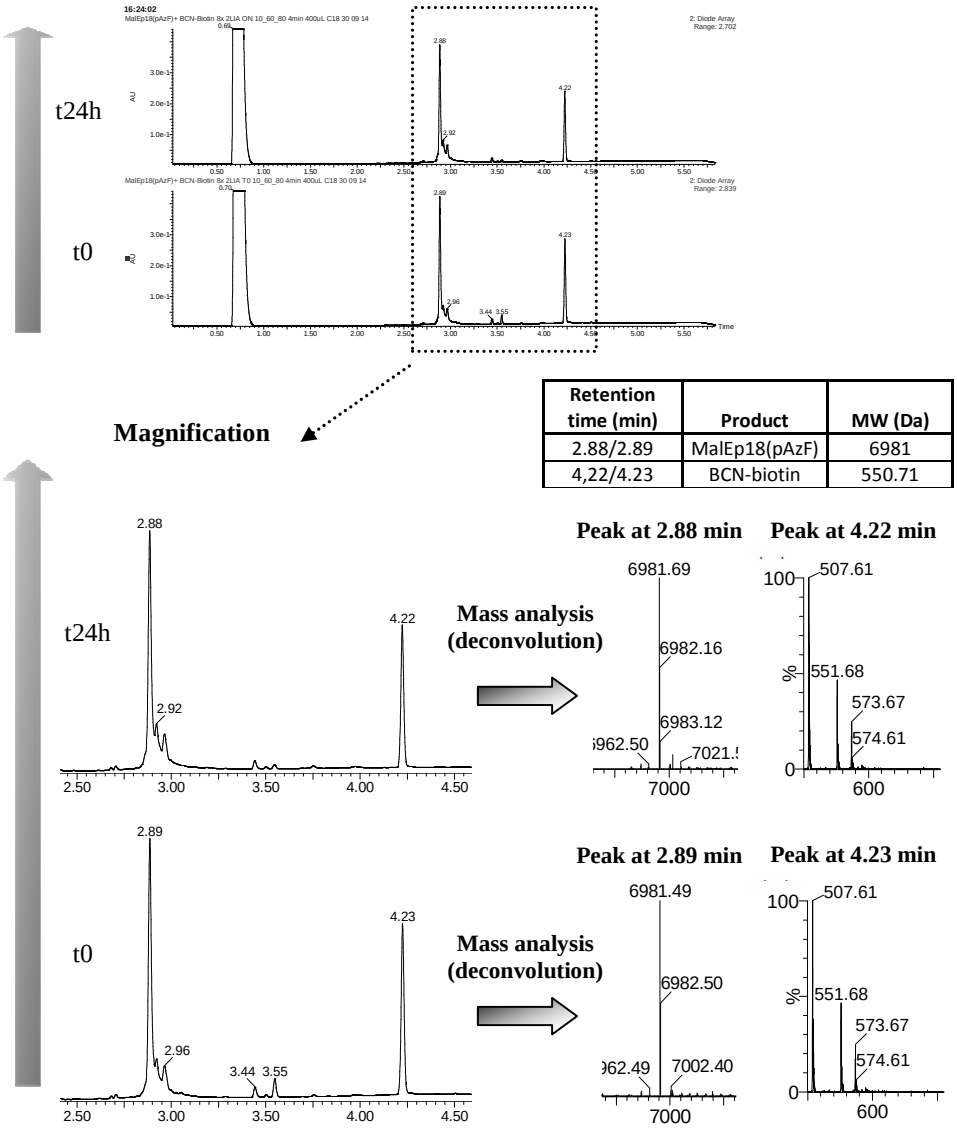

Figure 82. UPLC/MS analysis monitoring the N-terminal site-specific biotinylation of p18 antigen through SPAAC reaction between MalEp18(pAzF) and BCN-biotin.

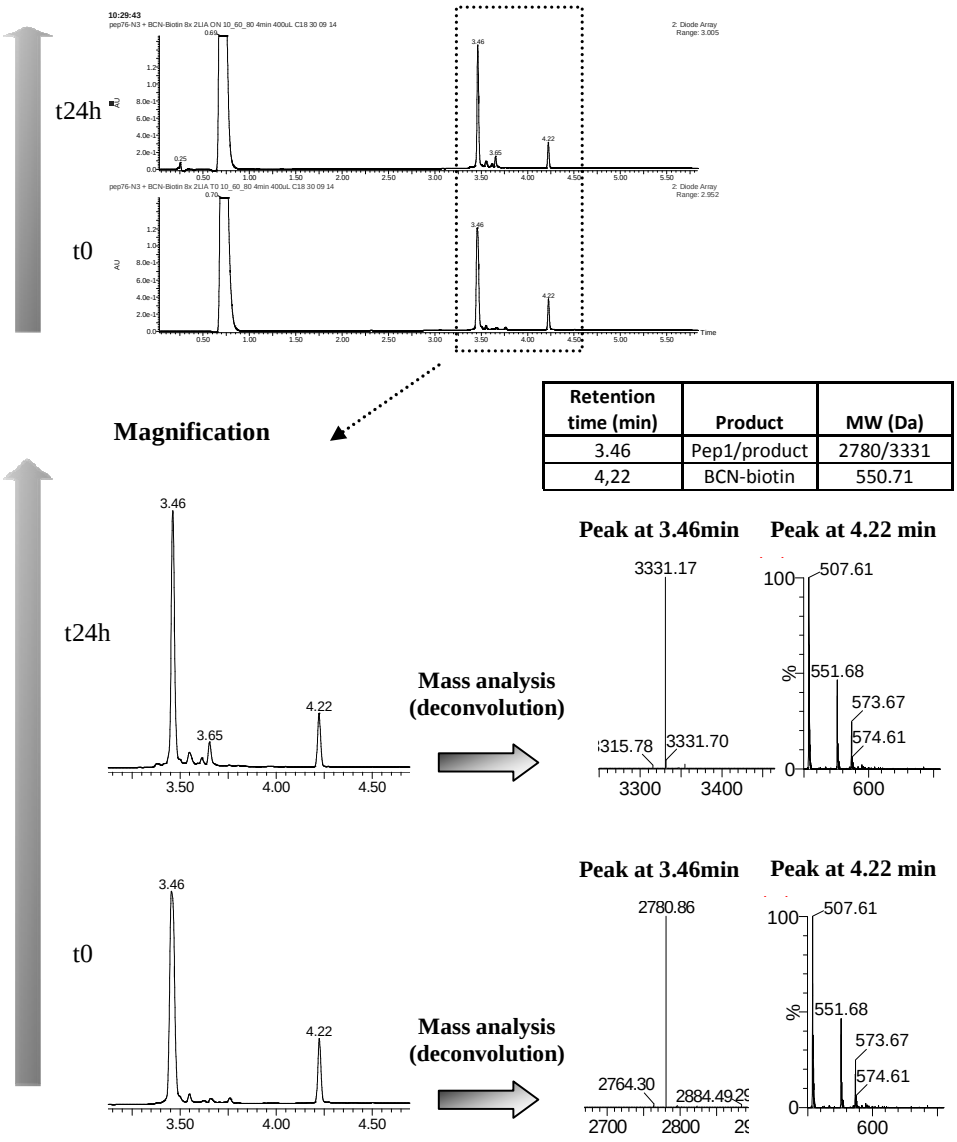

Figure 83. UPLC/MS analysis monitoring the SPAAC reaction between peptide 1 and BCN-biotin (positive control).

In order to promote the reaction between the MalEp18(pAzF) target protein and the BCN-biotin reactive, we then explored new conditions:

1. in organic buffer (DMSO) at low temperature (-20°C). As demonstrated by the experimental data reported in appendix relative to the study of click chemistry basic reaction, this condition, that provides a freeze and taw process, can promote the conjugation reaction.
2. In the presence of sulfo-betaine (NDSB-195) in phosphate buffer. These zwitterionic detergents appear to improve in a very efficient way the solubility of molecules in solution and thus promote the interaction between them (214).
3. Under denaturing conditions (8M Urea). This strategy was explored in the case in which the lack of reactivity of the azido group present on our target protein was due to particular structural conformations that prevent the exposure of the same azido functional group on the surface of the protein.

For each of these conditions, the reaction between peptide 1 and BCN-biotin was set up in parallel (positive controls). Also in this case, all reactions were carried out over night at 37°C and in presence of 8 fold molar excess of BCN-biotin (see Materials and Methods section). Moreover, the reactions were monitored by UPLC/MS analysis in the same conditions described above.
Figure 84 and Figure 85 respectively show the chromatographic profiles of the reaction between MalEp18 (pAzF) target protein + BCN-biotin and peptide 1 + BCN-biotin conducted in the three listed above conditions. Tables present in the same figures show instead the masses obtained by mass analysis of the peaks present in the corresponding reaction at time 0 and after 24 hours.

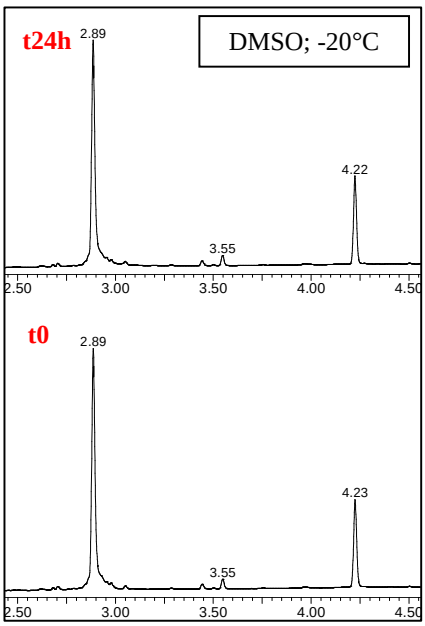

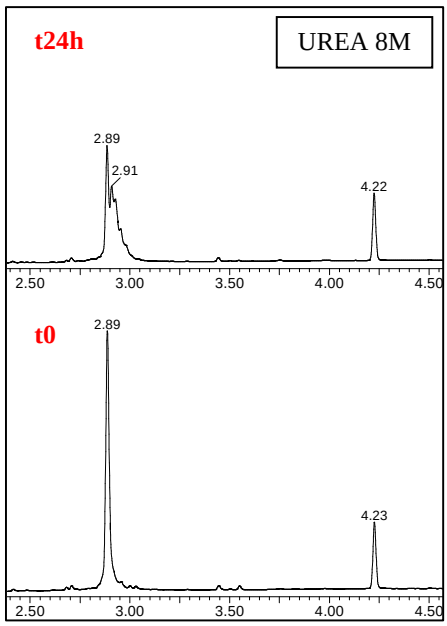

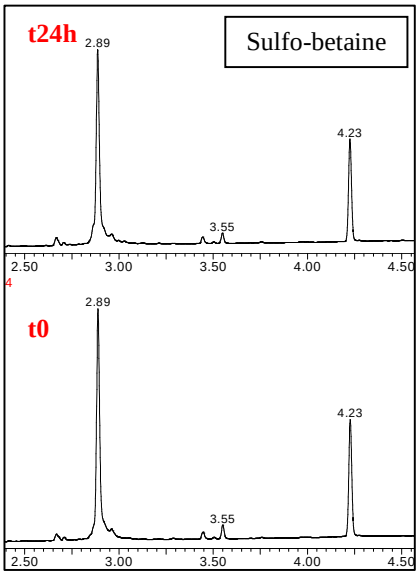

MalEp18/pAzF

	DMSO; -20°C	Sulfo-betaine	UREA 8M
Peak at 2,89 min; t0	6982,15 Da	6981,25 Da	6981,44 Da
Peak at 2,89 min; t24h	6981,67 Da	6980,8 Da	6981,17/7024,88 Da
Peak at 4,22 min; t0	551,68 Da	551,68 Da	551,68 Da
Peak at 4,22 min; t24h	551,68 Da	551,68 Da	551,68 Da

BCN-biotin

Figure 84. UPLC/MS analysis monitoring the SPAAC reaction between MalEp18(pAzF) and BCN-biotin in three dfferent conditions (DMSO -20°C; in presence of sulfo-betaine and UREA 8M).

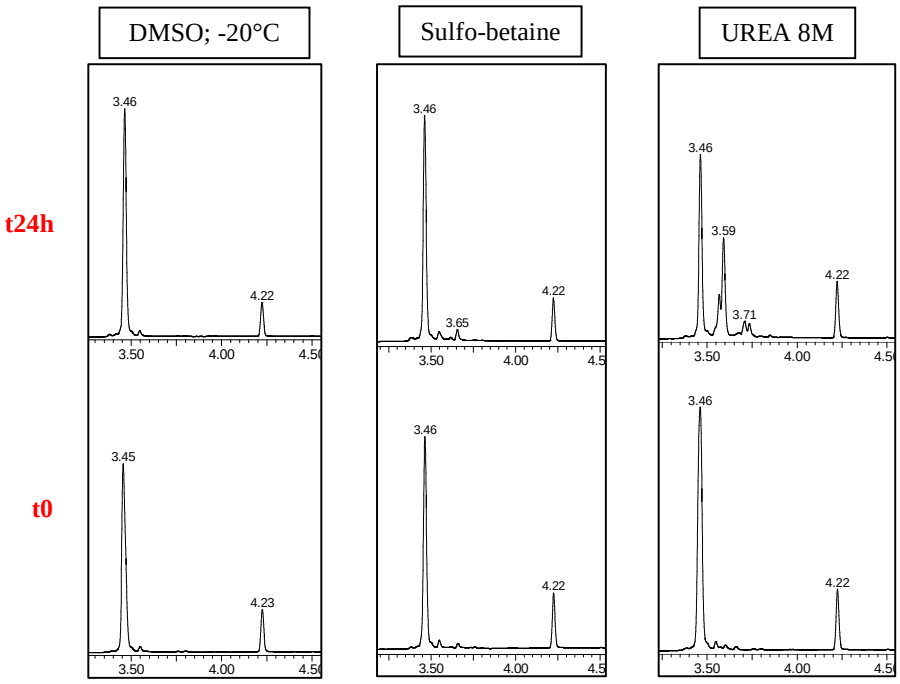

Peptide 1

	DMSO; -20°C	Sulfo-betaine	UREA 8M
Peak at 3,46 min; t0	2780,19 Da	2780,86 Da	2781,05 Da
Peak at 3,46/3.59 min; t24h	3331,01 Da	3331,66 Da	3331,51/3374,72 Da
Peak at 4,22 min; t0	551,6 Da	551,68 Da	551,68 Da
Peak at 4,22 min; t24h	551,6 Da	551,68 Da	551,68 Da

BCN-biotin

Figure 85. UPLC/MS analysis monitoring the SPAAC reaction between peptide 1 and BCN-biotin in three dfferent conditions (DMSO -20°C; in presence of sulfo-betaine and UREA 8M).

The results shown in Figure 84 indicate that the reaction did not occur also in these conditions. In all three cases, the chromatographic profile at time 0 was identical to that observed after 24 hours of reaction. Furthermore, the mass relative to the peaks present in the reaction did not vary indicating the inability of the MalEp18(pAzF) protein to react with the cyclooctyne-biotin. Only in the reaction carried out under denaturing conditions (8M UREA) was identified, after 24 hours of reaction, a chromatographic profile slightly different than that found at time 0 and the appearance of a different mass that coincides, however, with the adduct of the target protein with urea present in the buffer.
The reactions carried out with the peptide 1 instead occurred in all three cases: the mass relative to the peak of peptide 1 appeared to be coincident with that of the product after 24 hours of reaction. Also in this case, we noted the formation of the adduct with urea in the reaction carried out under denaturing conditions. These reactions confirmed the characteristic of robustness of the click chemistry reaction which showed a good efficiency in a variety of conditions.
Regarding the protein MalEp18(pAzF) and the process of genetic incorporation of unnatural amino acids will be necessary to perform future investigations aimed to understand the lack of reactivity of our target protein containing a residue of para-azido-phenylalanine with the alkyne reagent.
The tests of expression in the absence of pAzF unnatural amino acid in the growth medium and the results of N-terminal sequencing of the purified target protein had led to believe that the process of pAzF incorporation into MalEp18 was successful. Now it is necessary to understand the cause of the unresponsiveness of incorporated azido functional group. A MALDI-TOF analysis after tryptic digestion will be necessary to confirm the presence of pAzF in third position and later it will be useful to re-start from the optimization of the constructs design.

p18 ANTIGEN IMMOBILIZATION ON SOLID PHASE THROUGH THE USE OF LEUCINE ZIPPER (OR "VELCRO") PEPTIDES

Immobilization of proteins in a functionally active form and proper orientation is crucial for effective surface-based analysis of proteins, such as Diasorin LIAISON® immunoassays based on immobilization of antigens or antibodies on paramagnetic microbeads. For this reason we explored a new technique of immobilization on solid phase for the p18 antigen to be applied in LIAISON® EBV VCA IgG/IgM immunoassays.
This technique is based on the use of leucine zipper or “velcro” peptides, as described in detail in the introduction. For this purpose two recombinant constructs were created; in the first, named ZE-ELP36, that represents the capture domain of the target protein, the acidic partner velcro, named ZE, was fused with the ELP[KV7F36] sequence, previously described for the ELP-intein purification method. The Elastin Like Polypeptides (ELP) sequence is the region of the construct that allows the interaction with the solid phase, in fact it is able to interact effectively with the tosyl groups present on paramagnetic microbeads thanks to the presence of several lysine residues in its sequence. Furthermore the ELP sequence can be exploited for the purification of the construct itself, through the use of Inverse Transition Cycling (ITC) method. In the second construct, named MalEp18-ZR, the basic partner velcro, called ZR, was fused to the target protein MalEp18 as affinity tag. As previously illustrated, the idea of this system is based on the interaction of the two velcro peptides, through the formation of coiled coil structures, to enable the indirect immobilization of the target protein on solid phase, in a oriented and stable way (Figure 86).

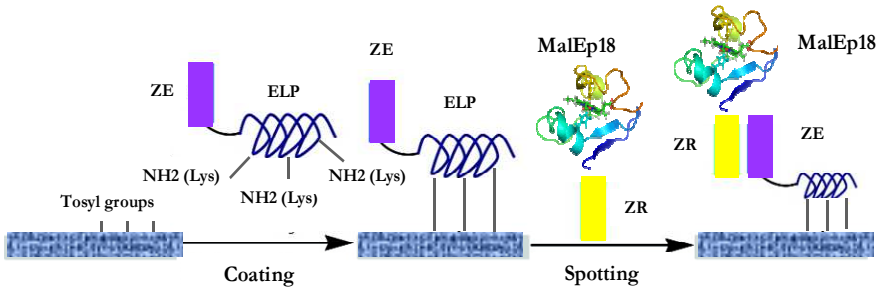

Figure 86. Schematic representation of p18 antigen indirect immobilization on solid phase through the use of velcro peptides.

Once the cloning was carried out for both constructs (pET24-ZE-ELP[KV7F36] and pET24-MalEp18-ZR; see materials and methods section for more details), we transformed the BL21(DE3) *E.coli* strain with the two different plasmids.
Table 11 shows the different expression conditions explored for both constructs.

Fermentation	Vector	Temperature (°C)	Induction Time (h)	[IPTG] (mM)
A	pET24-ZE-ELP[KV7F36]	37°C	3	1
B	pET24-ZE-ELP[KV7F36]	15°C	20	0,1
C	pET24-MalEp18-ZR	37°C	3	1
D	pET24-MalEp18-ZR	15°C	20	0,1

Table 11. Different conditions used for ZE-ELP36 and MalEp18-ZR fusion proteins expression.

The ZE-ELP36 (expected molecular weight of 21,55 kDa; black squares) and MalEp18-ZR (expected molecular weight of 12,24 kDa; gray squares) target proteins are well expressed in all conditions (Figure 87).

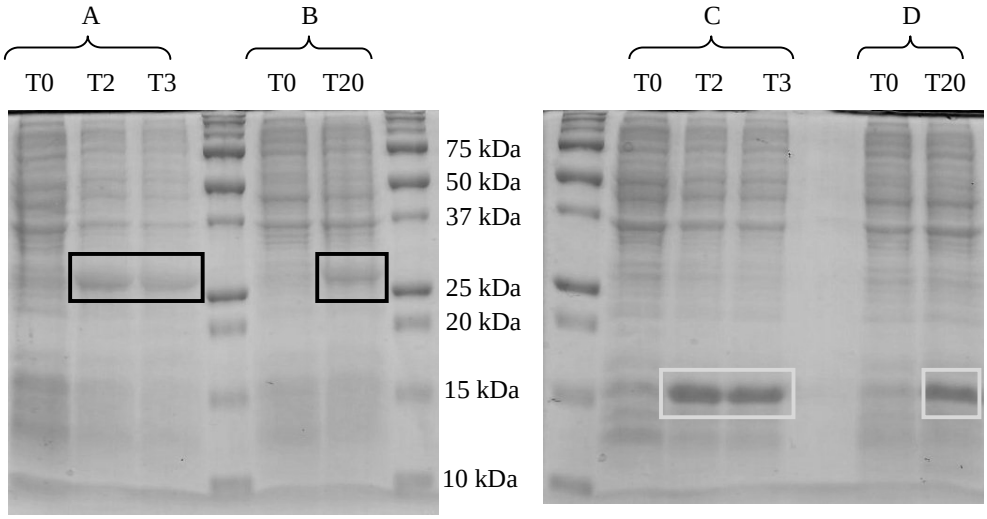

Figure 87. SDS-PAGE analysis showing the induction test of BL21(DE3) pET24-ZE-ELP[KV7F36] and BL21(DE3) pET24-MalEp18-ZR, fermented at 37°C and 15°C. Black squares indicate ZE-ELP36 target protein and gray squares indicate MalEp18-ZR target protein.

After ensuring the expression, we verified the solubility of the two fusion proteins in both conditions (37°C and 15°C) as detailed in Materials and Methods section.

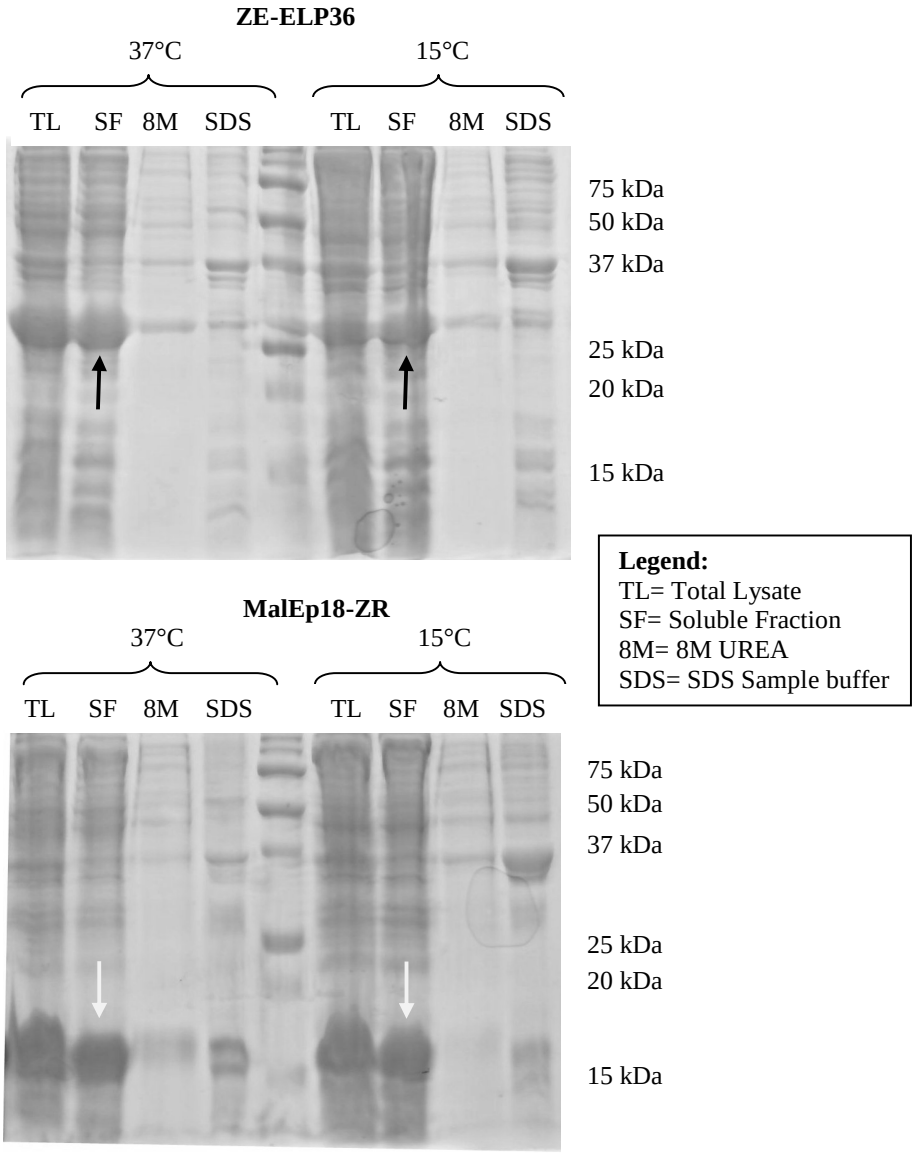

Figure 88. SDS-PAGE analysis showing the solubility test of BL21(DE3) pET24-ZE-ELP[KV7F36] and BL21(DE3) pET24-MalEp18-ZR, fermented at 37°C and 15°C. Black arrows indicate ZE-ELP36 and gray arrows indicate MalEp18-ZR fusion protein present in soluble fraction.

The SDS PAGE analysis of solubility test (Figure 88) shows that the ZE-ELP36 and MalEp18-ZR target proteins are completely soluble in both conditions of fermentation (37°C and 15°C). In fact, the band corresponding to ZE-ELP36 (expected molecular weight of 21,55 kDa; black arrows) and also that corresponding to MalEp18-ZR (expected molecular weight of 12,24 kDa, gray arrows) is visible, in both cases, in the total lysate (TL lane) and in the soluble fraction (SF lane), but it is not present, except in small part, in fractions containing urea or SDS sample buffer (insoluble fractions).
Also in this case (as for the MalEp18-*Mxe*GyrA-ELP36 fusion protein), we chose to use the fermentation carried out at 15°C for the purification of both target proteins.

For purification of the ZE-ELP36 fusion protein, we exploited the aggregation and solvation properties of ELPs by using the Inverse transition Cycling (ITC) process, as previously described.
First, in order to find the lowest NaCl concentration able to completely precipitate the ZE-ELP36 fusion protein, a large range of salt concentrations was explored: 2.5 M, 2.0 M, 1.5 M and 1.0 M of NaCl (Figure 89). Only the lowest NaCl concentration (1.0 M) determined the loss of the ZE-ELP36 protein (the presence of the target protein also in the supernatants obtained after the hot spin steps - 1°HS and 2°HS lanes - indicates that the concentration of salt added in solution was not sufficient to promote efficient precipitation of the ELP-fusion protein), while a complete recovery of protein was obtained at 1.5 M or higher NaCl concentrations. Therefore, all subsequent precipitation steps were performed at 1.5 M salt concentration. Two ITC rounds were performed for every purification batch, as illustrated in Figure 90.

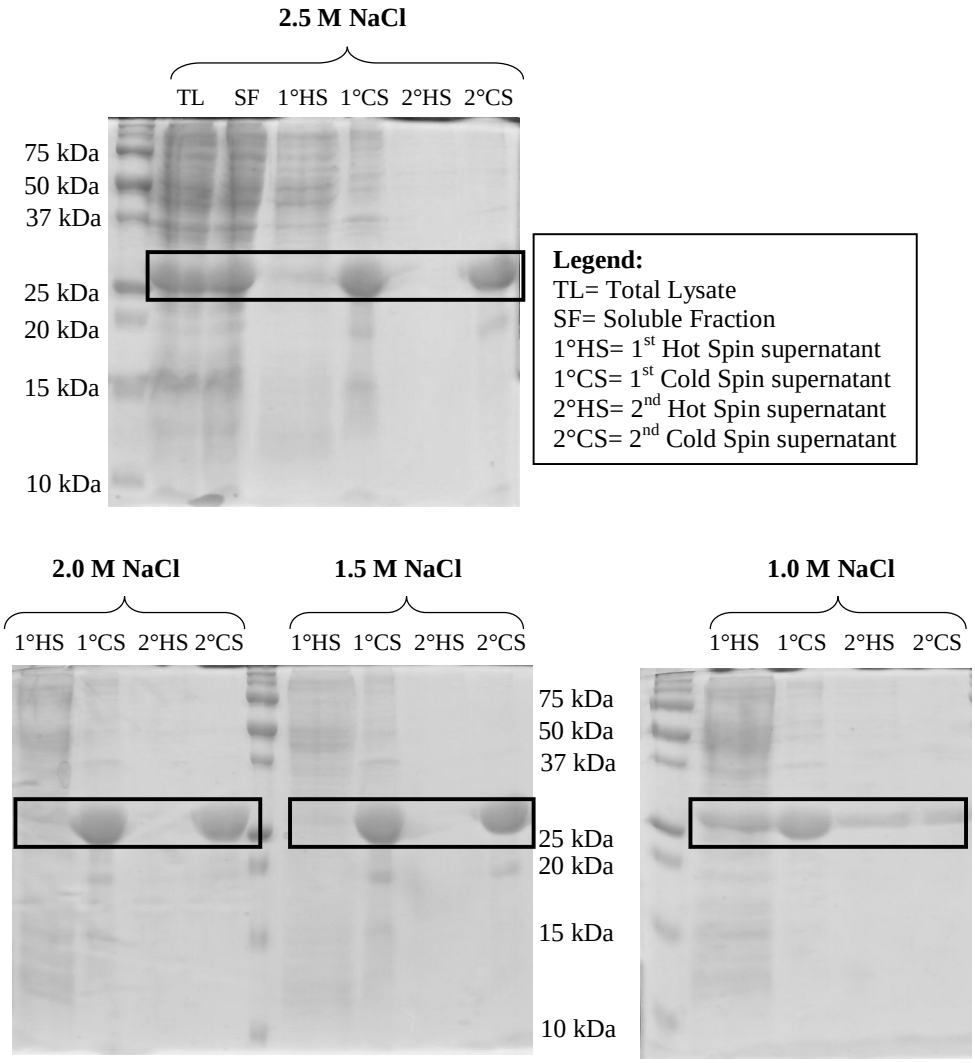

Figure 89. Precipitation tests of ZE-ELP36 fusion protein at different NaCl concentrations. Red squares indicated the band of ZE-ELP36 target protein.

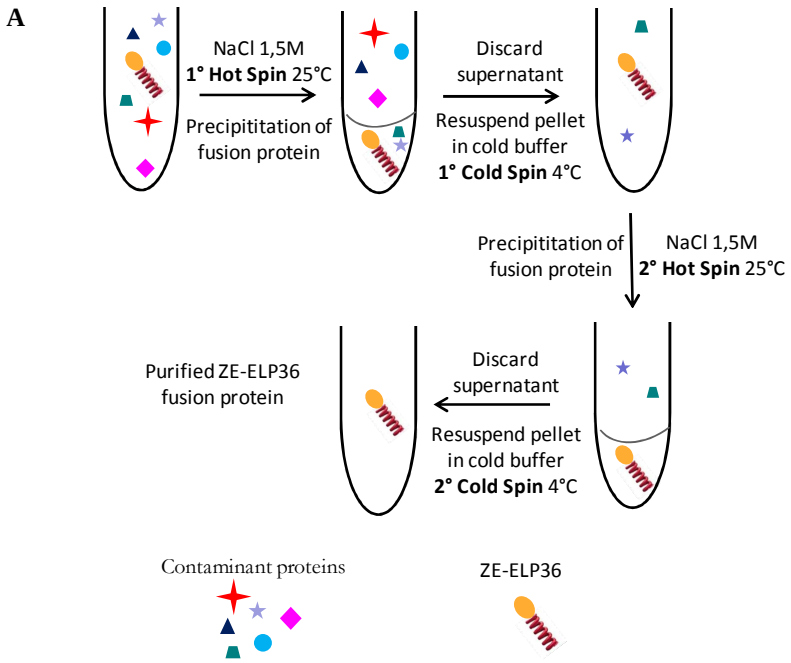

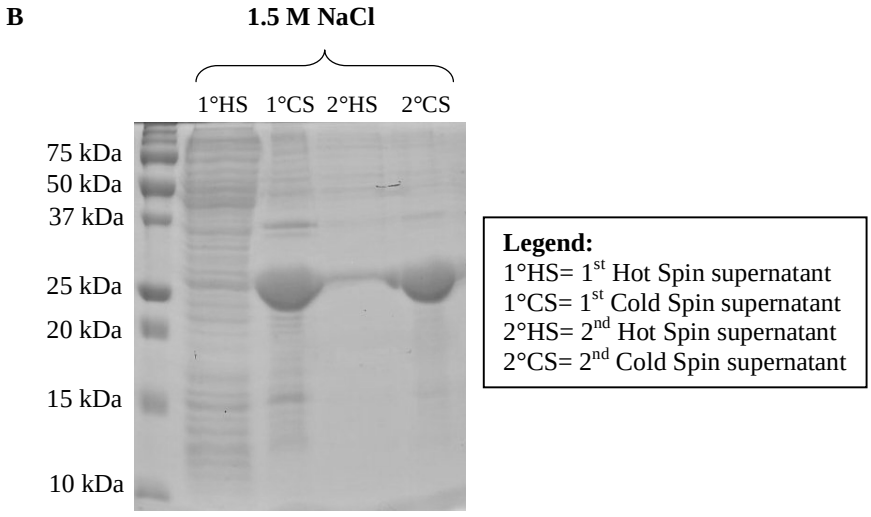

Figure 90. (A) ITC purification scheme and (B) SDS PAGE analysis monitoring ITC purification process.

After ITC process, a chromatographic step of purification was performed. The sample was loaded on a GFC column (Superdex 200 Hiload 16 60, see materials and methods section) previously equilibrated with PBS buffer. Elution was carried out with a isocratic gradient of the same PBS buffer. The ZE-ELP36 target protein was obtained with a good purity and yield (Figure 91).

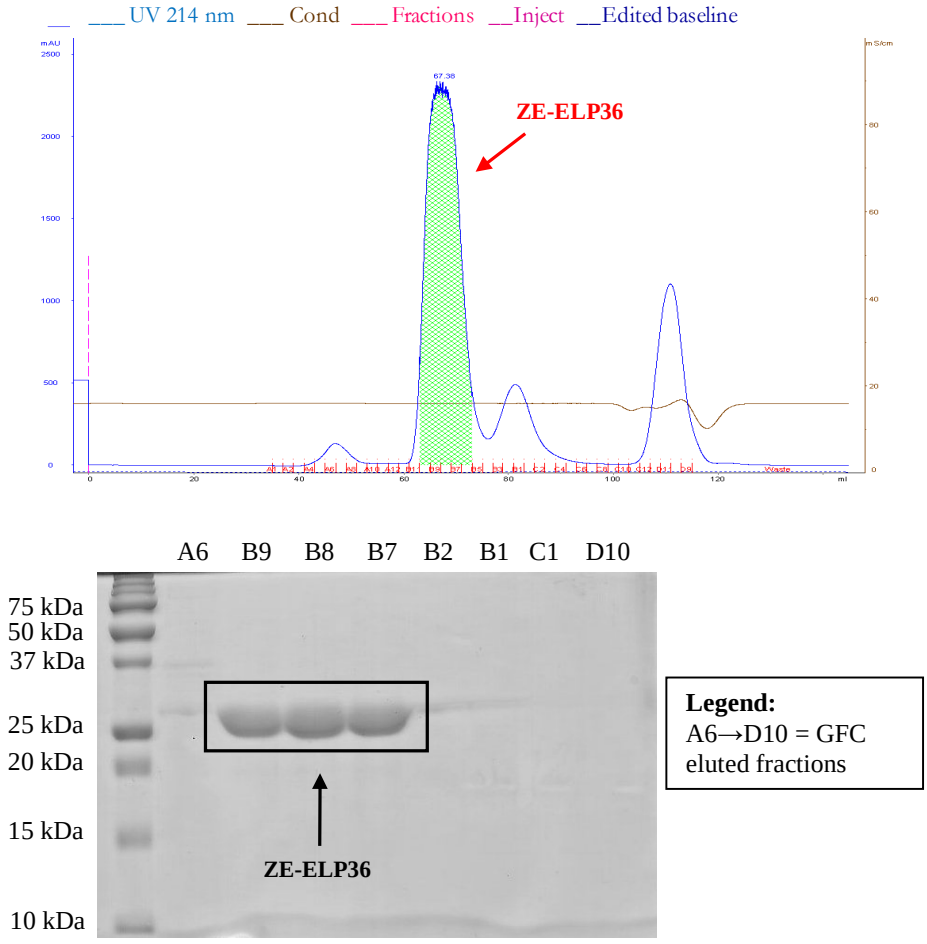

Figure 91. GFC chromatographic profile of ZE-ELP36 target protein (above) and corresponding SDS-PAGE analysis of eluted fractions (below).

Fractions corresponding to the ZE-ELP36 target protein (Figure 91) were then pooled together and quantified through densitometric analysis of bands corresponding to the purified target protein on SDS-PAGE (Biorad Image Lab software; data not shown).

For purification of the MalEp18-ZR fusion protein, we performed a Cation Exchange Chromatography (CEC) exploiting the high isoelectric point of the protein (pI:11.47). The sample was loaded on a CEC column (CM_Ceramic_HyperD_F_XK_16/5.5, see materials and methods section). This column was activated with buffer B CEC (25mM Sodium acetate, 1M NaCl; pH 5) and finally equilibrated with buffer A CEC (25mM Sodium acetate; pH 5). Protein elution was done with a linear gradient from 0% to 100% of buffer B CEC in 60 mL (Figure 92).

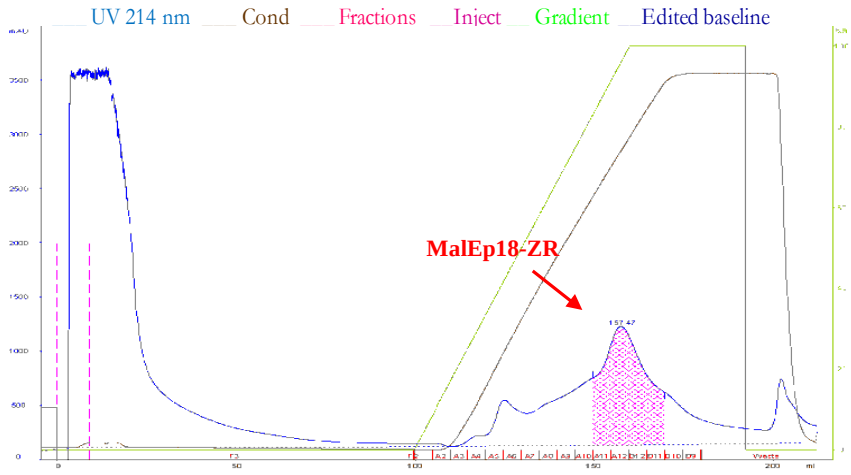

Figure 92. CEC chromatographic profile of MalEp18 target protein.

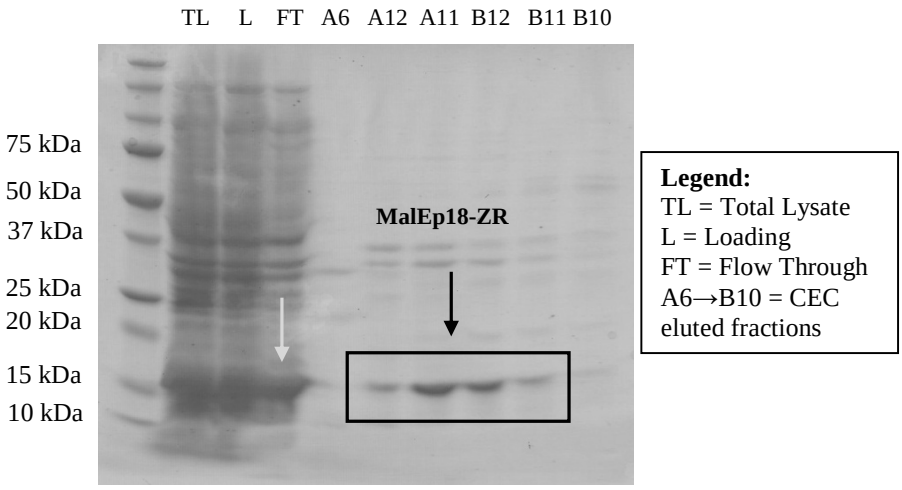

Figure 93. SDS-PAGE analysis monitoring CEC purification of MalEp18-ZR. Gray arrow indicates MalEp18-ZR target protein present in flow through.

As the SDS-PAGE analysis shows (Figure 93), the cation exchange chromatography as a method of purification did not permit to obtain the target protein with a good purity degree and yield. In the fractions containing the protein of interest, in fact, there were many bands of contaminating proteins (Figure 93; fractions A12 →B11); moreover, a large amount of protein was lost during the process (presence of a band corresponding to the target protein in the flow-through; Figure 93; FT lane, gray arrow).

For this reason, and due to the peptidic nature of the construct MalEp18-ZR, we decided to perform a Reversed Phase Chromatography (RPC) as purification method. The sample was loaded on a reversed phase column (Source15RPC 15µm 8.5x100mm, see materials and methods section) previously equilibrated with water/TFA 0.1% and CH3CN/TFA 0.1%. Elution was performed with a linear gradient of 10-60% CH3CN/TFA 0.1% in 35 mL. A good purity degree and yield was obtained for the MalEp18-ZR target protein (Figure 94) and the pool of fractions corresponding to the target protein was then subjected to lyophilization and quantified.

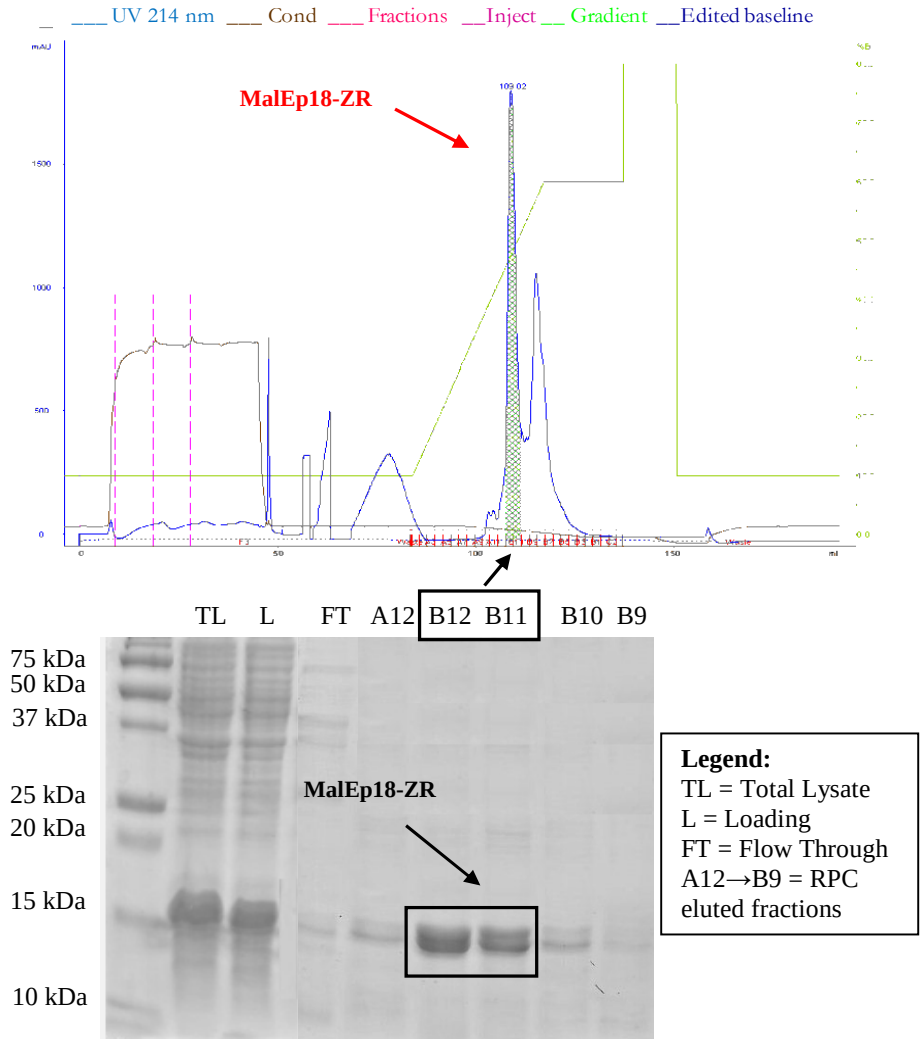

Figure 94. RPC chromatographic profile of MalEp18-ZR target protein (above) and corresponding SDS-PAGE analysis of eluted fractions (below).

Once expressed, purified and biochemically characterized, the ZE-ELP36 and MalEp18-ZR fusion proteins were tested in the Diasorin LIAISON ® EBV VCA IgM immunoassay for their ability to immobilize the p18 antigen on solid phase. This new method of coating was then compared with that currently used (Figure 95).

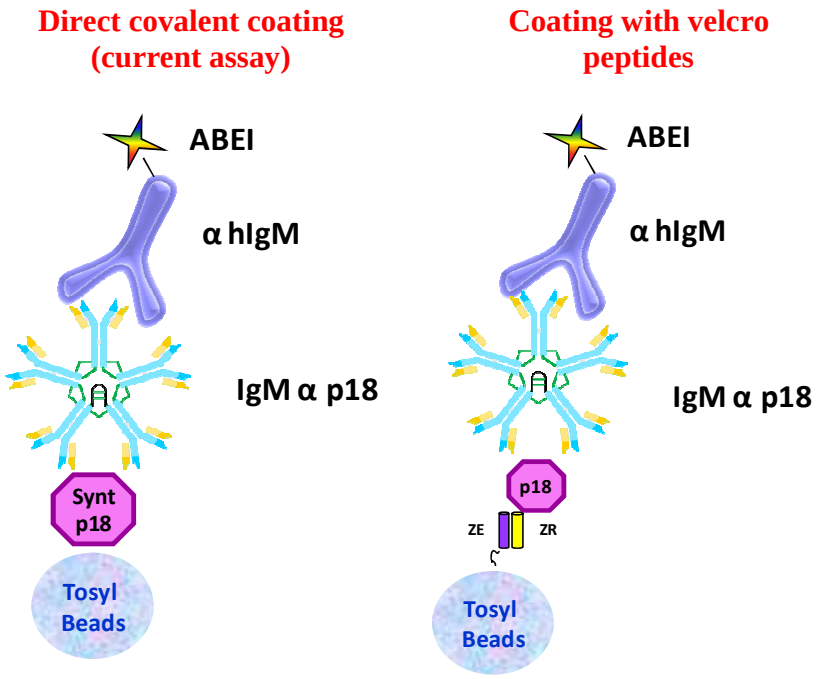

Figure 95. Schematic representation showing comparison between different techniques for p18 antigen immobilization on solid phase: direct covalent coating and through the use of velcro peptides.

In order to set up the immobilization system on solid phase that involves the use of Velcro Peptides (VP), two different assay protocols were explored. The first protocol provided a pre-incubation of the two constructs to allow the interaction of two velcro peptides before the reaction with the other bioreagents of the immunoassay (incubation off-line). The second protocol (incubation on-line) provided instead that the interaction between the 2 velcro peptides occurs during the assembly of

the reaction directly on the LIAISON® instrument (more details about the two protocols are described in materials and methods section). For the evaluation of these two protocols, two calibrators and the positive and negative controls present in the current kit were analyzed (in duplicate). In parallel, the current assay was run (Figure 96).

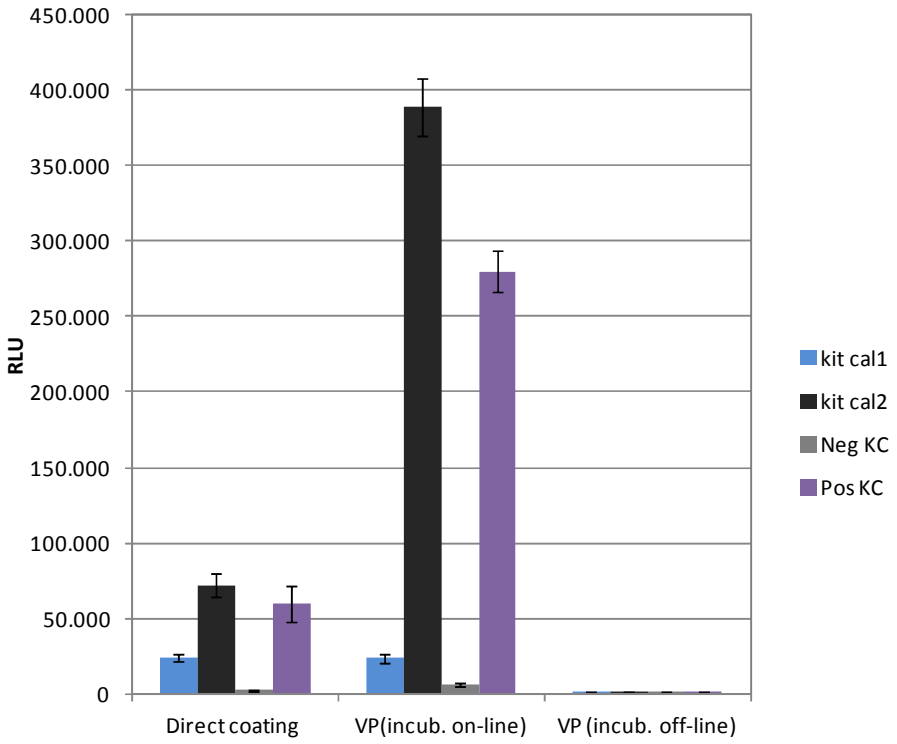

Figure 96. Comparison between direct covalent coating (current assay) and two different immobilization protocols on solid phase through the use of Velcro Peptides (VP) system. The different methods were tested on negative (Neg. KC) and positive (Pos KC) controls and two calibrators (kit cal1 and kit cal2) present in the current kit.

Experimental data (Figure 96) revealed that the assay protocol which provides the pre-incubation off-line of velcro peptides is not responsive. Using this type of protocol, in fact, neither the two calibrators nor the positive control were detected. The other protocol, characterized by incubation on-line of the two constructs, was found to be promising with signals relative to the positive control and calibrator 2 (kit cal2) much higher than those detected by the current kit. For this reason, this protocol was selected to perform the next experiments. In the following test, the immunochemical activity of the p18 antigen immobilized on solid phase through the velcro peptides system or through direct covalent coating (current assay) was tested on a standard curve composed by a high positive human serum sample in dilution. As described above for the different variants of the p18 antigen, in this curve there are known increasing concentrations of antibodies (IgM) directed specifically against the p18 antigen. Each test was conducted in triplicate and the response, in RLU, was plotted versus the increasing concentration (U/ml) of α p18 IgM antibodies present in the standard curve. Figure 97 shows the direct comparison between the analytical performance of p18 antigen immobilized on solid phase through direct covalent coating (gray) and through velcro peptides system (blue) in the EBV VCA IgM immunoassay.

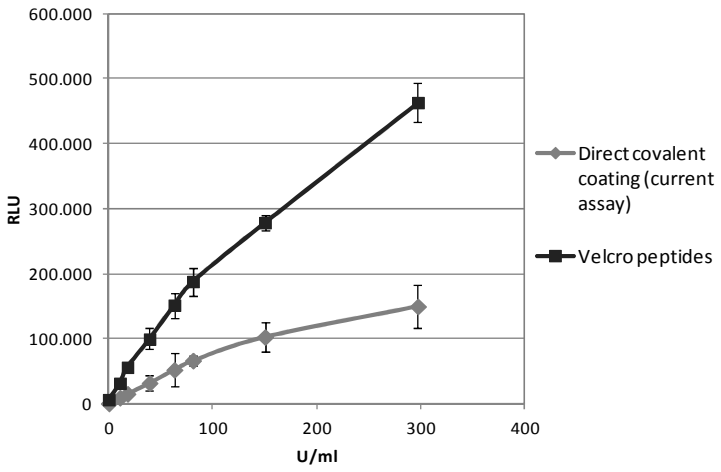

Figure 97. Comparison between the analytical performance of p18 antigen immobilized through direct covalent coating (gray) and velcro peptides system (blue) in the LIAISON® EBV VCA IgM immunoassay on a standard curve.

The immobilization of the p18 antigen on solid phase through the use of velcro peptide system had proven to be immunoresponsive: the signal values (RLUs) in fact follow the concentration increase of IgM α p18 antibodies of standard curve. Furthermore, the response given by the p18 antigen immobilized through velcro peptides system was considerably higher than that obtained with the p18 antigen directly coated on solid phase.

In order to evaluate the robustness of velcro peptides immobilization method, a panel of negative and positive samples was tested (Figure 98). In parallel, the current assay was run as reference. Final evaluation of the p18 antigen performance immobilized on solid phase through different techniques was expressed as the average of the signals of each panel. The p18 antigen immobilized on solid phase through velcro peptides system showed a slight increase of the signal relating to the positive samples (panel B; black bar) compared to the synthetic peptide directly coated on solid phase (panel B; gray bar). The negative aspect of the velcro peptides system was that also the signal of negative samples (panel A; black bar) was much higher than that detected for the direct covalent coating (panel A; gray bar). The result was an increase of the background with a consequent decrease of the ratio between the signal of the positive to negative samples. Unfortunately the lowering of the positive/negative signal ratio correlates with the reduction of immunoassay performance. Probably the high background related to the use of velcro peptides was provided by the presence of numerous charged residues in the sequence of the same peptides, that promotes the formation of aspecific interaction with other components present in the sample or in the assay itself.

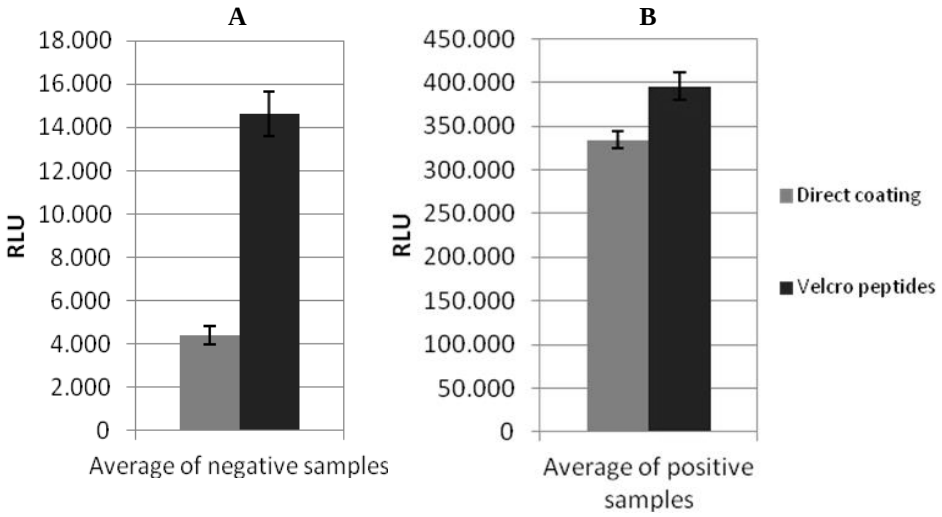

Figure 98. Comparison between the analytical performance of p18 antigen immobilized on microbeads through direct covalent coating (gray) and velcro peptides system (blue) in the LIAISON® EBV VCA IgM immunoassay on a panel of negative and positive samples.

This innovative system of immobilization has proven to be responsive; however the problem of high background needs further analyses in order to find strategies for its resolution, such as the use of specific detergents in the assay buffers or the sequence optimization of constructs themselves.

LIAISON® EBV VCA IgM REVERSE FORMAT

Despite the DiaSorin LIAISON® EBV VCA IgM immunoassay has a good analytical performance, in order to obtain an increase of specificity and therefore to exclude potential false positive samples, a new assay format was explored. Starting from the current indirect format (which includes the p18 antigen immobilization on solid phase), we tried to develop a "reverse" format, in which anti-human IgM antibodies, able to recognize human IgM present in the sample, are used as a capture element on solid phase, while the p18 antigen is used as a tracer (Figure 99). In this case the aim was to synthesize a tracer molecule characterized by the presence of the p18 antigen (p18 tracer). In order to optimize the emission of the signal relative to the tracer molecule and therefore the sensitivity of immunoassay, we used a particular non-proteic scaffold with a structure able to bind several chemiluminescent molecules (ABEI) together with the antigen of interest. In addition, for the synthesis of this tracer, we decided to applied the click chemistry, which, as described above, has proven to be a highly efficient and robust chemistry.

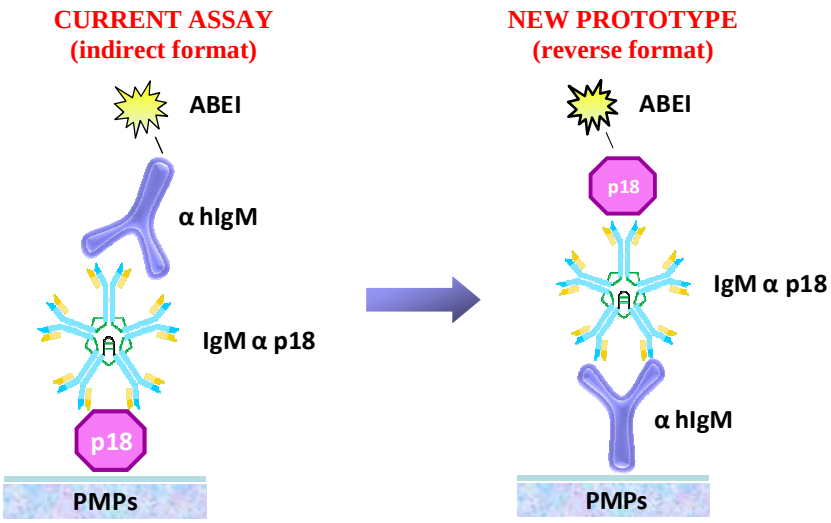

Figure 99. Schematic representation of LIAISON® EBV VCA IgM immunoassay format change. Starting from the current indirect format, we tried to develop a "reverse" format, in which the p18 antigen is used as a tracer.

The p18 tracer, necessary to perform the DiaSorin LIAISON® EBV VCA IgM immunoassay in its reverse format, was synthesized according to the following reaction steps (Figure 100). Figure 101 instead shows the chromatographic profiles of the GFC purifications carried out respectively in step 3 and in step 5 of process.
Briefly, in the first step the scaffold was labeled with a multiplicity of ABEI molecules; the reaction occured in an organic medium (DMSO) overnight. In the second step the other functionalities of the scaffold molecule were derivatized with the bicycle nonyne (BCN) reagent, necessary to carry out the subsequent reaction of click chemistry. This step which involved the reaction between the amino groups present on the scaffold and the NHS-ester group of the BCN molecule, was carried out in DMSO for 2 hours. The third step was represented by a gel fitration chromatography (GFC) to remove the excess of ABEI and BCN present in reaction (Superdex 200 Hiload 16 60 column, PBS buffer, isocratic gradient; see materials and methods section). In the fourth step the click chemistry reaction between the modified ABEI-BCN scaffold and the azido-p18 peptide (p18-N3), synthesized ad hoc in order to possess an N-terminal azido group (azido-lysine), was performed (see materials and methods session). The reaction was carried out overnight in PBS buffer. The final product (scaffold-ABEI-p18) was then subjected to an additional purification process to remove the excess of azido-p18 peptide (Superdex 200 Hiload 16 60 column, PBS buffer, isocratic gradient; see materials and methods section).
The immunoreactivity of these particular type of tracers, that includes the use of a non-proteic scaffold molecule as carrier for several chemi-luminescent probes and for the antigen of interest, was previously demonstrated in a model system that deviates from the main topics of the thesis, as a proof of concept. The model system is the LIAISON® Murex recHTLV-I/II prototype assay used for the detection of antibodies specific for the Human T-lymphotropic Virus type I and II (HTLV-I/II). The experimental details and the correlated results are detailed in the appendix session.

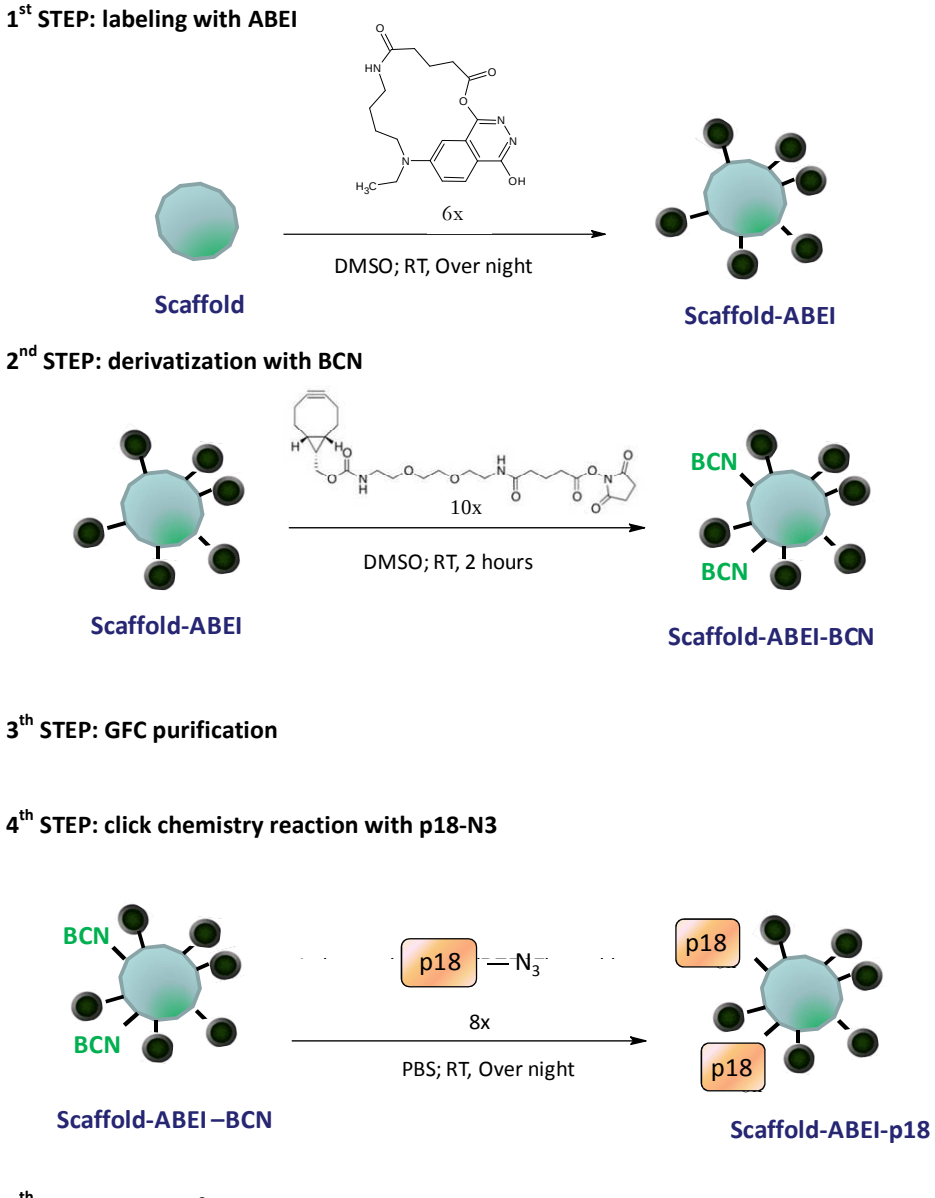

Figure 100. Schematic representation of p18-tracer synthetic process.

A_Scaffold-ABEI-BCN

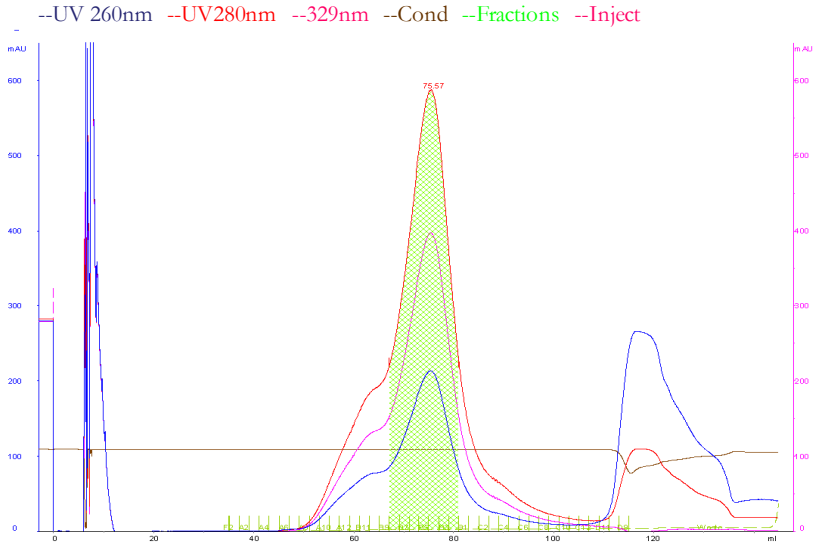

B_Scaffold-ABEI-p18

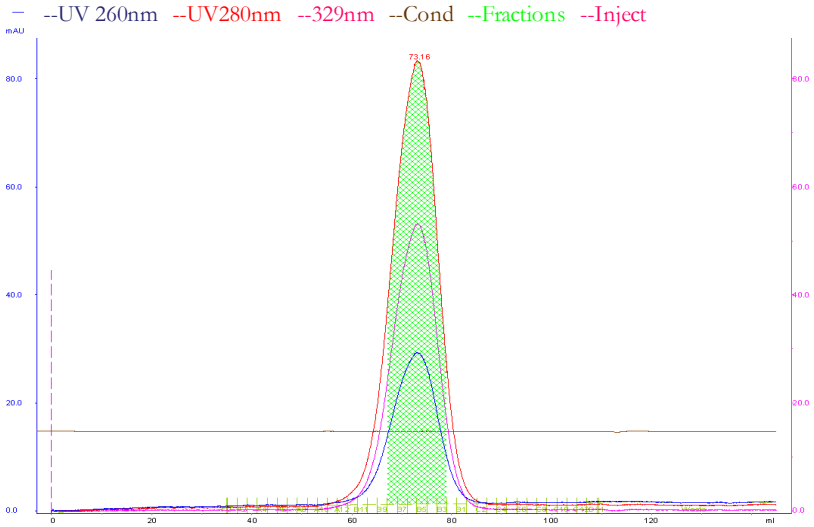

Figure 101. Chromatographic profiles of GFC purifications performed at the level of step 3 and 5 of p18-tracer synthetic process. The first chromatogram refers to scaffold-ABEI-BCN intermediate, while the second refers to scaffold-ABEI-p18 product.

The new p18-tracer thus obtained, was then tested in a reverse format assay and compared to the current one (indirect format). The analysis was performed in duplicate on the negative and positive controls present in the current kit and on a panel of negative (only 2) and positive samples (8 in total) (Figure 102).
The results indicated that this new type of format was not responsive, it was not able to detect neither the positive control nor the positive samples for EBV IgM. The signals (RLUs) related to the positive control (panel A) and to the positive samples (panel C) were in fact indistinguishable to those obtained for the negative samples (panel B). Probably the immobilization of anti-human IgM antibodies on solid-phase, which capture all of the IgM present in the sample and not only those specific to the p18 antigen, disadvantages the system and makes it ineffective. Moreover, the system could be disadvantaged by the fact that the immunoglobulins of type M are characterized by a quaternary structure with a high steric hindrance, and thus the interaction between anti-human IgMs coated on solid phase and other anti-p18 IgMs present in the samples is not favor.

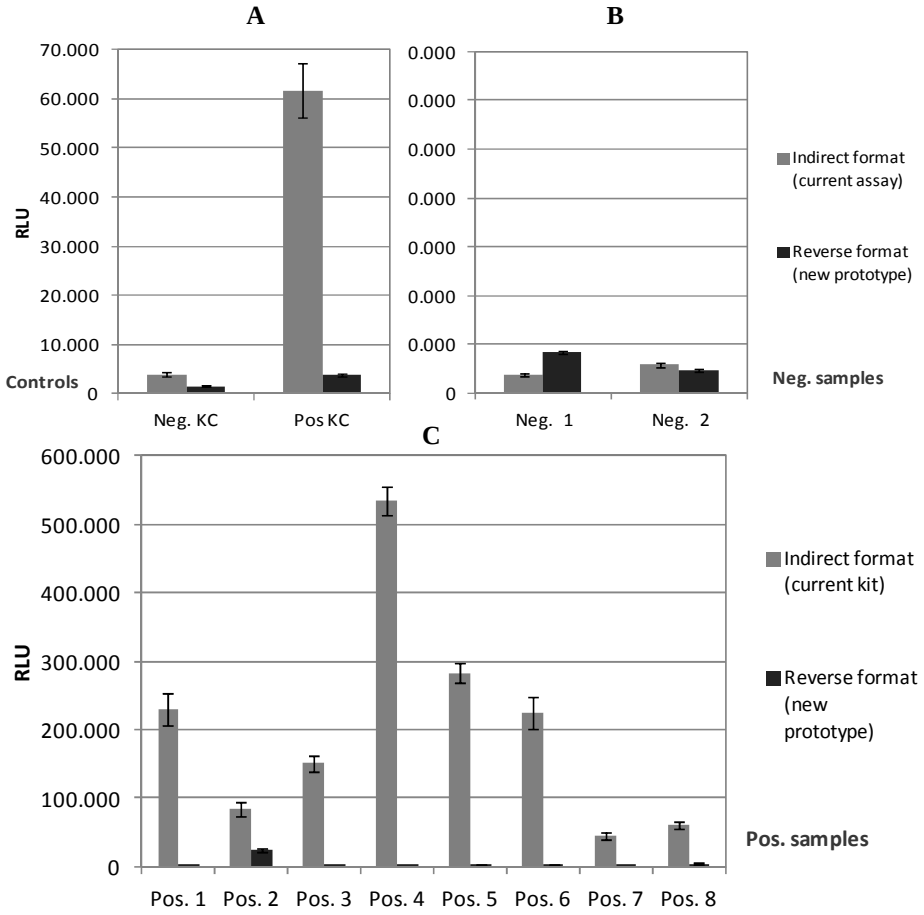

Figure 102. Comparison between the analytical performance of indirect format (current assay; gray) and reverse format (new prototype; blue) of LIAISON® EBV VCA IgM immunoassay on controls of current kit (Neg. KC and Pos. KC; panel A) and on a panel of negative (panel B) and positive samples (panel C).

We are confident that the problem of lack of responsiveness of the p18-tracer is not related to the nature of the same tracer, but to the type of assay format, specifically used for the detection of IgM antibodies to the p18 antigen. In fact, the same tracer was used in a similar reverse assay format for the detection of IgG in sera of mice immunized with the p18 antigen for other purposes, showing good results. Moreover, mouse sera before immunization shown the absence of reactivity (data not shown).

DISCUSSION

In the last years there have been great advances in immunodiagnostics. Despite the numerous advances in the field, there is a critical need for rapid and cost-effective immunoassay procedures and novel diagnostic solutions in order to increase the potentiality and the outreach of immunodiagnostics. Improvements in immunodiagnostic technologies and the exploration of new techniques provide the basis for developing immunoassays capable of meeting stringent requirements for sensitivity, specificity, robustness, and simplicity.

For this purpose and then with the objective to develop more performing bioreagents and to find new solutions for the improvement of immunodiagnostic assays performance, in this work numerous techniques and innovative procedures were explored and developed. As model systems for the application of these new technologies, the assays designated for the determination of antibodies directed specifically against the Epstein-Barr virus (Diasorin LIAISON® EBV VCA IgM and IgG assays) were selected.

EBV is the causative agent of infectious mononucleosis and is one of the most successful viruses, it is estimated that nearly 95% of the adult population worldwide is seropositive for EBV. Moreover, it is associated with a still growing spectrum of clinical disorders, ranging from acute and chronic inflammatory diseases to lymphoid and epithelial malignancies; for this reason it is necessary to develop diagnostic assays for EBV detection with high specificity and sensitivity. The minor viral capsid protein VCA p18 is one of the most important antigens for the diagnosis of EBV and for this reason it is a key bioreagent for LIAISON® EBV VCA IgM and IgG assays. The several methods explored in this thesis allowed to obtain different variants of the p18 antigen with the aim to improve the performance of immunoassays for the EBV detection mentioned above.

The first point on which we focused was the exploration of the ELP-intein system as an alternative production method for the p18 antigen. This method is based on the combination of two technological tools, the ELP aggregation ad solvation properties (physico-chemical tool) and the intein auto-cleavage activity (biochemical tool). ELPs are thermally responsive polypeptides that undergo an inverse temperature phase transition in response to thermal changes. The temperature-dependent, reversible self-

aggregation of ELPs is exploited for proteins purification, in particular in a non-chromatographic protein purification method named inverse transition cycling (ITC). ITC protein purification provides the use of ELPs as tag, in this way the target protein fused to an ELP sequence can be purified through repeated cycles of precipitation and re-solubilization in response to thermal and buffer salt concentration changes, exploiting the ELPs properties. The ELP-Intein system also relies on the self-cleaving properties of inteins: the insertion of an intein at the right position in the ELP fusion construct gives the opportunity to isolate the target protein from the ELP tag at the end of ITC process. Therefore, this new non-chromatographic method is characterized by the use of a self-cleavable temperature responsive tag and offers an alternative option for protein purification.

The considerable length (57 amino acids) of the p18 synthetic peptide, used as capture element coated on solid phase in LIAISON® EBV VCA IgM and IgG assays, makes its synthetic process very complex. Moreover the production of the same antigen in recombinant way, alone or as a fusion construct with classical fusion partners (e.g. MBP; GST; Trx), carried out in the past in our laboratories, did not allow to obtain good results in terms of efficiency and yield of purified antigen. For all these reasons we decided to apply the ELP-Intein system for the production of the p18 antigen. We first optimized the design of the construct for the expression of the ELP-Intein-fusion protein with the addition of the first six amino acids of the maltose binding protein at the N-terminus and we then determined the best conditions for the Inverse Transition Cycling (ITC) purification process in terms of salt concentration necessary to completely precipitate the ELP-fusion protein and in terms of ITC rounds numbers. Once obtained the ELP-fusion protein with a good purity degree, the adding of DDT with free thiol groups, allowed the self-cleavage activity of intein and therefore the release of the p18 antigen from the ELP-Intein tag. Finally, to separate the cleaved tag from the target protein, we performed a chromatographic step of purification (reversed phase purification). At the end of the entire process, the p18 recombinant antigen was successfully obtained with high purity and yield and the ELP-Intein method has proved to be an excellent system for the preparation of the same antigen. Numerous advantages are linked to the

use of this system: it is technically simple, fast and economical, in fact it avoids the expense associated with traditional chromatographic separations and requires no specialized equipment or reagents. Moreover, it is a very easy to scale-up process, from bench scale to industrial scale production. Furthermore, the intein insertion in the fusion construct allowed the avoidance of any protease for target protein release from the tag, differently from standard purification methods with affinity. Protease use correlates with increased process cost and time, introducing also the risk of undesired aspecific cleavage. For all these reasons and on the basis of the results obtained for the p18 antigen, ELP-Intein system appeared to be a very good alternative to currently used purification procedures that are generally more expensive, difficult to scale-up and that require several days to obtain a purified protein.

The use of inteins, and in particular the use of a C-terminal mutated intein (*Mxe*GyrA N198A) in the fusion construct, allowed us to obtain another p18 antigen variant characterized by a C-terminal site specific biotinylation. In fact p18-thioester derivative, obtained through the thiols induced N-terminus cleavage activity of a mutated intein, was exploited in expressed protein ligation technique, in which the reaction between the recombinant p18 antigen with a C-terminal thioester group and a synthetic peptide containing a thiol group at the N-terminus and a lysine-biotin at the C-terminus permitted to obtain a C-terminal site-specific biotinylation of target protein. The critical step of this reaction was the choice of reagent for the thiotransesterification and thus for the induction of intein-self cleavage reaction. A variety of molecules can be used to induce thiolysis of intein fusion proteins; the choice of MESNA (2-mercaptoethanesulfonic acid) allowed to obtain p18 antigen with a highly stable and sufficiently reactive for the reaction of expressed protein ligation C-terminal thioester.

In general this technique has proved to be simple, involving a single chemical step, and therefore a powerful tool for the chemical engineering of proteins.

p18 recombinant antigens (biotinylated and non-biotinylated derivative), obtained in the first case through ELP-Intein method and in the second exploiting the expressed protein ligation technique, were immunometrically characterized. The immunochemical activity of both

antigens, tested in the Diasorin LIAISON® EBV VCA IgM and IgG assays, was considerably higher than that associated to the synthetic peptide currently in use; this improvement in immunochemical activity was especially more evident for the biotinylated variant. The C-terminal site-specific biotinylation of p18 antigen, in fact, dramatically improved its immunochemical activity, most likely due to the oriented exposure of the antigen on solid phase, provided by the site-specific modification. In addition, the results obtained on a panel of real samples for both recombinant antigens showed an increase of the ratio between the signal of the positive and negative samples when compared to the synthetic peptide of current kit; the result was a great improvement of performance of immunoassays for EBV detection. Therefore both recombinant derivatives of p18 antigen represent potential antigen candidates for the re-development of the current Diasorin LIAISON® EBV VCA IgM and IgG assays with improved analytical performance. The use of biotinylated variant would also have the important advantage that the amount of antigen to be used in the immunoassay would be much lower than those necessary for the non-biotinylated antigen with a significant positive effect on the costs of production of the bioreagents assays.

The genetic incorporation of Unnatural Amino Acids (UAA) into target protein directly in *E. coli* cells was another technique explored to achieve the N-terminal site-specific biotinylation of the p18 antigen. The aim was to determine if the biotinylation on a different site could have benefits in terms of antigen immunochemical activity. The use of this technology offers considerable advantages over both chemical and *in vitro* biosynthetic strategies, such as the site-specific and homogeneous modification of recombinant proteins under physiological conditions, and then the possibility to chemoselective modify the protein preserving its structure, functionality and reactivity. In particular, we applied this strategy to incorporate a para-azido-phenylalanine (pAzF) at the N-terminal region of the p18 protein. This particular unnatural residue was then exploited to realize a Strain-Promoted Azide-Alkyne Cycloaddition (SPAAC**)** reaction with a molecule of cyclooctyne-biotin in order to obtain the N-terminal site specific biotinylation of the p18 antigen.

We first optimized the target protein expression conditions for this particular system which provides the concomitant expression of the p18

antigen with a stop codon at the level of unnatural amino acid incorporation site and the tRNA/aaRS pair specific for the introduction of pAzF. We then purified the p18 antigen containing the N-terminal azido-group using the previously set-up ELP-Intein system. Unfortunately, the subsequent reaction of click chemistry (SPAAC reaction) between the p18 antigen containing the pAzF residue and the cyclooctyne-biotin reagent did not occur, despite the various conditions explored to optimize the reaction. The various expression tests carried out as controls in the absence of pAzF in the growth medium and the results of N-terminal sequencing of purified target protein have confirmed the incorporation of the pAzF into p18 antigen, but future analyses aimed to understand the lack of reactivity of incorporated azido functional group will be necessary, as well as will be useful to re-start from the optimization of the constructs design.

The antigens' immobilization on solid phase was one of the other aspects investigated in order to improve immunoassays performance. Immobilization of proteins in a controlled and oriented manner is a critical step in the surface-based analysis, such as LIAISON® immunodiagnostic assays. We explored a new technique of immobilization on solid phase for the p18 antigen based on the use of velcro peptides to be applied in Diasorin LIAISON® EBV VCA IgM assay. The first part of this exploration was based on the development of expression and purification conditions, and then on the biochemical characterization, of the two key constructs of the system (capture binding domain of target protein - ZE-ELP36 - containing the ZE acidic partner velcro, and affinity tag fused to the target protein - MalEp18-ZR - characterized by the presence of ZR basic partner velcro). The principle of this system is based on the formation of stable coiled coil structures between the two velcro peptides, to permit the indirect immobilization of the target protein on solid phase. The advantage of this technique is provided by the oriented and stable immobilization of antigen on solid phase. The efficiency of this new system for the p18 antigen immobilization was tested in the current Diasorin LIAISON® EBV VCA IgM and compared with the direct covalent coating currently used: the results obtained showed a good responsiveness of the system but, at same time, revealed a problem of high background introduced by the system

itself. As already discussed in the results session, this problem is probably due to the presence of numerous charged residues in the sequence of the two velcro pepides that facilitates the interaction between themselves but which promotes, at the same time, the aspecific interactions with other immunoassay components. Due to the good responsiveness of the system, the problem of aspecific interactions and then the problem of high background, can be solved through the exploration of new strategies. For example the use of new buffers characterized by specific detergents able of minimizing these undesired interactions, or through the optimization of constructs sequences with the aim to reduce the number of charged residues without however affecting the electrostatic interactions of the two peptides, fundamental for the formation of highly stable leucine zipper domains.

Finally the last exploration was performed on the format of Diasorin LIAISON® EBV VCA IgM immunoassay in order to reach a greater level of specificity. The development of a reverse format from the indirect current format has required the synthesis of a new tracer constituted by the presence of the p18 antigen. For this purpose and to improve the sensitivity of the assay (in terms of signal potency), we synthesized a particular tracer composed of a non-proteic scaffold molecule carrying the p18 antigen and a multiplicity of chemiluminescent molecules, aimed to enhance the signal emission of the molecule itself. For the synthesis of this molecule, we wanted to explore the use of a non-traditional type of chemistry, the click chemistry, which in previous studies had proved to be highly stable and selective. The tracer thus synthesized and tested in the Diasorin LIAISON® EBV VCA IgM assay was found to be completely not-responsive. The next test of reactivity of this new tracer molecule made in the reverse format of EBV VCA IgG assay for mouse sera screening, however, revealed that the lack of response in the LIAISON® EBV VCA IgM reverse prototype of tracer molecule is not attributable to the reactivity of the p18-tracer but to the reverse type of format that is not functional and therefore not suitable for this specific immunoassay. Despite the negative results, with this latter exploration we were able to set up the best conditions for the use of a new type of chemistry, the "click chemistry", and we developed a protocol for the synthesis of tracer

molecules potentially able of amplifying the signal and thus potentially able to improve the sensitivity of the system.
In general through the exploration of all the techniques reported in this thesis, we obtained, in some cases, results that confirmed the potential of these methods in improving the immunodiagnostic assays performance and in other cases, characterized by negative results, we acquired information for the optimization of these same techniques and for the possible application in other more suitable immunoassays.

Chapter 2:

An alternative site-specific labeling method for monoclonal antibodies: application in immunodiagnostic assays

INTRODUCTION

Antibodies have been proved to be useful reagents for the detection and quantification of many types of analytes both *in vitro* and *in vivo* and have, therefore, found wide application in research laboratories and in the diagnostic or pharmaceutical industry. In particular, monoclonal antibodies (mAbs) have long been a potent tool due to their high specificity and affinity for target antigens and have been extensively used as carriers of fluorophores, radioisotopes, cytotoxic agents, and enzymes, yielding conjugates that find utility in therapeutic and diagnostic fields, and in basic research, as well.

In diagnostic field, immunoassays are carried out to detect the presence of a particular antigen or antibody in human body fluids (e.g. blood, urine, saliva); the use of mAbs allows a potentially unlimited supply of identical reagent which can be selected from a number of different clones to have the optimal characteristics for the intended assay. Several approaches have been investigated to improve the sensitivity of immunoassays by manipulation of the detection system. One of the key aspects to improve the sensitivity of an immunodiagnostic assay is the optimization of bioconjugation reactions necessary to label antibodies with a specific probe. The methods employed for making mAb-based conjugates can be classified in two general categories: those that involve the random modification of mAb amino acid residues, and those that are highly regioselective. Examples of random modification procedures include the acylation of lysine ε-aminogroups (185), alkylation of tyrosines (186), and amidation of carboxylates (187). Traditionally, conjugation of labeling molecules to an antibody takes place at lysines solvent accessible reactive amino acids. Lysine conjugation results in 0–8 conjugated molecules per antibody, and peptide mapping has determined that conjugation occurs on both the heavy and light chain at ~20 different lysine residues (40 lysines per mAb). The biological and functional properties of these conjugates are often acceptable; however, random modification of mAbs may impair antigen binding and thus the immunoreactivity of antibody (in fact random labeling can take place at the level of the antigen binding site thus affecting the reaction of recognition between antibody and antigen) and leads to conjugate heterogeneity (Figure 1; panel A). In the last years, a number of site-specific and selective methods have been described to introduce

molecules of interest onto mAbs. The ability to control the location and stoichiometry of conjugation can significantly improve the performance of mAb conjugates in applications such as the immunodiagnostic assays.
The greatest selectivities are obtained using recombinant technologies (188,189). Recently, the innovative techniques provide the site-specific conjugation of antibodies through engineered cysteine residues (190), through the incorporation of unnatural amino acids (191), as described above for recombinant proteins, or through the use of specific enzymes: glycotransferases (192) and transglutaminases (193). However, selective modification has also been reported for chemically based methods as reductive amination of oxidized mAb carbohydrates (194), photoaffinity labeling of unconventional mAb binding sites (195), and reduction-alkylation of antibody interchain disulfides (196,197). In this last case conjugates are formed through partial reduction of interchain disulfide bonds at the level of antibody hinge region, followed by alkylation with thioreactive labeling molecule (Figure 2). Conjugation of thioreactive probes to proteins through cysteine residues has long been a method for protein labeling, and it has been applied to the generation of antibody-probe conjugates. In this particular case (partial reduction of disulfide bridges), the resulting mAb-probe conjugates are quite homogeneous in composition, with a controlled number of labeling molecules introduced for mAb (Figure 1; panel B). In fact, the reduction of disulfide bridges can be performed in a controlled way by changing different parameters of reaction (molar excess of reductant, antibody concentration, temperature, pH, time of reaction, etc.). Therefore, this type of process allows to introduce a specific number of labeling molecules, depending on the used reaction conditions. Moreover, since mAb interchain disulfides are distant from the antigen binding site and are generally not essential to maintain mAb integrity (198), this site-specific conjugation strategy allows to have conjugates that are potent and selective.

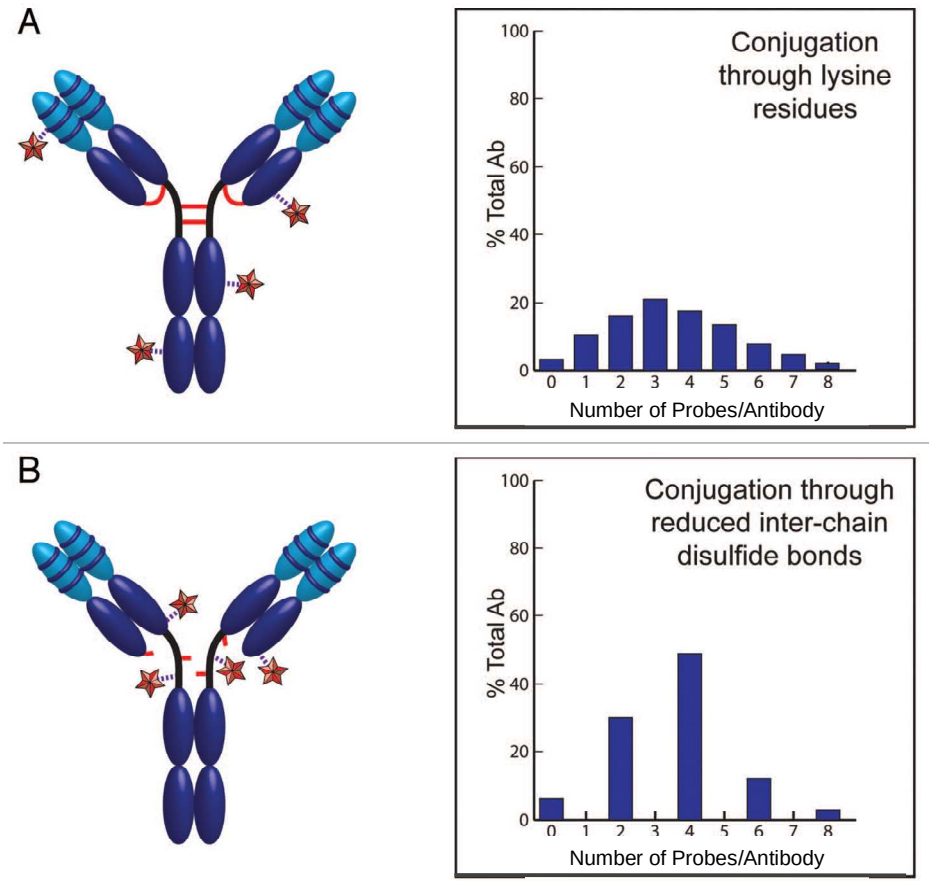

Figure 1. Conjugation methods for antibody-probe conjugates. (**A**) Traditional conjugation through lysine residues or (**B**) conjugation through reduced inter-chain disulfide bonds.
In the second case (**B**), the site-specific conjugation decreased the heterogeneity in both probes to antibody ratio and location of conjugation site.

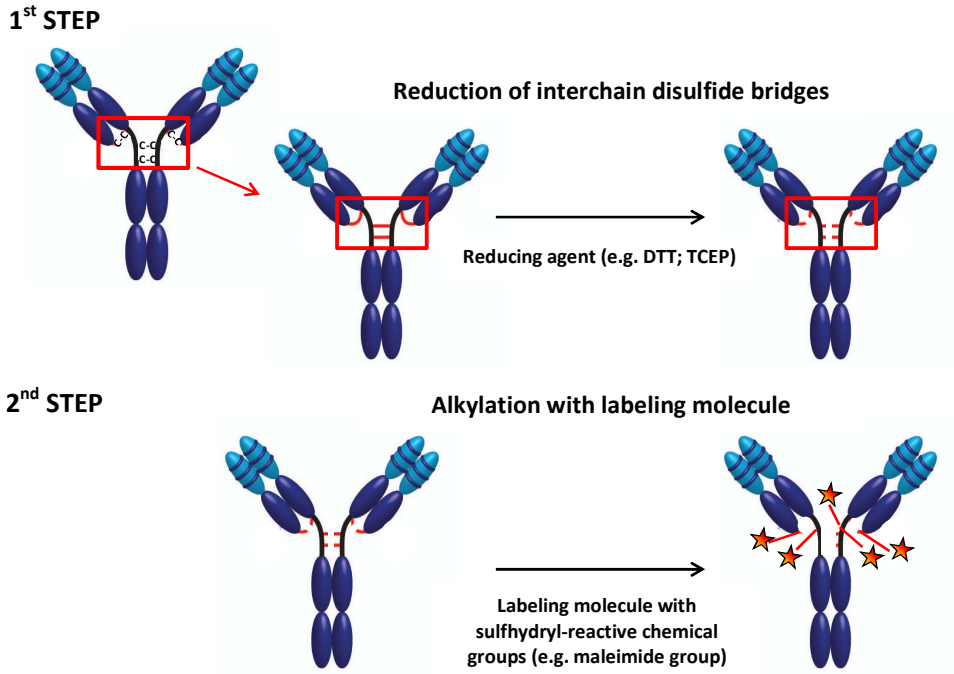

Figure 2. Scheme of conjugation through reduced inter-chain disulfide bonds. The procedure is based on two different steps: the first provides the partial reduction of interchain disulfide bonds at the level of antibody hinge region through the use of a reducing agent (e.g. DTT; TCEP), while the second step provides the alkylation of free thiol groups of reduced cysteines with the labeling molecule possessing sulfhydryl-reactive chemical groups (e.g. maleimide group).

As model systems to explore this new site-specific conjugation method two different monoclonal antibodies of solid phase were selected: the first belongs to the LIAISON® XL Murex HIV Ab/Ag HT immunodiagnostic assay and it is specifically direct against the p24 viral antigen of HIV virus; the second antibody of interest, instead, belongs to the LIAISON® chemiluminescent prototype for FGF23 detection.

THE LIAISON® Murex HIV Ab/Ag HT ASSAY

The LIAISON® XL Murex HIV Ab/Ag HT assay uses chemiluminescence immunoassay (CLIA) technology for the combined qualitative determination in human serum or plasma samples of p24 antigen and specific antibodies of human immunodeficiency virus (HIV).
The human immunodeficiency virus (HIV) is a lentivirus (a subgroup of retrovirus) that causes the acquired immuno-deficiency syndrome (AIDS), a pathology in humans in which progressive failure of the immune system allows severe opportunistic infections and cancers. HIV is transmitted by sexual contact between HIV-infected individuals, exposure to contaminated blood or blood products, and prenatal infection of a foetus or perinatal infection of a newborn from an infected mother. Within these bodily fluids, HIV is present as both free virus particles and virus within infected immune cells. HIV infects vital cells in the human immune system such as helper T cells (specifically CD4+ T cells), macrophages, and dendritic cells (200). HIV infection leads to low levels of CD4+ T cells through a number of mechanisms, including apoptosis of uninfected bystander cells, direct viral killing of infected cells, and killing of infected CD4+ T cells by CD8 cytotoxic lymphocytes that recognize infected cells. When CD4+ T cell numbers decline below a critical level, cell-mediated immunity is lost, and the body becomes progressively more susceptible to opportunistic infections.
HIV is different in structure from other retroviruses (Figure 3). It is roughly spherical with a diameter of about 120 nm (201). It is composed of two copies of positive single-stranded RNA that codes for the virus's nine genes enclosed by a conical capsid composed of 2000 copies of the viral protein p24. The single-stranded RNA is tightly bound to nucleocapsid proteins, p7, and enzymes needed for the development of the virion such as reverse transcriptase, proteases, ribonuclease and integrase. A matrix composed of the viral protein p17 surrounds the capsid ensuring the integrity of the virion particle (202). This is, in turn, surrounded by the viral envelope that is composed of two layers phospholipids taken from the membrane of a human cell when a newly formed virus particle buds from the cell. Embedded in the viral envelope are proteins from the host cell and about 70 copies of a complex HIV protein that protrudes through the surface of the virus particle. This

protein, known as “Env”, consists of a cap made of three molecules called glycoprotein (gp) 120, and a stem consisting of three gp41 molecules that anchor the structure into the viral envelope (203). This glycoprotein complex enables the virus to attach to and fuse with target cells to initiate the infectious cycle. Two types of HIV have been characterized: HIV-1 and HIV-2. HIV-1 is the virus that was initially discovered. It is more virulent, more infective, and is the cause of the majority of HIV infections globally. HIV-1 is classified by phylogenetic analysis into groups M (main or major), N (new, non-M, non-O), O (outlier) and P (Plantier et al., Nat. Med. 2009). The global AIDS pandemic was mainly caused by group M viruses, while group N and O viruses are relatively rare and endemic to West Central Africa. However, group O infections have been identified in Europe and the USA. Human immunodeficiency virus type 2 is similar to HIV-1 in its structural morphology, genomic organization, cell tropism, in vitro cytopathogenicity, transmission routes, and ability to cause AIDS. HIV-2 is less pathogenic than HIV-1, and HIV-2 infections have a longer latency period with slower progression to full-blown disease, lower viral titers, and lower rates of vertical and horizontal transmission. HIV-2 is endemic to West Africa, but HIV-2 infections, at a lower frequency compared to HIV-1, have been identified in the USA, Europe, Asia, and other regions of Africa.

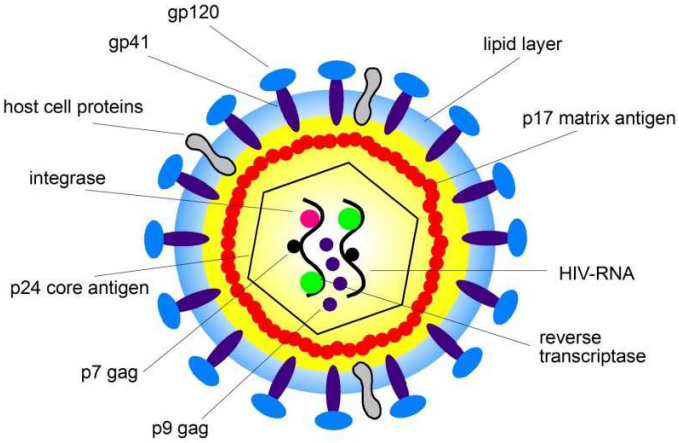

Figure 3. Structure of HIV virion.

Early after infection with HIV, but prior to seroconversion, HIV antigens may be detected in serum or plasma specimens. The HIV structural protein most often used as the marker of antigenaemia is the core protein, p24. The LIAISON® XL murex HIV Ab / Ag HT assay uses HIV p24 monoclonal antibodies to detect HIV p24 antigen prior to seroconversion, thereby decreasing the seroconversion window and improving early detection of HIV infection. As mentioned above, this immunoassay permits to obtain the simultaneous detection of anti-HIV antibodies and HIV p24 antigen. In particular, the part of the assay for qualitative determination of HIV p24 antigen provides a sandwich format in which a biotinylated monoclonal antibody anti-p24 acts on solid phase (streptavidinated magnetic particles) as capture binder for the p24 viral antigen, while a second monoclonal antibody anti-p24 linked to isoluminol-derivative (ABEI), is used as chemiluminescent tracer (Figure 4).

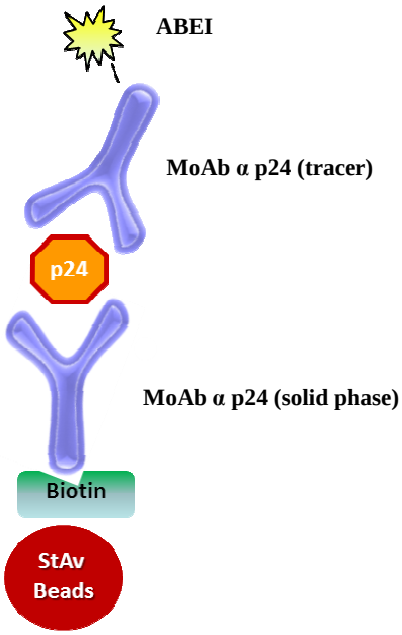

Figure 4. Schematic representation of the assay format for the qualitative determination of HIV p24 antigen in LIAISON® XL murex HIV Ab/Ag HT assay.

THE LIAISON® FGF23 PROTOTYPE ASSAY

Fibroblast Growth Factor 23 (FGF23) is a secreted, monomeric protein, belonging to the FGF family. The FGF23 gene is located on Chr12p13 and is phylogenetically grouped with FGF19 and FGF21 gene products. It plays a pivotal role as key regulator of phosphate homeostasis and vitamin D metabolism. It is able to induce urinary phosphate excretion by suppressing the expression of NaPi-2a and NaPi-2c cotransporters either directly or through affecting parathyroid hormone activity (204). It also suppresses 1,25(OH)2D by inhibition of 1a-hydroxylase that converts 25-hydroxyvitaminD (25(OH)D) to 1,25(OH)2D and stimulation of 24-hydroxylase that converts 1,25(OH)2D to inactive metabolites in the proximal tubule of the kidney.

A considerable number of metabolic bone diseases are associated with increased FGF23 levels; examples are vitamin-D-resistant rickets, tumor-induced osteomalacia (TIO) or chronic kidney diseases. Reduced FGF23 activity can also cause diseases in humans; examples are patients with familial tumoral calcinosis (FTC) (205). Since FGF23 is a major etiological factor in several diseases of phosphate homeostasis, it is important to develop informative assays for FGF23 plasma or serum levels that will be clinically and diagnostically useful.

FGF23 is an approximately 32-kD (251 amino acids) protein with a signal peptide necessary for its secretion (first 24 residue), followed by an N-terminal region that contains the FGF family homology domain and a 71–amino acid C-terminus that is characterized by a unique C-terminal motif with a specific three-dimensional configuration (i.e., disulfide bound and β sheet) (206). FGF23 activity is regulated by a proteolytic cleavage which occurs immediately after the $_{176}$RXXR$_{179}$ consensus sequence, sequence that is located at the boundary between the FGF core homology domain and the 72-residue-long C-terminal tail of FGF23 (207,208) (Figure 5). The proteolytic cleavage generates N-terminal (25-179) and C-terminal fragments (180-251). Neither of the processed N- or C-terminal fragments of FGF23 can exert its hormonal effects (209). Several studies have shown that the destruction of cleavage consensus sequence by missense mutations results in an increase in cleavage-resistant population of recombinant FGF23 in vitro mammalian cell culture systems (207-209). This leads to diseases such as autosomal

dominant hypophosphatemic rickets/osteomalacia (ADHR), X-linked hypophosphatemic rickets (XLH) and tumor-induced osteomalacia (TIO), mentioned above. In all these conditions, the increased FGF23 function that is predominantly characterized by elevated serum concentrations of FGF23 accounts for a pathogenic mechanism. Thus, internal cleavage is an important event to affect the specific biological activity of FGF23.

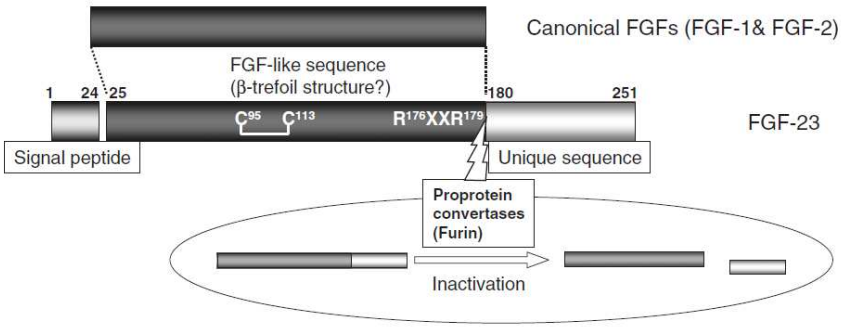

Figure 5. Schematic structure of hFGF23. FGF23 has a disulfide bond in the FGF23 like sequence and an internal cleavage site immediately after the RXXR consensus sequence.

The automatic chemiluminescent prototype for FGF23 detection relies on the use of high-affinity monoclonal antibodies that recognize the intact FGF23 molecule exclusively.
Since the cleaved fragments are inactive, it is important to distinguish the bioactive intact species of FGF23 protein from the inactive cleaved fragments. This requires two families of antibodies that recognize the N- and the C-terminal regions of the protein respectively, according to the scheme of immunoassay described in Figure 6. In details, the prototype provides a sandwich format in which a mouse monoclonal antibodies recognizing the N-terminal of FGF23 is used as capture binder coated on solid phase, while a mouse monoclonal antibody directed to the C-terminal of FGF23, linked to isoluminol-derivative (ABEI), is used as chemiluminescent tracer.

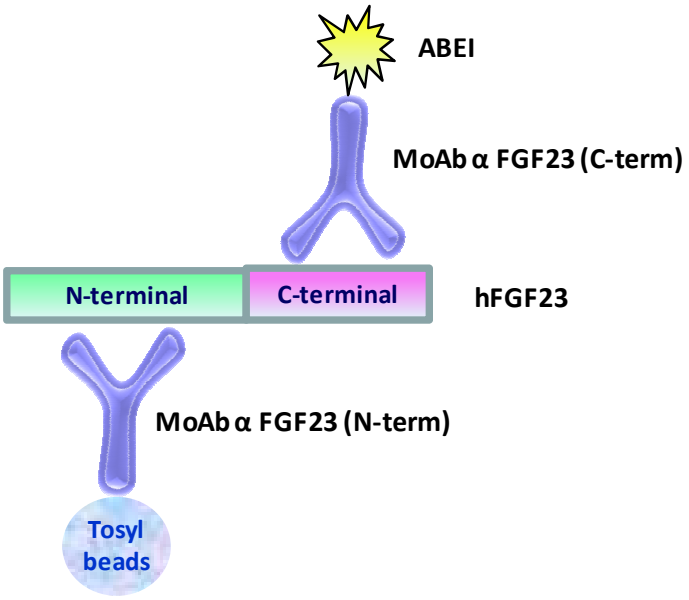

Figure 6. Prototype assay format for FGF23 detection.

AIM OF THE PROJECT

As mentioned in the introduction, the site-specific labeling of antibody molecule is one the most promising strategy to improve the sensitivity of an immunoassay. In fact, site-specific labeling approaches provide a means for both directing chemical modification to specific sites on the antibody molecule, located away from the antigen binding-site, and for controlling the stoichiometry of the reaction. Among the different strategies recently developed, one the most promising is based on reduction-alkylation of antibody interchain disulfides. This last approach is a simple method that provides a selective and controlled partial reduction of interchain disulfide bridge at the level of antibody hinge region using thiol-specific reagents (reductants), followed by alkylation with the thioreactive labeling molecule; it allows to introduce a specific number of labeling molecules, depending on the used reaction conditions. Due to these characteristics, the reduction-alkylation of antibody interchain disulfides represents a very powerful and selective tool for bioconjugation reactions. The aim of the last part of this thesis was to explore this innovative conjugation method in order to obtain a controlled and site-specific biotinylation of two different antibodies of solid phase belonging to the LIAISON® XL murex HIV Ab/Ag HT immunodiagnostic assay and to the LIAISON® chemiluminescent prototype assay for FGF23 detection, respectively. The purpose was to verify if, in these two specific case, a selective and oriented labeling promotes an increase of antibody performance and then of the related immunoassay. Both these type of diagnostic assays require a very high sensitivity (detection of antigens in order of few pg/ml) and specificity, therefore the optimization of principal bioreagents, including antibodies of solid phase, is needed to improve the characteristics of the assays and make them more powerful.

MATERIALS AND METHODS

REAGENTS

Boric acid, DTPA (diethylene triamine pentaacetic acid), MES (2-(*N*-morpholino)ethanesulfonic acid), TCEP (tris(2-carboxyethyl)phosphine), NEM (N-ethyl maleimide) were purchased by Sigma-Aldrich; EDTA (Ethylenediaminetetraacetic acid) and NaCl were purchased by Carlo Erba; EZ-link-Maleimide-PEG2-Biotin reagent was purchased by Thermo Scientific, PD-10 desalting columns were purchased by GE Healthcare.

PROCEDURE FOR REDUCTION-ALKYLATION OF ANTIBODY INTERCHAIN DISULFIDES (HINGE REGION LABELING)

A) 1 mg of mAb (anti-p24 or anti-hFGF23) was thawed from -30°C freezer in a ice bath. An aliquote of TCEP 10mM was diluted 1:10 in reduction buffer (25mM Boric acid; 25mM; NaCl; 1mM DTPA; pH 8) to obtain a 1 mM stock solution. 10 or 20 fold molar excesses of TCEP over the mAb were added and left reacting for 2 hours at 37°C.
B) Reaction sample was desalted using a PD-10 column previously pre-equilibrated in MES buffer (50mM MES; 5mM EDTA; pH 6.5). Elution of 0,5-1 mL fractions of volume were collected and analyzed by Nanodrop (Thermo Scientific). Fractions containing higher protein concentration were joined together.
C) Sample concentration was determined spectrofotometrically at 280 of wavelength in triplicate; MES buffer was used as blank.
D) At this point, 20 fold molar excesses of EZ-link-Maleimide-PEG2-Biotin over reduced mAb were added and left reacting for 1 hour at 4°C.
E) 5 fold molar excesses of N-Ethyl-Maleimide were then added to quench any unreacted, free cysteines and left reacting for 30 minutes at RT.
F) Final mAb-biotin conjugate was purified on a gel filtration column type Superdex 200 10/300 on a AKTA system (GE Heathcare).
Chromatographic conditions:
- column: Superdex 200 10/300 GL (CV ~ 24ml)
- flow rate: 0.5 mL/min
- isocratic elution in MES buffer

Eluted fractions containing the biotin-labeled mAb were pooled together and the conjugate concentration was determined spectrophotometrically: absorbance values were measured 3 times at 260 nm and at 280 nm wavelengths, respectively. Blank was made with MES buffer pH 6.5.

LIAISON® XL MUREX HIV Ab/Ag HT ASSAY

This immunoassay permits to obtain the simultaneous detection of anti-HIV antibodies and HIV p24 antigen. In particular, the part of the assay for qualitative determination of HIV p24 antigen provides a sandwich format in which a biotinylated monoclonal antibody anti-p24 acts on solid phase (streptavidinated magnetic particles) as capture binder for the p24 viral antigen, while a second monoclonal antibody anti-p24 linked to isoluminol-derivative (ABEI), is used as chemiluminescent tracer.

Coating protocol

1. Resuspension of microparticles (M-280 Streptavidin-coupled Dynabeads®) in resuspension buffer (10 mM PBS, pH 7.4) at 2% of concentration
2. Addition of the mAb α p24- biotin (40 μg/ml)
3. 18 h at 24°C
4. Blocking with 10 mM PBS, 0.1% BSA (w/v), pH 7.4
5. 5 h at 37°C
6. Washing with 10 mM PBS, 0.1% BSA (w/v), pH 7.4
7. Resuspension in PBS 10 mM, 0.1% BSA (w/v), pH 7.4 at final concentration of 0.15%

Assay protocol

During the first incubation, HIV p24 antigen present in calibrator, samples or controls binds to the solid phase (streptavidinated magnetic particles coated with biotinylated monoclonal antibodies anti-p24). During the second incubation monoclonal antibodies anti-p24 linked to the isoluminol derivative (ABEI-mAb conjugate) react with HIV p24 antigen already linked to the antibodies of solid phase. After each incubation, the unbound material is removed with a wash cycle. Subsequently, the starter reagents (hydrogen peroxide and 800 ng/ml deuteroferriheme in 1M NaOH) are added and a flash chemiluminescence

reaction is thus induced. The light signal, and hence the amount of isoluminol- monoclonal conjugate, is measured by a photomultiplier as relative light units (RLU) and is indicative of p24 antigen presence in calibrator, samples or controls.

STABILITY TESTS

The mAbs-biotin conjugates, obtained through reduction-alkylation of interchain disulfides at the level of antibody hinge region were tested in Diasorin LIAISON® XL Murex HIV Ab/Ag HT assay as described above, at time 0 (reference) and after 5 and 10 days at 37°C, and 3 and 5 days at 45°C. The immunochemical activity of the single tracer was then compared in the different conditions to determine the stability of the molecule reactivity after thermal stress.

LIAISON® FGF23 PROTOTYPE ASSAY

The automatic chemiluminescent prototype for FGF23 detection relies on the use of high-affinity monoclonal antibodies that recognize the intact bioactive FGF23 molecule exclusively, since the cleaved fragments are inactive. The immunoassay provides a sandwich format in which a mouse monoclonal antibodies recognizing the N-terminal of FGF23 is used as capture binder coated on solid phase, while a mouse monoclonal antibody directed to the C-terminal of FGF23, linked to isoluminol-derivative (ABEI), is used as chemiluminescent tracer.

Coating protocol

The M-280 Streptavidin-coupled Dynabeads® microparticles were used as solid phase at a final concentration of 0.25%. The biotinylated mAbs anti-FGF23 (N-terminal region) were diluted at a final concentration of 400 ng/ml in the assay buffer that was added as an additional component in the second incubation provided by the assay protocol described below.

Assay protocol

During the first incubation monoclonal antibodies anti-C-terminal region of FGF23 linked to the isoluminol derivative (ABEI-mAb conjugate) react with FGF23 antigen present in calibrator, samples or controls.

During the second incubation, biotinylated monoclonal antibodies anti-N-terminal region of FGF23, diluted in the assay buffer, bind to the solid phase (streptavidinated magnetic particles) and then FGF23 antigen already linked to the ABEI-mAb conjugate reacts with biotinylated mAb coated on solid phase. After each incubation, the unbound material is removed with a wash cycle. Subsequently, the starter reagents (hydrogen peroxide and 800 ng/ml deuteroferriheme in 1M NaOH) are added and a flash chemiluminescence reaction is thus induced. The light signal, and hence the amount of isoluminol- monoclonal conjugate, is measured by a photomultiplier as relative light units (RLU) and is indicative of FGF23 antigen presence in calibrator, samples or controls.

RESULTS/DISCUSSION

As extensively discussed in the introduction, the site-specific modification of antibodies results to be advantageous in the context of an immunodiagnostic assay; a controlled and located away from the antigen binding-site labeling significantly improves the performance of antibody molecule promoting the reaction of antigen recognition. A simple and promising method to site-specifically modify antibodies is represented by reduction-alkylation of interchain disulfides at the level of antibody hinge region. We then tried to apply this technology for the site-specific biotinylation of two different antibodies currently used in immunoassays for the HIV p24 viral protein and for the human FGF23 protein detection (Figure 7).

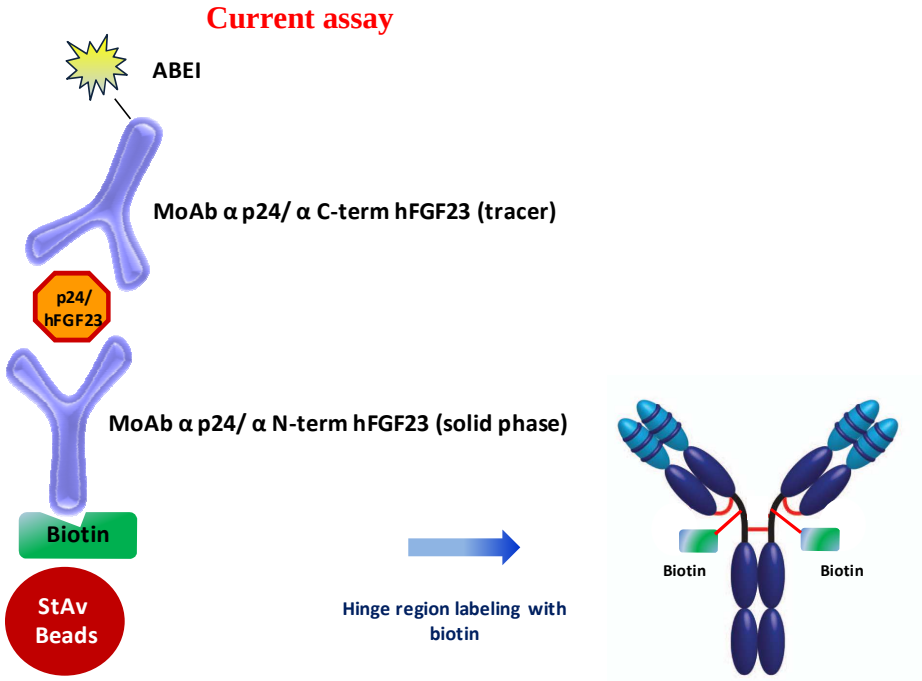

Figure 7. Schematic representation of site-specific biotinylation by reduction-alkylation of interchain disulfides of two different antibodies belonging to the LIAISON® XL Murex HIV Ab/Ag HT immunoassay and to the LIAISON® prototype assay for hFGF23 detection.

Figure 8 shows in detail the procedure used to obtain the hinge region site-specific biotinylation of the two antibodies mentioned above (more information are provided in the materials and methods session). The first step involved the partial reduction of the interchain disulfide bridges present at the level of the antibody hinge region with the reducing agent addition (TCEP - Tris (2-CarboxyEthyl) Phosphine - in our case). The reaction was conducted in borate buffer at pH 8 for 2 hours at 37°C. The excess of TCEP to be added in the reaction is a very critical parameter because it influences the degree of labeling in terms of number of label molecules introduced per molecule of antibody. We tested different molar excesses of TCEP in reaction (data not shown) and we identified the best conditions for our purposes: the addition of an excess ranging from 10 to 20 molar excesses of TCEP allowed us to obtain the desired degree of biotinylation. In the second step a desalting process was performed (see session material and methods) in order to remove the excess of TCEP present in reaction and to perform a change of buffer necessary for the subsequent alkylation reaction (from borate buffer at pH 8 to MES [2-(*N*-morpholino)ethanesulfonic acid] buffer at pH 6.5). The third step consisted in the alkylation reaction between the reduced cysteine residues and the biotin-maleimide reagent; in particular, in this step the reaction took place between the reduced thiol groups of cysteine residues of the hinge region and the maleimido-group of the reactive. The reaction was performed in MES buffer at pH 6.5 for 1h at 4°C. The fourth step involved a quenching reaction with N-ethyl-maleimide (NEM) to block free thiol groups that may lead to oxidation reactions with other reduced cysteine residues and thus to undesired structural rearrangements of the antibody molecule (aggregation). The reaction was carried out with 5 molar excess of NEM at room temperature for 30 minutes. Finally, the fifth step provided a GFC purification in order to remove the excess of biotin maleimide and NEM and to obtain a pure final product (Superdex 200 Hiload 10 300 column, MES buffer pH 6.5, isocratic gradient; see materials and methods section).

For the antibody of solid phase directed specifically against the p24 viral protein (LIAISON® XL Murex HIV Ab/Ag HT assay), we realized two different conjugates using two different conditions of reduction (10 and 20 molar excesses of TCEP). For the antibody of solid phase belonging to

the prototype assay for the detection of hFGF23 protein, we made a single conjugate; in this case the reduction reaction was carried out with 20 molar excesses of TCEP. Figure 9 shows the GFC purification chromatographic profiles carried out at the end of reduction/alkylation process of the three different conjugates.

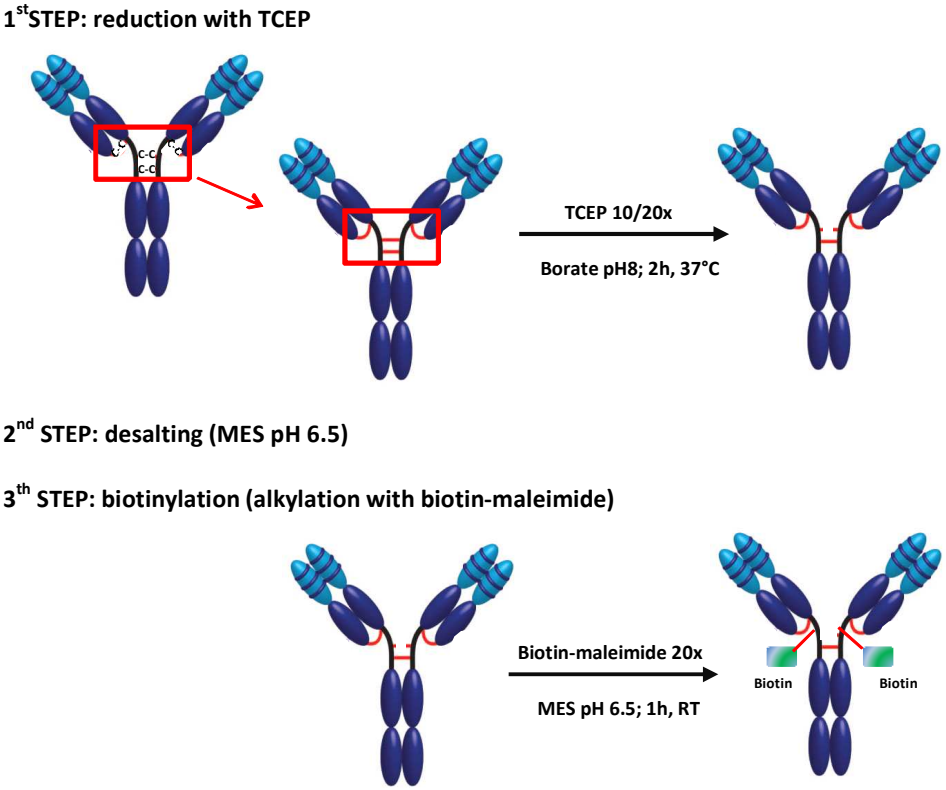

Figure 8. Schematic representation of hinge region site-specific biotinylation procedure.

A_mAb α p24-biotin (reduction with TCEP 10x)

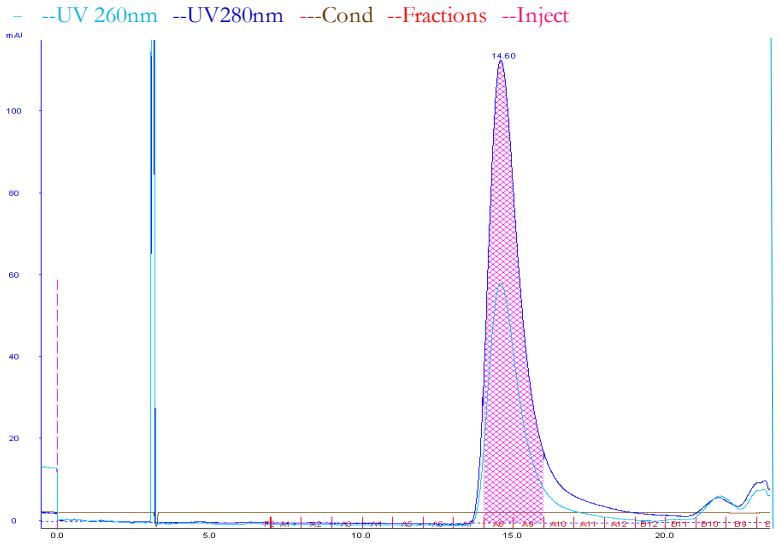

B_mAb α p24-biotin (reduction with TCEP 20x)

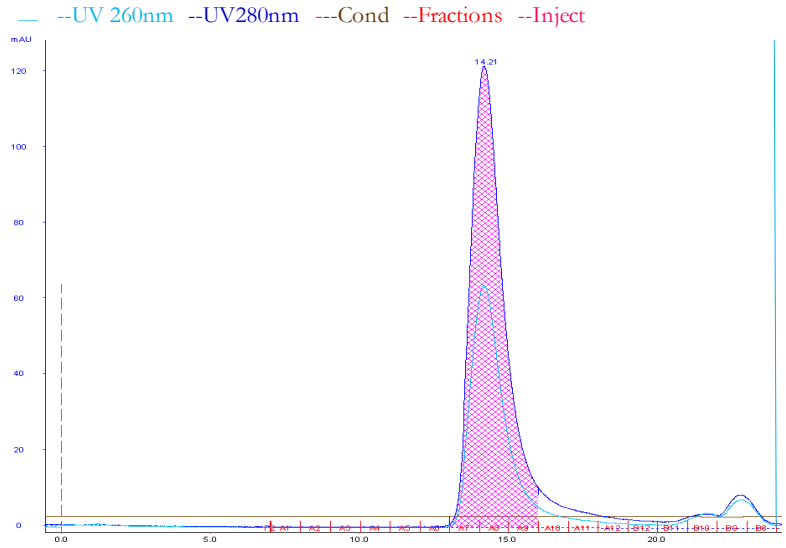

C_mAb α hFGF23(N-term)-biotin (reduction with TCEP 20x)

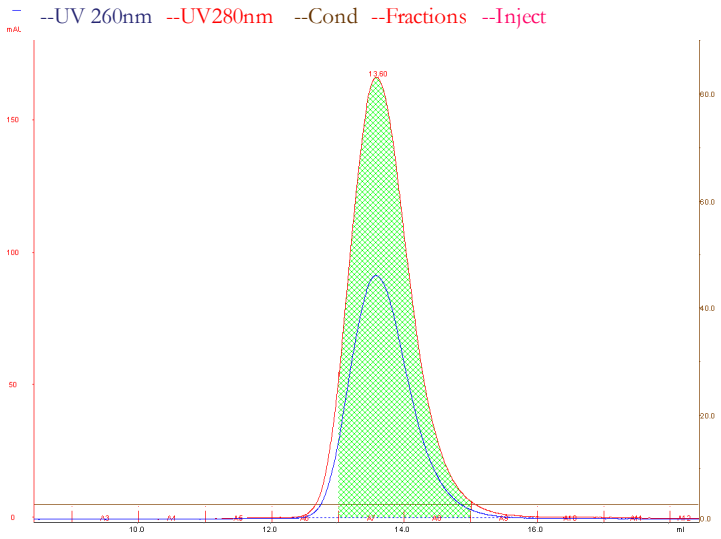

Figure 9. Chromatographic profiles of GFC purifications performed at the end of reduction/alkylation process. The first and second chromatograms refer to mAb α p24-biotin conjugates (reduction with TCEP 10x and TCEP 20x respectively), while the third chromatogram refers to mAb α hFGF23 (N-term)-biotin (reduction with TCEP 20x) conjugate. mAb → monoclonal Antibody.

LIAISON® XL Murex HIV Ab/Ag HT assay: mAb α p24-biotin

The two biotinylated preparations of the monoclonal antibodies α p24 obtained by reduction-alkylation of interchain disulfides at the level of the hinge region, were then tested in the LIAISON® XL Murex HIV Ab/Ag HT immunodiagnostic assay. As reference was taken the current HIV test which uses the same antibody, but biotinylated with a traditional random method on lysine residues. The analysis was performed in duplicate on a panel of negative and positive samples. Antibodies analytical performance was expressed as the average of the signals of each panel (Figure 10).

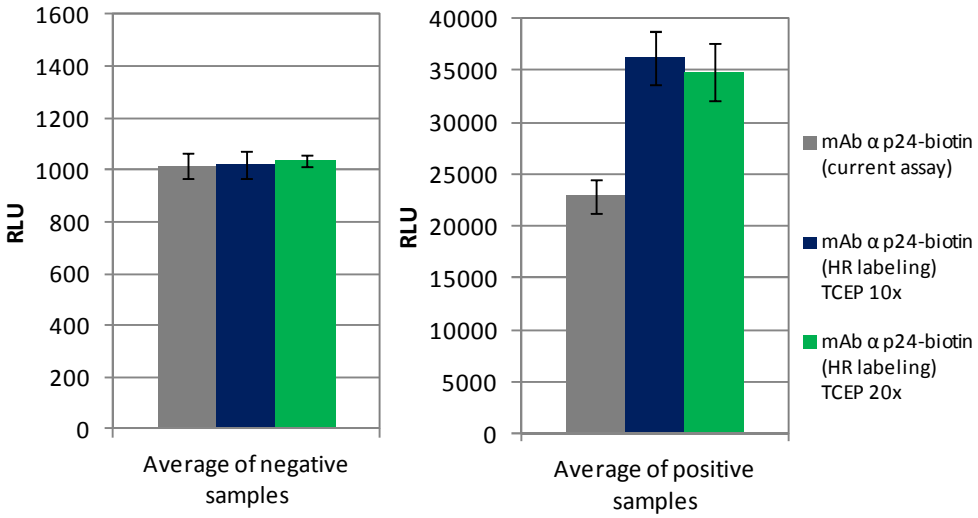

Figure 10. Comparison between the immunochemical activity of mAb α p24 - biotin currently used in LIAISON® XL Murex HIV Ab/Ag HT assay obtained through traditional method of biotinylation on lysine residues (gray) and mAbs α p24-biotin conjugates obtained through Hinge Region (HR) labeling (blue → reduction with TCEP 10x; green → reduction with TCEP 20x).

The results indicated that the new anti-p24 conjugates, obtained through reduction and alkylation of cysteines located at the level of hinge region, have a much better performance than that currently in use. In particular the new conjugates showed a great increase of the signal relating to the positive samples (panel B; blue and green bars) compared to the mAb α p24-biotin of current kit (panel B; gray bar). Moreover, the signal of negative samples for both new biotinylated mAbs α p24 (panel A; blue and green bars) was comparable to that detected for current biotinylated α p24 mAb (panel A; gray bar). The result was a great increase of the ratio between the signals of the positive and negative samples and therefore a great increase of immunodiagnostic assay performance.

Since the technique used for the site-specific biotinylation of antibodies involves the cleavage of interchain bonds, stability tests were carried out on these new conjugates to understand if this type of modification may alter the structure of the antibody molecule and consequently its immunochemical stability. In particular the two new conjugates were

subjected to thermal stress (37°C and 45°C) for a short period of time (from 3 to 10 days). The results of the analysis are shown in Figure 11.

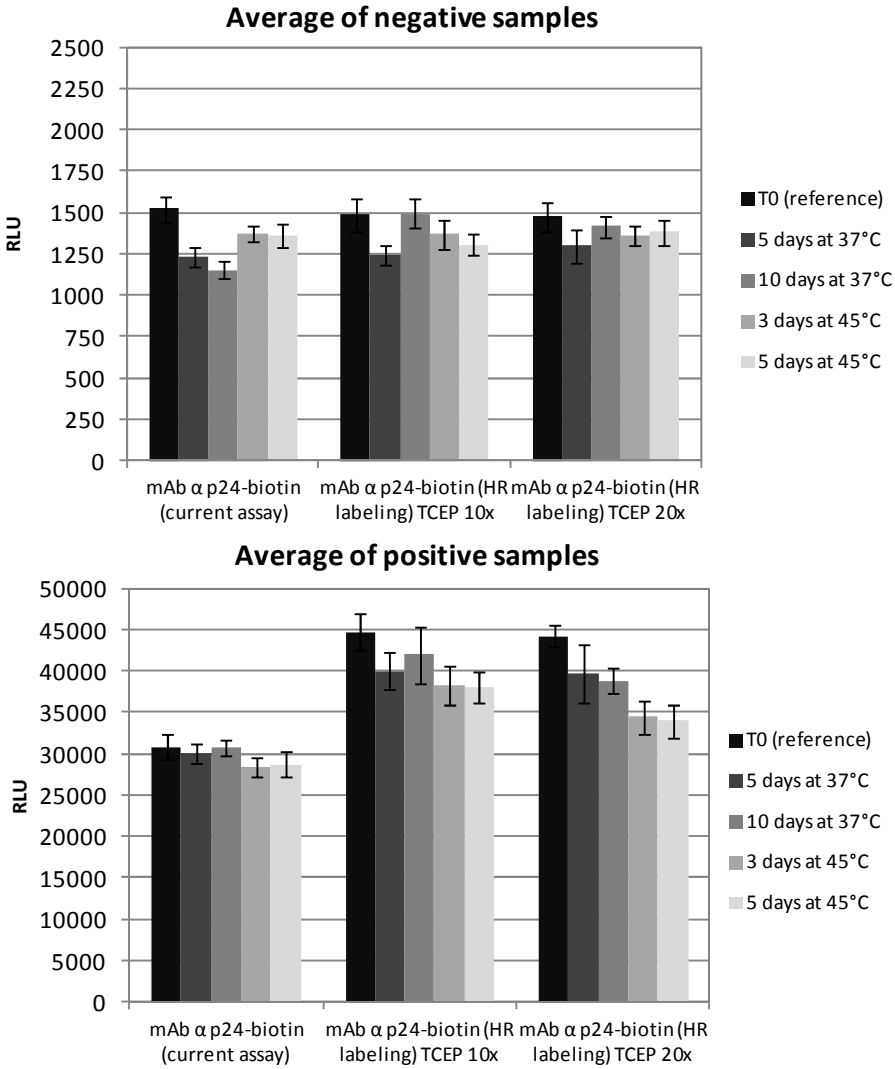

Figure 11. Short stability test of new and currently used mAbs α p24-biotin conjugates on a panel of positive and negative samples.

The new conjugates mAbs α p24-biotin showed, when subjected to thermal stress for a few days, a slight higher loss of reactivity (especially for positive samples; ~ 15% of loss) compared to that observed for the conjugate currently used. However, this loss of reactivity is still acceptable. Therefore the site-specific labelling at the level of disulfide bonds of the hinge region does not seem to alter the structural stability of the antibody molecule and thus does not seem to affect its immunochemical activity and the consequent performance of immunodiagnostic assay.

LIAISON® prototype assay for hFGF23 detection: mAb α hFGF23 (N-term)-biotin

The biotinylated monoclonal antibody α hFGF23 (N-term), obtained by reduction-alkylation of interchain disulfides, was tested on a standard curve composed by a high positive human serum sample in dilution. In this curve there are known increasing concentrations of FGF23 protein. Each test was conducted in triplicate and the response, in RLU, was plotted versus the increasing concentration (pg/ml) of FGF23 antigen present in the standard curve.
Figure 12 shows the direct comparison between the immunochemical activity of monoclonal antibody α hFGF23 (N-term) biotinylated on lysine residues (traditional random method; gray) and monoclonal antibody α hFGF23 (N-term) biotinylated in a site-specific way at the level of hinge region (blue).

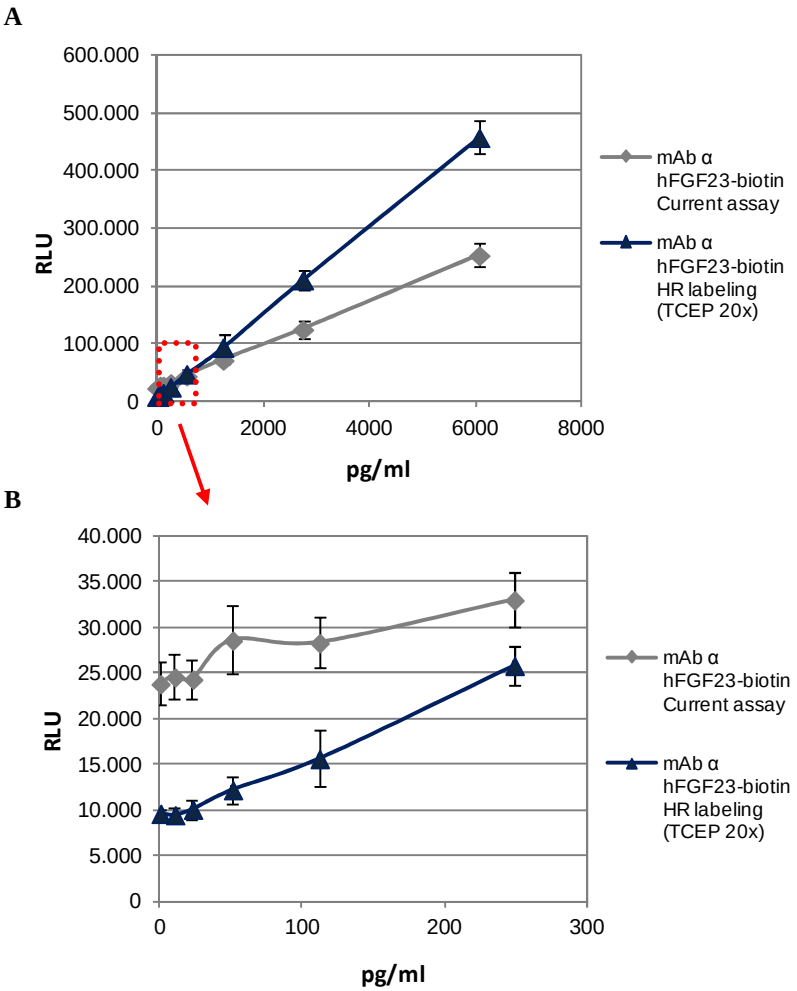

Figure 12. Comparison between the immunochemical activity of mAb α hFGF23 (N-term) biotinylated with traditional method (gray) and through reduction-alkylation of interchain disulfides (blue) in LIAISON® prototype assay for hFGF23 detection on a standard curve.

Results showed that the response given by monoclonal antibody α hFGF23 (N-term) biotinylated in a site-specific way at the level of hinge region (blue) was considerably higher than that obtained with the use of monoclonal antibody α hFGF23 (N-term) biotinylated with a traditional method (Figure 12; panel A), with a consequent increase in the assay performance. In addition, the site-specific biotinylation allowed to achieve a greater degree of sensitivity, in fact the use of a site-specific biotinylated monoclonal antibody α hFGF23 (N-term) permitted a better separation between the first points of the standard curve with the lowest FGF23 concentration (Figure 12; panel B). Therefore this new conjugate was also able to differentiate between samples containing a very low concentration of antigen. The antibody biotinylated with a traditional random method was not able to discriminate these samples that were all detected with the almost same RLU value (Figure 12; panel B).
In immunodiagnostic assays such as that for the FGF23 detection is essential to optimally detect and distinguish samples containing a low concentration of antigen. The results described above have revealed that the biotinylation, and more generally the site-specific modification of antibodies at the level of the hinge region, appears to be a powerful tool to significantly improve the immunoassay sensitivity. Even the data obtained for the antibody α p24 of solid phase belonging to LIAISON® XL Murex HIV Ab/Ag HT assay showed the ability of this site-specific labeling technique to enhance significantly the signal of positive samples leaving unchanged at low levels the signal of background (negative samples). As widely discussed above, the result is a great improvement of immunodiagnostic assay performance. Therefore, this type of methodology, simple to set up and to realize, has proven to be applicable on a wide variety of immunodiagnostic assays that require an improvement of sensitivity and in general an improvement of performance.

APPENDIX

SITE-SPECIFIC BIOTYNILATION OF p18 ANTIGEN THROUGH GENETIC INCORPORATION OF UNNATURAL AMINO ACIDS

STUDY OF CLICK CHEMISTRY BASIC REACTION

In order to set the best conditions of click chemistry to use in bioconjugation reactions, we studied the basic reaction through the evaluation of different parameters (pH, temperature, buffers, reagent concentration) and efficiency of reaction (time, yield, reproducibility). Two peptides were synthesized as model systems for these analyses (Figure 1): the first (peptide 1) was characterized by possessing an N-terminal azido group and in particular a residue of azidolysine, and the second peptide (peptide 2) was synthesized and conjugated to a molecule of BCN (bicyclo nonyne).

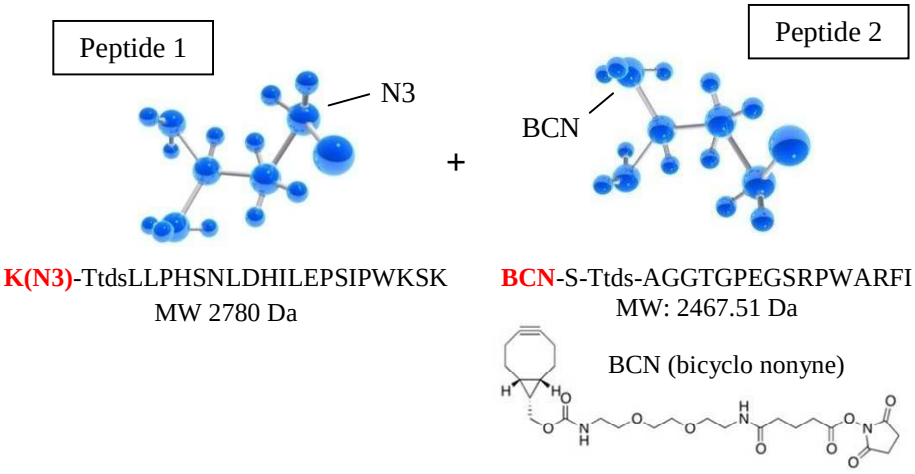

Figure 1. Schematic representation, sequence and molecular weight (MW) of the two peptides (peptide 1 and peptide 2) used as a model system for the study of click chemistry basic reaction. The chemical structure of BCN (bicyclo nonyne) is reported below.

The reaction between two peptides was monitored by UPLC/MS analysis. In particular, since the peak relative to the reaction product overlaps with that relating to peptide 1, to follow the progress of the reaction, we analyzed during the time the lowering of the peak relative to peptide 2, put into the reaction as limiting reagent (Figure 2; more details are reported in materials and methods section).

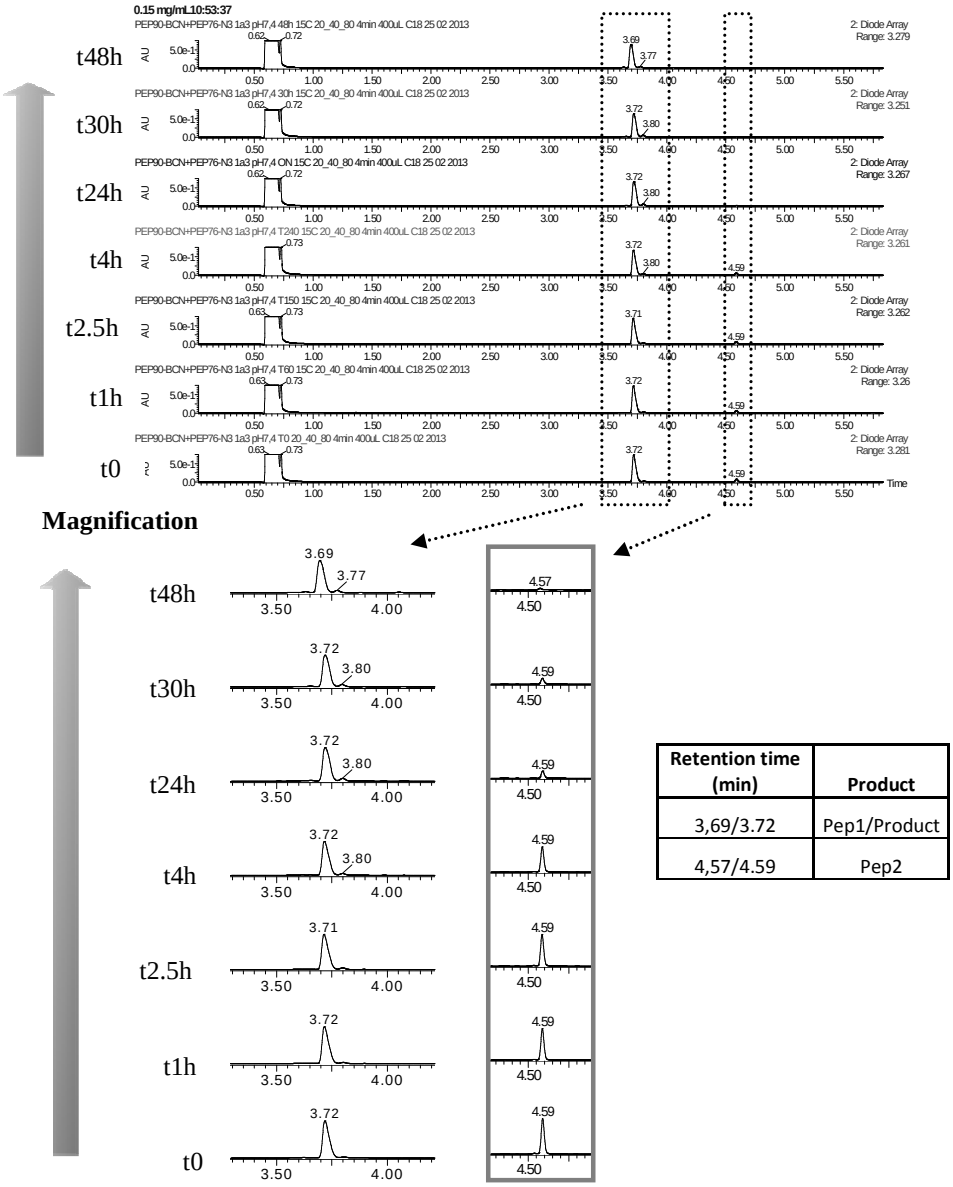

Retention time (min)	Product
3,69/3.72	Pep1/Product
4,57/4.59	Pep2

Figure 2. Example of UPLC/MS analysis of click chemistry kinetic reaction between peptide 1 and peptide 2. In order to follow the progress of the reaction, we analyzed the lowering of the height of the peak relative to peptide 2 (gray square). Column Acquity UPLC BEH300 C4 1.7µm, 2.1x100 mm, Waters; buffer A: H2O/TFA 0.1% v/v, buffer B: CH3CN/TFA 0.1% v/v; gradient 10-60% buffer B in 4 minutes.

The following graphs show the results obtained from the reaction of click chemistry between peptide 1 and peptide 2 at different molar ratios (Figure 3), at different temperatures (Figure 4) and at different pH (Figure 5).

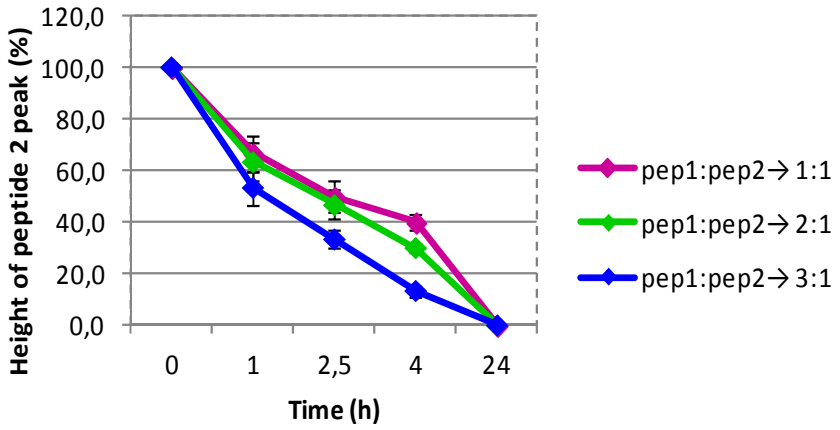

Figure 3. Analysis of influence of the reagents concentration in the click chemistry basic reaction between peptide 1 and peptide 2. Only the concentration of peptide 1 was varied (from 1 to 3 molar excess) compared to that of peptide 2, which remained unchanged (limiting reagent). The reaction was carried out at a concentration of 0,15 mg/ml for peptide2-BCN in presence of 1 (0,176 mg/ml), 2 (0,35 mg/ml) or 3 (0,53 mg/ml) fold molar excesses of peptide1-N3.

The variation of reagents concentration seems to affect the reaction kinetic. In fact, the increase of concentration of one of the two components involved in the click chemistry reactions (in our case the peptide with azido group; peptide 1) determines an acceleration of the reaction kinetic (Figure 3). For this reason, all subsequent reactions were performed using 3 fold molar excesses of peptide1-N3 (molar ratio 1:3 between peptide2-BCN and peptide1-N3).

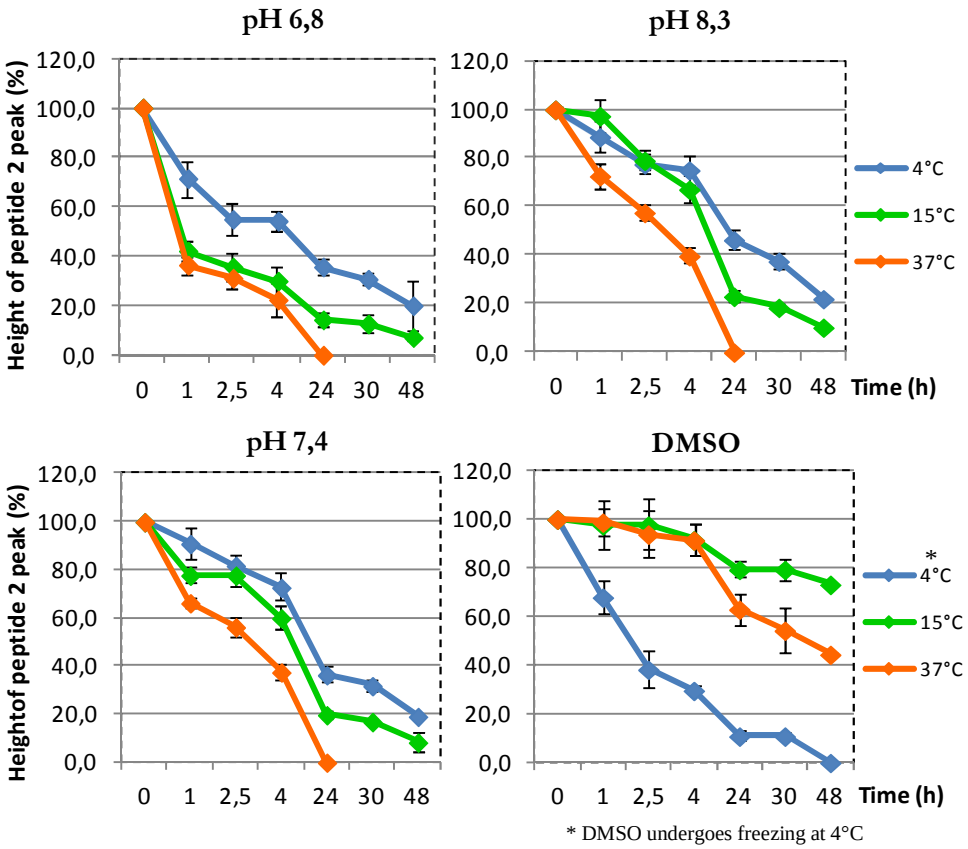

Figure 4. Analysis of influence of the temperature in the click chemistry basic reaction between peptide 1 and peptide 2. Three different temperatures were tested (4°C; 15°C; 37°C) in combination with four different buffers (Hepes pH 6.8; PBS pH 7.4; Borate pH 8.3 and DMSO). The reaction was carried out at a concentration of 0,15 mg/ml for peptide2-BCN in presence of 3 (0,53 mg/ml) fold molar excesses of peptide1-N3.

The temperature also affects the reaction of click chemistry. The kinetics of the reaction appears to be improved at higher temperatures in aqueous buffers: at 37°C, the click chemistry reaction goes to completeness much faster than at 15°C or 4°C (Figure 4). A separate discussion must be made for the reaction carried out in organic medium at 4°C. In DMSO (dimethyl sulfoxide) in fact, the reaction is faster at 4°C than at 37°C or 15°C. At 4°C, the DMSO undergoes freezing and it seems that this phenomenon can promote the interaction between molecules. In the

literature is reported a work (213) that explains how freeze-thawing of the reaction solution substantially increases the conjugation rate possibly because of the reactant concentration at the microenvironment scale with a consequent increase of collision opportunities between the reactants in the reaction solutions. Authors explain how the freezing of the reaction solution results in the phase separation of the solute rich phase and solute-poor phase. The solute-rich phase is a highly reactive environment that accelerates the conjugation reaction.

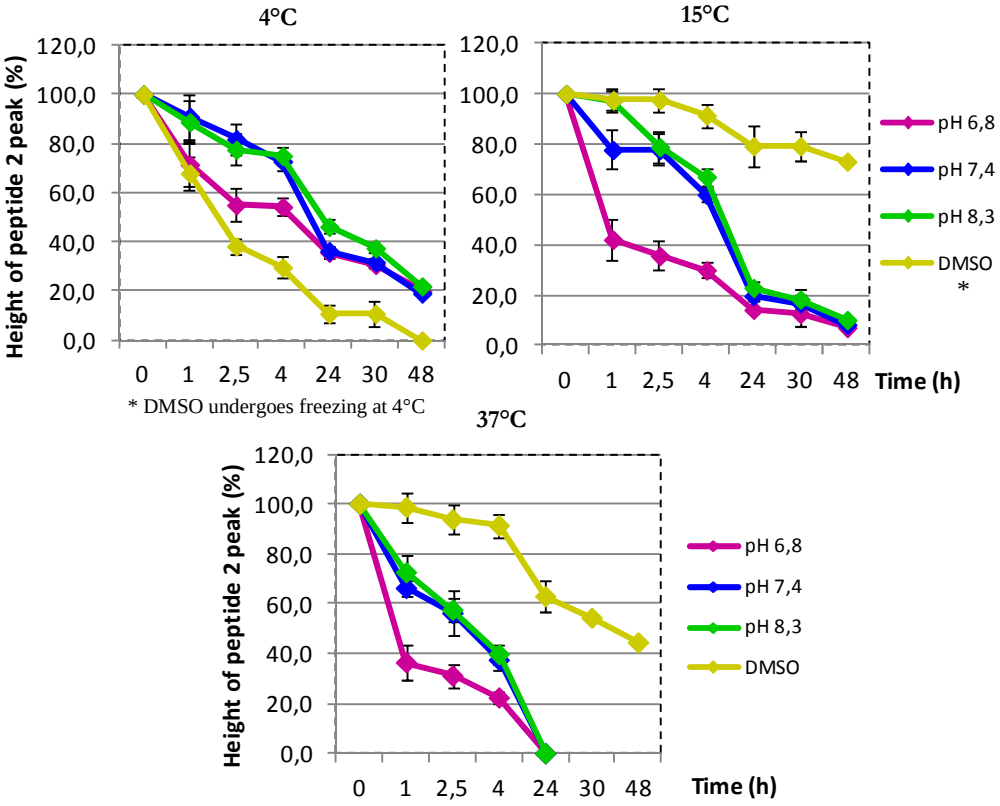

Figure 5. Analysis of influence of the pH in the click chemistry basic reaction between peptide 1 and peptide 2. Four different buffers were tested (Hepes pH 6.8; PBS pH 7.4; Borate pH 8.3 and DMSO) in combination with three different temperatures (4°C; 15°C; 37°C). The reaction was carried out at a concentration of 0,15 mg/ml for peptide2-BCN in presence of 3 (0,53 mg/ml) fold molar excesses of peptide1-N3.

The pH seems to affect the reaction in a less significant way (Figure 5). The profiles of the reaction kinetic are in fact very similar at pH 7.4 and 8.3; only at pH 6.8 the reaction seems to be faster especially in the first points of the kinetic (0 to 4 hours). Moreover, these last graphs clearly show how the reaction kinetic is much slower in the organic medium (DMSO) than in an aqueous buffer (Hepes pH 6.8; PBS pH 7.4; Borate pH 8.3). Even in this case, however, the peculiar kinetic of the reaction carried out in DMSO at 4°C, which is faster than those conducted at 15°C or 37°C in the same buffer, is confirmed.
In this regard, on the basis of information obtained by the paper mentioned above (213), we have conducted studies of the click chemistry reaction kinetics at low temperatures in organic medium (Figure 6). In parallel to the reaction carried out at room temperature for 24 hours, a reaction subjected to a freeze and thaw treatment was set up: the reaction was frozen at time 0 (at 4°C, left panel or -20°C, right panel), and thawed at room temperature after 24 h (time zero); at this point the kinetic was monitored for 24 hours at room temperature.

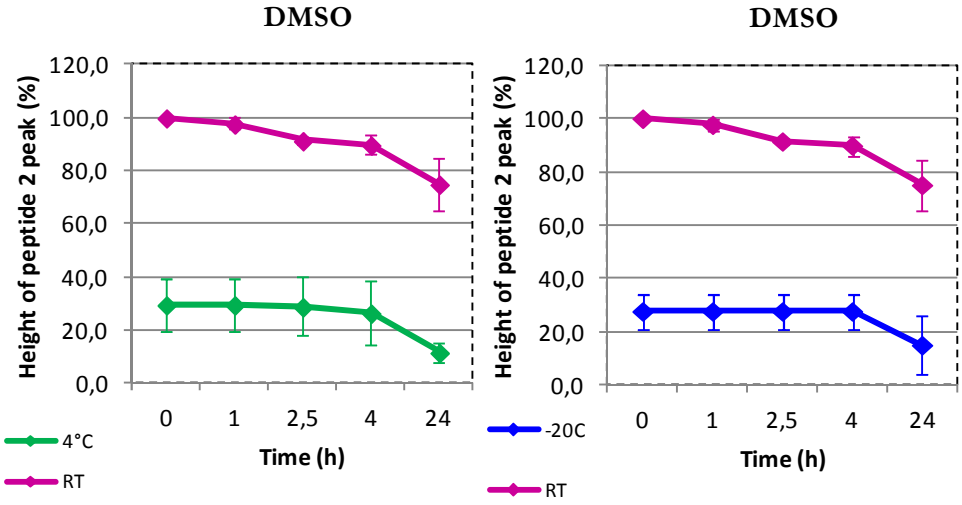

Figure 6. Comparison between the kinetic of click chemistry reaction carried out at room temperature (pink line) and after freeze and thaw treatment (green line → 4°C; blue line → -20°C). The reaction was carried out at a concentration of 0,15 mg/ml for peptide2-BCN in presence of 3 (0,53 mg/ml) fold molar excesses of peptide1-N3.

The graphs illustrated in Figure 6 show that after 24 hours of freezing (both at 4°C and at -20°C), the reaction reaches a completeness degree of 80% and it then remains at this constant level in the other 24 hours at room temperature. This characteristic offers a great advantage in the case of reactions that must necessarily be conducted in organic medium. These latter are in fact characterized by a very slow kinetic at room temperature, as shown in the previous graphs (Figures 4 and 5); the freeze and thaw treatment of these reactions allows to reach a greater completeness and then to obtain a good degree of efficiency even in conditions in which the reaction is not favored.

LIAISON® EBV VCA IgM REVERSE FORMAT

SYNTHESIS OF HTLV-I/II TRACERS THROUGH CLICK CHEMISTRY

DiaSorin LIAISON® Murex recHTLV-I/II immunoassay is an immunoassay used for the detection of antibodies specific for the Human T-lymphotropic Virus type I or II (HTLV-I/II). HTLV-I is a group of human retroviruses that are known to cause a type of cancer called adult T-cell leukemia/lymphoma and a demyelinating disease called HTLV-I associated myelopathy/tropical spastic paraparesis (HAM/TSP). HTLV-II is associated with rare lymphoproliferative diseases and neuro-degenerative disorders, although its etiological role remains to be fully established. The current assay is characterized by a high complexity (Figure 7) and, among the various components, it involves the use of two peptidic tracers (Figure 7, red arrows) consisting of a proteic carrier conjugated to several molecules of ABEI (Amino Butyl Ethyl isoluminol) cyclic and peptide molecules of HTLV-I (tracer 1) or HTLV-II (tracer 2). Since the production of the carrier protein is a very complex process, a prototype of immunoassay that involves the use of a non-proteic scaffold for the synthesis of two tracers, is under development. Even these tracers, like those present in the current assay, are synthesized through the use of a classical chemistry (thiol-chemistry). We explored the possibility to synthesize these two new HTLV-I/ II tracers switching from a thiol-chemistry (traditional chemistry) to a more innovative type of chemistry, the click chemistry.

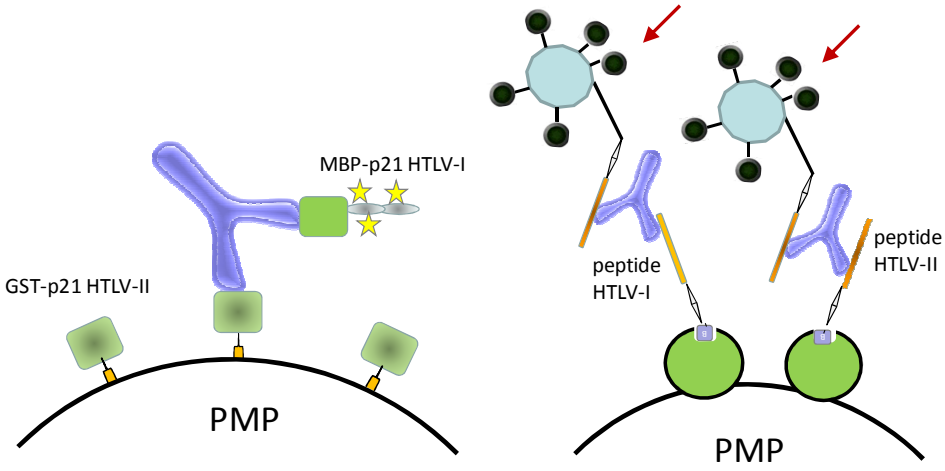

Figure 7. Schematic representation of DiaSorin LIAISON® Murex recHTLV-I/II immunoassay

Figure 8 shows in detail the procedure used to obtain the new HTLV-I/II tracers. In the first step the scaffold was labeled with a multiplicity of ABEI molecules; the reaction occured in an organic medium (DMSO) overnight. In the second step the BCN (bicyclo nonyne) reagent was added for the derivatization of the other functionalities present on the scaffold. This step which involved the reaction between the amino groups present on the scaffold and the NHS-ester group of the BCN molecule, was carried out in DMSO for 2 hours. Subsequently (third step) a GFC purification was carried out to remove the excess of BCN and ABEI molecules present in the reaction (Superdex 200 Hiload 16 60 column, PBS buffer, isocratic gradient; see materials and methods section). In the fourth step, an excess of HTLVI-N3 or HTLVII-N3 peptide (previously synthesized ad hoc with an N-terminal azido-lysine) was added in order to promote the click chemistry reaction between the same azido-peptides and BCN molecules present on the scaffold. The reaction was carried out overnight in PBS buffer. In the fifth step, the final product (scaffold-ABEI-HTLV-I/II) was then subjected to an additional purification process to remove the excess of azido-peptides (Superdex 200 Hiload 16 60 column, PBS buffer, isocratic gradient; see materials and methods section). Figure 9 shows the chromatographic profiles of the GFC purifications carried out respectively in step 3 and in step 5 of process.

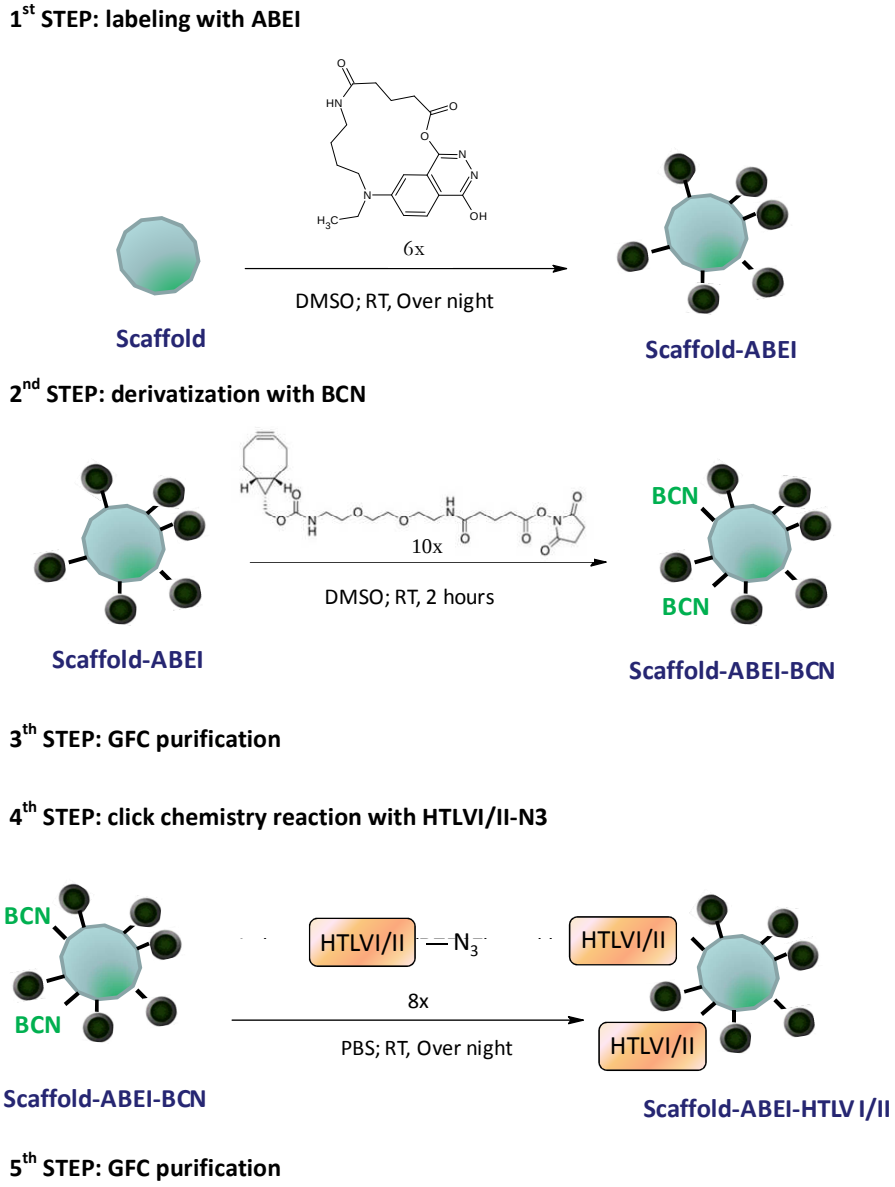

Figure 8. Schematic representation of HTLV-I/II-tracer synthetic process.

A_Scaffold-ABEI-BCN

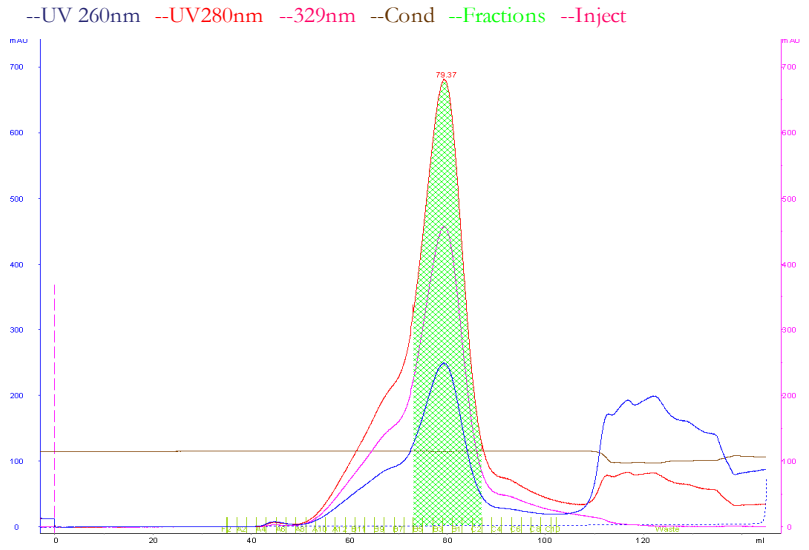

B_Scaffold-ABEI-HTLV-I

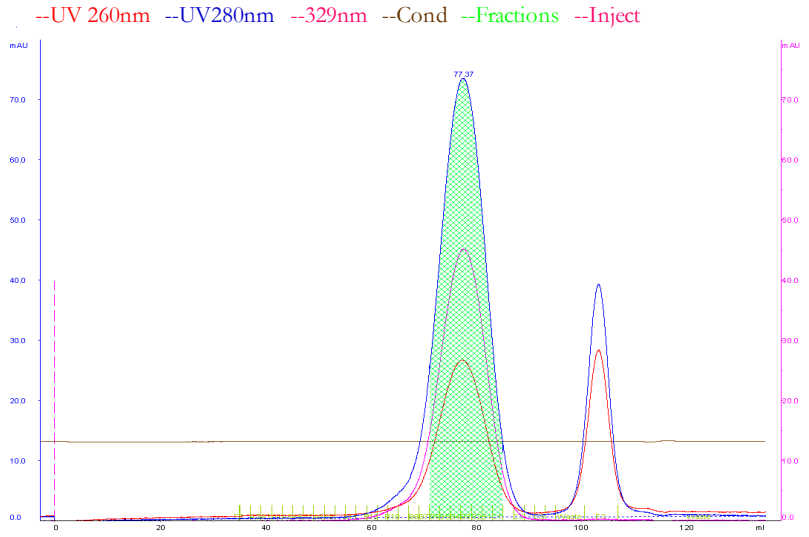

C_Scaffold-ABEI-HTLV-II

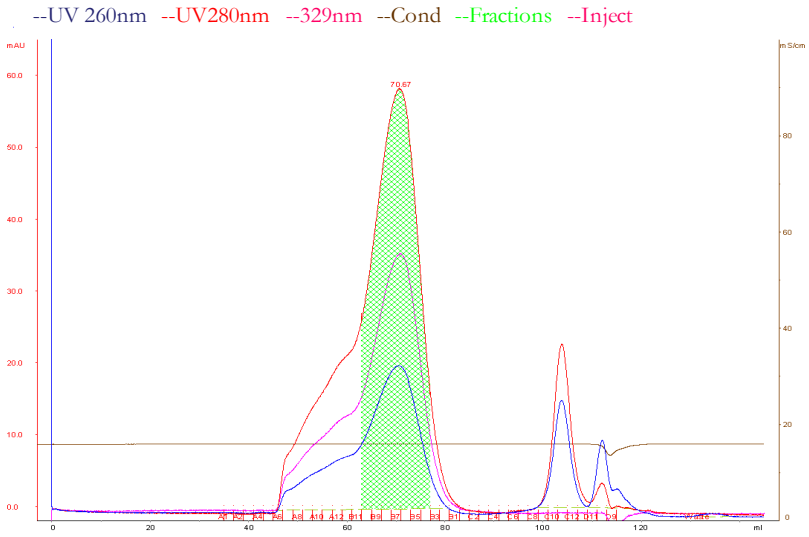

Figure 9. Chromatographic profiles of GFC purifications performed at the level of step 3 and 5 of HTLV-I/II-tracer synthetic process. The first chromatogram refers to scaffold-ABEI-BCN intermediate, while the second and third refer to scaffold-ABEI-HTLV-I and scaffold-ABEI-HTLV-II products respectively.

The new HTLVI/II tracers obtained as described above, were then tested in the LIAISON® Murex recHTLV-I/II chemiluminescent immunoassay and compared with the tracers currently in use in the prototype. The analysis was performed in duplicate on a panel of negative and positive samples and the final evaluation of analytical performance of tracer molecules was done on the average of the signals of each panel (Figure 10). As suggested from the LIAISON® Murex recHTLV-I/II current kit, the tracers currently used in the prototype were tested as a mix (HTLV-I tracer + HTLV-II tracer) in order to detect positive samples for both HTLV-I and HTLV-II; the new tracers, obtained through the use of click chemistry, instead, were individually analysed in order to verify the immunochemical activity of each of the two molecules (for this purpose a panel of HTLV-I positive samples only for the first tracer and a panel of HTLV-II positive samples only for the second tracer were then selected).

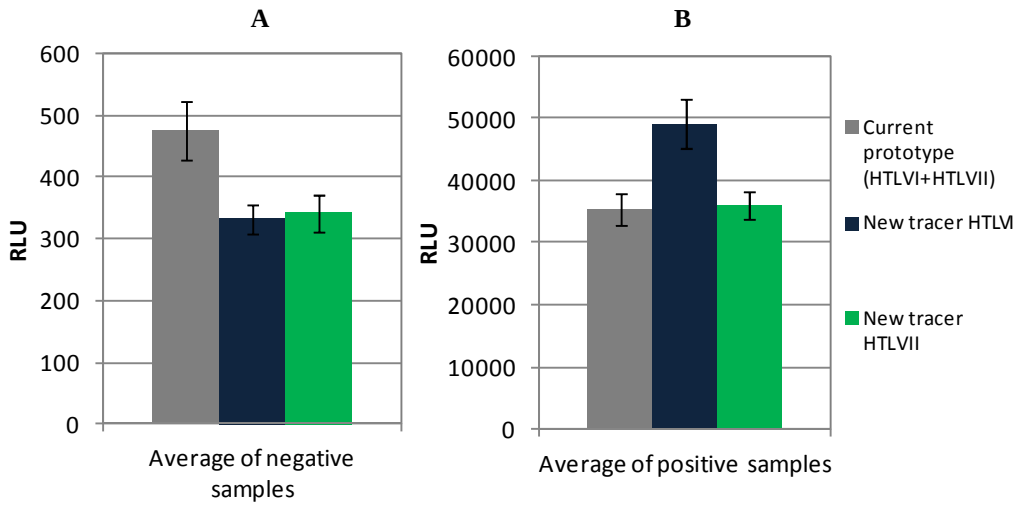

Figure 10. Comparison between the immunochemical activity of tracers currently used in LIAISON® Murex recHTLV-I/II prototype obtained through classical chemistry (gray; mix HTLV-I+HTLV-II) and new tracers obtained through click chemistry (blue → HTLV-I; green → HTLV-II).

The results obtained indicated that the tracers synthesized through the use of click chemistry have a performance comparable, if not slightly better than that of the tracers currently in use in prototype. In particular the new HTLV-I tracer showed a great increase of the signal relating to the positive samples (panel B; blue bar) compared to the mix of current tracers of prototype (panel B; gray bar), while the performance of the new HTLV-II tracer (panel B; green bar) on the detection of positive samples was almost comparable to that of the current tracers. Moreover, the signal of negative samples for both new tracers (panel A; blue and green bars) was lower than that detected for the mix of current tracers of prototype (panel A; gray bar). The result was an increase of the ratio between the signal of the positive and negative samples and therefore an increase of immunodiagnostic assay performance.

In addition to the analysis of immunochemical activity of tracers, also the stability of the same molecules was tested. In particular a short stability test (5 days at 37°C; for HTLV-I new tracer only) and long stability test (6 months at -20°C) were carried out (Figure 11).

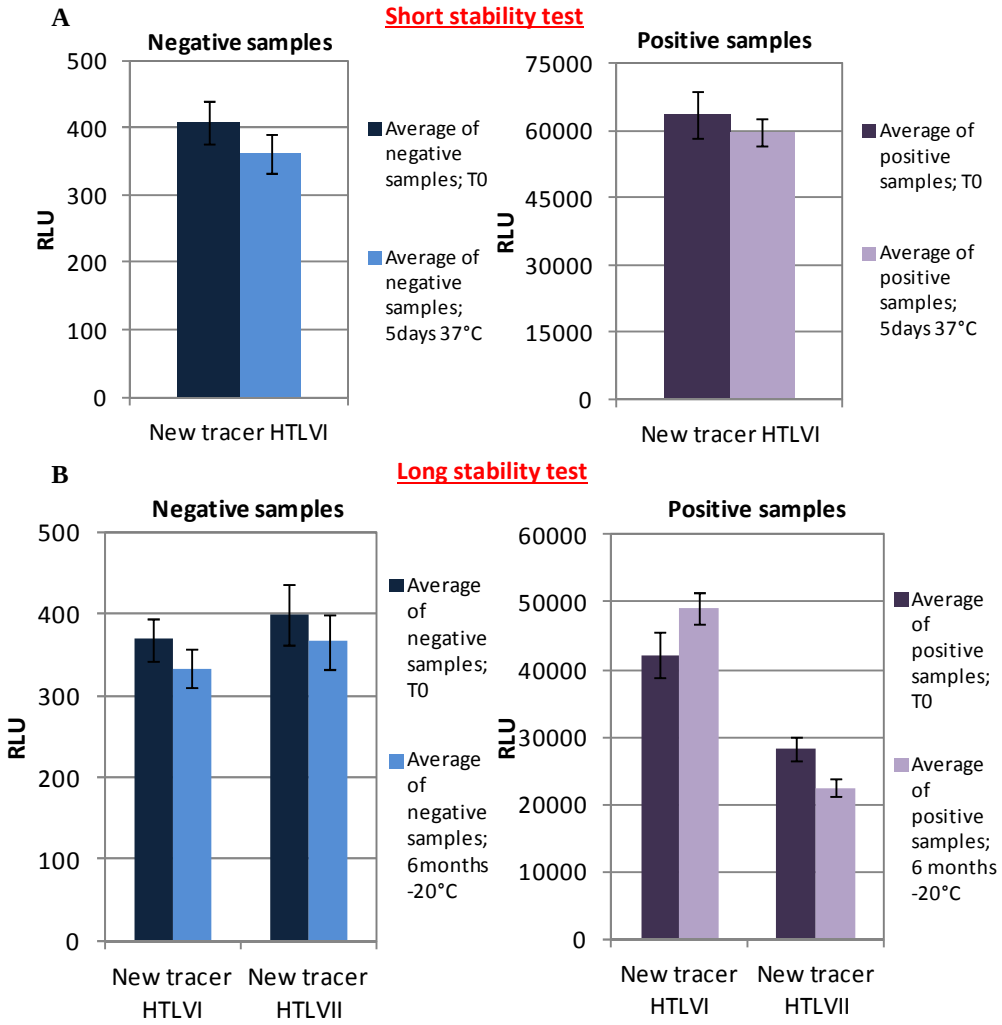

Figure 11. Short stability test (5 days at 37°C; only for HTLV-I new tracer; panel A) and long stability test (6 months at -20°C; for both new HTLV-I and HTLV-II tracers; panel B) on a panel of positive and negative samples.

As illustrated in Figure 11, the stability tests showed that the new tracers analyzed on a panel of positive and negative samples (also in this case the final evaluation of analytical performance of tracer molecules was done on the average of the signals of each panel), undergo an almost irrelevant loss of immunochemical activity whether they are subjected to thermal stress for a short period of time (5 days at 37°C; panel A. Data carried out only for the new HTLV-I tracer) or after storage at -20°C for 6 months (long stability test; panel B). The data thus obtained demonstrated that the new tracers synthesized through the use of an alternative chemistry (click chemistry) retained their immunochemical reactivity over time and therefore they resulted to be stable molecules.

REFERENCES

(1) Yalow RS and Berson SA. Immunoassay of Endogenous Plasma Insulin in Man. *Journal of Clinical Investigation*. 1960; 39 (7): 1157–1175.

(2) Ekins RJ. Radioimmunoassay of Thyroid and Steroid Hormones. *British Journal of Radiology*. 1970; 43 (515): 828.

(3) Epstein MA, Achong BG, Barr YM. Virus particles in cultured lymphoblasts from Burkitt's lymphoma. *Lancet*. 1964; 1:702-3.

(4) Henle G, Henle W, Diehl V. Relation of Burkitt's tumor-associated herpes-type virus to infectious mononucleosis. *Proc Natl Acad Sci USA.* 1968; 59:94-101.

(5) zur Hausen H, Schulte-Holthausen H, Klein G, et al. EBV DNA in biopsies of Burkitt tumours and anaplastic carcinomas of the nasopharynx. *Nature*. 1970; 228:1056-8.

(6) Zieglar JL, Drew WL, Miner RC, et al. Outbreak of Burkitt's-like lymphoma in homosexual men. *Lancet.* 1982; 2:631-3.

(7) Greenspan JS, Greenspan D, Lennette ET, et al. Replication of Epstein–Barr virus within the epithelial cells of oral "hairy" leukoplakia, an AIDS-associated lesion. *N. Engl. J. Med.* 1985; 313:1564-71.

(8) Jones JF, Shurin S, Abramowsky C, et al. T-cell lymphomas containing Epstein–Barr viral DNA in patients with chronic Epstein–Barr virus infections. *N. Engl. J. Med.* 1988; 318:733-41.

(9) Weiss LM, Movahed LA, Warnke RA, Sklar J. Detection of Epstein–Barr viral genomes in Reed–Sternberg cells of Hodgkin's disease. *N. Engl. J. Med.* 1989; 320:502-6.

(10) Nalesnik, M. A. 1999. Epstein-Barr virus, p. 385–407. In E. H. Lennette and T. F. Smith. Laboratory diagnosis of viral infections, 3rd ed. Marcel Dekker, Inc., New York, NY.

(11) Roizman B. Herpesviridae: general description, taxonomy and classification. In: Roizman B, editor. *The herpes viruses. London: Plenum Press*. 1996; 1-23.

(12) Fingeroth JD, Weis JJ, Tedder TF, Strominger JL, Biro PA, Fearson DT.Epstein-Barr virus receptor of human B lymphocytes in the C3d receptor CR2. *Proc Natl Acad Sci USA*. 1984; 81:4510-4.

(13) Sixbey JW, Vesterinen EH, Nedrud JG, Raab-Traub N, Walton LA, Pagano JS. Replication of Epstein-Barr virus in human epithelial cells infected in vitro. *Nature*. 1983;306:480-3.

(14) Kieff E. Epstein-Barr virus and its replication. In: Fields BN, Knipe DM, Howley PM, eds. Fields virology. *Philadelphia: Lippincott-Raven*. 1996; 3 (2):2343-96.

(15) Yao QY, Rickinson AB, Epstein MA. A re-examination of the Epstein-Barr virus carrier state in healthy seropositive individuals. *Int J Cancer*. 1985; 35:35-42.

(16) Sixbey JW, Nedrud JG, Raab-Traub N, Hanes RA, Pagano JS. Epstein–Barr virus replication in oropharyngeal epithelial cells. *N Engl J Med*. 1984; 310:1225-30.

(17) Allday MJ, Crawford DH. Role of epithelium in EBV persistence and pathogenesis of B-cell tumours. *Lancet*. 1988; 1:855-7.

(18) Anagnostopoulos I, Hummel M, Kreschel C, Stein H. Morphology, immunophenotype, and distribution of latently and/or productively Epstein-Barr virus-infected cells in acute infectious mononucleosis: implications for the interindividual infection route of Epstein-Barr virus. *Blood*. 1995; 85:744-50.

(19) Niedobitek G, Agathanggelou A, Herbst H, Whitehead L, Wright DH, Young LS. Epstein-Barr virus (EBV) infection in infectious mononucleosis: virus latency, replication and phenotype of EBV-infected cells. *J Pathol*. 1997; 182:151-9.

(20) Babcock GJ, Decker LL, Volk M, Thorley-Lawson DA. EBV persistence in memory B cells in vivo. *Immunity*. 1998; 9:395-404.

(21) Yao QY, Ogan P, Rowe M, Wood M, Rickinson AB. Epstein-Barr virus-infected B cells persist in the circulation of acyclovir-treated virus carriers. *Int J Cancer*. 1989; 43:67-71.

(22) Gratama JW, Oosterveer MAP, Zwann FE, Lepoutre J, Klein G, Ernberg I. Eradication of Epstein-Barr virus by allogeneic bone marrow transplantation: implications for sites of viral latency. *Proc Natl Acad Sci USA*. 1988; 85:8693-6.

(23) Birx DL, Redfield RR, Tosato G. Defective regulation of Epstein–Barr virus infection in patients with acquired immunodeficiency syndrome (AIDS) or AIDS-related disorders. *N. Engl. J. Med.* 1986; 314:874-9.

(24) Xiao, J., J. M. Palefsky, R. Herrera, J. Berline, and S. M. Tugizov. EBV BMRF-2 facilitates cell-to-cell spread of virus within polarized oral epithelial cells. *Virology.* 2009; 388**:**335-343.

(25) Xiao, J., J. M. Palefsky, R. Herrera, and S. M. Tugizov. Characterization of the Epstein-Barr virus glycoprotein BMRF-2. *Virology*. 2007; 359:382-396.

(26) Chesnokova, L. S., S. L. Nishimura, and L. M. Hutt-Fletcher. Fusion of epithelial cells by Epstein-Barr virus proteins is triggered by binding of viral glycoproteins gHgL to integrins alphavbeta6 or alphavbeta8. *Proc. Natl. Acad. Sci. U. S. A.* 2009; 106:20464-20469.

(27) Tsurumi, T., M. Fujita, and A. Kudoh. Latent and lytic Epstein-Barr virus replication strategies. *Rev. Med. Virol.* 2005; 15:3-15.

(28) Hadinoto, V., et al. On the dynamics of acute EBV infection and the pathogenesis of infectious mononucleosis. *Blood.* 2008; 111:1420-1427.

(29) Kieff, E., et al. The biology and chemistry of Epstein-Barr virus. *J. Infect. Dis.* 1982; 146:506-517.

(30) Kieff, E., et al. Biochemistry of latent Epstein-Barr virus infection and associated cell growth transformation. *IARC Sci. Publ.* 1985; 1985:323-339.

(31) Amon, W., and P. J. Farrell. Reactivation of Epstein-Barr virus from latency. *Rev. Med. Virol.* 2005; 15:149-156.

(32) horley-Lawson, D. A., and A. Gross. Persistence of the Epstein-Barr virus and the origins of associated lymphomas. *N. Engl. J. Med.* 2004; 350:1328-1337.

(33) Speck, S. H. Regulation of EBV latency-associated gene expression, p. 403-427. In E. S. Robertson (ed.), Epstein-Barr virus. *Caister Academic Press, Norfolk, England*. 2005.

(34) Blake, N., et al. Human CD8+ T cell responses to EBV EBNA1: HLA class I presentation of the (Gly-Ala)-containing protein requires exogenous processing. *Immunity.* 1997; 7:791-802.

(35) Bornkamm, G. W., and W. Hammerschmidt. Molecular virology of Epstein-Barr virus. *Philos. Trans. R. Soc. Lond. B Biol. Sci.* 2001; 356:437-459.

(36) Speck, S. H. Regulation of EBV latency-associated gene expression, p. 403-427. In E. S. Robertson (ed.), Epstein-Barr virus. *Caister Academic Press, Norfolk, England.* 2005.

(37) Israel, B. F., and S. C. Kenney. EBV lytic infection, p. 571-611. In E. S. Robertson (ed.), Epstein-Barr virus. *Caister Academic Press, Norfolk, England.* 2005.

(38) Bhaduri-McIntosh, S., and G. Miller. Cells lytically infected with Epstein-Barr virus are detected and separable by immunoglobulins from EBV-seropositive individuals. *J. Virol. Methods.* 2006; 137:103-114.

(39) Henke CE, Kurland LT, Elveback LR. Infectious mononucleosis in Rochester, Minnesota, 1950 through 1969. *Am. J. Epidemiol.* 1973; 98:483-90.

(40) Straus SE, Cohen JI, Tosato G, Meier J. NIH conference: Epstein-Barr virus infections: biology, pathogenesis, and management. *Ann. Intern. Med.* 1993; 118:45-58.

(41) Evans AS. Clinical syndromes associated with EB virus infection. *Adv. Intern. Med.* 1972; 18:77-93.

(42) Skare JC, Milunsky A, Byron KS, Sullivan JL. Mapping the X-linked lymphoproliferative syndrome. *Proc Natl Acad Sci USA.* 1987; 84:2015-2018.

(43) Morra M, Simarro-Grande M, Martin M, et al. Characterization of SH2D1A missense mutations identified in X-linked lymphoproliferative disease patients. J. Biol. Chem. 2001; 276: 36809-36816.

(44) Sayos J, Wu C, Morra M, et al. The X-linked lymphoproliferative disease gene product SAP regulates signals induced through the co-receptor SLAM. *Nature.* 1998; 395:462-469.

(45) Latour S, Gish G, Helgason CD, et al. Regulation of SLAM-mediated signal transduction by SAP, the X-linked lymphoproliferative gene product. *Nat Immunol.* 2001; 2:681-690.

(46) Provisor AJ, Iacuone JJ, Chilcote RR, et al. Acquired agammaglobulinemia after a life-threatening illness with clinical and laboratory features of infectious mononucleosis in three related male children. *New Engl J Med.* 1975; 293:62-65.

(47) Williams LL, Rooney CM, Conley ME, et al. Correction of Duncan's syndrome by allogeneic bone marrow transplantation. *Lancet*. 1993; 342:587-588.

(48) Seemayer TA, Gross TG, Maarten Egeler R, et al. X-linked lymphoproliferative disease: 25 years after the discovery. *Pediatr Res.* 1995; 38:471-478.

(49) Pathmanathan R, Prasad U, Sadler R, Flynn K, Raab-Traub N. Clonal proliferations of cells infected with Epstein–Barr virus in preinvasive lesions related to nasopharyngeal carcinoma. *N Engl J Med.* 1995; 333:693-698.

(50) de Thé G, Zeng Y. Population screening for EBV markers: toward improvement of nasopharyngeal carcinoma control. In: Epstein MA, Achong BG, eds. The Epstein-Barr virus: recent advances. *New York: John Wiley.* 1986; 237-49.

(51) Halprin J, Scott AL, Jacobson LJ, et al. Enzyme-linked immunosorbent assay of antibodies to Epstein-Barr virus nuclear and early antigens in patients with infectious mononucleosis and nasopharyngeal carcinoma. *Ann Intern Med.* 1986; 104:331-337.

(52) Inghirami G, Grignani F, Sternas L, Lombardi L, Knowles DM, Dalla-Favera R. Down-regulation of LFA-1 adhesion receptors by C-myc oncogene in human B lymphoblastoid cells. *Science*. 1990; 250:682-686.

(53) de-The G, Geser A, Day NE, et al. Epidemiological evidence for causal relationship between Epstein-Barr virus and Burkitt's lymphoma from Ugandan prospective study. *Nature*. 1978; 274:756-761.

(54) Weiss LM, Movahed LA, Warnke RA, Sklar J. Detection of Epstein– Barr viral genomes in Reed–Sternberg cells of Hodgkin's disease. *N. Engl. J. Med.* 1989; 320:502-6.

(55) Lukes RJ, Butler JJ. The pathology and nomenclature of Hodgkin's disease. *Cancer Res.* 1966;26:1063-1081.

(56) Marafioti T, Hummel M, Anagnostopoulos I, et al. Origin of nodular lymphocyte-predominant Hodgkin's disease from a clonal expansion of highly mutated germinal-center B-cells. *New Eng.l J. Med.* 1997; 337:453-458.

(57) Jarrett AF, Armstrong AA, Alexander E. Epidemiology of EBV and Hodgkin's disease. *Ann Oncol.* 1996 ;7:S5-S10.

(58) World Health Organization/International Agency for Research on Cancer. IARC Monographs on the Evaluation of Carcinogenic Risks to Humans. Epstein/Barr virus and Kaposi's Sarcoma Herpesvirus/Human Herpesvirus 8, vol. 70. Geneva: IARC Press, 1997.

(59) Glaser SL, Lin RJ, Stewart SL, et al. Epstein-Barr virus associated Hodgkin's disease: epidemiologic characteristics in international data. *Int. J. Cancer.* 1997; 70:375-382.

(60) Ambinder RF. Gammaherpesviruses and 'hit-and-run' oncogenesis.. *Am. J. Pathol.* 2000;156:1-3.

(61) Cohen JI. Epstein-Barr virus lymphoproliferative disease associated with acquired immunodeficiency. *Medicine (Baltimore)*. 1991; 70:137-60.

(62) Paya CV, Fung JJ, Nalesnik MA, et al. Epstein-Barr virus-induced posttransplant lymphoproliferative disorders. *Transplantation.* 1999; 68: 1517-25.

(63) Riddler SA, Breinig MC, McKnight JLC. Increased levels of circulating Epstein-Barr virus (EBV)-infected lymphocytes and decreased EBV nuclear antigen antibody responses are associated with the development of posttransplant lymphoproliferative disease in solid-organ transplant patients. *Blood.* 1994; 84:972-984.

(64) Rooney CM, Smith CA, Ng CY, et al. Infusion of cytotoxic T cells for the prevention and treatment of Epstein-Barr virus-induced lymphoma in allogeneic transplant recipients. *Blood.* 1998; 92:1549-55.

(65) Randhawa PS, Jaffe R, Demetris AJ, et al. Expression of Epstein–Barr virus–encoded small RNA (by the EBER-1 gene) in liver specimens from transplant recipients with post-transplantation lymphoproliferative disease. *N. Engl. J. Med.* 1992; 327:17101714.

(66) Tosato G, Jones K, Breinig MK, McWilliams HP, McKnight JL. Interleukin-6 production in posttransplant lymphoproliferative disease. J Clin. Invest. 1993; 91:2806-2814.

(67) Hochberg FH, Miller G, Schooley RT, Hirsch MS, Feorino P, Henle W. Central-nervous-system lymphoma related to Epstein–Barr virus. *N. Engl. J. Med.* 1983; 309:745-8.

(68) Lee ES, Locker J, Nalesnik M, et al. The association of Epstein–Barr virus with smooth-muscle tumors occurring after organ transplantation. *N. Engl. J. Med.* 1995; 332:19-25.

(69) Imai S, Koizumi S, Sugiura M, et al. Gastric carcinoma: monoclonal epithelial malignant cells expressing Epstein-Barr virus latent infection protein. *Proc. Natl. Acad. Sci. U S A.* 1994; 91:9131-9135.

(70) Pallesen G, Hamilton-Dutoit SJ, Zhou X. The association of Epstein-Barr virus (EBV) with T cell lymphoproliferations and Hodgkin's disease: two new developments in the EBV field. *Adv. Cancer. Res.* 1993;62:179-239.

(71) Jenson H, McIntosh K, Pitt J, et al. Natural history of primary Epstein-Barr virus infection in children of mothers infected with human immunodeficiency virus type 1. *J. Infect Dis*. 1999; 179:1395-1404.

(72) Kersten MJ, Klein MR, Holwerda AM, Miedema F, van Oers MH. Epstein-Barr virus-specific cytotoxic T cell responses in HIV-1 infection: different kinetics in patients progressing to opportunistic infection or non-Hodgkin's lymphoma. *J. Clin. Invest*. 1997;.99:1525-1533.

(73) Pedneault L, Lapointe N, Alfieri C, et al. Natural history of Epstein-Barr virus infection in a prospective pediatric cohort born to human immunodeficiency virus-infected mothers. *J. Infect. Dis.* 1998; 177:1087-1090.

(74) Triantos D, Porter SR, Scully C, Teo CG. Oral hairy leukoplakia: clinicopathologic features, pathogenesis, diagnosis, and clinical significance. *Clin. Infect. Dis.* 1997; 25:1392-1396.

(75) Andiman WA, Eastman R, Martin K, et al. Opportunistic lympho-proliferations associated with Epstein-Barr viral DNA in infants and children with AIDS. *Lancet* 1985; 2:1390-1393.

(76) Shibata D, Weiss LM, Nathwani BN, Brynes RK, Levine AM. Epstein-Barr virus in benign lymph node biopsies from individuals infected with the human immunodeficiency virus is associated with concurrent or subsequent development of non-Hodgkin's lymphoma. Blood 1991;77:1527-33.

(77) Hamilton-Dutoit SJ, Pallesen G, Franzmann MB, et al. AIDS-related lymphoma: histopathology, immunophenotype, and association with Epstein-Barr virus as demonstrated by in situ nucleic acid hybridization. *Am. J. Pathol.* 1991; 138:149-163.

(78) Shibata D, Weiss LM, Hernandez AM, Nathwani BN, Bernstein L, Levine AM. Epstein-Barr virus-associated non-Hodgkin's lymphoma in patients infected with the human immunodeficiency virus. *Blood*. 1993; 81:2102-2109.

(79) MacMahon EME, Glass JD, Hayward SD, et al. Epstein-Barr virus in AIDS-related primary central nervous system lymphoma. *Lancet*. 1991; 338:969-973.

(80) Antinori A, Ammassari A, De Luca A, et al. Diagnosis of AIDS-related focal brain lesions: a decision-making analysis based on clinical and neuroradiologic characteristics combined with polymerase chain reaction assays in CSF. *Neurology*. 1997; 48:687-694.

(81) McClain KL, Leach CT, Jenson HB, et al. Association of Epstein–Barr virus with leiomyosarcomas in young people with AIDS. *N. Engl. J. Med.* 1995; 332:12-18.

(82) Li, J.-H. et al. Tumour-targeted gene therapy for nasopharyngeal carcinoma. *Cancer Res.* 2002; 62: 171–178.

(83) Li, J.-H. et al. Efficacy of targeted FasL in nasopharyngeal carcinoma. *Mol. Ther.* 2003; 8: 964–973.

(84) Israel, B. F. & Kenney, S. C. Virally targeted therapies for EBV-associated malignancies. *Oncogene*. 2003; 22:5122–5130.

(85) Feng, W.-H., Hong, G., Delecluse, H. J. & Kenney, S. C. Lytic induction therapy for Epstein–Barr virus-positive B-cell lymphomas. *J. Virol.* 2004; 78:1893–1902.

(86) Ambinder, R. F., Robertson, K. D. & Tao, Q. DNA methylation and the Epstein–Barr virus. *Semin. Cancer Biol*. 1999; 9:369–375.

(87) Chodosh, J. et al. Eradication of latent Epstein–Barr virus by hydroxyurea alters the growth-transformed cell phenotype. *J. Infect. Dis.* 1998; 177: 1194–1201.

(88) Slobod, K. S. et al. Epstein–Barr virus-targeted therapy for AIDS-related primary lymphoma of the central nervous system. *Lancet.* 2000; 356: 1493–1494.

(89) Piche, A., Kasono, K., Johanning, F., Curiel, T. J. & Curiel, D. T. Phenotypic knockout of the latent membrane protein 1 of Epstein–Barr virus by an intracellular single-chain antibody. *Gene Ther.* 1998; 5: 1171–1179.

(90) Kenney, J. L., Guinness, M. E., Curiel, T. & Lacy, J. Antisense to the Epstein–Barr virus (EBV)-encoded latent membrane protein 1 (LMP-1) suppresses LMP-1 and Bcl-2 expression and promotes apoptosis in EBV-immortalised B cells. *Blood.* 1998; 92: 1721–1727.

(91) Cahir-McFarland, E. D., Davidson, D. M., Schauer, S. L., Duong, J. & Kieff, E. NFκB inhibition causes spontaneous apoptosis in Epstein–Barr virus-transformed lymphoblastoid cells. *Proc. Natl Acad. Sci. USA.* 2000; 97: 6055–6060.

(92) Farrell, C. J. et al. Inhibition of Epstein–Barr virus-induced growth proliferation by a nuclear antigen EBNA2-TAT peptide. *Proc. Natl Acad. Sci. USA.* 2004; 101: 4625–4630.

(93) Kirchmaier, A. L. & Sugden, B. Dominant-negative inhibitors of EBNA-1 of Epstein–Barr virus. *J. Virol.* 1997; 71: 1766–1775.

(94) Rooney, C. M. et al. Use of gene-modified virus-specific T lymphocytes to control Epstein–Barr virus-related lymphoproliferation. *Lancet.* 1995; 345: 9–13.

(95) Khanna, R. et al. Activation and adoptive transfer of Epstein–Barr virus-specific cytotoxic T cells in solid organ transplant patients with post-transplant lymphoproliferative disease. Proc. Natl Acad. Sci. USA. 1999; 96: 10391–10396.

(96) Haque, T. et al. Treatment of Epstein–Barr virus-positive post-transplantation lymphoproliferative disease with partly HLA-matched allogeneic cytotoxic T cells. Lancet. 2002; 360: 436–442.

(97) Roskrow, M. A. et al. Epstein–Barr virus (EBV)-specific cytotoxic T lymphocytes for the treatment of patients with EBV-positive relapsed Hodgkin's disease. *Blood.* 1998; 91: 2925–2934.

(98) Wagner, H. J. et al. Expansion of EBV latent membrane protein 2a specific cytotoxic T cells for the adoptive immunotherapy of EBV latency type 2 malignancies: influence of recombinant IL12 and IL15. Cytotherapy. 2003; 5: 231–240.

(99) Paludan, C. et al. Epstein–Barr nuclear antigen 1-specific CD4+ Th1 cells kill Burkitt's lymphoma cells. J. Immunol. 2002; 169: 1593–1603.

(100) Taylor, G. S. et al. Dual stimulation of Epstein–Barr virus (EBV)-specific CD4+/– and CD8+/– T cell responses by a chimeric antigen construct: Potential therapeutic vaccine for EBV-positive nasopharyngeal carcinoma. J. Virol. 2004; 78: 768–778.

(101) Frisan, T. et al. Local suppression of Epstein–Barr virus (EBV)-specific cytotoxicity in biopsies of EBV-positive Hodgkin's disease. Blood. 1995; 86: 1493–1501.

(102) Wagner, H. J. et al. A strategy for treatment of Epstein–Barr virus-positive Hodgkin's disease by targeting interleukin 12 to the tumour environment using tumour antigen-specific T cells. Cancer Gene Ther. 2004; 11: 81–91.

(103) Klutts, J. S., B. A. Ford, N. R. Perez, and A. M. Gronowski. 2009. Evidence-based approach for interpretation of Epstein-Barr virus serological patterns. J. Clin. Microbiol. 47:3204-3210.

(104) Baer R.A. et al. DNA-sequence and expression of the B95-8 Epstein-Barr virus genome. *Nature (London).* 1984; 310: 207-211.

(105) Berbers G.A. et al. Localization and quantification of HSP84 in mammalian cells. *Exp. Cell.Res.* 1988; 177:257-271.

(106) Chee M.S. et al. Analysis of the protein-coding content of the sequence of human cytomegalovirus strain AD169. *Curr. Top. Microbiol. Immunol.* 1990; 154:125-169.

(107) Chen M.R. et al. Cloning and characterization of cDNA clones corresponding to transcripts from the BamHI G region of the Epstein-Barr virus genome and expression of BGLF2. J. Gen. Virol. 1991; 72: 3047-3055.

(108) Wout M.J. et al. Localization and diagnostic application of immunodominant domains of the BFRF3-encoded Epstein-Barr virus capsid protein. *The J. of Infectious Diseases.* 1994; 70:13-9.

(109) Xu MQ, Perler FB. The mechanism of protein splicing and its modulation by mutation. *EMBO J.* 1996; 15(19):5146-5153.

(110) Meyer D.E., Chilkoti A. Purification of recombinant proteins by fusion with thermally-responsive polypeptides. *Nat. Biotechnol.* 1999; 17: 1112–1115.

(111) Hirata R., et al. Molecular structure of a gene, VMA1, encoding the catalytic subunit of H(+)-translocating adenosine triphosphatase from vacuolar membranes of *Saccharomyces cerevisiae*. *J. Biol. Chem.* 1990; 265:6726–6733.

(112) Kane PM., et al. Protein splicing converts the yeast *TFP1* gene product to the 69-kD subunit of the vacuolar H(+)–adenosine triphosphatase. *Science*. 1990; 250:651–657.

(113) Perler FB., et al. Protein splicing elements: inteins and exteins-a definition of terms and recommended nomenclature. Nucl. Acids Res. 1994; 22:1125–1127.

(114) Perler FB. InBase: the Intein Database. *Nucl. Acids Res*. 2002; 30:383–384.

(115) Liu XQ. Protein-splicing intein: genetic mobility, origin, and evolution. Ann. Rev. Genet.2000; 34:61–76.

(116) Belfort M, Derbyshire V, Stoddard BL, Wood DW. Homing endonucleases and inteins. Berlin Heidelberg New York: Springer; 2005.

(117) Chong S, Xu MQ. Protein splicing of the *Saccharomyces cerevisiae* VMA intein without the endonuclease motifs. J.Biol. Chem. 1997; 272:15587–155890.

(118) Amitai G, Callahan BP, Stanger MJ, Belfort G, Belfort M. Modulation of intein activity by its neighboring extein substrates. *Proc. Natl. Acad. Sci. U S A.* 2009.

(119) Saleh L, Perler FB. Protein splicing in cis and in trans. *Chem. Rec.* 2006;6:183–193.

(120) Telenti A, Southworth M, Alcaide F, Daugelat S, Jacobs WR Jr, Perler FB. The Mycobacterium xenopi GyrA protein splicing element: characterization of a minimal intein. *J. Bacteriol.* 1997; 179 (20): 6378-6382.

(121) Arnold U. Incorporation of non-natural modules into proteins: structural features beyond the genetic code. *Biotechnol. Lett.* 2009; 31:1129–113.

(122) Charalambous A, Andreou M, Skourides PA. Intein-mediated site-specific conjugation of Quantum Dots to proteins in vivo. *J. Nanobiotechnology*. 2009; 7:9.

(123) Oeemig JS, Aranko AS, Djupsjobacka J, Heinamaki K, Iwai H. Solution structure of DnaE intein from Nostoc punctiforme: structural basis for the design of a new split intein suitable for site-specific chemical modification. *FEBS Lett.* 2009; 583:1451–1456.

(124) Seyedsayamdost MR, Yee CS, Stubbe J. Site-specific incorporation of fluorotyrosines into the R2 subunit of E. coli ribonucleotide reductase by expressed protein ligation. *Nat. Protoc.* 2007; 2:1225–1235.

(125) Züger S, Iwai H. Intein-based biosynthetic incorporation of unlabeled protein tags into isotopically labeled proteins for NMR studies. *Nat. Biotechnol.* 2005; 23:736–740.

(126) Chong S, Xu MQ. Harnessing inteins for protein purification and characterization. In: Belfort M, Derbyshire V, Stoddard BL, Wood

DW, editors. Homing endonucleases and inteins. *Berlin Heidelberg New York: Springer*; 2005. pp. 273–292.

(127) Ozawa T, Nishitani K, Sako Y, Umezawa Y. A high-throughput screening of genes that encode proteins transported into the endoplasmic reticulum in mammalian cells. *Nucleic Acids Res.* 2005; 33:e34.

(128) Evans TC Jr, Benner J, Xu MQ. The cyclization and polymerization of bacterially expressed proteins using modified self-splicing inteins. *J. Biol. Chem.* 1999;2 74:18359–18363.

(129) Muir TW, Sondhi D, Cole PA. Expressed protein ligation: a general method for protein engineering. *Proc. Natl. Acad. Sci. USA.* 1998; 95:6705–6710.

(130) Mar ley J, Lu M. & Bracken C. A method for efficient isotopic labeling of recombinant proteins. *J. Biomol. NMR.* 2001; 20: 71–75.

(131) Jansson M, Li Y.C, Jendeberg L, Anderson S, Montelione B.T. & Nilsson B. High-level production of uniformly 15N- and 13C-enriched fusion proteins in Escherichia coli. *J. Biomol. NMR*; 1996; 7: 131–141.

(132) Chin J.W, Cropp T.A, Anderson J.C, Mukherji M, Zhang Z. & Schultz P.G. An expanded eukaryotic genetic code. *Science.* 2003; 301: 964–967.

(133) Wang L. & Schultz P.G. Expanding the genetic code. *Chem. Commun.* 2002; 1– 11.

(134) Wallace C.J. Peptide ligation and semisynthesis. *Curr. Opin. Biotechnol.* 1995; 6: 403–410.

(135) Dawson P.E, Muir T.W, Clark-Lewis I. & Kent S.B. Synthesis of proteins by native chemical ligation. *Science.* 1994; 266: 776–779.

(136) Burns J.A, Butler J.C, Moran J. & Whitesides G.M. Selective reduction of disulfides by tris (2-carboxyethyl) phosphine. *J. Org. Chem.* 1991; 56: 2648–2650.

(137) Dawson P.E, Churchill M, Ghadiri M.R. & Kent S.B.H. Modulation of reactivity in native chemical ligation through the use of thiol additives. *J. Am. Chem. Soc.* 1997; 119: 4325–4329.

(138) Canne L.E, Botti P, Simon R.J, Chen Y, Dennis E.A, Kent S.B.H. Chemical protein synthesis by solid phase ligation of unprotected peptide segments. *J. Am. Chem. Soc.* 1999; 121: 8720–8727.

(139) Muir T.W, Sondhi D. & Cole P.A. Expressed protein ligation: a general method for protein engineering. *Proc. Natl Acad. Sci. USA.* 1998; 95: 6705–6710.

(140) Hofmann, R.M. & Muir, T.W. Recent advances in the application of expressed protein ligation to protein engineering. *Curr. Opin. Biotechnol.* (2002); 13: 297–303.

(141) Evans T.C. Jr & Xu M.Q. Intein-mediated protein ligation: harnessing nature's escape artists. *Biopolymers*. 2000; 51: 333–342.

(142) Keeley, F.W. et al. Elastin as a self-organizing biomaterial: Use of recombinantly expressed human elastin polypeptides as a model for investigations of structure and self-assembly of elastin. *Philos. Trans. R. Soc. Lond. B Biol. Sci.* 2002; 357: 185–189.

(143) Rosenbloom, J. et al. Extracellular matrix 4: The elastic fiber. FASEB J. 1993; 7: 1208–1218.

(144) Daamen, W.F. et al. Comparison of five procedures for the purification of insoluble elastin. *Biomaterials.* 2001; 22: 1997–2005.

(145) Urry, D.W. Free energy transduction in polypeptides and proteins based on inverse temperature transitions. *Prog. Biophys. Mol. Biol.* 1992; 57: 23–57.

(146) Urry, D.W. Entropic elastic processes in protein mechanisms. I. Elastic structure due to an inverse temperature transition and elasticity due to internal chain dynamics. *J. Protein Chem.* 1988; 7: 1–34.

(147) Serrano, V. et al. An infrared spectroscopic study of the conformational transition of elastin-like polypeptides. *Biophys. J.* 2007; 93: 2429–2435.

(148) Girotti, A. et al. Influence of the molecular weight on the inverse temperature transition of a model genetically engineered elastin-like pH-responsive polymer. *Macromolecules.* 2004; 37: 3396–3400.

(149) Meyer, D.E. and Chilkoti, A. Quantification of the effects of chain length and concentration on the thermal behavior of elastin-like polypeptides. *Biomacromolecules.* 2004; 5: 846–851.

(150) Urry, D.W. et al. Temperature of polypeptide inverse temperature transition depends on mean residue hydrophobicity. *J. Am. Chem. Soc.* 1991; 113: 4346–4348.

(151) Ribeiro, F.J. et al. Influence of the amino-acid sequence on the inverse temperature transition of elastin-like polymers. *Biophys. J.* 2009; 97: 312–320.

(152) Liu C. C. and Schultz P. G. Adding new chemistries to the genetic code. Annu. Rev. Biochem. 2010; 79: 413−444.

(153) Nakamura Y, Gojobori T, and Ikemura T. Codon usage tabulated from international DNA sequence databases: status for the year 2000. *NucleicAcids Res.* 2000; 28: 292.

(154) Xie J. and Schultz P. G. An expanding genetic code. *Methods.* 2005b; 36: 227–238.

(155) Wang L, Brock A, Herberich B, Schultz P. G. Expanding the genetic code of Escherichia coli. *Science.* 2001; 292: 498–500.

(156) Normanly J, Kleina L. G, Masson J. M, Abelson J, Miller J. H. Construction of Escherichia coli amber suppressor tRNA genes. III. Determination of tRNA specificity. *J. Mol. Biol.* 1990; 213, 719–726.

(157) Steer B. A, Schimmel P. Major anticodon-binding region missing from an archaebacterial tRNA synthetase. *J. Biol. Chem.* 1999; 274: 35601–35606.

(158) Xie J, Schultz P. G. Adding amino acids to the genetic repertoire. *Curr. Opin. Chem. Biol*. 2005a; 9: 548–554.

(159) Armen R. S, Schiller S. M, Brooks C. L, 3rd. Steric and thermodynamic limits of design for the incorporation of large unnatural amino acids in aminoacyl-tRNA synthetase enzymes. *Proteins.* 2010; 78: 1926–1938.

(160) Ryu Y, and Schultz P. G. Efficient incorporation of unnatural amino acids into proteins in Escherichia coli. *Nat. Methods.* 2006; 3: 263−265.

(161) Cellitti, S. E, Jones D. H, et al. In vivo incorporation of unnatural amino acids to probe structure, dynamics, and ligand binding in a large protein by nuclear magnetic resonance spectroscopy. *J. Am. Chem. Soc.* 2008; 130: 9268−9281.

(162) Young T. S, Ahmad I, Yin J. A, and Schultz P. G. An enhanced system for unnatural amino acid mutagenesis in E. coli. *J. Mol. Biol.* 2010; 395: 361−374.

(163) Anderson J. C, Wu N, Santoro S. W, Lakshman V, King D.S. and Schultz P. G. An expanded genetic code with a functional quadruplet codon. *Proc. Natl. Acad. Sci. U.S.A.* 2004; 101: 7566−7571.

(164) Rusmini F, Zhong Z, Feijen J. Protein immobilization strategies for protein biochips. *Biomacromolecules.* 2007; 8(6):1775-1789.

(165) Zhang K, Diehl M. R, and. Tirrell D. A. Artificial polypeptide scaffold for protein immobilization. *J. Am. Chem. Soc.* 2005; 127: 10136-10137.

(166) Wolf E, Kim PS, Berger B. MultiCoil: a program for predicting two- and three-stranded coiled coils. *Protein Sci.* 1997; 6 (6):1179-89.

(167) Landschulz WH, Johnson PF, McKnight SL. The leucine zipper: a hypothetical structure common to a new class of DNA binding proteins. *Science.* 1988; 240 (4860): 1759-64.

(168) Kohn WD, Mant CT, Hodges RS. Alpha-helical protein assembly motifs. *J. Biol. Chem.* 1997; 272(5): 2583-2586.

(169) O'Shea EK, Klemm JD, Kim PS, Alber T. X-ray structure of the GCN4 leucine zipper, a two-stranded, parallel coiled coil. *Science.* 1991; 254(5031):539-44.

(170) Moll JR, Ruvinov SB, Pastan I, Vinson C. Designed heterodimerizing leucine zippers with a ranger of pIs and stabilities up to 10(-15) M. *Protein Sci*. 200; 10 (3) :649-55.

(171) Kolb HC, Sharpless KB. The growing impact of click chemistry on drug discovery. *Drug Discov Today*. 2003; 8 (24): 1128-1137.

(172) Lutz JF1. 1,3-dipolar cycloadditions of azides and alkynes: a universal ligation tool in polymer and materials science. *Angew. Chem. Int. Ed. Engl*. 2007; 46(7):1018-1025.

(173) Prescher JA, Bertozzi CR. Chemistry in living systems. Nat Chem Biol. 2005; 1(1):13-21.

(174) Mahal LK, Yarema KJ, Bertozzi CR. Engineering chemical reactivity on cell surfaces through oligosaccharide biosynthesis. *Science*. 1997; 276 (5315):1125-1128.

(175) Saxon E, Bertozzi CR. Cell surface engineering by a modified Staudinger reaction. *Science*. 2000; 287(5460): 2007-2010.

(176) Bräse S, Gil C, Knepper K, Zimmermann V. Organic azides: an exploding diversity of a unique class of compounds. *Angew. Chem. Int. Ed. Engl*. 2005; 44(33): 5188-5240.

(177) Köhn M, Breinbauer R. The Staudinger ligation-a gift to chemical biology. *Angew. Chem. Int. Ed. Engl*. 2004; 43(24):3106-3116.

(178) Rostovtsev VV, Green LG, Fokin VV, Sharpless KB. A stepwise huisgen cycloaddition process: copper(I)-catalyzed regioselective "ligation" of azides and terminal alkynes. *Angew. Chem. Int. Ed. Engl.* 2002; 41(14): 2596-2599.

(179) Tornøe CW, Christensen C, Meldal M. Peptidotriazoles on solid phase: [1,2,3]-triazoles by regiospecific copper(i)-catalyzed 1,3

dipolar cycloadditions of terminal alkynes to azides. J. Org. Chem. 2002; 67(9):3057-3064.

(180) Baskin JM, Prescher JA, Laughlin ST, Agard NJ, Chang PV, Miller IA, Lo A, Codelli JA, Bertozzi CR. Copper-free click chemistry for dynamic in vivo imaging. *Proc. Natl. Acad. Sci. USA.* 2007;104(43):16793-16797.

(181) Agard NJ, Baskin JM, Prescher JA, Lo A, Bertozzi CR. A comparative study of bioorthogonal reactions with azides. *ACS Chem. Biol.* 2006; 1(10):644-648.

(182) Agard NJ, Bertozzi CR. Second-Generation Difluorinated Cyclooctynes for Copper-Free Click Chemistry. *J. Am. Chem. Soc.* 2008; 130:11486–11493.

(183) Debets MF, van Berkel SS, Schoffelen S, Rutjes FPJT, van Hest J. CM, van Delft FL. Aza-dibenzocyclooctynes for fast and efficient enzyme PEGylation via copper-free (3+2) cycloaddition. *Chem. Commun.* 2010; 46: 97–99.

(184) Antony-Meyer C, Meier H. Bicyclo[6.1.0]nonyne. *Chem. Ber*. 1988, 121, 2013–2018.

(185) Wisdom GB. Conjugation of antibodies to fluorescein or rhodamine. *Methods Mol. Biol.* 2005; 295: 13113-4.

(186) Gudmundsson BM, Young NM, and Oomen RP. Characterization of residues in antibody binding sites by chemical modification of surface-adsorbed protein combined with enzyme immunoassay. *J. Immunol. Methods*. 1993; 158: 215-227.

(187) Wines BD and Easterbrook-Smith SB. Carbodiimide cross-linking of human C1q and rabbit IgG. *Mol. Immunol.* 1990; 27: 221-226.

(188) Hayashi N, Kipriyanov S, Fuchs P, Welschof M, Dorsam H. and Little M. A single expression system for the display, purification and conjugation of single-chain antibodies. *Gene.* 1995; 160: 129-130.

(189) Schneider P. Production of recombinant TRAIL and TRAIL receptor: Fc chimeric proteins. *Methods Enzymol.* 2000; 322: 325-345.

(190) Junutula JR, Bhakta S, Raab H, Ervin KE, Eigenbrot C, Vandlen R, Scheller RH, Lowman HB. Rapid identification of reactive cysteine residues for site-specific labeling of antibody-Fabs. *J. Immunol. Methods.* 2008; 332:.41-52.

(191) Liu W, Brock A, Chen S, Chen S, Schultz PG. Genetic incorporation of unnatural amino acids into proteins in mammalian cells. *Nat. Methods.* 2007; 4: 239-244.

(192) Boeggeman E, Ramakrishnan B, Pasek M, Manzoni M, Puri A, Loomis KH, Waybright TJ, Qasba PK. Site specific conjugation of fluoroprobes to the remodeled Fc N-glycans of monoclonal antibodies using mutant glycosyltransferases: application for cell surface antigen detection. *Bioconjug. Chem.* 2009; 20: 1228-1236.

(193) Yokoyama K, Nio N, Kikuchi Y. Properties and applications of microbial transglutaminase. *Appl. Microbiol.. Biotechnol.* 2004; 64: 447-454.

(194) Rodwell JD et al. Site-specific covalent modification of monoclonal antibodies: in vitro and in vivo evaluations. *Proc. Natl. Acad. Sci. U.S.A.* 1986; 83: 2632-2636.

(195) Chang IN, Lin JN, Andrade JD and Herron JN. Photoaffinity labeling of antibodies for applications in homogeneous fluoroimmunoassays. *Anal.Chem.* 1995; 67: 959-966.

(196) Doronina SO et al. Development of potent monoclonal antibody auristatin conjugates for cancer therapy. *Nat. Biotechnol.* 2003; 21: 778-784.

(197) Trail PA et al. Cure of xenografted human carcinomas by BR96-doxorubicin immunoconjugates. *Science.* 1993; 261: 212-215.

(198) Saphire EO et al. Contrasting IgG structures reveal extreme asymmetry and flexibility. *J. Mol. Biol.* 2002; 319 9-18.

(199) Douek DC, Roederer M, Koup RA. Emerging Concepts in the Immunopathogenesis of AIDS. *Annu. Rev. Med.* 2009; 60: 471–484.

(200) Cunningham AL, Donaghy H, Harman AN, Kim M, Turville SG. Manipulation of dendritic cell function by viruses. *Current opinion in microbiology.* 2010; 13 (4): 524–529.

(201) McGovern SL, Caselli E, Grigorieff N, Shoichet BK. A common mechanism underlying promiscuous inhibitors from virtual and high-throughput screening. *Journal of Medical Chemistry*. 2002; 45 (8): 1712–1722.

(202) National Institute of Health (June 17, 1998). Crystal Structure of Key HIV Protein Reveals New Prevention, Treatment Targets Archived from the original on February 19, 2006. Retrieved September 14, 2006.

(203) Chan DC, Fass D, Berger JM, Kim PS. Core structure of gp41 from the HIV envelope glycoprotein. *Cell.* 1997; 89 (2): 263–273.

(204) Shimada T, Hasegawa H, Yamazaki Y, Muto T, Hino R, Takeuchi Y, Fujita T, Nakahara K, Fukumoto S, Yamashita T. FGF-23 is a potent regulator of vitamin D metabolism and phosphate homeostasis. *J. Bone Miner. Res*. 2004; 19(3):429-435.

(205) Razzaque MS. The FGF23-Klotho axis: endocrine regulation of phosphate homeostasis. *Nat. Rev. Endocrinol.* 2009; 5(11):611-609.

(206) Yamashita T. Structural and biochemical properties of fibroblast growth factor 23. *Ther Apher Dial*. 2005; 9 (4):313-318.

(207) White KE, Carn G, Lorenz-Depiereux B, Benet-Pages A, Strom TM, Econs MJ. Autosomal-dominant hypophosphatemic rickets (ADHR) mutations stabilize FGF-23. *Kidney Int.* 2001; 60(6): 2079-2086.

(208) Isakova T. et al. Fibroblast growth factor 23 is elevated before parathyroid hormone and phosphate in chronic kidney disease. *Kidney Int.* 2011; 79 (12):1370-1378.

(209) Shimada T, Muto T, Urakawa I, Yoneya T, Yamazaki Y, Okawa K, Takeuchi Y, Fujita T, Fukumoto S, Yamashita T. Mutant FGF-23 responsible for autosomal dominant hypophosphatemic rickets is resistant to proteolytic cleavage and causes hypophosphatemia in vivo. Endocrinology. 2002; 143(8): 3179-3182.

(210) Meyer DE, Trabbic-Carlson K, Chilkoti A. Protein purification by fusion with an environmentally responsive elastin-like polypeptide: effect of polypeptide length on the purification of thioredoxin. *Biotechnol. Prog.* 2001; 17(4):720-728.

(211) Lim DW, Trabbic-Carlson K, Mackay JA, Chilkoti A. Improved non-chromatographic purification of a recombinant protein by cationic elastin-like polypeptides. *Biomacromolecules.* 2007; 8 (5): 1417-1424.

(212) Stenström CM, Jin H, Major LL, Tate WP, Isaksson LA. Codon bias at the 3'-side of the initiation codon is correlated with translation initiation efficiency in Escherichia coli. *Gene*. 2001; 263(1-2): 273-284.

(213) Takemoto H, Miyata K, Ishii T, Hattori S, Osawa S, Nishiyama N, Kataoka K. Accelerated polymer-polymer click conjugation by freeze-thaw treatment. *Bioconjug. Chem.* 2012; 23(8):1503-6.

(214) Emily K. Perttua and Francis C. Szoka. Zwitterionic sulfobetaine lipids that form vesicles with salt-dependent thermotropic properties. *Chem. Commun.* 2011; 47: 12613-12615.